Boron removal from saline water.

Bin Darwish, Nawaf Naif

Swansea University
Prifysgol Abertawe

Boron Removal from Saline Water

Nawaf Naif Bin Darwish

BEng in Chemical Engineering (King Fahd University of Petroleum and Minerals, Saudi Arabia)

MSE in Chemical Engineering (King Saud University, Saudi Arabia)

Submitted to Swansea University in fulfilment of the requirements for the Degree of Doctor of Philosophy

Swansea University

2014

ProQuest LLC.
789 East Eisenhower Parkway
P.O. Box 1346
Ann Arbor, MI 48106 – 1346

DEDICATION

I want to warmly dedicate this work

To My Father, My Wife (Areej) , My Daughters (Reef and Deem), My mother in law (Fatima), My Brothers, My Sisters and all other family members

SUMMARY

Although boron is an essential micronutrient for some plants, animals and humans, the range between deficiency and excess is narrow. The effects of excess boron on plants includes the reduction of root cell division, retarded shoot and root growth, inhibition of photosynthesis, deposition of lignin and suberin and decrease in leaf chlorophyll. A report by the World Health Organization (WHO) suggests a safe maximum level of boron daily intake of 13 mg/d an excessive level of boron can be toxic to and can causes serious diseases.

There are several methods applied for boron removal from aqueous solutions and seawater. Among these methods, ion exchange, which is the most extensively method. Ion-exchange and adsorption are widely used techniques to remove metals and other solutes from aqueous solutions. This includes the removal of boron from reverse osmosis (RO) permeate in the process of seawater desalination.

The use of boron-selective ion exchange resins based on macroporous polystyrene matrices with the active group N-methyl-D-glucamine (NMG) seems to still have the highest importance for the elimination of boron. Kinetics of adsorption or IEX is in many cases strongly influenced by diffusion resistance in particles of adsorbent. This resistance can be decreased by using smaller particles. Sorbents can be used as very fine particles which results in increase of the surface area and the process rate, considerably. Hybrid adsorption membrane filtration has gained the interest lately as it can be used for the removal of very small quantities of harmful substances from water. This thesis deals used hybrid system on both lab and pilot scale where a pilot plant was designed for the removal of boron. Boron separation combines two phenomena: i) sorption with fine sorbent particles and ii) membrane separation of B-loaded macromolecules/particles. The hybrid system includes two separation loops, Loop 1: Binding of boron (B) on Amberlite IRA743 resin (S), which is subsequently followed by separation of this (BS) complex from the water by means of semi-permeable microfiltration membrane. Here, pure water (W) is the main product whereas the complex (BS) passes to the second stage of separation.

The effects of different parameters on boron removal using Amberlite IRA743 resin were investigated in this thesis. These parameters are, resin particle size, solution pH, temperature, contact time, initial boron concentration, resin concentration and the existence of different salts and ions like NaCl, Na_2SO_4 and $MgCl_2$. The removal increased with increasing pH, temperature, contact time and resin dosage while it decreased with increasing initial boron concentration and resin particle size.

For the microfiltration stage, three Polyvinylidene fluoride (PVDF) with different pore size have been used in this thesis. The effects of operational parameters like membrane pore size, transmembrane pressure, resin concentration and pH on permeate flux for hybrid adsorption-microfiltration were studied. The permeate flux increased with increasing the transmembrane pressure and pH but it decreased with increasing the resin concentration.

The regeneration of loaded resin with boron was investigated. Hydrochloric acid (HCl) and sulfuric acid (H_2SO_4) at different concentrations have been used for the elution of boron from the saturated resin and then washing with sodium hydroxide (NaOH). There was an improvement in the boron removal after cycles of regeneration.

The integrated adsorption-microfiltration was applied for boron removal from water and encouraging results were achieved.

Declaration

This work has not previously been accepted in substance for any degree and is not being concurrently submitted in candidature for any degree.

Signed: ---------- (Candidate)

Date: 15/9/2014

STATEMENT 1

This thesis is the result of my own investigations, except where otherwise stated. Where correction services have been used the extent and nature of the correction is clearly marked in a footnote(s).

Other sources are acknowledged by footnotes giving explicit references. A bibliography is appended.

Signed: ---------- (Candidate)

Date: 15/9/2014

STATEMENT 2

I hereby give consent for my thesis, if accepted, to be available for photocopying and for inter-library loans **after expiry of a bar on access approved by the Swansea University**

Signed: ---------- (Candidate)

Date: 15/9/2014

ACKNOWLEDGEMENTS

I would like to express my ultimate gratitude to my supervisor Professor Nidal Hilal, Director of the Centre for Water Advanced Technologies and Environmental Research (CWATER) at Swansea University, for his continuous guidance, help, support, ideas throughout the entire period of my thesis. My deepest appreciation is extended to Dr. Victor Kochkodan for his motivation and significant comments on my work.

I would like to thank Dr. Daniel Johnson for his excellent contribution on imaging and analysis of Atomic Force Microscopy and Scanning Electron Microscope.

I would like to thank Dr. Mabrouk Zanain for his help in using Malvern Mastersizer-2000 analyzer and Surface area analyzer.

Many thanks to Gary Tuckett for his help and contribution in designing and constructing the semi-pilot plant.

A special thanks is dedicated to King Abdulaziz City for Science and Technology (KACST), Saudi Arabia for funding my study.

Finally, I would like to extend my appreciation and thanks to my family and friends for their continuous care and support.

CONTENTS

FIGURES

TABLES

NOMENCLATURE

K	kinetic rate constant
A	Arrhenius factor
R	Gas constant
E	activation energy
S	Salinity
T	Temperature
R_g	Radius of gyration
C	Concentration
V	Volume
J	Permeate flux
A	Membrane effective area
R	Removal percentage
C_0	Initial boron concentration
C_e	Final boron concentration in the solution
q_e	amount of boron sorbed per amount mass of sorbent
b	Langmuir equilibrium constant
q	Adsorption capacity
q_t	amount of boron adsorbed at time t
q_e	amount of boron adsorbed at equilibrium
K_1	pseudo-first-order rate constant
K_2	pseudo-second-order rate constant
K_F	constant related to adsorption capacity
1/n	constant related to adsorption intensity
SPAN	the width of the distribution based on the 10%, 50% and 90% quantile
K_a	Dissociation constant
E	Activation energy

ABBREVIATIONS

AMF	Adsorption microfiltration
RO	Reverse osmosis
NMG	N-methyl-D-glucamine
NMR	Nuclear magnetic resonance
IBPD	imino-bis propanediol
GVPA	Poly(vinyl amino-N, N′-bis-propane diol
VBC	vinylbenzyl chloride
TG	tannin gel
PEU	polymer enhanced ultrafiltration
PNS	Poly(glycidylmethacrylate)
COP	Poly(4-Vinyl-1,3-dioxalan-2-one-co-vinylacetate)
GPVA	poly (vinyl amino-N, N′-bis-propane diol)
TMP	Trans membrane pressure
CFMF	cross flow microfiltration
BET	Brunauer – Emmet – Teller
AFM	Atomic force microscopy
SEM	scanning electron microscope
GMA	glycidyl methacrylate
ATRP	transfer radical polymerization
PS-DVB	poly(styrene-divinyl benzene)
PAA	Polyallylamine
TEOS	tetraethoxysilane
GPTMS	(3-glycidoxypropyl)trimethaoxysilane
EGDE	Ethyleneglycoldiglycidylether
GMHP	N-D-glucidol-N-methyl-2-hydroxylpropyl methacrylate
PEI	Polyethylenimine
LAc	3-5- bis(hydroxymetyl) -4-hydroxybenzoil acid
WHO	World Health Organization
DCMD	Direct contact membrane distillation
PVDF	polyvinylidene fluoride

LDHs	Layered double hydroxides
HT	Hydrotalcite
HDTMA	hexadecyl trimethyl ammonium
HFO	hydrous ferric oxide
TSPA	bis(trimethoxysilylpropyl) amine
IEX	Ion exchange

CHAPTER 1

Introduction

1.1 General Introduction

Over the last years the increased attention given to boron concentration in aqueous solutions has been favouring the upgrading of conventional water treatment processes and an emergence of novel technologies in order to improve an efficiency of boron removal. Boron is of special concern in desalinated seawater and irrigation water because of its possible toxic effects for both human and plants.

Ion-exchange and adsorption are widely techniques used to remove metals and other solutes from aqueous solutions. This includes the removal of boron from reverse osmosis (RO) permeate in the process of seawater desalination.

The use of boron-selective ion exchange resins based on macroporous polystyrene matrices with the active group N-methyl-D-glucamine (NMG) seems to have still the highest importance for the elimination of boron. The presence of two vicinal hydroxylic groups allows boric acid and borates to form stable complex with the fixed group on the resin.

Kinetics of adsorption or ion exchange are in many cases strongly influenced by diffusion resistance in particles of adsorbent. This resistance can be decreased by using smaller particles.

Sorbents can be used as very fine particles which results in increase of the surface area and the process rate, considerably.

Basic concept of the hybrid adsorption-membrane (AMF) process is the adsorption of solute onto fine sorbent particles to get fast adsorption and followed by separation of loaded adsorbent by microfiltration. The second step of AMF is the separation of the complex (BC) into free sorbent (C) and pure boron (B) and their separation carried out by membrane.

The main advantage of the hybrid AMF compared with the classical column sorption on the fixed bed is the high efficiency and low costs. Sorbents can be used at a very small particle size which leads to increase of the surface area and the process rate considerably.

1.2 Objective of the Study

Many technologies have been applied for boron removal from water. Due to either low boron removal or high cost of these technology, the ion exchange method most extensively used and the most efficient for boron removal .

Combination of two separation processes such as sorption and membrane filtration reveals many advantages comparing with conventionally used fixed bed systems. The main advantage of this separation method is the high efficiency and lower costs of the process comparing with classical sorption in fixed bed system. The sorbents can be used as very fine particles that increase the interface area and in consequence, the rate of the process is enhanced. The low-pressure driven membrane techniques such as microfiltration and ultrafiltration have been considered as indispensable treatment methods in the water and wastewater treatment applications to remove specific pollutants which are not normally removed by the conventional processes.

A hybrid adsorption-microfiltration (AMF) process is the adsorption of solute onto microparticle sorbent to obtain fast adsorption and separation of loaded adsorbent by microfiltration.

Fine particles of Amberlite IRA743 will be used in this study for boron removal from water at different boron concentration ranging from 1.5 – 15 mg/L. The regeneration of loaded resin will be take part in this study.

The integrated process of boron removal which combine AMF and regeneration of the loaded resin as a continuous process will be evaluated in this thesis.

This technique will be applied in this thesis to study the following:

1. The effect of contact time, particle size, resin dosage, temperature, pH, boron concentration, and the existence of salts (NaCl, Na_2SO_4 , $MgCl_2$) on boron removal by Boron-Specific Ion Exchange Resin.

2. The effect of membrane porosity, pressure, resin concentration, pH and salts (NaCl, Na_2SO_4 , and $MgCl_2$) on permeate flux.
3. The regeneration of loaded resin and its reusability using different acid at different concentration.
4. The application of integrated hybrid adsorption-microfiltration process for the removal of boron from saline water.

1.3 Outline of the Thesis

This thesis consists of eight chapters and the general overview of each chapter is described in the following paragraphs. Beside this chapter which shows introduction including general information about boron and its importance to life and a brief description of the hybrid adsorption-microfiltration process and its application for boron removal from water, chapter two presents a comprehensive review of boron and its chemical properties in nature and in water. Chapter two also presents the standards or guideline values for boron concentration in drinking water around the world. The technologies used for boron removal from waters also presented in chapter two.

All experimental equipment and related procedures used in this thesis are covered in chapter three. In Chapter four, the results of the influences of different parameters on boron removal by complexation with boron-selective ion exchange Amberlite IRA743 resin are discussed. These parameters include, particle size of the resin, pH of the boron solution and its temperature, the contact time of boron with the resin, initial boron concentration, resin dosage and the impact of different salts like NaCl, $MgCl_2$ and Na_2SO_4.

The results of the microfiltration of the suspension are presented in Chapter five. The effect of some operational parameters on permeate flux are discussed in this chapter. These parameters include membrane pore size, transmembrane pressure, resin concentration in the feed solution, and pH of the feed solution. The regeneration of loaded resin with boron using different acids with different concentrations is discussed in Chapter six. Hydrochloric acid (HCl) and sulfuric acid (H_2SO_4) are used at different concentrations to elute boron from the loaded resin. The effect of time of elution and acid concentration on the elution are discussed. The loaded resin regeneration consists of

two steps: the elution of boron from the saturated resin using acid and regeneration (washing) with base (NaOH).

The integrated hybrid adsorption-microfiltration process is presented in Chapter seven. This process includes two separation loops, binding of boron (B) on Amberlite IRA743 resin (S), which is subsequently followed by separation of this (BS) complex from the water by means of semi-permeable microfiltration membrane. Then, splitting of the complex BS onto the free resin (S) and boron (B) followed by membrane separation is carried out in the second stage of separation (regeneration). This step allows to reuse the resin and to recycle it to the system. This system is applied experimentally in this chapter and the results are presented. Finally, conclusions as well as recommended works for the future are outlined in chapter Eight.

CHAPTER 2

Literature Review

2.1 Boron and its chemical properties

Boron (B) is the fifth element in the Periodic Table with atomic mass of 10.81. It is the most electronegative element of Group 13 and its chemical properties closely resemble the non-metals, particularly silicon. Pure element of boron was first isolated simultaneously and independently in 1808 by H. Davy in England, who observed that electric current sent through a solution of borates produced a brown precipitate on one of the electrodes, and J. Gay-Lussac and L. Thenard in France, who obtained boron by reducing of boric acid with iron at high temperatures (Greenwood, 1973).

Elemental boron exists as a solid at room temperature, either as black monoclinic crystals or as a yellow or brown amorphous powder when impure. The amorphous boron can be obtained by reduction of the boron oxide with sodium or a fluoborate with potassium (Greenwood, 1973):

$$B_2O_3 + 6Na \rightarrow 2B + 3Na_2O \qquad 2.1$$

$$4KBF_3 + 3K \leftrightarrow 3KBF_4 + B \qquad 2.2$$

Crystalline boron was first prepared when hydrogen and boron bromide vapour at rather less than atmospheric pressure were passed over a tantalum filament heated to 1000-1300 °C (Kemp, 1956). At this temperature the bromide is reduced and the boron thus becomes deposited on the filament as black hexagonal flakes and needles:

$$2BBr_3 + 3H_2 \leftrightarrow 6HBr + 2B \qquad 2.3$$

Two crystalline modifications of boron, namely α-rhombohedral boron and β-rhombohedral boron exist at atmospheric pressure. The latter is believed to be thermodynamically stable at high temperatures, whereas α-boron is sometimes called the low-temperature form (Albert and Hillebrecht, 2009).

The chemical nature of boron is influenced primarily by its small size (covalent radius of boron of 0.8-1.01 A) and high ionization energy (344.2 kJ/mol) (Greenwood, 1973). The high affinity for oxygen is another dominant characteristic of boron, which forms the basis of the extensive chemistry of borates and related oxo-complexes (Kemp, 1956).

The chemical properties of the boron element depend also on its morphology and particle size. Micron sized amorphous boron reacts easily and sometimes intensely, whereas crystalline boron is very inert chemically and resistant to attack even by boiling hydrofluoric or hydrochloric acid. It should be noted that boron is difficult to prepare in a state of high purity owing to its very high melting point of 2079°C (Emsley, 1991). Boron boiling point is 2250°C and its density is 2.37 g/m^{-3} (Krebs, 2006).

The electron structure of the element is $1s^2\ 2s^2\ 2p^1$ and hence boron can form three or four valence bonds (Ali *et al.*, 2005). In its most common compounds, such as oxides, sulphides, nitrides, and halides boron has the formal oxidation state +3. In these compounds the bonds are coplanar, with interbond angles of 120 °. The lower oxidation states +1 or 0 are present only in compounds such as higher boranes (e.g. B_5H_9), subvalent halides (e.g. B_4Cl_4), metal borides (e.g.Ti_2B), or in some compounds containing multiple B–B bonds (Kemp, 1956). In naturally occurring compounds boron usually has a coordination number of either 3 or 4.

Boron salts are generally well water soluble, e.g. borax has a water solubility of 25.2 g/L, while boron trifluoride is the least water soluble boron compound, with a water solubility of 2.4 g/L (Kemp, 1956).

2.2 Boron in nature

Boron element is composed of ^{8}B, ^{10}B, ^{11}B, ^{12}B and ^{13}B isotopes. The most stable isotopes are ^{10}B and ^{11}B. The occurrence of these isotopes in nature is 19.1-20.3% and 79.7-80.9%, respectively (Greenwood, 1973).

2.2.1 Boron in lithosphere

Boron is widely distributed in lithosphere of the earth (Morgan, 1980). It is found in rocks and soils, particularly in clay rich marine sediments. The concentration of boron in the earth's crust varies from 1 to 500 mg/kg, depending on the nature of the rock (Aubert

and Pinta, 1997). An average of boron in the earth's crust is around 10 mg/kg, representing 0.001% of the elemental composition of the earth (Krauskopf, 1972). The amount of boron in soils ranges from 2 to 100 mg/kg with an average of 30 mg/kg (Aubert and Pinta, 1997). Most soils have low boron content (<10 mg B/kg), while high boron content soils (10–100 mg B/kg) are usually associated with volcanic activity.

The total amount of boron stored in the lithosphere is estimated as: the continental and oceanic crusts (1018 kg B), coal deposits (1010 kg B), commercial borate deposits (1010 kg B), and biomass (1010 kg B) (Argust, 1998).

It should be noted that boron is never found free in nature, but invariably occurs as the oxide B_2O_3 in combination with the oxides of other elements to form borates of greater or lesser complexity. There are more than 200 boron compounds in the Earth (Beatty, 2005), but only twelve are found commercially significant (Adair, 2007). The first known borate mineral to antiquity is sodium tetraborate decahydrate $Na_2B_4O_7.10H_2O$ or borax (Figure 2.1a). An early use of borax was to make perborate, the bleaching agent once widely used in household detergents. The other important boron containing minerals are ulexite ($NaCaB_5O_9.8H_2O$), colemanite ($Ca_2B_6O_{11}.5H_2O$) (Figure 2.1b) and kernite ($Na_2B_4O_7.4H_2O$). Borax, colemanite, ulexite and kernite provide more than 90% of the word's boron demand (Adair, 2007). The occurrence of concentrated deposits of borate minerals is intimately connected with past or present volcanic activity and arid climatic conditions are essential for continued preservation of such deposits, which are being exploited in the United States, Turkey, Italy, Spain, Russia, Chile and some other countries.

a) b)

Figure 2.1 Photos of boron-containing minerals: borax (a) and (b) colemanite

2.2.2 Boron in aqueous environmental

The majority of the Earth's boron is found in the oceans, with an average concentration of 4.5 mg/L, but ranges from 0.5 to 9.6 mg/L (Weast *et al.*, 1985). Geographical location and seasonal effects play a significant role in the boron concentration in the oceans and seas (Farhat *et al.*, 2013). Boron content in Mediterranean sea may be as high as 9.6 mg/L (Argust, 1998). In the Arabian Gulf, boron levels have been reported to be as high as 7 mg/L (Farhat *et al.*, 2013).

The natural borate content of ground water and surface water is usually small and is a result of leaching from rocks and soils containing borates and borosilicates. Concentrations of boron in ground water throughout the world range widely, from <0.3 to >100 mg/L. In EU, concentrations of boron changes from 0.5 to 1.5 mg/L for southern Europe (Italy, Spain) and up to approximately 0.6 mg/L for northern Europe (Denmark, Germany, UK) (Butterwick *et al.*, 1989).

The amount of boron in surface water depends on factors such as the proximity to marine coastal regions, inputs from industrial and municipal effluents and the geochemical nature of the drainage area. Boron concentrations in surface water range from <0.001 to 2 mg/L in EU, with mean values typically below 0.6 mg/L (Butterwick *et al.*, 1989). Similar boron content has been reported for water bodies within Turkey, Russia and Pakistan, from 0.01 to 7 mg/L, with most values below 0.5 mg/L. Concentrations of boron in surface waters of North America (Canada, USA) range from 0.02 mg/L to 360 mg/L, indicative of boron-rich deposits, up to 0.01 mg/L in Japan and up to 0.3 mg/L in South African surface waters.

A wide variation of boron concentrations in surface water is due to both natural and anthropogenic factors (Jahiruddin *et al.*, 1998). Natural factors include the weathering of rocks and the leaching of salt deposits. In coastal areas, rain containing sea salt from ocean spray provides another source of boron (Jahiruddin *et al.*, 1998).

The anthropogenic factors include water pollution with boron-containing wastes from glass/ceramic industry (a largest market of 56% global borate demand) and metallurgy. Boron may also be discharged to the environmental as drainage from disused coal mines and leaching of tips and landfills from the mining industry (Hebblethwaite and Emberson, 1993).

Domestic wastewater effluents may be also extremely enriched in boron, with concentrations varying from several hundred μg/L to several mg/L (Fox *et al.*, 2000). By far the most common reason for this enrichment is the presence of sodium perborate that used as a bleaching agent in detergents and cleaning products.

Boron-containing fertilizers can also be a major source of anthropogenic boron due to their widespread application. Boron is an essential micronutrient for plants and consequently is included in many fertilizers at levels ranging from 0.01 to 0.06 wt.% , most commonly in the form of borax (Brady and Weil, 2008). Wyness et al. (2003) found that rivers draining high intensity agricultural areas of south-eastern England can have average boron concentrations of up to 387 μg/L.

The total distribution of boron contents in the hydrosphere was identified by Argust (1998) as the oceans (1015 kg B), groundwater (1011 kg B), ice (1011 kg B), and surface waters (108 kg B).

2.3 Physico-chemistry of boron compounds in water

In nature, boron is released from rocks and soils through weathering, and subsequently ends up in aqueous environment as boric acid $B(OH)_3$ or borate ion $B(OH)_4^-$.

2.3.1 Physical properties of boric acid

Boric acid was first prepared from borax (sodium tetraborate decahydrate) by the reaction with hydrochloric acid (Kemp, 1956):

$$Na_2B_4O_7.10H_2O + 2HCl \rightarrow 4B(OH)_3 + 2NaCl + 5H_2O \qquad 2.4$$

It crystallizes from aqueous solutions normally as white, shining, waxy plates of orthoboric acid, $B(OH)_3$. On heating above 100 °C the boron acid gradually loses water, changing to metaboric acid HBO_2:

$$B(OH)_3 \rightarrow HBO_2 + H_2O \qquad 2.5$$

At higher temperature all the water is lost and anhydrous boric oxide forms:

$$2B(OH)_3 \rightarrow B_2O_3 + 3H_2O \qquad 2.6$$

Crystalline boric acid consists of layers of $B(OH)_3$ molecules held together by hydrogen bonds shown in Figure 2.2 (Kemp, 1956). The dimension of the unit cell, which contains

four molecules of $B(OH)_3$, being a_0=7.04 A, b_0=7.05 A, c_0=6.56 A with α= 92°30′, β=101°10′ and γ=120° (Kemp, 1956). The lattice is of the layer type (which explains the ready cleavage into flakes), consisting of sheets of coplanar BO_3 groups. Each oxygen atom, besides being linked to boron, is joined to two other oxygen atoms by means of hydroxyl bonds. The distance between each pair of sheets is 3.18 A (Kemp, 1956).

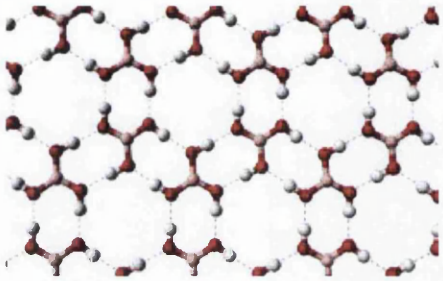

Figure 2.2 A schematic presentation of one sheet of H_3BO_3 lattice, (Kemp, 1956)

The solubility of boric acid in water increases rapidly with temperature at atmospheric pressure as shown in Table 2.1 (Owen, 1934, Kemp, 1956)

Table 2.1 Effect of the temperature on water solubility and the first dissociation constant K_a of boric acid, (Kemp, 1956, Owen, 1934)

Temperature, °C	**Solubility of $B(OH)_3$, wt. %**	**$K_a \times 10^{10}$**
0	2.70	
15	4.17	4.72
20	4.65	5.26
25	5.44	5.79
50	10.24	8.32
75	17.41	
100	27.53	

Boric acid in water is uncharged and has trigonal structure. Figure 2.3 shows an actual size comparison between boric acid molecule, sodium and chloride ions in water.

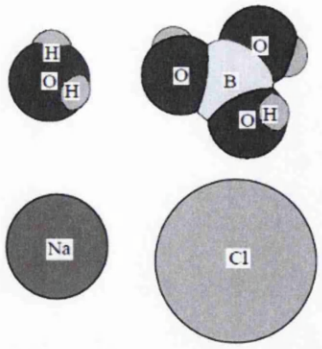

Figure 2.3 Size comparison between boron acid and some other species in aqueous Solutions

2.3.2 Dissociation of boric acid in water

Boric acid is a very weak acid and does not dissociate in aqueous solution as a Bronsted acid but acts as a Lewis acid by accepting a hydroxyl ion to form the tetrahydroxyborate ion, as confirmed by Raman spectroscopy (Jolly, 1984):

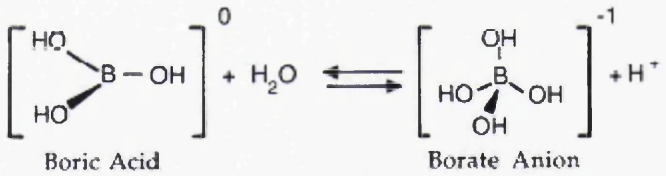

Thus the dominant forms of inorganic boron in natural aqueous systems are mononuclear species such as boric acid $B(OH)_3$ and borate ion $B(OH)_4^-$. The distribution of these two components depends on the first dissociation constant K_a of boric acid. It was shown that the first dissociation constant is equal of 5.8×10^{-10} mol/L in fresh water at temperature 25 °C, while values of 1.8×10^{-13} and 3×10^{-14} have been reported for the second and third dissociation constant of boric acid respectively. As seen in Table 2.1, K_a increase with an increase of water temperature (Owen, 1934).

In solutions more concentrated than 0.1 M, boric acid acts as a much stronger acid than in diluted solutions, becoming comparable to acetic acid; the apparent ratio of the

concentration of borate ions to that of boric acid molecules in the solution progressively increased from 1:1000 at 0.2 M to 1:5 at 3.5 M (Kemp, 1956).

The pK values (= - log(K_a)) of boric acid has been determined to be pK_a=8.60 in artificial seawater at T=258 °C/salinity of 35 g/L (Dickson, 1990) and pK_a =9.24 at 25 °C in fresh waters (Dean, 1999).

In general, due to a relatively high pK_a, boron acid has limited dissociation at neutral or low pH values. Being a weak acid, the actual pK_a value of boric acid (and distribution of boric acid and borate ion) essentially varies depending on pH, ionic strength and temperature of the feed solution. The most important parameter, which determines a ratio of boric acid molecules to borate ions in water, is pH of the medium. As shown in Figure 2.4, the distribution of boron species in seawater is changes dramatically with pH at temperatures of 10 and 35 °C (Edzwald and Haarhoff, 2011). As can be seen in this Figure, the borate monovalent anion $B(OH)_4^-$ dominates at higher pH while non-ionized boric acid $B(OH)_3$ at lower pH.

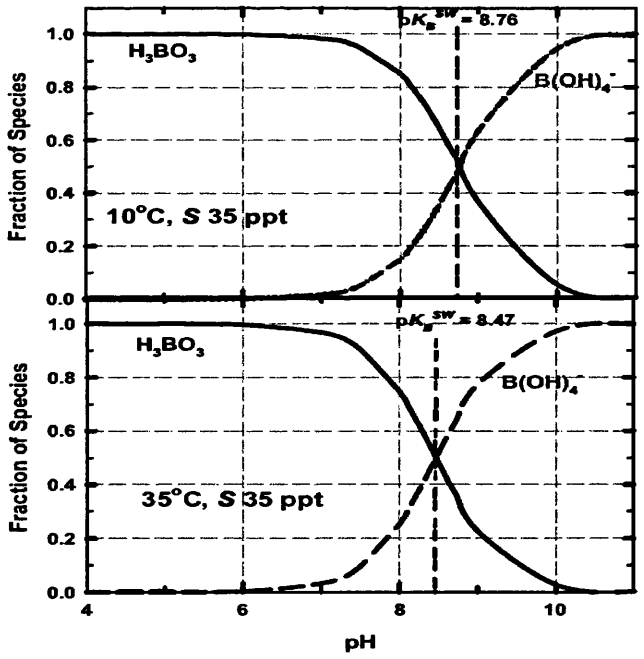

Figure 2.4 Fraction of $B(OH)_3$ and $B(OH)_4^-$ as a function of pH for seawater with salinity of 35 %: top Figure at 10 °C, bottom Figure at 35 °C, (Edzwald and Haarhoff, 2011)

Dickson (1990) investigated the dissociation of boric acid in seawater over a wide ranges of salinity (5000–45,000 mg/L) and temperature (0–45 °C). Based on the obtained results, he suggested an equation to estimate the dissociation constant of boric acid depending on salinity (S) and temperature of seawater (T):

$$lnK_a = \frac{-8966.90 - 2890.51S^{0.5} - 77.942S + 1.726S^{1.5} - 0.0993S^2}{T} + (148.0248 + 137.194S^{0.5} + 1.62247S) + (-24.4344 - 25.085S^{0.5} - 0.2474S).\ln(T) + 0.053105S^{0.5}.(T) \quad 2.7$$

Roy *et al.* (1993) have subsequently found that the measurement of the dissociation constant by using Dickson approach is quite reliable. It was reported that the pK_a of boric acid decrease from 9.23 to 8.60, when the salinity increased from 0 to 40,000 mg/L (Choi and Chen, 1979) and the pK_a changed from 9.38 to 9.079 as the solution temperature increase from 10 to 50 °C (Owen, 1934).

The distribution of boric acid and borate in seawater at different salinity and temperatures is shown in Figure 2.5 (Hilal *et al.*, 2011) and it is seen that a fraction of borate ion increases with an increase of salinity and temperature of seawater.

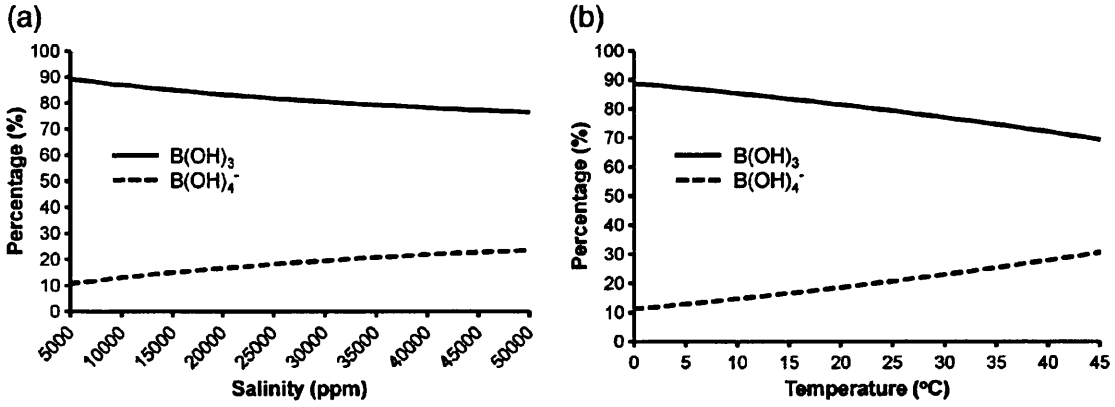

Figure 2.5 The distribution of boric acid molecules and borate ions in seawater at different salinity and temperature, (Hilal et al., 2011)

The dependence of pK_a of boric acid on pressure has been investigated by (Tsuda *et al.*, 1976) and was found an increase in pK_a value of up to 2 units as pressure increased from 0 to 6 kbar.

The kinetics of the boric acid–borate equilibrium at various temperatures and ionic strengths of aqueous solutions was studied by (Waton *et al.*, 1984). The authors suggested that the temperature dependence of kinetic rate constant can be fit by an Arrhenius equation:

$$k = A \exp(\frac{-E_a}{RT}) \qquad 2.8$$

where A is the pre-exponential factor or Arrhenius factor, R=8.3145 J/(mol×K) is the gas constant, T is the absolute temperature in Kelvin, and E is the activation energy.

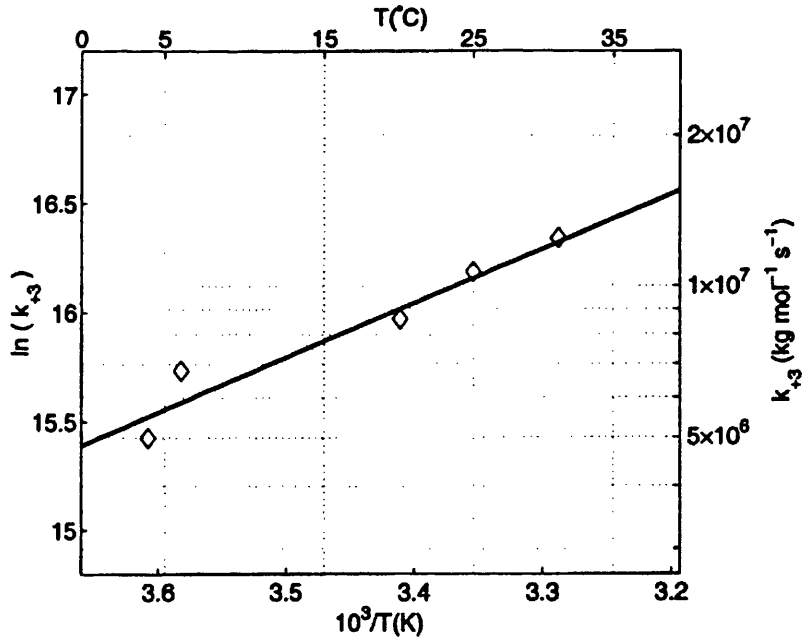

Figure 2.6 Arrhenius plot of the rate constant k_{+3} of boric acid dissociation at ionic strength I=0.1. The solid line represents the best linear fit to the data when $ln\ k_{+3}$ is plotted vs. $10^3/T\ (K)$, (Waton et al., 1984)

A linear regression of ln k_{+3} versus $1/T$ (Figure 2.6) yields A=4.58x10^{10} kg/mol×s and E=20.8±5.1 kJ/mol. Thus, the rate constant k_{+3} can be expressed as:

$$k_{+3} = 4.58x10^{10} \exp(-20.8 \times \frac{10^8}{RT}) \qquad 2.9$$

Which yields k_{+3} =1×10^7 kg/mol× s at 258 °C.

It should be noted that, in contrast to many other acid–base equilibriums, the dissociation of boric acid in aqueous solutions is not diffusion-controlled. This is probably due to the substantial structural change that is involved in the conversion from planar $B(OH)_3$ to tetrahedral $B(OH)_4^-$ species (Mellen *et al.*, 1983). As a result, the rate constant is two to four orders of magnitude smaller than typical rate constants of diffusion-controlled reactions which are on the order of 10^9–10^{11} kg/mol×s (Eigen and Hammes, 1963).

Zeebe *et al.* (2001) showed that the theoretically calculated relaxation time for chemical and isotopic equilibrium is ~95 and ~125 μs, respectively, for typical seawater conditions at temperature T=258 °C and salinity S=35 %. It follows that for practical purposes i.e., when time scales of minutes and hours are considered, it can safely be assumed that the dissolved boron species are in equilibrium.

2.3.3 Polyborates ions in aqueous solutions

Depending on boron concentration in aqueous solutions various boron-containing species may be found in water. At low boron concentration (<0.02 M), dissolved boron is mainly presented as the mononuclear boron species, $B(OH)_3$ and $B(OH)_4^-$.

At higher concentrations (0.025-0.6 M) and with an increase in pH from 6 to 10, water soluble polyborate ions such as $B_3O_3(OH)_4^-$, $B_4O_5(OH)_4^-$ and $B_5O_6(OH)_4^-$ are formed (Power and Woods, 1997).

The formation of these polynuclear ions is attributed to the interaction of boric acid and borate ions in solution according to following equations (Cotton and Wilkinson, 1980):

$$2B(OH)_3 + B(OH)_4^- \leftrightarrow B_3O_3(OH)_4^- + 3H_2O \quad 2.10$$

$$2B(OH)_3 + B(OH)_4^- \leftrightarrow B_3(OH)_{10}^- \quad 2.11$$

$$2B(OH)_3 + 2B(OH)_4^- \leftrightarrow B_4O_5(OH)_4^{2-} + 5H_2O \quad 2.12$$

$$4B(OH)_3 + 2B(OH)_4^- \leftrightarrow B_5O_6(OH)_4^- + 6H_2O \quad 2.13$$

The structural formulas of some polymeric borate ions and their distribution as a function of pH of the aqueous solutions are presented in Figures 2.7 (Salentine, 1983) and 2.8 (Anderson *et al.*, 1964), respectively. An increase in pH usually results in higher nuclearity borates, but at pH >10 $B(OH)_4^-$ is mainly formed. It should be noted that formation of polyborate ions in aqueous solutions are negligible at boron concentrations lower than 290 mg/L (Matsunaga and Nagata, 1995).

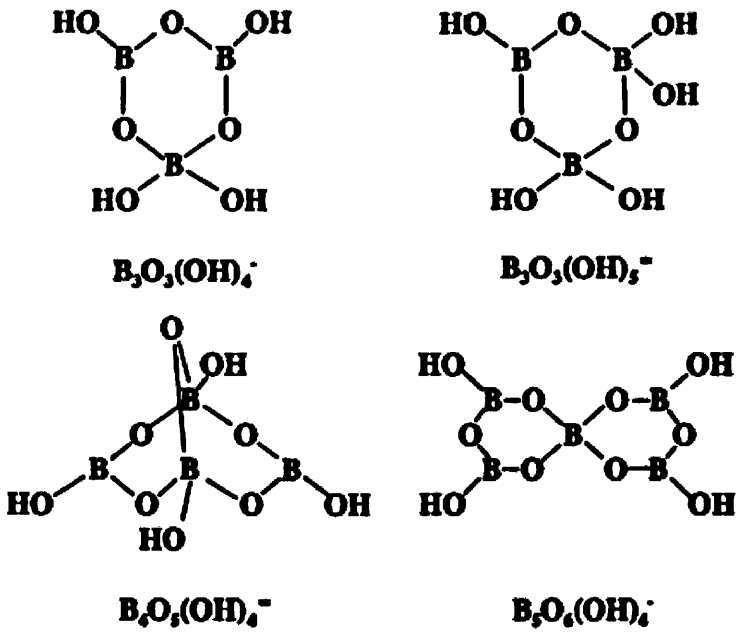

Figure 2.7 Chemical structures of polymeric borate anions in aqueous solutions, (Salentine, 1983)

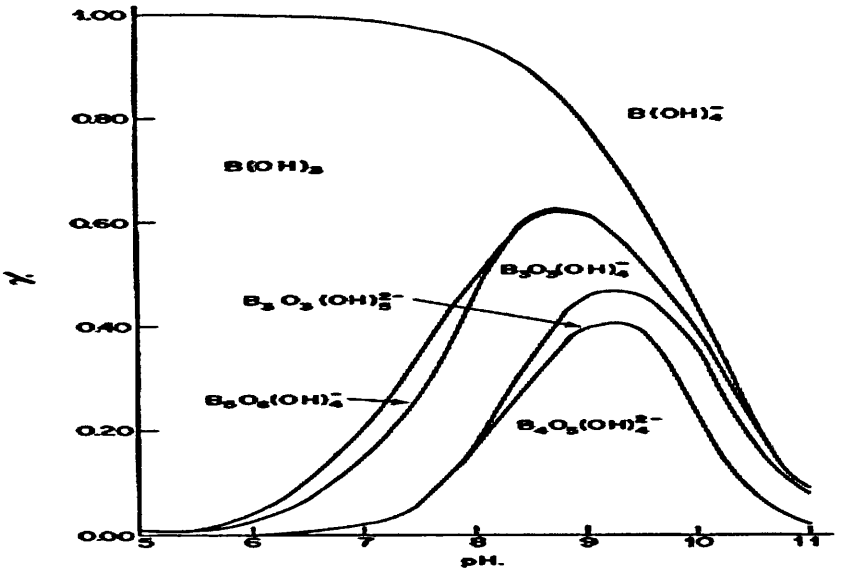

Figure 2.8 Distribution of polyborate species as a function of pH in 0.4 M boric acid, (Anderson et al., 1964)

2.4 Complexation of boron species in water

2.4.1. Boron complexes with alcohols and polyols

In aqueous environment boric acid and borates reacts with alcohols and multiple-hydroxyl containing compounds (polyols) forming boron esters, neutral *cis*-diol monoborate esters, monoborate complexes or bis(diol)borate complexes (Figure 2.9) (Eigen and Hammes, 1963) .

$$B(OH)_3 + 3ROH \leftrightarrow B(OR)_3 + 3H_2O \qquad 2.14$$

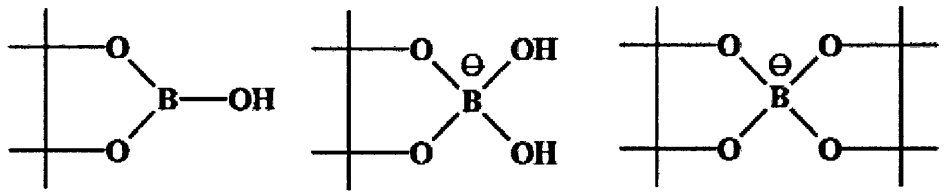

(a) (b) (c)

Figure 2.9 Chemical structures of (a) *cis*-diol monoborate esters ,(b) monoborate complexes or (c) bis(diol)borate complexes, (Eigen and Hammes, 1963)

The complexation with polyols increases the acidity of boron acid due to the formation of cyclic borate esters. For example, the dissociation constant of boric acid becomes about 7×10^{-6} in presence of mannitol, i.e. a ten–thousand fold increase comparing without the polyol (Kemp, 1956). Such behavior is not shown on addition of monofunctional alcohols, nor of glycols, nor of the trans-form of cyclopentane-diols, but it is shown on addition of the *cis*-form of the latter compounds. The phenomenon depends on the formation of mono-or dicyclic compounds with the polyol groups, which are more highly dissociated that the boric acid itself, and it follows that the only compounds with two hydroxyl groups suitably placed on the same side of the $C-C$ link can react in this way. Thus, the stability of the borate complex formed is strongly dependent on the type of diol used. If the diol involves the OH groups oriented in such a way that they accurately match the structural parameters required by tetrahedrally coordinated boron, a strong complex is formed. The complexation with polyols with an increase of the acidity of boric acid has been used for many years for boric acid quantitative analysis. The boric acid could be titrated to a phenolphthalein endpoint, which is not possible in the absence of the polyols (Belcher *et al.*, 1970). The complexation process with polyols involves two distinct mechanisms: interaction of boric acid with polyol or borate ion with polyol (Figure 2.10) (Tu et al., 2013). Contribution of each mechanism in the overall complexation depends on the solution pH where either boric acid or borate ion is dominantly present.

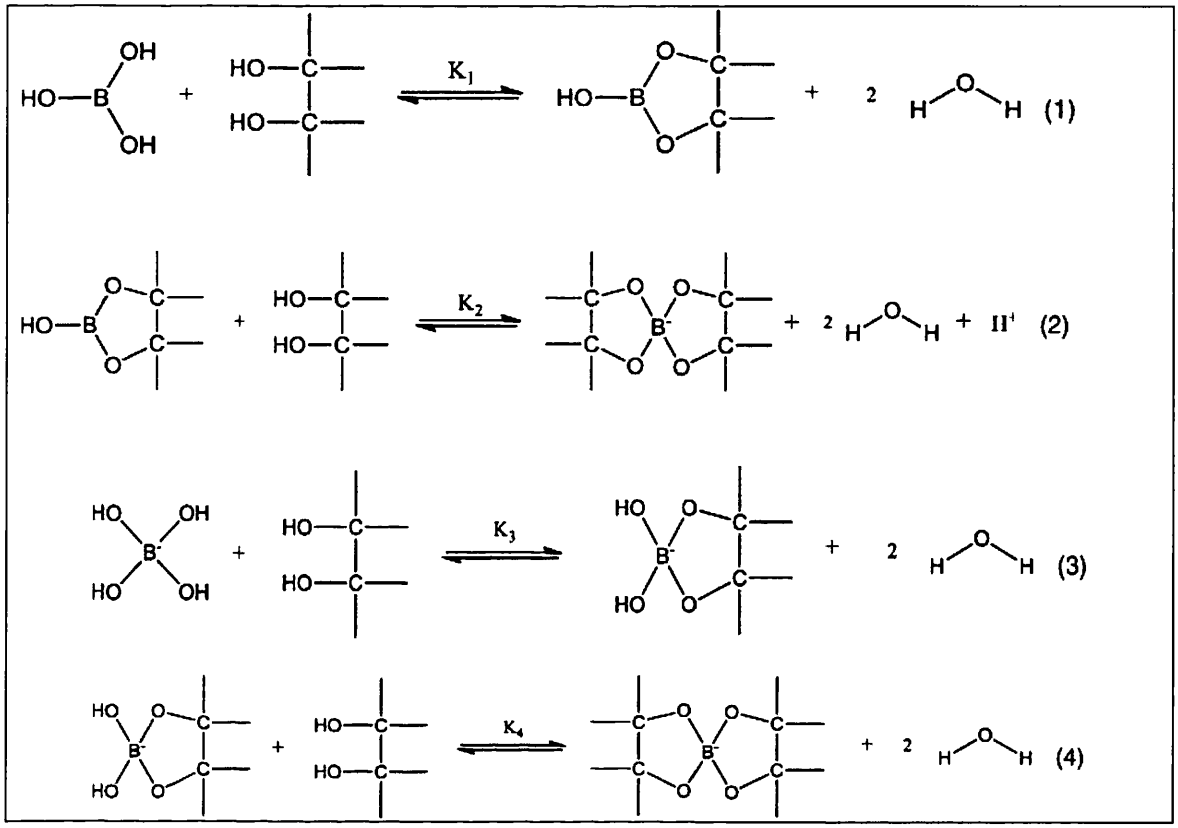

Figure 2.10 General scheme of boron complexation with polyols, (Tu et al., 2013)

The equilibrium constants of borate complexes have been investigated by several studies (Vanduin *et al.*, 1984, Vanduin *et al.*, 1985, Makkee *et al.*, 1985) and some of the data are listed in Table 2.2 (Sanderson, 1980). In general, the stability of the borate complex is strongly dependent on the type of diol used. As have been discussed above, if the orientation of OH groups in diol molecule is favourable for tetrahedral boron coordination, a stable complex will be formed.

Table 2.2 Equilibrium constant for boric acid complexes with polyols, (Sanderson, 1980)

Polyol	K_1	K_2
1,2-etanediol	2.15	1.15
1,3-propanediol	1.27	0.11
glycerol	16.0	41.2
catechol	7.8×10^3	1.42×10^4
D-mannitol	1.1×10^2	1.37×10^5
D-glucose	1.50×10^3	7.6×10^2
D-sorbitol		4.44×10^5
D-ribose		1.57×10^7

A variety of physical, spectroscopic and chemical techniques have been utilized for the studies of the formation of borate complexes. It was shown that the amount of acidification produced upon the addition of polyol is proportional to the extent of ester formation and that the monitoring of the electrical conductivity of the solution may be used to study the boron complex formation (Power and Woods, 1997, Kemp, 1956). Later, ^{1}H, ^{11}B and ^{13}C NMR spectroscopy have been increasingly applied to the measurement of solution equilibrium in borate complex formation (Lenz and Heeschen, 1961). Thereafter it was shown that complex formation between various carbohydrates and borates could be detected by signal broadening and/or chemical shift changes in the ^{13}C NMR or ^{11}B NMR spectra of the parent compounds (Gorin and Mazurek, 1973, Makkee *et al.*, 1985).

Makkee *et al.* (1985) showed that boric acid/borate reacts with mannitol generating anionic mono (1:1) and bis(1:2) diol-borate complexes. It was found that for 0.1M boric acid and 0.01M D-mannitol, the monoborate complex is formed and, even at pH values as high as 12, 90% of the boric acid remains uncomplexed. On the other hand, at mannitol concentration of 0.5 M, boric acid concentration is essentially zero at pH>8 and the bis(mannitol) ester and the monomannitol ester are present in a ratio of 9:1. Due to the reversible nature of the reactions between boric acid and the polyol, concentration

of the produced hydrogen ion should be kept low to assure a considerable extent of dichelate complex formation.

Geffen *et al.* (2006) used ^{11}B NMR spectroscopy to analyze the complexation of boron (0.1M) with mannitol as a function of pH and found that at pH 7.7 for boron: mannitol molar ratio of 1:5 and at pH 8.8 for boron: mannitol molar ratio of 1:2, complexation goes to completion.

Theoretical calculations of ionized boron species products as a function of pH using Mineql+ program revealed that the reactants concentration have a strong influence on the ionized boron species: for 32 mg/L and 7 mg/L boron content an almost complete ionization of boron species is expected at a pH values of approximately 9.5 and 10, respectively (Geffen *et al.*, 2006).

The similar anionic mono (1:1) and bis (1:2) diol-monoborate species are also formed with carbohydrates possessing 1,2-diol systems (Chapelle and Verchere, 1988).

It is interesting to note that natural boron-containing polyolcomplexes have been isolated from the phloem sap of celery (*Apium graveolens*) and extrafloral nectar of peach *(Prunus persica*) (Hu *et al.*, 1997).

Pizer *et al.* (1993) studied thermodynamic parameters of aliphatic 1,2-diol –boron complexation by variable-temperature ^{1}H and ^{11}B NMR spectroscopy. The systems studied were: $B(OH)_4^-$/1,2-ethanediol; $B(OH)_4^-$/1,2-propanediol; $C_6H_5B(OH)_3^-$/1,2-ethanediol; $CH_3B(OH)_3^-$/1,2-propanediol; and $CH_3B(OH)_3^-$/1,2-dihydroxybenzene. The first four systems have very similar stability constants and thermodynamic parameters. The reactions are all exothermic ($\Delta H° \sim$ -20 kJ/mol) and values of $\Delta S°$ are quite negative ($\Delta S° \sim$ -60 J/(mol×K)). The negative entropy is attributed primarily to a loss of configurational entropy in the ligand on complexation. This assertion was further investigated by studying the complexation of $CH_3B(OH)_3^-$with the rigid ligand 1,2-dihydroxybenzene. The $CH_3B(OH)_3^-$/1,2-dihydroxybenzene reaction is characterized by a stability constant which is greater by four orders of magnitude than those of the other systems and this increase is shown to be entirely due to a much more positive value of $\Delta S°$.

Complexation of boric acid with high molecular weight organic alcohols may results in gelation of polymeric solutions. It was shown that polyvinyl alcohol undergoes rapid gelation when contacted with boric acid solution, due to complexation of boron by hydroxyl groups located at different polymeric chains (Sinton, 1987, Kurokawa *et al.*, 1992). It was considered that the gelation can be avoided by specially designed polymers possessing boron chelating sites such as imino-bis propanediol (IBPD) groups. Poly(vinyl amino-N, N′-bis-propane diol) (GVPA) polymer containing four hydroxyl groups for boron complexation was synthesized by reaction of high molecular weight polyvinyl amine with glycidole (Sinton, 1987). During complexation three hydroxyl groups of four are involved in boron complexation while the fourth one remains unoccupied. The experiments showed that the reaction of IBPD functional polymer with boric acid in aqueous solution does not result in observed precipitation during 1 week.
Dynamic and static light scattering method was used for studying conformation of the polymer macromolecules upon changes in experimental conditions such as pH, polymer concentration and presence of boron (Zerze et al., 2013a). Effect of pH and concentration on radius of gyration (R_g) was investigated for aqueous polyvinyl amine solutions and the results are shown in figure 2.11.

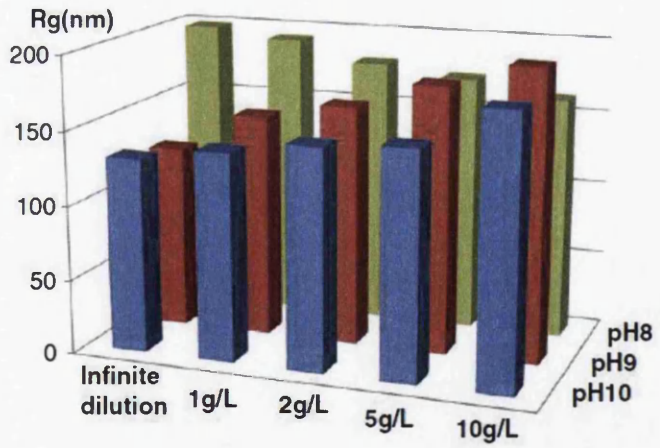

Figure 2.11 Effect of pH and polymer concentration on gyration radius of GPVA in the presence of boron at loading 0.001, (Zerze et al., 2013a)

As seen in Figure 2.11, radius of gyration of the polymer chains is proportional to polymer concentration at pH 9.0 and 10.0, whereas at pH 8.0 the proportionality becomes reverse. This controversy was explained by residual hydroxyl groups retained after complexation of boron with three of the hydroxyl groups. The residual hydroxyl groups would probably form relatively weak intermolecular boron bridging among the macromolecular chains. Thus, at low polymer concentration they may be too far from each other for the boron bridging.

Synthesized three water-soluble polyethylenimine (PEI) based polymers containing linear alkyl monool, 1,2-diol, and 1,2,3-triol groups for boron complexation. It was suggested that boron acid/borate can interact with the functionalized polymers via ion pairing and/or borate ester formation. The ultrafiltration experiments showed that the boron rejection essentially decreased when NaCl was added to the solutions. This finding indicates the presence of significant ion pairing in boron-PEI systems. To suppress the ion-pairing effect of PEI, a high chloride/boron ratio of about 10 was used. It was found that monool-PEI polymer does not form any borate esters and boron binding occurs only through the ion-pairing mechanism. For the 1,2-diol-PEI and 100 mg/L boron concentration, almost 43% of the boron was rejected when sodium sulphate was added to the solution. For 1,2,3-triol and the same boron concentration, an even larger rejection of boron (76%) was shown when NaCl was added to the solution. These results indicate that boron interacts with polymers, which contains 1,2-diol, and 1,2,3-triol groups, by means of ion pairing and also via borate ester formation.

2.4.2 Boron complexation with organic acids and enzymes

Besides alcohols and polyols, boric acid reacts with some organic acids in water with forming boron-containing complexes. For example, neutral borate complex, monomalic acid borate complex and the bis(malic acid) borate complex are formed with malic acid and its derivatives as shown in Figure 2.12 (Dembitsky *et al.*, 2002). These boron-containing compounds were also found in apple juice and wine (Matsunaga and Nagata, 1995, Lutz *et al.*, 1991).

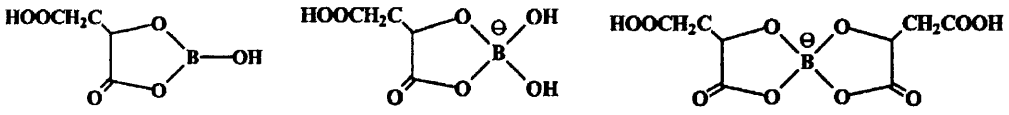

(a) (b) (c)

Figure 2.12 Chemical structures of borate complexes with maleic acid: (a) neutral borate complex,(b) monomalic acid borate complex,(c) bis(malic acid) borate complex, (Dembitsky et al., 2002)

The complexation of boric acid with salicylic acid, salicyl alcohol and bis(hydroxymethyl)phenol derivatives has been investigated using ^{11}B NMR spectroscopy by (Miyazaki *et al.*, 2008). It was shown that boric acid accepts an electron pair through the nucleophilic attack of the salicylic acid (Ac), followed by a condensation reaction, to form the 1:1 monochelate complex (Figure 2.13a). The monochelate complex then reacts with the ligand through the condensation reaction to give the 1:2 bischelate complex (Figure 2.13 b).

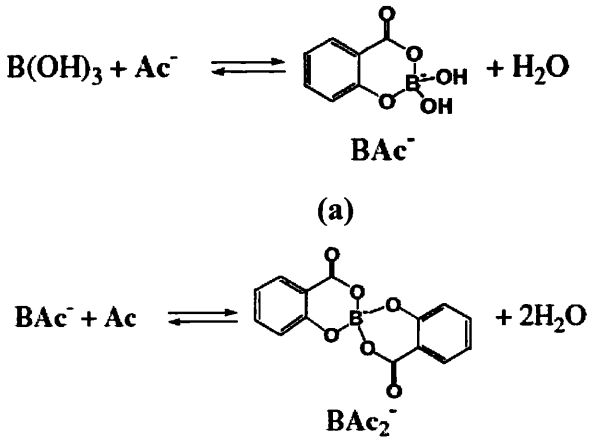

Figure 2.13 Complexation of boric acid with salicylic acid with forming of (a)1:1 monochelate complex (b) 1:2 bischelate complex, (Miyazaki et al., 2008)

The chemical shifts and formation constants of boric acid complexes with salicyl compounds are shown in Table 2.3 (Miyazaki *et al.*, 2008). As seen from data in this Table, bis(hydroxymethyl)phenol derivatives formed quite stable chelate complexes among the used salicyl compounds. It was assumed that boron complexation with bis(hydroxymethyl)phenol compounds was highly favorable from an enthalpy viewpoint (Lutz *et al.*, 1991).

Table 2.3 ^{11}B NMR chemical shifts and formation constants of boric acid complexes with salicyl derivatives (Ionic strength is 0.10 mol/L KCl, 25 °C), (Miyazaki et al., 2008)

Ligand	pK_{a1}	pK_{a2}	Complex	δ	$\log K_f$
Salicylic acid (**Ac**)	2.98*	13.61*	BAc^-	2.9	1.05 ± 0.01
			BAc_2^-	3.3	2.15 ± 0.03
Salicyl alcohol (**Ol**)	9.54		BOl^-	1.6	3.60 ± 0.01
			BOl_2^-	1.8	1.50 ± 0.06
2,6-Bis(hydroxymethyl)-*p*-cresol (**LMe**)	9.44		$BLMe^-$	1.7	4.23 ± 0.03
			$B(LMe)_2^-$	1.9	2.45 ± 0.10
3,5-Bis(hydroxymethyl)-4-hydroxybenzoic acid (**LAc**)	4.20	8.57	$BLAc^{2-}$	1.8	3.74 ± 0.04
			$B(LAc)_2^{3-}$	2.0	2.42 ± 0.09

The 3-D structures of boron acid complexes with salicyl derivatives are presented in Figure 2.14 (Miyazaki *et al.*, 2008).

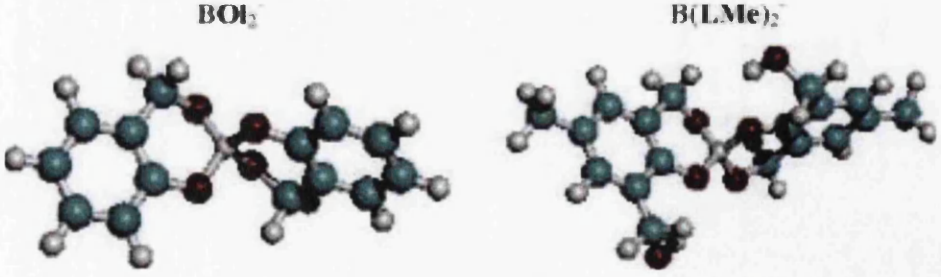

Figure 2.14 Optimized structures of the 1:2 complexes of boric acid with salicyl alcohol $(Ol)^-$ and 2,6-Bis(hydroxymethyl)-p-cresol $(LMe)^-$, (Miyazaki et al., 2008)

As seen in Figure 2.15, where the pH dependence of the equilibrium concentrations of the boron species in a large excess of 3-5- bis(hydroxymetyl) -4-hydroxybenzoil acid (LAc) is presented, at the pH range of 6–9, the negatively charged 1:2 bischelate complex prevails in the aqueous solution (Miyazaki *et al.*, 2008).

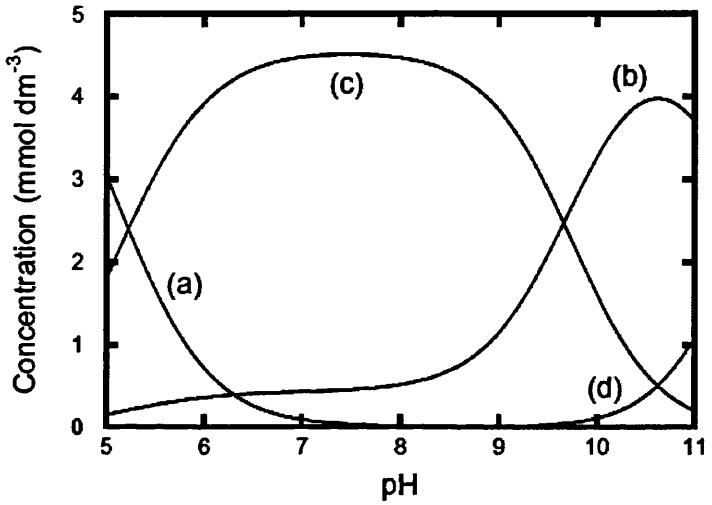

Figure 2.15 pH dependent equilibrium concentrations of boron species for a solution containing 5 mmol/L boric acid/borate and 50 mmol/L LAc. (a): $B(OH)_3$; (b): $B(LAc)^{2-}$; (c): $B(LAc)_2^{3-}$; (d): $B(OH)_4^-$, (Miyazaki et al., 2008)

A possible complexation of boron with humic substances in aqueous solutions should be also mentioned. Schmitt-Kopplin et al. (1998) postulated that $B(OH)_3$ binds to carboxylate groups (COO^-) within humic acids where it forms a transient hydrogen bonded structure. A schematic presentation of this complexation mechanism is shown in Figure 2.16 (Banasiak and Schafer, 2009).

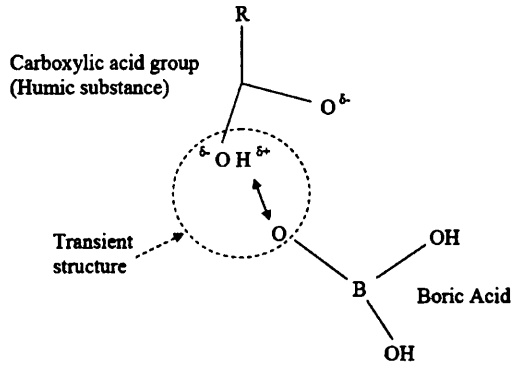

Figure 2.16 Schematic presentation of $B(OH)_3$ complexation with humic substances, (Banasiak and Schafer, 2009)

Complexation of boron compounds with different enzymes of plants, microorganisms, animals and humans, that results in stimulation, stabilization and/or inhibition of the ferments in the aqueous solutions have been also reported (Kliegel, 1980).

It was found that the enzyme urease is inhibited by boric acid (Zaborska, 1995). This inhibition is attributed to borate occupying the active site, as for example, the active site of a serine protease (Figure 2.17) (Kliegel, 1980).

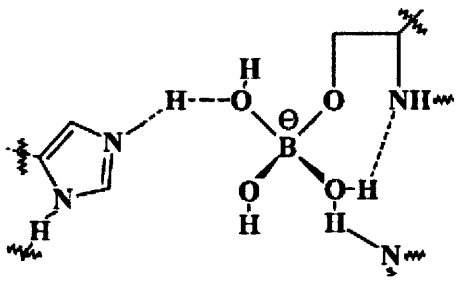

Figure 2.17 Boron inhibition of the active site of a serine protease, (Kliegel, 1980)

An another example is the complexation of borate ion with the ribose group of nicotinamide adenine dinucleotide (Kliegel, 1980). The charge separated complex is favoured over the reduced nicotinamide adenine dinucleotide and leads to inhibition of this enzyme (Figure 2.18).

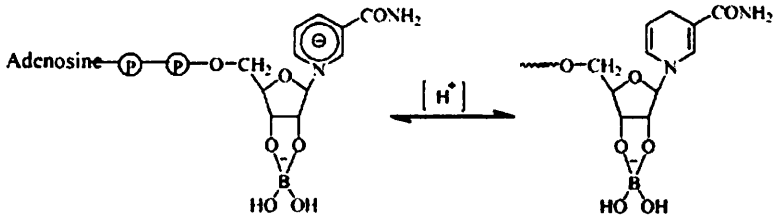

Figure 2.18 Borate inhibition of hydrogenase coenzyme by fibityl group complexing, (Kliegel, 1980)

It should be noted that boron complexation ability in the aqueous solutions is used as a basis of selective ion exchange technology for boron removal from water (Simonnot *et al.*, 2000). Commercial boron selective resins are primarily classified as macroporous crosslinked polystyrenic resins, functionalized with N-methyl-D-glucamine (NMG) group (Güler *et al.*, 2011a). The functional NMG group includes a tertiary amine and a polyol groups. The role of the tertiary amine is to neutralise the proton brought by the formation of tetra borate complex. NMG groups capture boron through a covalent attachment and formation of an internal coordination complex as shown in Figure 2.19 (Hilal *et al.*, 2011)

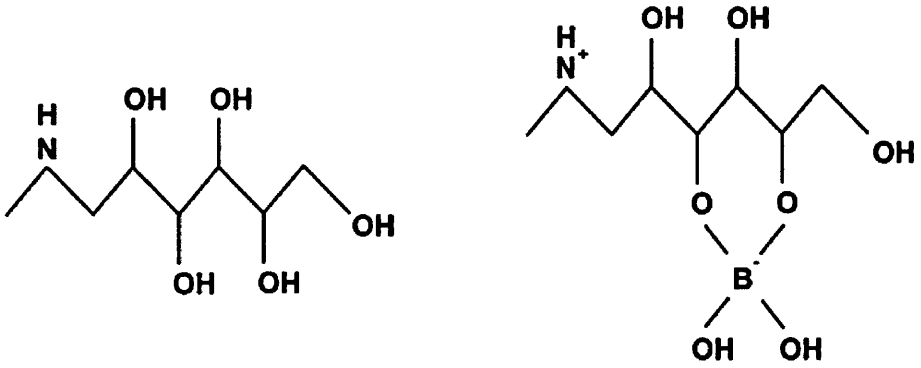

Figure 2.19 Chemical structure of NMG group (left) and monoborate complex (right), ((Hilal et al., 2011)

Boron complexation ability is used for development of novel boron selective sorbents. Recently the new sorbent NMG functionalized calix[4]arene based magnetic sporopollenin sorbent has been synthesized and used for boron removal from aqueous environment (Kamboh and Yilmaz, 2013). It was shown, that boron complexation takes place between the borate ion $B(OH)_4^-$ and hydroxyl groups of the synthesised sorbent (Figure 2.20). It was found that the highest sorption value (84%) was obtained at pH of 7.5. On the contrary, lower boron sorption above the pH 7.5 may be due to the abundance of OH^- ions in the solution, which compete with $B(OH)_4^-$ ions for the sorption sites. Also boron complexation with some specific organic reagents such as curcumin and carmine are widely used in spectrophotometric techniques for determination of boron concentration in water (Sah and Brown, 1997).

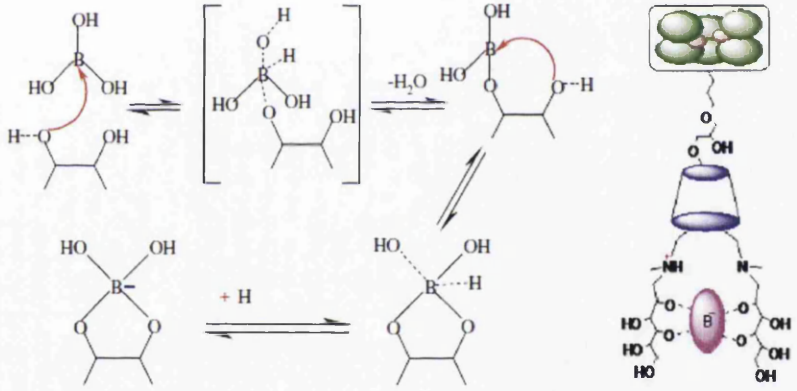

Figure 2.20 Boric acid complexation with vicinal-OH groups and boron sorption by calix[4]arene based magnetic sporopollenin, (Kamboh and Yilmaz, 2013)

2.5 Boron and drinking water regulations

Boron aquatic chemistry primarily determines the boron concentration in water, including drinking water. It should be noted that for many years boron content in drinking water was not considered as an important issue regarding a possible impact on human health. In 1958, 1963 and 1971 there was no mention of boron in the WHO International Standards for drinking water. Since boron has been shown to induce several harmful effects on animals in laboratory studies (Weir and Fisher, 1972, Lee *et al.*, 1978), provisional guidelines for boron concentration in drinking water by WHO were first introduced in 1993 as 0.3 mg/L, based on no observed adverse effect level. This guideline value was increased to 0.5 mg/L in 1998 due to a lack of financially viable boron removal technologies from water. However, extensive data from the UK and the USA on dietary boron intakes showed that the intake from air and food is lower than expected. This lead the increase in the boron intake allocated to drinking water from 10% to 40% (WHO, 2009), without approaching the tolerable boron daily limit. Accordingly to current WHO guidelines on drinking water quality, the recommended boron content in drinking water is established as 2.4 mg/L (WHO, 2011). It was noted (WHO, 2011), that short- and long-term oral exposures to boric acid or borax in laboratory animals have demonstrated that the male reproductive tract is a consistent target of toxicity. Testicular lesions have been observed in rats, mice and dogs given boric acid or borax in food or drinking-water. Developmental toxicity has been demonstrated experimentally in rats, mice and rabbits. Negative results in a large number of mutagenicity assays indicate that boric acid and borax are not genotoxic. In long-term studies in mice and rats, boric acid and borax caused no increase in tumour incidence (WHO, 2011).

As seen in Table 2.4, standards or guideline values for boron concentration in drinking water vary widely around the world, ranging from 0.5 to 5.0 mg/L. In general the maximum permissible boron concentration in drinking water is commonly determined by considering a range of factors including human and ecological health, social and natural characteristics, and cost of the available water treatment technologies. Because the influence of boron on human health has not been thoroughly elucidated, most of the existing guidelines are still provisional values that are subject to further discovery of

boron toxicity on human beings. In 2011, the World Health Organization issued a guideline document that indicates that boron content in drinking water should not exceed 2.4 mg/L (Dydo, 2013). The revised Guideline Value was incorporated into the Guidelines for Drinking-Water Quality, 4th Edition, 2011. In this context, Water Desalination Report implied that '*Although the new guideline value is based on a human health perspective, some utilities may set seawater desalination plants product water limits as low as 0.5 mg/L to reflect agricultural-related issues. These issues include boron's herbicidal effect on some plant species, which is a particular concern in areas of low rainfall*' (Kabay *et al.*, 2013a). The WHO guideline was formulated on the basis of human health consideration only. It was not related to irrigation water where old standards should still be applied (Wolska and Bryjak, 2013). It is recommended that the maximum concentration of boron for the protection of irrigated crops should not exceed the values as shown in Table 2.5 (Xu and Jiang, 2007).

Table 2.4 Regional standards for boron in drinking water

Region	Maximum boron concentration (mg/L)	References and comments
Saudi Arabia	0.5	SASO (SASO, 2000). Bottled and unbottled drinking water
United States of America (USA)	-	USEPA (USEPA, 2006). No federal regulations of boron
State of Minnesota	0.6	USEPA (USEPA, 2008)
State of New Hampshire	0.63	USEPA (USEPA, 2008)
State of Florida	0.63	USEPA (USEPA, 2008)
State of Maine	0.63	USEPA (USEPA, 2008)
State of Wisconsin	0.9	USEPA (USEPA, 2008)
State of California	1	USEPA (USEPA, 2008)
European Union (EU) including UK	1	EEA (EEA, 1998)
South Korea	1.4	Ministry of Environment (MOE, 2009), changed from 0.3 mg/L
Japan	1	NIPH (NIPH, 2006)
New Zealand	1.4	Ministry of Health (MOH, 2005)
Australia	4	NHMRC (NHMRC, 2004)
Canada	5	CDW (CDW, 2008) It has not changed since 1990
WHO recommendation	0.5	WHO (WHO, 2003); changed from 0.3 mg/L (WHO, 1993)

Table 2.5 Relative tolerance of agricultural crops to boron, (Xu and Jiang, 2007)

Maximum concentration of B in irrigation water (mg/L)	**Agricultural crops**
< 0.5	blackberry
0.5-1.0	peach, cherry, plum, grape, cowpea, onion, garlic, sweet potato, wheat, barley, sunflower, mung bean, sesame, lupin, strawberry,Jerusalem artichoke, kidney bean, lima bean
1.0-2.0	red pepper, pea, carrot, radish, potato, cucumber
2.0-4.0	lettuce, cabbage, celery, turnip, kentucky bluegrass, oat,corn, artichoke, tobacco, mustard, clover,squash, muskmelon
4.0-6.0	sorghum, tomato, alfalfa, purple vetch, parsley, red beet, sugar beet
6.0-15.0	asparagus

2.6 Technologies for boron removal from water

2.6.1 Membrane Technologies

2.6.1.1 Boron removal with reverse osmosis (RO) membranes

Many technologies are used for water desalination. Among them, seawater reverse osmosis getting the leading position (Güler *et al.*, 2011a).

Reverse Osmosis (RO) is a membrane technology used widely for seawater desalination. The term 'osmosis' is a natural phenomena that means that water flows from a low concentration solution into a high concentration solution. By applying an external pressure greater than the osmotic pressure of the solution, the water flows in the reverse direction i.e. from the high concentration solution to the low concentration one and this is the concept of RO technology.

With the recent rapid growth of reverse osmosis technology used in seawater desalination, the removal of boron becomes an essential subject and become a scientific spotlight.

Many researchers studied the ability of reverse osmosis technology in removing boron and the parameters that affect the removal of boron.

The removal of boron by RO is affected by many factors, such as, temperature, pressure, pH, feed flow rate, feed salinity or ionic strength, an initial boron concentration, and recovery ratio (Table 2.6).

Boron removal increases with increasing pH. When pH increases, $B(OH)_3$, which is a Lewis acid reacts with water resulting in the production of $B(OH)_4^-$ and H_3O^+. Especially, $B(OH)_4^-$ becomes the dominant species at pH between 9 and 10 and at pH 11 almost 100% of the boric acid exists as $B(OH)_4^-$ species (Georghiou and Pashalidis, 2007).

Applied pressure also affects the removal of boron from sea water . If the applied pressure increases, the boron rejection increases (Koseoglu *et al.*, 2008a, Sutzkover *et al.*, 2000, Prats *et al.*, 2000, Koseoglu *et al.*, 2010), The dissociation constant increases 2 units as pressure increased from 0 to 6 kbar as shown in Figure 2.3 (Güler *et al.*, 2011a).

No effect of initial boron concentration (Koseoglu *et al.*, 2008a, Cengeloglu *et al.*, 2008, Magara *et al.*, 1998) and feed flow rate on boron rejection (Koseoglu *et al.*, 2008a).
There is an inverse relationship between boron rejection and feed temperature, recovery ratio, ionic strength. It was reported that pKa of boric acid would shift about 1 unit lower at higher ionic strength (Choi and Chen, 1979, Hilal *et al.*, 2011), i.e., pKa is 9.25 at 0% salinity and would be about 8.5 at 30% salinity as shown in Fig. 2.21 (Choi and Chen, 1979).

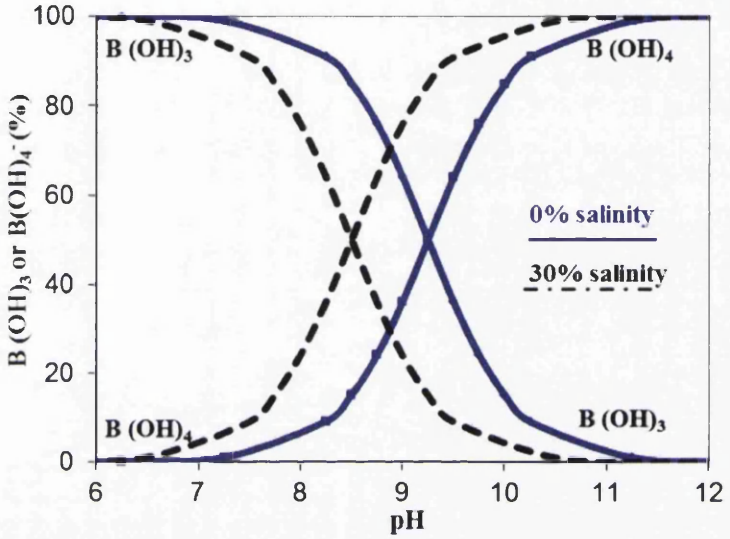

Figure 2.21: Distribution of $B(OH)_3$ and $B(OH)_4^-$ at different pH, (Choi and Chen, 1979)

Existence of biofouling will lead to a decrease in boron rejection and decline in water flux (Huertas *et al.*, 2008). *P. aeruginosa* PAO1 was used as a biofouling agent with the aim of studying the influence of biofilm formation on permeate flux and boron rejection by NF (NF-70) and RO (LFC-1) membranes. The decrease in boron rejection is attributed to biofilm growth that enhances concentration polarization of salts, including boron, near the membrane surface. The decline in permeate water flux is attributed to the increase of both hydraulic resistance (by EPS) and transmembrane osmotic pressure (by the phenomenon of biofilm-enhanced osmotic pressure).

Parameters	Boron rejection	References	Used membranes	Parameters
pH	increase	(Prats *et al.*, 2000)	Hydranautics CPA2 Toray SU-710, SUL-G10	5.5-10.5
		(Koseoglu *et al.*, 2008a)	the Torary™ UTC-80-AB and Filmtec™ SW30HR	8.2 and 10.5
		(Cengeloglu *et al.*, 2008)	SWHR, BW-30 and AG	6-11
		(Hung *et al.*, 2009)	Woongjin Chemical RE8040-SR, RE8040-SHN	6.5-10.5
		(Oo and Song, 2009)	BWRO, ESPA1, LFC1 and CPA2	6-11.5
		(Hyung and Kim, 2006)	SWRO, SR, SWC4+, SW30HR XLE, SW30HR LE, TM820, and TM820A	6.2-9.5
		(Mnif *et al.*, 2009)	RO (AG2514TF) and NF (HL2514T)	7-12
		(Koseoglu *et al.*, 2010)	SWRO: UTC-80AB and SW30HR, BWRO: UTC-70C, BW30 and TFC-HR, NF: NF90, NP030 and NF99 HF	8-10.5
		(Huertas *et al.*, 2008)	NF-70 and LFC-1	6.8-10.5
		(Dydo *et al.*, 2005)	BW-30, TW-30, NF-90 and NF-45	8.5-11
		(Magara *et al.*, 1998)	Nitto Denko NTR-70SWC, ES10-D4	5.5-11
		(Koseoglu *et al.*, 2008a)	the Torary™ UTC-80-AB and Filmtec™ SW30HR	8.2 and 10.5

Feed pressure	Increase	(Prats *et al.*, 2000)	Hydranautics CPA2 Toray SU-710, SUL-G10	15–35 bar
		(Koseoglu *et al.*, 2008a)	Toray UTC-80-AB Filmtec SW30HR	600–800 psi , No effects for SW30HR
		(Koseoglu *et al.*, 2010)	SWRO: UTC-80AB and SW30HR, BWRO: UTC-70C, BW30 and TFC-HR, NF: NF90, NP030 and NF99 HF	6.9, 15.5, 20.7, 31 ba (decrease at 31 bar)
		(Cengeloglu *et al.*, 2008)	SWHR, BW-30 and AG	15-35 bar
		(Güler *et al.*, 2011a)	SW30-2540 and XUS SW30XHR-2540	55-63 bar
		(Koseoglu *et al.*, 2008a)	the Torary™ UTC-80-AB and Filmtec™ SW30HR	41.3-55.2 bar
		(Hung *et al.*, 2009)	RE4040-SHN, SW30HRLE-4040 and TM810L	600-850 psi
Initial boron concentration	No effect	(Koseoglu *et al.*, 2008a)	Toray UTC-80-AB Filmtec SW30HR	No significant effect up to 6.6 mg/L
		(Cengeloglu *et al.*, 2008)	SWHR, BW-30 and AG	5-40 mg/L
		(Magara *et al.*, 1998)	Nitto Denko NTR-70SWC, ES10-D4	No remarkable effect lower than 35 mg/L
Feed temperature increase	decrease	(Hung *et al.*, 2009)	Woongjin Chemical RE8040-SR, RE8040-SHN	15 –35 °C and pH conditions (8.1–8.3)
		(Hyung and Kim, 2006)	SWRO, SR, SWC4+, SW30HR XLE, SW30HR LE, TM820, and TM820A	15 °C, 25 °C, 35 °C a two pH conditions (6.
		(Güler *et al.*, 2011a)	SW30-2540 and XUS SW30XHR-2540	11, 13, 14, 16 °C (pH=7-7.5)

		(Kim *et al.*, 2010)	RE4040-SHN, SW30HRLE-4040 and TM810L	5-35 °C
Feed flow rate	No effect	(Koseoglu *et al.*, 2008a)	Toray UTC-80-AB Filmtec SW30HR	Cross flow velocity 0.5–1.0 m/s
Recovery ratio increases	Decreases	(Magara *et al.*, 1998)	Nitto Denko NTR-70SWC, ES10-D4	50%, 80%, 90%
		(Mnif *et al.*, 2009)	RO (AG2514TF) and NF (HL2514T)	10%-70%
		(Dydo *et al.*, 2005)	BW-30, TW-30, NF-90 and NF-45	5%-75%
Ionic strength increase	Decrease	(Oo and Song, 2009)	BWRO, ESPA1, LFC1 and CPA2	0-15000 mg/L NaCl
		(Kim *et al.*, 2010)	RE4040-SHN, SW30HRLE-4040 and TM810L	30000 - 45000 mg/L
Biofouling	decrease	(Huertas *et al.*, 2008)	NF-70 and LFC-1	Aeruginosa PAO1 (pH=8.5)

Dominguez-Tagle *et al.* (2011) studied the boron removal efficiency of 14 commercial RO membranes at pH 8, temperature 30°C, recovery ratio 40% and the boron concentration was 5 mg/L. The results are summarized in Table 2.7.

Table 2.7 Boron removal efficiency of 14 commercial RO membranes, (Dominguez-Tagle et al., 2011)

Manufacturer	Model	Boron rejection (%)
SAHEAN Industries Inc.	RE8040-SR400	68
	RE8040-SHN400	83
Toray Industries Inc	TM820A-400	82
	TM820C-400	81
	TM820E-400	76
	TM820F-400	68
The DOW Chemical Company	SW30XHR-400i	84
	SW30HRLE-400	79
	SW30XLE-400i	69
	SW30ULE-400i	67
Hydranautics	SWC4+	89
	SWC4+B	92
	SWC5	81
	SWC6	72

Yavuz *et al.* (2013a) evaluated the effect of applied pressure and membrane configuration on boron removal from geothermal water using two spiral wound FilmTech BW30-2540 elements. The maximum boron rejection was 47% and 49% at 12 and 15 bars respectively using a single membrane mode of operation. When the pH of geothermal water was increased from 8 to 10.5, boron rejection obtained was 94.5–95% for both single and double membrane configurations at 12 bar of operating pressure while the average permeate flux and water recovery values decreased.

2.6.1.2 Boron removal with ion-exchange membranes and membrane distillation

Donnan dialysis is a useful membrane process used for recovery of valuable ions and removal of undesirable ions from water and wastewater (Ayyildiz and Kara, 2005, Kir and Alkan, 2006). In the Donnan dialysis process, an ion exchange membrane (anion-exchange or cation exchange one) separates two solutions: the feed (containing anions or cations that should be removed) and the receiver (electrolyte with relatively high concentration of the neutral driving anion or cation). The chemical potential gradient of the components on both sides of the membrane causes the flow of the driving counter ion from the receiver to the feed, and resulting electric potential evokes the transport of counter ions in the opposite direction (Rozanska *et al.*, 2006).

Ayyildiz and Kara (2005) applied Donnan dialysis method to remove boron from aqueous solution using three anion exchange membranes (Neosepta- AHA, AFN and AMH). The results showed that the transport of boron increased with increasing pH value to 9.5 and then decrease due to the formation of $B(OH)_4^-$ in the solution which also led to an increase in transport of boron. The transport of boron with respect of different receiver composition was affected by the increasing hydrated radius of ions as follow: NaCl>$NaHCO_3$>Na_2SO_4. It is observed that the most of the boron transport occurred when HCO_3^- ion was in both the feed and receiver solution because its rate was lower than $Cl^-$and SO_4^- ions. The AFN membrane was found to be the most effective in boron recovery followed by AMH one. Increasing the boron concentration in the feed will lead to increase the flux increase proportionally.

The mechanism of the diffusive boron transfer through the anion exchange AMX (Neosepta) membrane was evaluated by multiple regression methods (Turek *et al.*, 2009). It was found that Donnan dialysis (OH^--$B(OH)_4^-$ exchange) phenomena dominate over simple boric acid diffusion dialysis. Thus to enhance boron fluxes as well as its removal efficiency, the process should be carried out at as high as possible receiving solution pH while the feed solution pH should be maintained low.

Plasma modified and unmodified ion exchange membranes were used by Kir *et al.* (2011) for boron removal from aqueous solution at boron concentration ranges from 0.1-0.001 M by Donnan dialysis. When diluting the feed phase from 0.1 to 0.001 M, the flux of boron decreased proportionally (Ayyildiz and Kara, 2005). At theses concentrations,

the removal of boron and flux are higher in the plasma modified membrane than the unmodified one. The increase of boron transport and boron flux is due to the fact that nitrogen plasma treatment increases the surface wettability and hydrophilicity of the membrane and improves the flux (Kir and Alkan, 2006, Nunes and Peinemann, 2006, Bryjak *et al.*, 2002).

Direct contact membrane distillation (DCMD) experiments were carried out for boron removal, in which the feed and the distillate are directly separated by the hydrophobic membrane using self-prepared polyvinylidene fluoride (PVDF) hollow fiber membranes (Hou *et al.*, 2010). The feed pH, Temperature and boron concentration had no significant influence on the permeate flux and boron rejection.

2.6.2 Adsorption methods

The application of low cost and easily available materials for the treatment of wastewater and seawater has been investigated during recent years (Kavak, 2009). Adsorption is one of the useful and economical techniques at low pollutant concentration (Ozturk and Kavak, 2005).

2.6.2.1 Boron removal with activated carbon

Activated carbon is currently the most widely used for boron removal from water. Rajaković and Ristić (1996) found the amount of boron adsorbed on activated carbon around 1.59 mg/g. The impregnation of activated carbon with $CaCl_2$ and $BaCl_2$ decreased the amount of boron adsorbed to 1.05 and 0.59 for Ba^{2+} and Ca^{2+} respectively because the presence of Ba^{2+} and Ca^{2+} reduced the number of available adsorption sites while Kluczka et al. (2007) found the impregnation with calcium chloride will increase the adsorption capacity and precipitated sparingly soluble calcium borate.. The impregnation of activated carbon with citric acid (Rajaković and Ristić, 1996, Kluczka *et al.*, 2007) , tartaric acid (Kluczka *et al.*, 2007, Rajaković and Ristić, 1996), salicyclic acid (Celik *et al.*, 2008) , orthophosphoric(V) acid, glucose (Kluczka *et al.*, 2007) and mannitol (Kluczka *et al.*, 2007) will lead to the increase the amount of boron adsorbed. Köse *et al.* (2011) prepared activated carbon from olive bagasse by physical activation. The maximum boron removal was obtained at initial pH (5.5) of the solution. The adsorption of boron decreased as temperature increased while it increased as the initial

boron concentration increased. The amount of boron adsorbed increased from 0.05 to 1.5 mg/g of adsorbent as the initial boron concentration increased from 40 to 100 mg/L.

Recognizing the high cost of activated carbon, many investigators have studied the feasibility of cheap, commercially available materials as its possible replacements (Ozturk and Kavak, 2005).

Several investigations are reported in the literature on the utilization of fly ash for adsorption of individual pollutants in an aqueous solution or flue gas. The results are encouraging for the removal of heavy metals and organics from industrial wastewater (Ahmaruzzaman, 2010).

Fly ash with particle size between 250 and 400 μm was obtained from a textile plant where Soma coals were used (Ozturk and Kavak, 2005). These surfaces are suitable for adsorption of borate ions. So, the maximum uptake of boron takes place at pH 2. The boron extraction increases with decreasing pH from 12 to 6 (Hollis *et al.*, 1988). The amount of boron adsorbed increased with agitation time and decreased with increasing temperature which means an exothermic nature of the adsorption process. The increase in adsorbent dosage increased the removal of boron due to the increase in surface area. The adsorption yield decreased by increasing boron concentration. The existence of Na_2SO_4 and $CaCl_2$ will decrease the boron adsorption by 3-4 %.

Coal and fly ash were used by Polat *et al.* (2004) as adsorbents of boron. The effect of material type on boron removal from seawater is presented in Figure 2.22. The removal varies from 60% to 98% for coal and ash samples which almost the same of synthetic ion exchange resin while the removal only about 20% for zeolite. The removal increase with increasing the reaction time and reduce liquid/solid ratio for Yenikoy coal and South African ash samples and not for Yenikoy ash.

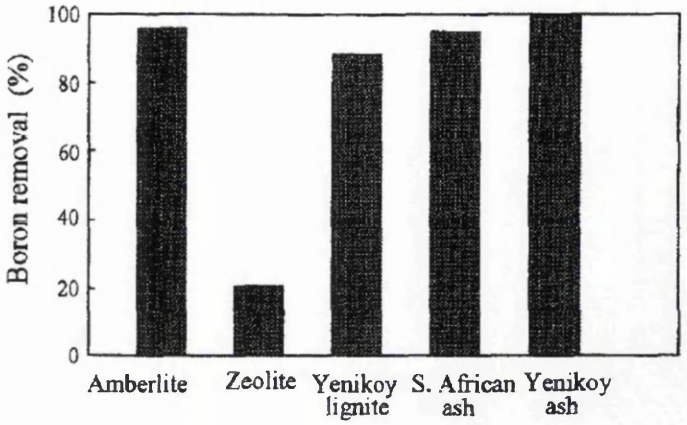

Figure 2.22 The effect of material type on boron removal from seawater, (Polat et al., 2004)

The fly ash agglomerates with particle size (1.0-1.6 mm) was used in batch and column experiments (Polowczyk *et al.*, 2013). The effects of pH, temperature, adsorbent dosage, initial boron concentration and contact time on the adsorption were investigated. The maximum adsorption capacity was found as 6.9 mg/g, while the maximum removal achieved was about 90%.

2.6.2.2 Boron removal with mineral adsorbents

Mineral adsorbents include siliceous materials, clay and natural zeolites have been used to remove boron from geothermal water, wastewater and seawater.

Red mud is a widely available fine-grained mixture of oxides and hydroxides, capable of removing several contaminants including phosphate, fluoride, cadmium, lead, copper, nitrate, arsenic, phenol and dye. The adsorption of boron from aqueous solution containing 43mg boron/L using the neutralized red mud was studied by Cengeloglu *et al.* (2007) in batch equilibration technique. Because of the repulsive forces between $B(OH)_4^-$ and the negative charged surface of the red mud at pH above 8, the effect of pH experiments were done at pH 2-7 and there was a fluctuation of the amount of boron adsorbed. The removal of boron increased with increasing the amount of the red mud due to the increase in surface area of the red mud.

Layered double hydroxides (LDHs) or hydrotalcite (HT)-like compounds have the chemical formula as written: $[M^{2+}_{1-x}M^{3+}_{x}(OH)_2](A^{n-})_{x/n}.mH_2O$, Where M^{2+} is a divalent cation (Mg^{2+}, Co^{2+}, Ni^{2+}, Zn^{2+}, Mn^{2+}, Cd^{2+}), M^{3+} is a trivalent cation (Al^{3+}, Fe^{3+}, Cr^{3+}, Ga^{3+}), A^{n-} is an anion and x is defined as the $M^{3+}/M^{2+} + M^{3+}$.

The adsorption of boron from aqueous solution by LDHs with different metal ions (Mg-Al and Mg-Fe) was investigated by Ferreira *et al.* (2006). The adsorption equilibrium was reached after 120 min. the adsorption was not effected by increasing pH because of the high buffering capacity of the LDHs while the adsorption increased with increasing adsorption quantity,

Hydrotalcite (HT) compound, Mg-Al-NO_3-layered double hydroxide (LDH) was prepared by Ay *et al.* (2007) by using co-precipitation method. The effect of adsorbent dose was investigated by varying the amount of HT and calcined-HT (CA-HT) and both adsorbent have a maximum adsorption (>95%) at 0.6 g of HT and CA-HT and the maximum adsorption capacity was 20 mg of boron per gram of adsorbent.

Vermiculite sample consists of Si, Al, Mg, O, K and traces of Fe and Ca as the constitutive elements was modified by thermal shock at 700°C, chemical exfoliation at 80°C in the presence of H_2O_2 and ultrasonic treatments at 20 kHz in the presence of H_2O or H_2O_2 and its ability for boron adsorption was observed by Kehal *et al.* (2010). The adsorption of boron depends of the method of modification. The boron uptake increased from 0.015 mmol/g for raw Vermiculite to 0.151 mmol/g for modified one by ultrasound in the presence of H_2O_2 for 1 h.

Natural zeolite was modified by hexadecyl trimethyl ammonium bromide (HDTMA-Br) and the effect of pH; adsorbent dosage and initial solution concentration in a batch system were investigated (Demirçivi and Nasün-Saygili, 2010). The boron removal efficiency was studied at pH values of 2-12 and initial boron concentration of 10 mg/L. The highest value of boron removed was observed at pH 8.5. The effect of adsorbent amount was examined and changed from 0.1 to 10 g while the initial boron concentration and pH were kept constant at 10 mg/L and 8.5 respectively. The boron removal increased with increasing the amount of adsorbent and the removal efficiency varied from 3 to 44 %. The adsorption of boron on HDTMA-zeolite increased when the initial boron concentration increased from 10 to 40 mg/L. The adsorption isotherms of batch system were analysed by Langmuir and Freundlich isotherm models and it was

shown that Freundlich isotherm represents the adsorption very well. The effect of bed height, flow rate and initial boron concentration were examined in column experiments. Boron removal increased with increasing bed height and decreased with increasing flow rate and initial boron concentration.

Alunite which has a composition of 43.47% SiO_2, 27.12% Al_2O_3, 23.50% SO_3 and 5.50% K_2O was calcined at temperatures between 100 and 900°C and used by Kavak (2009) in batch adsorption experiments for boron removal from aqueous solution containing 10 mg boron/l. Boron adsorption increased with increasing pH and adsorbent dosage and decreased with increasing temperature. The optimum conditions were found as pH 10, temperature =25°C and the mass of the adsorbent = 1g/25ml solution. Maximum adsorbent capacity was found as 3.39 mg/g.

Seyhan *et al.* (2007) used two kinds of iron-rich natural clays, CB1 (48.21% SiO_2, 13.10% Al_2O_3, 9.97% Fe_2O_3) and CB2 (44.55% SiO_2, 11.91% Al_2O_3, 12.12% Fe_2O_3) for boron sorption from aqueous media. The optimum conditions when using these clays found by factorial design were found to be pH 10, 45°C, 0.25 g of clay and 20 ml of sample volume. The equilibrium state was reached in 180 min with a boron sorption percentage of 80% for CB1 and 30% for CB2.

Karahan *et al.* (2006) modified clays to increase their adsorption capacities of boron from aqueous solution. Bentonite, sepiolite and illite clays were modified by nonylammonium chloride to produce nonylammonium bentonite, nonylammonium sepiolite and nonylammonium illite. The results showed the modification of bentonite and illite with nonylammonium chloride will increase the adsorption of boron in aqueous solution at pH 8-10 and high ionic strength. The data were will described by Freundlich and Dubinin-Radushkevich adsorption isotherm.

Adsorption of boron on Siral 5 (4.5% SiO_2 , 95.5% Al_2O_3), Siral 40 (39.7% SiO_2, 60.3% Al_2O_3) and Siral 80 (78.3% SiO_2, 21.7% Al_2O_3) was studied in a batch system (Karahan *et al.*, 2006). The results showed that as the boron equilibrium concentration in solution and temperature increased the amount adsorbed increased. The adsorption process can be described with Freundlich equation and Dubinin-Radushkevich equation. The results showed that the Siral samples can be used for boron removal from aqueous solution.

$Ni(OH)_2$, $Co(OH)_2$, $Al(OH)_3$, $Fe(OH)_3$, $Zn(OH)_2$ and $Mg(OH)_2$ were applied in adsorption/co-precipitation stage in adsorption/co-precipitation-reverse system to remove boron from high boron-containing waters (Turek *et al.*, 2007). Nickel hydroxide, $Ni(OH)_2$, was the most efficient in boron removal since it removed 93 to 70% when boron concentration increases from 10 to 300 mg/L. The efficiencies of the other metal hydroxides were in the order: Al-Co-Fe-Zn≈Mg. For all the metal hydroxides (except Co and Zn), the percentage of boron removed decreases as the initial boron content increased, while for all the metal hydroxide, the boron uptake increases with the initial boron content increase. Due to the toxicity of theses metal hydroxide and the additional clean-up process required to match the requirements of the industrial wastes discharged to the environment, iron and aluminium were found to suitable for boron removal in adsorption/co-precipitation stage. Percentage of boron removed increased and the boron uptake decreased as the concentrations of Al^{3+} and Fe^{3+} increased. To avoid a large precipitation load which leads to high RO feed water salinity, the adsorption/co-precipitation step should be operated at high boron content.

Remy *et al.* (2005) investigated the effects of temperature, lime concentration and temperature on the removal of boron from wastewater by calcium hydroxide. Experimental results showed that under optimum conditions (50g/l of powdered calcium hydroxide, a temperature of 90°C and process time of 2 h) the concentration of boron reduced from 700 mg/L to 50 mg/L. XRD analysis showed that $CaB_3O_3(OH)_5.4H_2O$, which is a borate mineral called inyoite, occurred between Ca(OH)2 and borate ions (Yilmaz *et al.*, 2012):

$$Ca^{2+}_{(aq)} + 3H_3BO_{3(aq)} + 2OH^- + H_2O \rightarrow CaB_3O_3(OH)_{5(s)} + 4H_2O \qquad 2.15$$

Cerium oxide was used as granule and powdered (200-275 mesh) at two levels of pH (6.18 and 10) and two temperature values 20 and 40°C for boron removal from aqueous solution (Öztürk and Kavak, 2008). 2^3 full factorial design (3 parameters effect performance and two levels of these parameters) was applied in order to examine the main factors and their interactions for the boron removal by adsorption. Maximum boron removal was obtained at original pH (6.18) and 40°C by powdered cerium oxide and the adsorbed boron amount was 21 g/L.

The adsorption of boric acid and borate on hydrous ferric oxide (HFO) was investigated by Peak *et al.* (2003) using Attenuated Total Reflectance Fourier transform Infrared (ATR-FTIR) spectroscopy. The adsorption of boric acid and borate on hydrous ferric oxide can happen via physical adsorption on outer sphere ligand exchange on inner sphere reactions. Both trigonal (boric acid) and tetrahedral (borate) boron are complexed on the HFO surface.

The adsorption of boron on iron-oxide (FeO(OH)) has been investigated in aqueous solutions as a function of pH, ionic strength, temperature, boron concentration and amount of the adsorbent (Demetriou and Pashalidis, 2012). The adsorption is based on inner-sphere complexation and is an exothermic reaction . The optimum pH for boron removal by sorption on iron-oxide was 8 and the maximum removal capacity was found to be 0.03 mol/kg.

del Mar de la Fuente García-Soto and Camacho (2006) used magnesium oxide to remove boron from aqueous solution containing 500 mgB/L. The optimum pH value was found between 9.5 and 10.5. The removal increases with increasing temperature and the quality of reagent added.

Pure Fe_3O_4 particles and two kinds of composites of Fe_3O_4 particles derived from Fe_3O_4 and bis(trimethoxysilylpropyl) amine (TSPA), and from $Fe_3O_4$and a flocculating agent 1010f (a copolymer of acrylamide, sodium acrylate, and [2-(acryloyloxy)ethyl]trimethylammonium chloride) were used to adsorb boron from aqueous solution (Liu *et al.*, 2009b). Fe_3O_4–TSPA particles presented the highest adsorption capacity, whereas the pure Fe_3O_4 particles showed the lowest capacity. For all particles, amount of boron adsorbed decreased with the initial pH in the order of 6.0 > 2.2 > 11.7, and decreased with the increase in ionic strength.

Kluczka *et al.* (2013) prepared a new adsorbent based on natural clinoptilolite and amorphous zirconium dioxide (ZrO_2) for the removal of boron from fresh water. It was found that the removal of boron increased while the adsorbent dose increased and the temperature decreased at an optimum pH *(*pH = 8*)* and a contact time of 30 min. the maximum adsorption capacity for zirconium oxide was found 0.428 mg/L at pH 6 and temperature 20 °C.

Three samples of aluminum-based water treatment residuals (Al-WTR1, Al-WTR2, and Al-WTR3) which are mainly composed of Al_2O_3, Fe_2O_3, and SiO_2 were applied to remove boron from a solution containing 200 mgB/L (Irawan *et al.*, 2011). The batch maximum adsorption capacities were found as 0.980, 0.700, and 0.190 mg/g using Al-WTR1, Al-WTR2, and Al-WTR3, respectively, at pH value of 8.3±0.2.

Bouguerra *et al.* (2008) used activated alumina to evaluate the potential of activated alumina for the removal of boron from aqueous solution containing 5 mgB/l and 50 mgB/l. Boron adsorbed increase with stirring time and attains equilibrium at about 30 minutes. The amount of boron adsorbed increased with increasing boron concentration. Maximum adsorption was achieved in the pH range of 8 and 8.5 for both concentrations (5 and 50 mg/L).The amount of removed boron increased with increasing adsorbent dose due to the increase in the total available surface area of the adsorbent particles. Adsorption of boron decreased significantly by the addition of other anions like nitrate, fluoride, hydrogen, carbonate and silica. The maximum adsorption capacity for activated alumina was 2 mg/g at initial pH 6 and temperature 20 °C.

2.6.2.3 Boron removal by biosorption

Biosorption is an alternative technology in water treatment based on the property of different kinds of inactive and dead biomass to bind and concentrate hazardous ions from dilute aqueous solutions (Liu *et al.*, 2007). Figure 2.23 schematically summarizes alternative process pathways to produce biosorbent materials which are effective and durable in repeated long-term applications aimed mainly at removing metals from large quantities of toxic industrial metal bearing effluents (Vieira and Volesky, 2010).

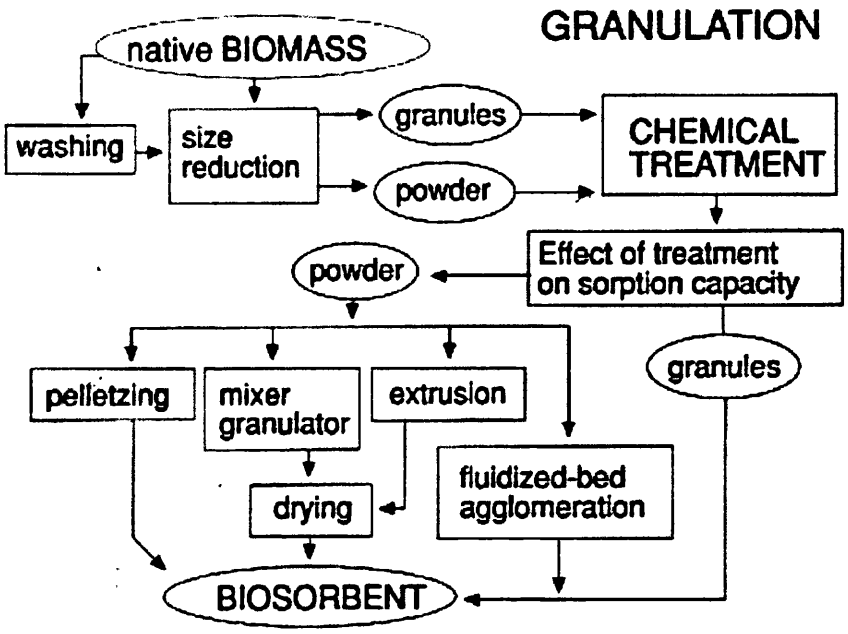

Figure 2.24 Schematic diagram of processing different types of microbial biomass into usable biosorption materials, (Vieira and Volesky, 2010)

Cotton cellulose was used as a biosorbent for boron removal. With high pH, there was lower removal boron and the maximum uptake of boron was 11.3 mg/g at pH 7. The boron removal increased with boron concentration. The boron adsorption into cotton is described by linear Freundlich isotherm.

The adsorption of boron on activated sludge was studied and its adsorption capacity with other adsorbents was found in the order: activated alumina > activated carbon > activated sludge > soil (Fujita *et al.*, 2005).

2.6.3 Electrochemical methods

Electrochemical methods such as electrocoagulation and electrochemical separation become interesting processes for water treatment since it is a simple and efficient method where the flocculating agent is generated by electro-oxidation of a sacrificial anode, generally made of iron or aluminum (Yilmaz *et al.*, 2005a).

Electrocoagulation is a process consist several steps such as electrolytic reactions at electrode surfaces, formation of coagulants in aqueous phase, adsorption of soluble pollutants on coagulants which are removed by sedimentation or flotation (Yilmaz *et al.*, 2005a).

Aluminium electrode is used and has the main reaction (Picard *et al.*, 2000):

Anode: $$Al_{(s)} \rightarrow Al^{3+}_{(aq)} + 3e^{-} \quad 2.16$$

Cathode: $$3H_2O + 3e^{-} \rightarrow 3/2\ H_{2\,(g)} + 3OH^{-}_{(aq)} \quad 2.17$$

At high pH

$$2Al_{(s)} + 6H_2O + 2OH^{-}_{(aq)} \rightarrow 2Al(OH)^{-}_{4\,(aq)} + 3H_{2(g)} \quad 2.18$$

Al^{3+} and OH^{-} for equations 2.16 and 2.17 react to form various monomeric species such as : $Al(OH)^{2+}$, $Al(OH)_2^{+}$, $Al_2(OH)_2^{2+}$, $Al(OH)_4^{-}$, and polymeric species such as $Al_6(OH)_{15}^{3+}$, $Al_7(OH)_{17}^{4+}$, $Al_8(OH)_{20}^{4+}$, $Al_{13}O_4(OH)_{24}^{7+}$, $Al_{13}(OH)_{34}^{5+}$, which transform finally into $Al(OH)_3$ according to the following reaction :

$$Al^{3+}_{(aq)} + 3H_2O \leftrightarrow Al(OH)_{3(s)} + 3H^{+}_{(aq)} \quad 2.19$$

Electrocoagulation method using aluminium electrode for boron removal from wastewater was investigated by (Yilmaz *et al.*, 2005a). Boron removal increased with increasing pH up to 8 then it decreased. In the case of increasing current density, boron removal increased due to the increase in Al^{3+} passed to solution at higher density which leads to increasing of $Al(OH)_3$ formation. Boron removal efficiency decreased with increasing boron concentration and this result can be explained as follows: the amount of Al^{3+} passed to the solution at the same current density was insufficient for solution with high boron concentration. Same results were obtained by Yilmaz *et al.* (2008) and Bektaş *et al.* (2004) who examined different supporting electrolytes (15 mM NaCl, 15 mM KCl, 10 mM Na_2SO_4 and 10 mM $CaCl_2$) and the results show high boron removal with all these electrolytes and the highest value was obtained with 10mM $CaCl_2$.

2.6.4 Ion Exchange Method

Boron-specific ion exchange resins were developed in the 1970s in the ceramic industry to remove borate from magnesium brine (Jacob, 2007). Resins used today are the same and they have a macroporous polystyrene matrix on which N-methyl glucamine functional groups are attached. The general mechanism for boron adsorption by glucamine-type resins is given in Figure 2.24 (Baek *et al.*, 2007):

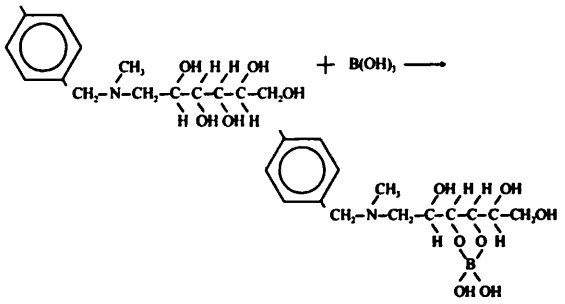

Figure 2.25 The general mechanism for boron adsorption by glucamine-type resins, (Jacob, 2007)

In the environment, boron is mostly in borate or boric acid form. In water, these two species are in chemical equilibrium:

$$B(OH)_3 + H_2O \leftrightarrow B(OH)_4^- + H^+ \qquad pK_a = 9.14 \qquad 2.20$$

According to this reaction, borate-to-boric acid ratio is higher at higher pH values. In addition, there is a difference between the complexation mechanisms of these two species: boric acid makes ester bond with hydroxyl groups due to valence orbital on boron while borate anion can make ionic interaction with polyelectrolytes. However, borate-to-boric acid ratio in the original solution may not be important for bonding to hydroxyl groups due to a possible shift to boric acid from borate anion during complexation. The important thing concerning the effect of pH on complexation is most probably the optimum conformation of the polymer molecules (Zerze *et al.*, 2013a).

2.6.4.1 Commercial Resins

Boncukcuoğlu *et al.* (2004) and Yilmaz *et al.* (2005b) used Amberlite IRA 743 as boron specific resin. The ratio of resin/boron solution, boron concentration, stirring speed and temperature were selected as experimental parameters. The removal of boron from wastewater increased with increasing temperature (Baek *et al.*, 2007) and ratio of resin/solution (Pelin Demirçivi, 2008, Yilmaz *et al.*, 2005b). The removal rate of boron increases with decreasing the feed boron concentration (Baek *et al.*, 2007, Pelin

Demirçivi, 2008) while the was no effect of stirring speed on boron removal , but the removal decreased with increasing the flow rate (Yilmaz *et al.*, 2005b) . High boron removal was achieved at pH 8.5-10 (Pelin Demirçivi, 2008, Baek *et al.*, 2007, Yoshimura *et al.*, 1998).

Kim *et al.* (2010) used two different columns containing ion exchange resin Amberlite IRA743 using the permeates of RE4040-SHN, SW30HRLE-4040 and TM810L membranes with concentration of boron in between 0.7 and 0.9 mg/L. The permeate from these membranes was passed through and the removal was efficient with 98% rejection and 1.8 mgB/ml resin sorption capacity.

Badruk and Kabay (2003) used the chelating resin Diaion CRB 02 for boron removal from 0.01M H_3BO_3 solution and Kizildere geothermal brine (30 mg B/L). The largest removal was 49% for 0.01M H_3BO_3 and 98% for Kizildere geothermal brine. The breakthrough capacity decreased with increasing in speed volume (SV). 10 cycles of sorption-washing-elution-regeneration-washing in the geothermal field was performed and the results showed a small decrease in the capacity between cycles 2-7 and reached a plateau in cycles 7 (Kabay *et al.*, 2004a, Kabay *et al.*, 2004b).

The column performance of two selective resins (Diaion CRB 02 and Dowex XUS 43594) on boron removal at concentration 5mg/L was investigated by Kabay *et al.* (2007). The increase in resins amount will lead to improve boron removal. By reduction the particle size of both resins from 0.355-0.500 μm to 45-75 μm, the optimum resin amount decreased from 2g/L to 1g/L. Increasing the speed volume (SV) will decrease the breakthrough capacities of both resins. Dowex resin has larger breakthrough capacity (6.69mg/g) than Diaion resin (6.27 mg/g).

Kabaya *et al.* (2008) evaluated Diaion CRB02 and Dowex (XUS 43594.00) from aqueous solution containing boron concentration similar to the typical permeate concentration (1.5-1.6 mg/L). Equilibrium half-time can be estimated between 30-45 min for Dowex resin and 20-30 min for Diaion. The sorption equilibrium was reached after 180 min when 93.5% of boron was removed by Diaion resin and 240 min when 90.8% of boron was removed with Dowex resin.

Yılmaz İpek *et al.* (2013) evaluated the performance of boron selective ion exchange resins Diaion CRB 02 and Dowex (XUS 43594.00) in a fixed-bed column for boron

removal from geothermal water containing 8.5-13 mgB/L by applying different operating parameters such as flow rate and pH. The sorption kinetics data of these resins can be fitted using pseudo-second-order mechanism compared with pseudo-first-order equation.

A comparative study between four resins was performed to obtain the optimum amount of resin for boron removal from geothermal wastewater which contains 18-20 mg B/l (Kabay *et al.*, 2004a). The optimum amount of CRB 01, CRB 02, Purolite S 108 (1) and Purolite S 108 (2) to remove 90% of boron was 3g-resin/l-wastewater. Breakthrough capacity of Purolite S 108 (1) was faster than Diaion CRB 01 and that for Diaion CRB 02 was better than Purolite S 108 (2).

A strong basic anion exchange resin, Dowex 2X8, was applied for boron removal from aqueous solution containing 600 mgB/L (Bektaş and Öztürk, 2004). The maximum boron removal was obtained at pH 9 (Öztürk and Kavak, 2008, Öztürk and Köse, 2008) due to presence of $B(OH)_4^-$ and the equilibrium was obtained of 15 min of sorption time. The sorption process is an exothermic, so as the temperature increases the sorption of boron decreases. The maximum adsorption of the resin was found to be 22.27 mg B/g resin. Due to the increase in exchangeable ions of the resin, the increase in resin dosage will lead to increase in boron removal and the amount of boron adsorbed increases when initial boron concentration increases (Öztürk and Köse, 2008). They applied Sorption-elution-washing-regeneration-washing cycles the resin to check the reusability of the resin. After three cycles using 0.5 HCl solution, the total capacity of the resin remained the almost the same.

Yan *et al.* (2008) used Ion exchange resin, XSC-800 for boron removal form refined brine which was used for the production of low-boron lithium salts. The effect of flow rate, boron concentration, temperature, pH, height/diameter (H/D) of the column, anion concentration, stirring speed and diameter of the resin particles were studied. The results indicated that, boron removal increased with increasing temperature, pH, H/D and decreased with increasing flow rate, boron concentration, chloride anion concentration and diameter of resin particles. There was no effect of stirring speed and the regeneration of the resin on the removal of boron.

The boron adsorption by XSC-700 resin increases with increasing boron concentration, temperature and increases with decreasing resin/brine ratio, while the stirring speed has no significant effect on the boron adsorption (Xiao *et al.*, 2012).

A relationship between an amount of boron bounded with an ion-exchange resin and the boron concentration remaining in solution is described by an appropriate isotherm (Cengeloglu *et al.*, 2007). The analysis of the isotherm data is important to develop an equation which accurately represents the results and which could be used for design purposes. Several adsorption isotherm models have been used to describe the experimental boron adsorption data (Kavak, 2009).

The adsorption of boric acid on a strong-base anion-exchange resin, Amberlite IRN-78LC at different temperatures and concentration was investigated (Na and Lee, 1993).The amount of boric acid adsorbed increased as the temperature increased from 10 to 60°C and with concentration ranging from 0-1500 mg/L. The adsorption expression was proposed as :

$$q = q^{\infty}(K_l C/K_c C + K_0) \qquad 2.21$$

Where q^{∞} is the adsorption capacity of the resin, q is the amount of boron adsorbed, C is the boron concentration in the solution, K_l is Langmuir type adsorption of boric acid at low concentration, K_c can be interpreted as a so-called polymerization effect representing that borate ions with less boron atoms in the resin turn into polyborate ions with more boron atoms as the boron concentration in solution increases, and K_0 is the initial adsorption take place at low boron concentration.

Şahin (2002) studied the behaviour of the boron selective resin Amberlite XE 243 which was ground to 55-100 mesh size. The adsorption capacity of the resin was found to be 5.2 mgB/ml. The experimental results were converted to dimensionless variables by taking the ratios of volume and concentrations at different initial concentration for different boron flow rates:

$$C/C_0 = 0.05(V_1/V_2)^{2.72} \qquad 2.22$$

Where C and C_0 are the boron concentration at any time and initial time respectively.

Hanay *et al.* (2003) studied the effect of temperature, ratio of solid/liquid and stirring speed on boron removal from geothermal water using Amberlite IRA743.

Three types of adsorbent, CRB 03, CRB 05 and Chelest Fiber, were investigated by Nishihama *et al.* (2013). Chelest Fiber has a higher adsorption rate for boron than CRB 03 and CRB 05 and all of the adsorbents follow Langmuir kinetics with the maximum amounts adsorbed were 1.18 (CRB 05)≈1.15 (Chelest Fiber) >0.989 mmol/g (CRB 03), respectively.

2.6.4.2 Synthetic Resins

As the performance of the resins depends on its polymeric support and functional groups, many research have been done to develop new resins.

Biçak *et al.* (2001) concluded the preparation of a perfect chelating resin for boron extraction from aqueous solutions as follow:

- The adjacent carbon atoms of the functional group should have at least two hydroxyl groups.
- For a high removal, an amine function per one mole of boric acid is essential.
- For regeneration by base and acid, the sorbent must not have hydrolysable linkages.
- The backbone of polymer sorbent must be as inert as possible and it must not contain electron-rich substituents on phenyl rings.
- For continuous column extractions, the polymer sorbent must have moderate swelling ability.

They prepared terpolymer of glycidyl methacrylate (0.4 mol) with methyl methacrylate (0.5 mol) and divinyl benzene (0.1 mol) in spherical beads and modified with N-methyl-D-glucamine as functional groups. They found that the resin has a high activity in boron sorption and can be regenerated more than 20 times without any activity loss. The effect of Ca(II), Mg(II) and Fe(III) ions was positive and the capacity of the resin rises in the presence of these ions due to coprecipitation of borates by the metal hydroxides formed on the resin particles.

Having six hydroxyl functions, sugar derivatives such as sorbitol and mannitol have exceptionally high boron binding abilities (Bicak *et al.*, 2005). They prepared polymer supported amino bis-(*cis*-propane 2,3 diol) functions for boron removal. This resin with cis-diol functionality was found to be rapid in boron uptake while the capacity per chelating group was retaining almost the same. But the recovery of sorbed boron by acid leaching was very slow due to formation of highly stable tetra coordinated borate esters Gazi and Bicak (2007). For that reason, they prepared 2-hydroxylethylamino propylene glycol functions having one hydroxyl group less than the formers. They prepared terpolymer of glycidyl methacrylate with methyl methacrylate and divinyl benzene in spherical beads and modified with 2-hydroxyethylamino propylene glycol as functional groups. Maximum boron loading capacity of this resin was found to be 1.60 mmol/g in non-buffered conditions and increased with increasing pH until reaching 1.68 mmol/g at pH 8. Basicity of the amino group of the resin gives additional contribution in boron binding. The presence of calcium, magnesium and iron ions doesn't reduce the boron uptake of this resin. This resin needs 30-35 min to reduce boron concentration to less than 1 mg/L.

Senkal and Bicak (2003) tested polymer supported iminopropylene glycols as a boron specific sorbent. The results showed high efficiency of this resin in removing boron from water with a boron loading capacity of 3 mmol/g. the polymer used was efficient in chelation with boric acid at mg/L levels in contact time of 12 min . Splitting of sorbed boron can be achieved by simple acid leaching (4 M HCl) and regenerated by NaOH solution (0.1 M).

Poly(GMA-co-TRIM) was prepared by radical suspension polymerization by Wang *et al.* (2007) and functionalized with N-methylglucamine (MG). By applying the resin for removal of boron from aqueous solution, it showed low swelling degree with a capacity of 1.84 mmol/g. The removal increased as pH increased to 8 and decreased after that. It can be used for 10 cycles without losing its sorption capacity.

Parschová *et al.* (2007) compared the performance of number of sorbents possessing N-methyl-D-glucamine functional groups with different polymeric supports, polypropylene–styrene, polypropylene–GMA, viscose–GMA and commercially used polystyrene–DVB (Purolite D-4123). The breakthrough capacity of the commercial resin

was greater than the synthesized resins under the conditions investigated. However, viscose–GMA based sorbent showed much faster sorption kinetics and was easy to regenerate even with diluted (0.1 mol/L) hydrochloric acid.

Li-na *et al.* (2006) prepared two kinds of novel chelating adsorbents for boron removal from aqueous solution. The first resin was synthesized by functionalization of poly(GMA-co-TRIM) by N-methylglucamine and the other one was an organic-inorganic hybrid mesoporous SBA-15 with polyol functional group prepared by two-step post-grafting method. The two adsorbents were examined at pH between 2.6 and 8.6 and the results showed that the maximum boron uptake for the resin was 1.25 mmol/g while 0.63 mmol/g for the poly-grafted SBA-15 due to its lower amount of functional groups.

Gazi *et al.* (2008) applied atom transfer radical polymerization (ATRP) to prepare poly(styrene-divinyl benzene) (PS-DVB) microspheres having poly(glycidyl methacrylate) surface grafts and functionalized with 2-hydroxyethylamino-2,3-propanediol . Boron loading capacity of this resin was found as 3.29±0.01 mmol/g. The presence of Ca(II), Mg(II) and Fe(III) didn't affect the boron uptake capacity of the resin.

A new polymeric resin with glucose sulphonamide functions was prepared by Gazi *et al.* (2004) using copolymerization of styrene with DVB using suspension polymerization methodology. This resin has a boron loading capacity of 2.365 mmol/g and the size fraction of the resin was 210-420 μm. Almost 2.254 mmol of boric acid were recovered from 1 g of the resin when treated with 2 M H_2SO_4.

Harada *et al.* (2011) synthesized Polyallylamine-beads-Glucose (PAA-Glu) and compared its adsorption characteristic with polyvinyl alcohol (PVA) and commercially available N-methylglucamine type resins (CRB03 and CRB05). The results showed that the synthesised resin (PAA-Glu) has the highest boron loading capacity at 26.7 mg/g resin while PVA has the lowest value at 7.5 mg/g. The commercial resins (CRB03 and CRB05) have boron loading capacity 13.1 and 13.9 mg/g respectively.

Bicak and Senkal (1998) prepared crosslinked polystyrene sulfonamide with sorbitol functions. The boron loading capacity of this resin was found to be 1.22 mmol/g and reached in about 30 min. This material has high boron loading capacities in buffered solutions whereas in non-buffered conditions its capacity is somewhat less.

A new hybrid gel with boron-selective functional groups was prepared by Liu *et al.* (2009c) from tetraethoxysilane (TEOS), (3-glycidoxypropyl)trimethaoxysilane(GPTMS) and a new precursor (W) prepared from GPTMS and N-methylglucamine (MG). The adsorption of boron onto this hybrid gel compared with the commercial resin D564 with the particle size of 250-830 μm for both resins. By increasing temperature, the adsorption becomes more rapidly and the equilibrium time decreased especially for the hybrid gel. Boron adsorption is suppressed by H^+ ions at low pH. At high pH, the electrostatic repulsion between $B(OH)_4^-$ and the negatively charged adsorbents weakens the complexation reaction. With increasing the ionic strength of the solution, the boron adsorption amount on the hybrid gel decreased. Adsorption of boron onto both resins can be described by second-order kinetics and the hybrid gel shows the lower rate constant.

Sabarudin *et al.* (2005) synthesized a chitosan resin with N-methyl-D-glucamine (CCTS-NMDG) by two steps: the first on is the synthesis of CCTS with the cross-linker of ethyleneglycoldiglycidylether (EGDE) and the second step is the chemical bonding of NMDG to the CCTS. The boron uptake capacity of the resin was found to be 2.1 mmol/g. Boron concentration in solution containing 100 mg/L of boron goes to zero in 10 min when using CCTS-NMDG, while it takes 60 min when using Amberlite IRA 743.

Kaftan *et al.* (2005) prepared Glucamine-modified MCM-41 by functionalized the support material MCM-41 with propyl bromide then reacted with N-methylglucamine. The maximum boron uptake capacity of the resin was 0.8 mmol/g. This sorbent can be used at any pH greater than 6 since the considered form of boron absorbed is $B(OH)_4^-$. The new resin was compared with the commercial one Amberlite IRA 743 and found that the new one has higher sorption efficiency than the commercial resin.

Inukai *et al.* (2004) synthesized two forms (powder and fiber) of N-methylglucamine-type cellulose derivative by the reaction of grafted cellulose with N-methylglucamine. The grafted cellulose was obtained by the graft polymerization of two forms of cellulose with vinyl monomer having epoxy groups. The maximum boron uptake capacity of the resin is 1.1 mmol/g at pH 9. This capacity of the cellulose powder was at the same level as those of a branched-saccharide-chitosan resins (Inukai *et al.*, 1997).

Liu *et al.* (2009a) prepared Hybrid gel with tetraethoxysilane (TEOS) and bis (trimethoxysilylpropyl) amine (TSPA) as precursors. As the temperature increases from 25°C to 55° C, the amount of boron adsorbed decreased and the adsorption occurs more rapidly due to the diffusion limit adsorption. The maximum amount of boron adsorbed was between pH 4-10. Increasing the ionic strength will lead to increase in the adsorption amount due to the role of nonelectrostatic interactions and hydrophobic attraction on the adsorption process. Electrostatic interaction is known to decrease with the increase in ionic strength because of the suppression of the electrical double layer (You *et al.*, 2006) while hydrophobic attraction increases with the increase in ionic strength due to the "salting-out" effect (Grover and Ryall, 2004).

A macromonomer N-D-glucidol-N-methyl-2-hydroxylpropyl methacrylate (GMHP) was prepared by Bıçak *et al.* (2000) by the reaction of glycidyl methacrylate in 2-methyl pyrrolidone solution with n-methyl-D-glucamine (NMG). Two approaches were followed for the crosslinking polymerization of the macromonomer. In the first approach N,N′-tetraallylpiperazinium was used as a crosslinker, while in the second approach, the excess of diglycidel deravitive of N-methyl-D-glucamine was used as a crosslinker. Both gels showed a rapid binding of boron and needs 15 min to remove almost all boron from solutions containing 30.7 mgB/L with capacities of 2.12 mmol/g and 2.18 mmol/g for G1 and G2 respectively. The difference in capacities was due to the used crosslinker (N,N′-tetraallylpriperazinium dichloride) possessing quaternary ammonium groups which increase the osmotic pressure.

M. Suzuki *et al.* (1999) used an anion exchange resin loaded with chromotropic acid (disodium 2,7-dihydroxynaphthalene-4,5-disulfate) for complexation and removal of trace boron and the results were compared with disodium 4,5-dihyroxybenzene-1,3-disulfonate (Tiron) and a chelating resin functionalized with N-methylglucamine. The highest adsorption of boric acid/borate by chromotropic acid was reached at pH less than 4.5, and the adsorption by Tiron happens at a neutral region but N-methylglucamine resin can adsorbs borate at a wide pH range. The maximum uptake capacity of chromotropic acid, Tiron, and N-methylglucamine was 0.82, 1 and 1.2 mmol/g respectively.

Yasuhiko *et al.* (2002) synthesized D(+)-mannose-type polyallylamine by the reaction of polyallylamine and D(+)-mannose. The maximum amount of boron adsorbed at pH 8.2

was 2.06 mmol/g which three times greater than the amount adsorbed by Amberlite IRA-743. The adsorbed boron was eluted successfully with 1.0 M/l hydrochloric acid solution.

Wolska and Bryjak (2011) prepared VBC/S/DVB matrices by membrane emulsification followed by suspension polymerization from vinylbenzyl chloride (VBC), styrene (S) and divinylbenzene (DVB) with different VBC to S ratios. The microspheres were modified with N-methyl-D-glucamine at reflux (BP) and a microwave reactor (MW). The maximum uptake of boron by these resins was ranging between 0.25 and 1.06 mmol/g. Five sorption/desorption cycles were conducted for two resins with high boron uptake using 5% H_2SO_4 solution. For both sorbents, a small decrease in the sorption capability was observed after the first cycle.

The adsorption of boron on a tannin gel (TG) synthesized from condensed tannin molecules and the amine-modified tannin gel (ATG) prepared with ammonia treatment of the TG was examined at various pH and temperatures (Morisada *et al.*, 2011). The adsorption was small and constant at pH below 7 and the adsorbed amount increased with increasing pH above 7. The adsorption rates onto both gels increase with increasing temperature, and the ATG can adsorb boron more quickly than the TG.

Poly(hydroxypropyl methacrylate) gel beads were synthesized, then it was functionalized to yield glucamine carrying hydrogel beads as a sorbent for boron uptake (Ersan and Pinarbasi, 2011). The equilibrium adsorption amount of boron is 13.5 mmol/g at optimum conditions.

Bursalı *et al.* (2011) prepared chitosan solution by the dissolution of 2.0 g of chitosan flakes into 50 mL of a 5% (v/v) acetic acid solution for 24 hr and then dropped into 0.5M NaOH. Parameters, such as pH, temperature, initial boron concentration, adsorbent dosage, and ionic strength, affecting boron adsorption onto chitosan beads were examined. The boron removal increased with increasing pH from 4.5 to 7.5 then remains constant until pH 8.5 then decreased . The removal increased with increasing resin dosage and ionic strength. The following values were obtained as the optimum conditions in the studied ranges: pH 8.0, temperature = 308 K, amount of chitosan beads = 0.15 g, initial boron concentration = 4 mg/ L , and ionic strength = 0.1 M NaCl.

Glycidyl methacrylate-divinylbenzene microspheres (GD) with epoxy groups of high reactivity were synthesized by suspension polymerization method and functionalized

with four different amino alcohol compounds such as 3-amino-1, 2-propanediol (AP), 2-amino-2-methyl-1 ,3-propanediol (AMP) , 2-amino-2-hydroxymethyl-1,3-propandiol (AHMP) and N-methyl-D(-)-glucamine (MG) (Ohe *et al.*, 2003). Their adsorption capacities for boron are the following order: AHMP>MG>AP>AMP. These results suggest that boron prefers the five-membered chelate ring to the six-membered chelate ring.

An adsorbent was prepared by radiation induced graft polymerization of glycidyl methacrylate (GMA) onto non-woven polyethylene fabrics in aqueous medium, and following chemical modification with NMDG (Hoshina *et al.*, 2007). Effect of pH on boron adsorption was investigated at pH range from 2 to 11 by using 10 mg/L of boron solution. 90% of boron was removed in 1 hour between pH 3 and pH 8 while the removal decreased at pH 2 and pH higher than 8. The adsorbed boron can be eluted using 1M HCl.

A new N-methylglucamine functionalized calix[4]arene based magnetic sporopollenin (4) was synthesized and applied for the removal of boron from aqueous environment containing 5 mgB/L (Kamboh and Yilmaz, 2013). Boron removal efficiency improved with increasing the resin dosage and ionic strength. The highest sorption value (84%) was obtained at pH 7.5,while above pH 7.5 the sorption of boron decreased.

Poly(glycidyl methacrylate) was grafted onto partially Dehydrochlorinated poly(vinyl chloride) (DHPVC) by using atom transfer radical polymerization (ATRP) technique. Epoxy group on the polymeric sorbent was functionalized via ring opening of epoxide group by using amine and acid (Yavuz *et al.*, 2013b). The capacity of the resin was calculated as 2.5 mmol/g. The polymeric sorbent has a potential as an adsorbent for removal of boron from wastewater because it can be used over a wide pH range.

Santander *et al.* (2013) produced a chelating resin by polymerization of N-(4-vinylbenzyl)-N-methyl-Dglucamine (VbNMDG) monomer unit in presence of N,N-methylenebis-acrylamide (MBA) as the crosslinking agent. It was compared with boron selective commercial resin Diaion CRB02. This resin gave a higher sorption capacity and faster kinetics than that of Diaion CRB02 for boron removal from geothermal water.

Boron-selective adsorbent was synthesized by grafting the glycidyl methacrylate onto polyethylene (PE) non-woven fiber using electron beam ionizing radiation and functional groups, NMDG, are introduced to the monomer grafted on polymer backbone

(Ting *et al.*, 2013). The adsorbent was tested in batch and column modes. The maximum adsorption capacity was 14.5 mg B/g.

2.6.5 Hybrid membrane methods for boron removal

These separation methods, which include polymer enhanced ultrafiltration (PEU) and adsorption membrane filtration (AFM) has gained the interest lately as it can be used for the removal of very small quantities of harmful substances from water. Usually, boron separation combines two phenomena: i) complexation with macromolecules (PEU) or sorption with fine sorbent particles (AFM) and ii) membrane separation of Boron-loaded macromolecules/particles. The main advantage of these separation methods is the high efficiency and lower costs of the process comparing with classical ultrafiltration or sorption in fixed bed system. In the last case, the sorbents can be used as very fine particles that increase the interface area and in consequence, the rate of the process is enhanced (Kabay *et al.*, 2009, Yilmaz Ipek *et al.*, 2007).

2.6.5.1 Polymer Enhanced Ultrafiltration (PEUF)

Polymer Enhanced Ultrafiltration (PEUF) is a relatively new membrane separation technique in which a small target species complex with a special water soluble functional polymer and the separation is achieved by the ultrafiltration of this feed solution containing macromolecular complexes (Zerze *et al.*, 2013a, Zerze *et al.*, 2013b). Water-soluble polymers are generally used in the PF process on a low weight-to-volume basis (ca. 1%) to maintain reasonable membrane flux rates (Smith *et al.*, 2005).

Hydroxyethylamino Glycerol Functioned Poly(glycidylmethacrylate) (PNS) and Poly(4-Vinyl-1,3-dioxalan-2-one-co-vinylacetate) (COP) were synthesized and applied in PEUF for boron removal from aqueous solution containing 10 mgB/L using Polyether sulfone membranes (Doğanay *et al.*, 2011). The boron retention values obtained were 52 % and 57% for PNS and COP respectively.

Zerze *et al.* (2013b) synthesized a copolymer, poly (vinyl amino-N, N′-bis-propane diol-co-DADMAC) (GPVA-co-DADMAC) in three comonomer ratios (2%, 5% and 10%) and applied for boron removal by PEUF. Boron concentration could be reduced from 10

mg/L down to 0.8 mg/L by using of novel copolymer in continuous PEUF at pH 9 and boron-to-polymer mass ratio (loading) of 0.001.

Newly synthesized poly (vinyl amino-N, N′-bis-propane diol) (GPVA) is presented as an excellent chelating polymer for boron removal (Zerze *et al.*, 2013a). Boron concentration could be reduced from 10 mg/L down to 0.4 mg/L via total recycle PEUF.

Smith *et al.* (2005) prepared three water-soluble polymers containing linear alkyl monool, 1,2-diol, and 1,2,3-triol groups, mostly on the primary amines of polyethylenimine, and characterized, and tested for their ability to recover boric acid from solutions with boron concentrations ranging from 50 to 5000 mg/L. At low boron concentrations, the 1,2,3-triol polymer performed better than the 1,2-diol, whereas at high boron concentrations, the 1,2-diol outperformed the 1,2,3-triol.

2.6.5.2 Adsorption Membrane Filtration (AMF)

Basic concept of a hybrid adsorption-membrane (AMF) process is the adsorption of solute onto microparticle sorbent to obtain fast adsorption and separation of loaded adsorbent by microfiltration (Blahušiak *et al.*, 2009, Blahušiak and Schlosser, 2009, Kabay *et al.*, 2008, Onderková *et al.*, 2009, Schlosser *et al.*, 2008).The hybrid system consists of two separation steps as shown in Figure 2.25 (Kabay *et al.*, 2006, Yilmaz *et al.*, 2006) :

1. Binding of boron (B) on sorbent (C) which leads to the separation of boron from the aqueous solution (W) by semi-permeable membrane.
2. Separation of the complex (BC) into free sorbent (C) and pure boron (B) and their separation carried out by membrane

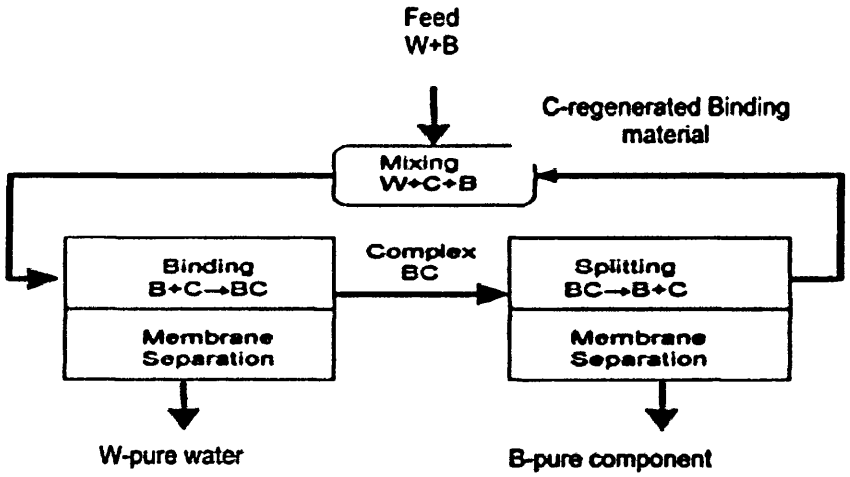

Figure 2.26 Flow sheet of the hybrid ion-exchange–membrane system, (Kabay et al., 2006)

The main advantage of the hybrid AMF compared with the classical column sorption on the fixed bed is the high efficiency and low costs (Güler *et al.*, 2011a, Güler *et al.*, 2011b). Sorbents can be used at a very small particle size which leads to increase of the surface area and the process rate considerably (Yilmaz-Ipek *et al.*, 2011). It is quite difficult to avoid pressure drop in conventional packed beds (Yilmaz-Ipek *et al.*, 2011). Diffusion resistance in adsorbent particles strongly influences the kinetics of adsorption or ion exchange. This resistance can be avoided by using small particles (Blahušiak *et al.*, 2009, Blahušiak and Schlosser, 2009, Onderková *et al.*, 2009).

The efficiency of boron removal from geothermal water was investigated by a hybrid process coupling ion exchange with UF using submerged hollow fiber type UF membrane module (ZW-1, GE) (Kabay *et al.*, 2013a, Kabay *et al.*, 2013b). Boron selective chelating ion-exchange resins Dowex XUS-43594.00 with an average particle diameter of 20 μm were used for boron separation from geothermal water . It was possible to decrease the boron concentration of the geothermal water below 1.0 mg B/L by coupling ion exchange with UF.

Two chelating resins (CRB 02 and XUS 43594.00) were used by Kabay *et al.* (2006) as binding materials to find out the performance of hybrid AMF process for boron removal from aqueous solution. A flat-type hydrophobic Teflon-Fluropore membrane with a pore

size of 0.2 μm and thickness of 200 μm was used. Both sorbents (50 μm) showed a rapid sorption of boron which enough to use it in hybrid AFM process. CRB 02 resin needed 5 min to decrease boron concentration to half of the initial concentration while for XUS 43594.00 resin it took 30 min. After five cycles of regeneration with NaOH, the performance of both resins was improved due to the better access to functional groups through the regeneration of resins with the NaOH solution following each cycle.

Same experiment was done by Yilmaz *et al.* (2006) by using hollow fiber polypropylene membranes with 0.4 μm pores as filtration material. CRB02 can remove 72% of boron while Dowex remove 80 %. On the other hand, boron level drops to 50% after 5 min for Diaion CRB02 and 30 min for Dowex XUS 43594.00. CRB02 seems to be more suitable for use in a sorption-membrane process.

Bryjak *et al.* (2008a) and Bryjak *et al.* (2008b) used Dowex XUS 43594.00 as ion exchange resin with particle size of 0-20 μm and Hollow-fiber Polypropylene membranes with 0.40 μm pores were used as filtration materials. Dowex XUS 43594.00 showed a great performance for boron removal from seawater permeate containing 1.7 mgB/L. The concentration of boron in product water was 0.3 mg/L in 5 min.

Dowex XUS 43594 and Diaion CRB 02 with particle size ranging from 0.355 to 0.500 mm were ground to obtain particles of 45-75 μm diameters (Kabay *et al.*, 2008). The filtration materials used were two polypropylene microfiltration membranes with pore diameter of 0.4 μm. The equilibrium half time for boron removal was reached in 15-20 min with large resin beads (0.355-.500 μm) and 3 min with fine resins beads (45-75 μm).

Bryjak *et al.* (2009) used Dowex XUS 43594 of average particle size of 20, 75 and 500 μm as a sorbent while polypropylene capillaries with pore size of 0.4 micrometer was used as a filtration materials. After 3 min of sorption, the concentration of boron drop from 2mg/L to value that permissible by the WHO (0.5 mg/L), when using the fine particles (20μm) while it took 24 h to reach this value when using particles with the size of 500μm. The optimum amount of the resin to be used was found to be 1g/L. To check the stability of the system, the AMF was running for 48 h without any fouling of the membrane with the sorbent particles.

Blahušiak and Schlosser (2009) and Onderková *et al.* (2009) examined Dowex XUS 43594 with particles size of 550±50 μm a sorbent with two types of membranes:

microfiltration polypropylene hollow fiber hydrophobic membrane Oxyphan with pore size of 0.2 μm and proprietary hydrophilic capillary membrane. With increasing trans-membrane pressure difference, the permeate flux increases at lower suspension concentrations, below 7% with a hydrophilic membrane and 4% for a hydrophobic membrane. The permeate flux was higher for the hydrophilic membrane than for the hydrophobic one.

The tubular ceramic microfiltration membrane Membralox (Pall) with a mean pore size of 0.1 μm was investigated by Onderková *et al.* (2009) using Dowex XUS-G3 as a sorbent. The permeate flux increased with increasing transmembrane pressure and decreased with increasing the suspension concentration. In general, the ceramic membrane is suitable for the AMF application as it showed acceptable permeate flux.

The optimum parameters for boron removal process form geothermal water containing 8-9 mgB/L such as feed flow rate, resin concentration and resin particle size were studied by Kabay *et al.* (2009). Diaion CRB02 and Dowex XUS 43594 were used as sorbents and a submerged-style hollow-fiber module containing two polypropylene membranes with pore diameter of 0.4 μm as filtration material. The concentration of boron in permeate increased slowly after 80 min of contact time when the flow rate increased from 0.5 ml/min to 1 ml/min. The smallest particles in the size 0-250 μm accumulate on the membrane module. The boron concentration in permeate satisfied the permissible limit with particles in the size range 45-125 μm. Increases in suspension concentration from 2g/l to 4.2 g/l lead to the increase of boron removal from geothermal water.

Wolska *et al.* (2010) prepared vinylbenzyl chloride–styrene–1,4-divinylbenzene (VBC/S/DVB) copolymer by membrane emulsification followed by suspension polymerization and modified with N-methyl-D-glucamine in two ways:

1- Dimethyl sulfoxide (DMSO)as solvent in a microwave reactor
2- 1,4-dioxane as solvent in a chemical reactor at boiling point (BP)

Resin 1 is more suitable to be used in the adsorption filtration hybrid system since it reduces boron concentration to 0.2 mg/L comparing with the other one which reduces the concentration to 0.5 mg B/L and 1.0 g/l of the resin is suggested.

2.7 Adsorption Isotherms

A relationship between an amount of boron bounded with an ion-exchange resin and the boron concentration remaining in solution is described by an appropriate isotherm (Cengeloglu *et al.*, 2007). The analysis of the isotherm data is important to develop an equation which accurately represents the results and which could be used for design purposes. Several adsorption isotherm models have been used to describe the experimental adsorption data (Kavak, 2009)..

Langmuir isotherm is the widely used sorption isotherm to model the equilibrium concentration of the species transferring from the liquid to the solid phase (Yilmaz-Ipek *et al.*, 2011).

A basic assumption of Langmuir isotherm is that the sorption takes place at specific homogeneous sites in the sorbent and no sorption takes place when the site is occupied by a solute (Demirçivi and Nasün-Saygili, 2010).

It is expressed as:

$$q_e = \frac{bq_m C_e}{1 + bC_e} \qquad 2.23$$

A linear form of this expression is:

$$\frac{C_e}{q_e} = \frac{1}{bq_m} + \frac{C_e}{q_m} \qquad 2.24$$

Where:

q_e : The amount of boron sorbed per amount mass of sorbent, (mg/g)

C_e : The remained amount of boron in solution at equilibrium, (mg/L)

b: the Langmuir equilibrium constant , (L/mg)

A plot of $\frac{C_e}{q_e}$ versus C_e will give a straight line with a slope of $1/q_m$ and an intercept of $(\frac{1}{bq_m})$.

Another adsorption isotherms which describe the adsorption process called Pseudo-second-order kinetic model and Pseudo-first-order kinetic model.

Pseudo-second-order kinetic is expressed as (Chowdhury and Saha, 2010):

$$q_t = \frac{k_2 q_e^2 t}{1 + k_2 q_e t} \qquad 2.25$$

Where q_t and q_e are the amount of boron adsorbed at time t and at equilibrium (mg/g) and k_2 (g/ mg.min) is the pseudo-second-order rate constant for the adsorption process. The different linearized forms of the pseudo-second-order equation are given in Table 2.8 (Chowdhury and Saha, 2010). The most popular form used is Type 1.

Table 2.8 The different linearized forms of the pseudo-second-order equation

Linear Regression	Expression	Plot
Type 1	$\frac{t}{q_t} = \frac{1}{k_2 q_e^2} + \frac{1}{q_e} t$	t/q_t vs. t
Type 2	$\frac{1}{q_t} = \frac{1}{q_e} + \frac{1}{k_2 q_e^2} \frac{1}{t}$	$\frac{1}{q_t}$ vs. $\frac{1}{t}$
Type 3	$q_t = q_e - \frac{1}{k_2 q_e} \frac{q_t}{t}$	q_t vs. $\frac{q_t}{t}$
Type 4	$\frac{q_t}{t} = k_2 q_e^2 - k_2 q_e q_t$	$\frac{q_t}{t}$ vs. q_t

Pseudo-first-order kinetic model is expressed as (Fox *et al.*, 2000, Ho and McKay, 1998, Neal *et al.*, 1998, Schmitt-Kopplin *et al.*, 1998):

$$\log(q_1 - q_t) = \log(q_1) - \frac{k_1}{2.303} t \qquad 2.26$$

Where:

q_1 : the amount of adsorbent sorbed at equilibrium, (mg/g)

q_t : is the amount of boron sorbed at time t (mg/g),

k_1 : is the equilibrium rate constant of first order sorption (l/min).

The intercept of the straight line plots of $\log(q_1 - q_t)$ against t should equal $\log(q_1)$, otherwise the reaction is not likely to be a first order reaction even this plot has high correlation coefficient with the experimental data.

An isotherm which can be applied to non-ideal sorption on heterogeneous surfaces as well as multilayer sorption is called The Freundlich isotherm. It was derived by assuming an exponentially decaying sorption site energy distribution (Demirçivi and Nasün-Saygili, 2010). The Freundlich isotherm has the following formula:

$$\log q_e = \log K_F + \frac{1}{n}\log c_e \qquad 2.27$$

Where:

q_e : the amount adsorbed at equilibrium, (mg/g)

K_F : a constant related to adsorption capacity

$\frac{1}{n}$: a constant related to adsorption intensity

c_e : the equilibrium concentration, (mg/L)

The graph of $\log q_e$ versus $\log c_e$ gives a straight line with slope $\frac{1}{n}$ and intercept $\log K_F$.

Among the several methods of boron removal from aqueous solutions, the use of boron-selective resins seems to have still the highest importance. The combination of the adsorption of boron by ion exchange resins with their separation on membranes seems be an attractive alternative to the commonly used column-mode technology. The integrated hybrid adsorption-microfiltration process and the regeneration of the loaded resin have been investigated in this study. A continuous adsorption-microfiltration-regenration process is a cost-effective process and has a high boron removal efficiency.

CHAPTER 3

Experimental equipment and procedures

This chapter covers the experimental equipment used in this thesis and all related procedures.

3.1 Chemicals and water samples:

The water used for the experiments for preparation the salt solutions was purified with a Milli-Q system from Millipore, where the conductivity was measured as 0.055 μS/cm and the resistivity was 18.2 MΩ.cm.

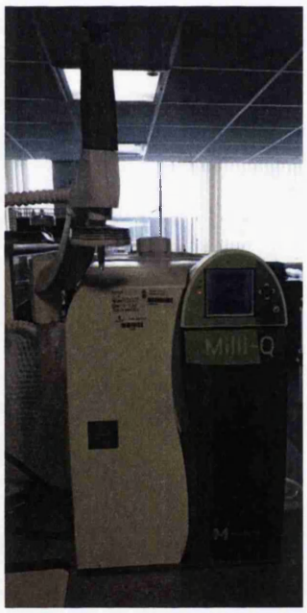

Figure 3.1 Milli-Q system

Boric acid 99.8+%, sodium hydroxide and hydrochloric acid at different concentrations were obtained from Fisher Scientific, UK. A weakly basic anion exchange resin Amberlite IRA743 with properties shown in Table 3.1 was provided from Sigma-Aldrich, UK. The chemical structure of the resin is shown in Figure 3.2. All the chemicals used in the experiments were reagent grade. All glassware used in the experiments were rinsed with deionized water and dried at 110 C overnight.

Table 3.1 Properties of Amberlite IRA743

Vapor density	**<1 (vs air)**
Vapor pressure	17 mmHg (20 °C)
Description	weakly basic anion exchange resin
Autoignition temp.	~800 °F
Moisture	48-54%
Matrix	styrene-divinylbenzene (macroporous)
Matrix active group	N-methylglucamine (free base form) functional group
Particle size	500-700 µm
Capacity	0.7 meq/mL by wetted bed volume

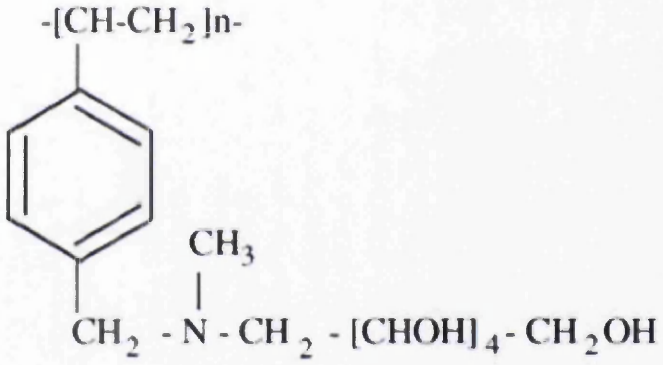

Figure 3.2 Chemical structure of the Amberlite IRA 743 resin, (Yilmaz et al., 2005b)

3.2 Microfiltration Membranes

Membranes used during the study were hydrophilic polyvinylidene fluoride (PVDF) with pore size of 0.1, 0.22, and 0.45 µm were supplied by Merck Millipore.

3.3 Batch IX Experiments

The initial Amberlite IRA743 resin with particle size of 500-700 µm was ground using a ball mill and sieved by 150-180 and 45 µm sieves to get the resin fractions with particle size of 1-45 and 150-180 µm, respectively. The powdered resin was regenerated using

0.2 M NaOH solution, and then washed with a large amount of water and dried in the oven at 70 °C.

Boric acid solution was prepared in 5 L volumetric flask by dissolving the appropriate amount of boric acid in Milli-Q water to prepare a solution with required boron concentration.

The adsorption experiments were carried out using a batch method. Various amounts of the resin were added to 500 ml of boron solution in 500 ml beakers for 1 hour at continuous stirring using a hot-plate stirrer. The range of the parameters investigated is summarized in Table 3.2.

Table 3.2 Investigated Parameters for boron removal (Batch Experiments)

Parameter	Range
pH	4-10.5
Temperature	15-35
Boron Concentration	1.5-15 mg/L
Resin Concentration	0.2-3 mg/L

At the end of each experiments the suspension solution samples were filtered using vacuum filter flask with filter paper (100% cellulose 0.15mm thickness,13 μm pore size 90mm circles) and stored in 50 ml polypropylene centrifuge tubes for further analysis.

3.4 Adsorption Membrane Filtration (AMF) Experiments

For a membrane study, the membrane unit set-up has been designed and fabricated on semi-pilot scale (Figure 3.3 and 3.4). The system consists of three 5 L tanks, tank 1 is the suspension tank where the boron solution is mixed with the resin and fed to microfiltration cell 1 (MF1), tank 2 is the concentrate tank where the concentrate from MF1 is collected and an acid is added to decrease pH for desorption of boron and then concentrated by MF2 into tank 3 where the solution is diluted by some of the permeate

from MF1 and pH of the permeate from MF3 is adjusted and returned to tank 1 as a regenerated resin. The effective membrane area in the membrane cell is 0.64 mm².

Figure 3.3 Adsorption Membrane Filtration (AMF) unit

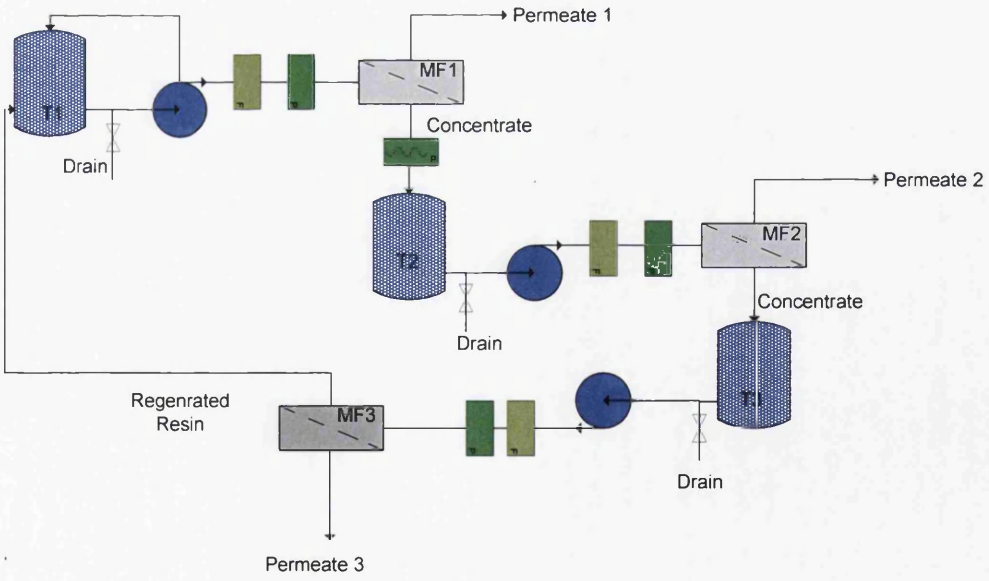

Figure 3.4 Schematic representation of the AMF unit

Water flux measurements were carried out with high purity water. The pure water permeability was determined from filtration tests at different transmembrane pressures (0.2 – 1.5 bar) at ambient temperature,. The pressure was varied between 0.2 -1.5 bars and pure water flux *is* defined as:

$$J_v = \frac{V_{F.R}}{A} \qquad 3.1$$

where J_v is the permeate flux (L/m^{2}h), A is the effective membrane area (m^2) and $V_{F.R}$ is the volume flow rate (L/h).

In this study, the pure water flux was determined by weighing the obtained permeate during a predetermined time using an electronic balance (Precisa, Model XB3200C) connected to a computer. By plotting the membrane flux (J_v) versus operating pressure (ΔP), the membrane permeability (pure water permeability), L_p can be obtained from the slope of the straight line as follows:

$$L_p = \frac{J_v}{\Delta P} \qquad 3.2$$

In filtration experiments with the suspensions of the powdered resin , 5 L of the suspension solution containing the resin at different concentration (0.2 – 1 g/L) was pumped through the membrane cell of AFM unit to collect the permeate. The effect of operating pressure at 0.2, 0.5, 1, and 1.5 bars, resin concentration at 0.2 , 0.4, 0.6, 0.8 and 1 g/L, and addition of different salts include sodium chloride (NaCl) at 5000 – 35000 mg/L, sodium sulfate (Na_2SO_4) at 3000-10000 mg/L and magnesium chloride ($MgCl_2$) at 5000-20000 mg/L. After each MF run the cell is flushed with Milli-Q water and the water flux is measured at 0.5 bar to check the membrane fouling by comparing water fluxes before and after filtration.

3.5 Experimental Equipment

3.5.1 Hach Spectrophotometer DR-2400

This technique was used to determine the concentration of the boron and the suspended solids in the samples. Boron concentration was determined using the carmine method (Gibbs, 1994, Hach-Company, 2004). This method adapted from Standard Methods for

the Examination of Water and Wastewater for the determination of boron. In this method, the boron is determined by the reaction sulfuric acid with BoroVer® 3 reagent to form reddish to bluish colour complex in proportion to the boron concentration. In the presence of concentrated sulfuric acid, boron exists as the cation B^{3+}. The cation complexes to the carmine indicator causing the solution to change color from red to blue according to the following reaction:

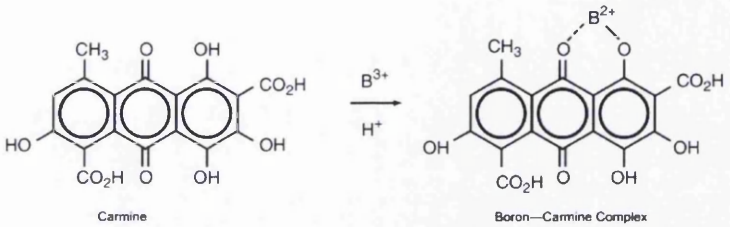

Carmine Boron—Carmine Complex

The blue-colored complex is read at 605 nm using a spectrophotometer, and the amount of color is proportional to the dissolved boron concentration. The coloured complex is then measured by the spectrophotometer Hach spectrophotometer DR-2400 (Hach method 8015) shown in Figure 3.5. The suspended solids were measured by method 8006 adapted from Sewage and Industrial Wastes, (Krawczyk and Gonglewski, 1959) for concentration ranging from 0-750 mg/L.

Figure 3.5 DR/2400 Portable Spectrophotometer

3.5.2 pH meter

Litmustik® Pocket pH tester (model PHH-3X) shown in Figure 3.6 was obtained from Omega , United Kingdom , used to measures pH at range from 0-14 with an accuracy of 0.1 and temperature at range from 0 to 70 °C at 1°C accuracy. The probe was calibrated before readings at 20±2°C using buffer solutions (pH = 4, 7 and 10 ±0.01) while the temperature is factory calibrated. The standard solutions were obtained from Fisher Scientific, UK.

Figure 3.6 Litmustik® Pocket pH Testers (model PHH-3X)

3.5.3 Ball Mill

The Ball Mill used in this study to grind Amberlite IRA743 is shown in Figure 3.7 is designed for use with Ball Mill Jars of up to 5 litres. It is a single tier machine with 2 rollers to fit the Jar filled with the resin. It is fitted with a speed controller giving a roller speed from 0-100RPM. Porcelain ball mill pot with a 5L capacity was used.

Figure 3.7 A photo of The Ball Mill

3.5.4 Malvern Mastersizer-2000 analyzer

A Malvern Mastersizer-2000 analyzer shown in Figure 3.8 was used to evaluate the particle size distribution of the Amberlite IRA743 resin. The device measures the intensity of light scattered as a laser beam passes through a dispersed particulate sample. Usually A particle-size instrument based on light scattering can distinguish the scattering patterns of large particles from small particles because large particles scatter strongly and principally to small angles away from the incident light beam while small particles scatter weakly and too much larger angles. Analysis of the scattering intensity as a function of observation angle can yield a particle size distribution (Wedd, 2003).

The advantages of the technique responsible for this popularity include (1) ease of use; (2) rapid data collection (measurements are typically completed within 60 seconds); (3) high reproducibility; (4) broad dynamic range (systems are available that cover the range from 0.02 μm to several millimeters); (5) volume distribution measurements ; and (6) flexibility (Kelly and Kazanjian, 2006) .

This technique was used in this work to measure the particle size distribution of the Amberlite IRA743 resin. The Mastersizer 2000 uses the technique of laser diffraction to measure the size of particles. It does this by measuring the intensity of light scattered as a laser beam passes through a dispersed particulate sample. This data is then analyzed to

calculate the size of the particles that created the scattering pattern. It can measure particle sizes from 0.02 μm to 2000 μm.

A typical Malvern Mastersizer-2000 system is made up of three main elements:

Optical bench - A dispersed sample passes though the measurement area of the optical bench, where a laser beam illuminates the particles. A series of detectors then accurately measure the intensity of light scattered by the particles within the sample over a wide range of angles.

Sample dispersion units (accessories). Sample dispersion is controlled by a range of wet and dry dispersion units. These ensure the particles are delivered to the measurement area of the optical bench at the correct concentration and in a suitable, stable state of dispersion.

Instrument software. The Mastersizer 2000 software controls the system during the measurement process and analyses the scattering data to calculate a particle size distribution.

Figure 3.8 The Mastersizer 2000 particle size analyzer

3.5.5 Surface area analyzer

In this study, surface area was determined using the Brunauer – Emmet – Teller (BET) method (Brunauer *et al.*, 1938). The fundamental of the BET theory is the concept that the forces which contribute to vapor condensation are also responsible for the bond

energy in multimolecular adsorption. The rate of condensation of gas molecules onto an adsorption layer is equal to the rate of their evaporation from the same layer (Nikitin and Petasyuk, 2008). The BET method is the most widely used standard procedure for the determination of the surface area of porous material The BET equation can be expressed as follows (Dubois, 2011):

$$\frac{p}{n^a(p_0 - p)} = \frac{1}{n^a C} + \frac{C-1}{n_m^a C}\left(\frac{p}{p_0}\right) \qquad 3.3$$

where p is the pressure and p_0 the saturation pressure of the gas. The parameter represents the amount adsorbed at the relative pressure p/p_0 and n_m^a is the monolayer capacity, i.e. the quantity of gas needed for the surface to be covered with exactly a completed physically adsorbed monolayer. The constant *C* is also called the BET constant. It is related exponentially to the enthalpy (heat) of adsorption in the first adsorbed layer. It is used to characterize the shape of the isotherm in the BET range, and gives an indication of the magnitude of the adsorbate-adsorbent interaction energy.

The BET equation requires a linear relation between $\frac{p}{n^a(p_0-p)}$ and $\frac{p}{p_0}$ (i.e. the BET plot). The range of linearity is restricted to a limited part of the isotherm —usually not outside the $\frac{p}{p_0}$ range of 0.05—0.30. Some adsorption systems give linear (or nearly linear) BET plots over several ranges of $\frac{p}{p_0}$, that the BET plot can be expected to yield the true value of n (Pierotti and Rouquerol, 1985). An example of a BET plot is presented in Figure 3.9 (Dubois, 2011).

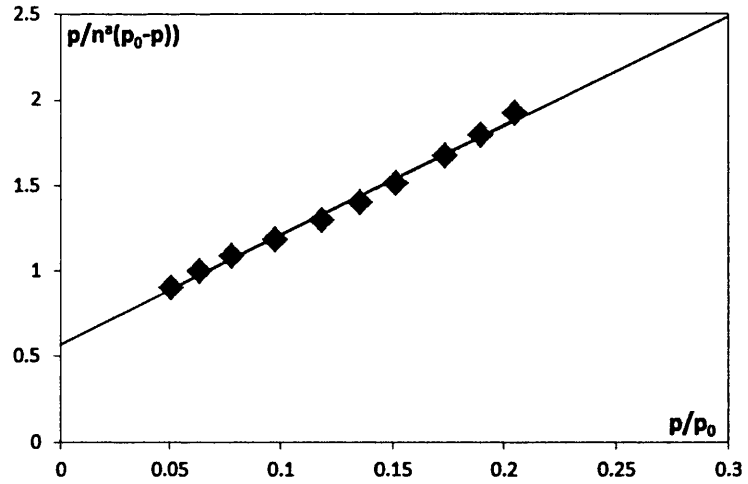

Figure 3.9 Example of BET plot for biotite, 0.125-0.250 mm, (Dubois, 2011)

The BET surface area of the fractions of the Amberlite IRA743 resin was determined with Nova 2000e, surface area and pore size analyzer using liquid nitrogen method (Nova 2000e, surface area and pore size analyzer, Swansea University, UK) shown in Figure 3.10.

To evaluate the surface area of the resin samples the following procedure was used:

- An empty cell was weighed, an Amberlite IRA743 sample was added, the sample cell placed in the pouch of the heating mantle and set with clamp, cell inserted into fitting, tighten place.
- The degasser was loaded and vacuum pulled on the sample for at least 10 minutes. Next, the temperature set to 248°C and the heating mantle switched on. After sufficient time for complete outgassing (overnight), the mantle was switched off.
- After cooling to room temperature, the degasser was unloaded and then cell removed and reweighed to obtain the dry, outgassed sample weight.
- The sample was analysed, the weighed cell was fitted in its place in the analysis part and the flask inside filled with liquid nitrogen then the analysis set up and applied for 8 hours.

Figure 3.10 Nova 2000e, surface area and pore size analyzer

3.5.6 Atomic force microscopy

Atomic force microscopy (AFM) is used to characterize the surface morphology of MF membranes. A sharp tip with a diameter smaller than 10 μm is scanning across a surface with a constant force. London-vanderWaals interactions will occur between the atoms in the tip and the surface of the sample and these forces are detected. This will result in a line scan or profile of the surface (Mulder, 1996).

Binnig *et al.* 1986 invented atomic force microscopy (AFM). Since then, it has become an important means of material characterization at up to atomic level resolution. From the different techniques used to study membrane morphology only the AFM can provide direct and detailed information on the size distribution, shape and topography of the pores (Al-Abri, 2007). AFM has four primary modes of operation: contact mode, non-contact mode, tapping mode or intermittent and the recently developed profile-imaging mode (Hilal *et al.*, 2006).

The basic set-up of a typical AFM is shown in Figure 3.11 (Bowen and Hilal, 2009). A probe is mounted at the apex of a flexible Si or Si_3N_4 cantilever. The cantilever itself or

the sample surface is mounted on a piezocrystal which allows the position of the probe to be moved in relation to the surface. Deflection of the cantilever is monitored by the change in the path of a beam of laser light deflected from the upper side of the end of the cantilever by a photodetector. As the tip is brought into contact with the sample surface, by the movement of the piezocrystal, its deflection is monitored. This deflection can then be used to calculate the interaction forces between probe and sample (Bowen and Hilal, 2009).

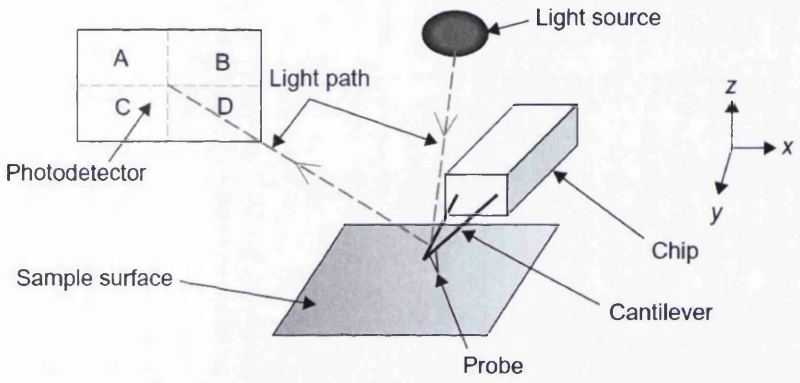

Figure 3.11 Basic AFM Set-Up, (Bowen and Hilal, 2009)

Figure 3.12 below shows schematic diagram of atomic force microscope operation (Al-Abri, 2007).

AFM can provide high-resolution 3D images of membrane surfaces in both air and liquid environments without needing prior surface modification.

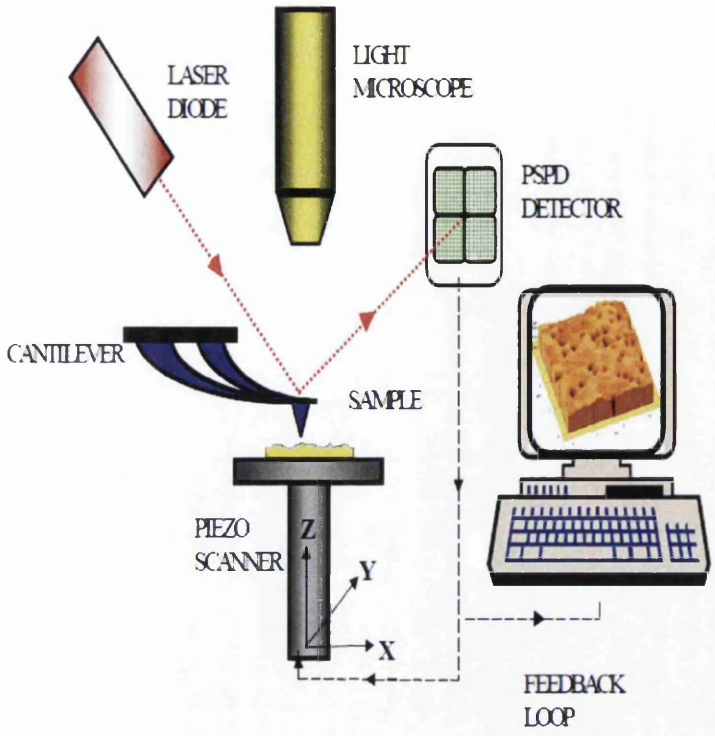

Figure 3.12 Schematic demonstration of the principle of AFM operation, (Al-Abri, 2007)

Three key parameters that influence membrane separation processes can be studied using AFM. These parameters are (i) pore size distribution and surface morphology, (ii) long range interaction forces, and (iii) surface adhesion, which can be related to membrane fouling (Mulder, 1996). AFM has been used to characterize several kinds of membranes such as MF, UF, NF, and RO membranes (Chahboun *et al.*, 1992, Singh *et al.*, 1998, Khulbe *et al.*, 2006). AFM is also used as a mean to characterize and identify the changes in membranes surface morphology and structure related parameters such as pore size, pore size distribution, porosity and roughness following modification process using different methods ((Bowen and Teodora, 2007, Freger *et al.*, 2002, Hilal and Kochkodan, 2003, Wahab Mohammad *et al.*, 2003, Hilal *et al.*, 2005, Xie *et al.*, 2005, Yan *et al.*, 2006, Al-Abri, 2007).

The surface of hydrophobic PVDF membranes were investigated by tapping mode atomic force microscopy (TM-AFM), to obtain mean pore size, pore size distribution, nodule size, pore density, surface porosity and roughness parameters (Khayet *et al.*, 2004, Khayet *et al.*, 2005, Alkhudhiri, 2013).

All AFM measurements were performed on a Multimode AFM with Nanoscope IIIa controller (Veeco, USA) using manufacturersupplied software (Figure 3.13). All measurements were carried out using tapping mode in air at room temperature, and were performed using TESP type cantilevers (nominal spring constant 20-80 N/m).

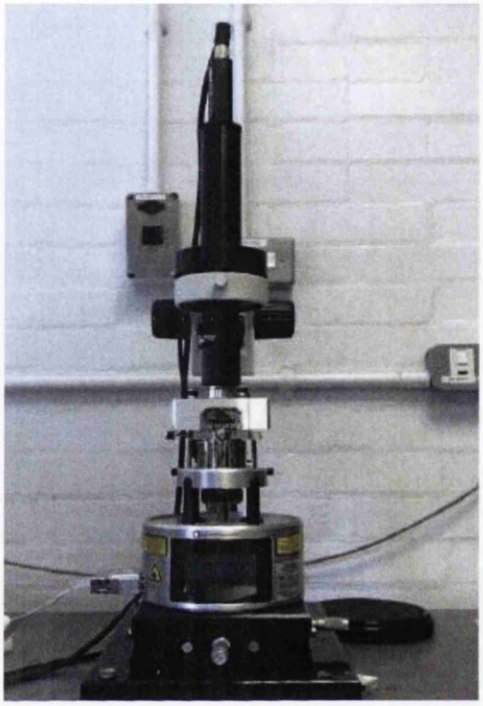

Figure 3.13 A photo of an atomic force microscope (Veeco, USA)

3.5.7 Scanning Electron Microscope (SEM)

The scanning electron microscope (SEM) is one of the most versatile instruments available for the examination and analysis of the microstructure morphology and chemical composition characterizations (Zhou *et al.*, 2007). The main components of a typical scanning electron microscope SEM are scanning system, electron column, detector(s), display, vacuum system and electronics controls as seen in Figure 3.14. The electron column of the SEM contains the following parts: an electron gun and two or more electromagnetic lenses operating in vacuum. The electron gun used to generate free electrons and accelerates them to energies in the range 1-40 keV in the SEM.

The electron lenses create a small, focused electron probe on the specimen.

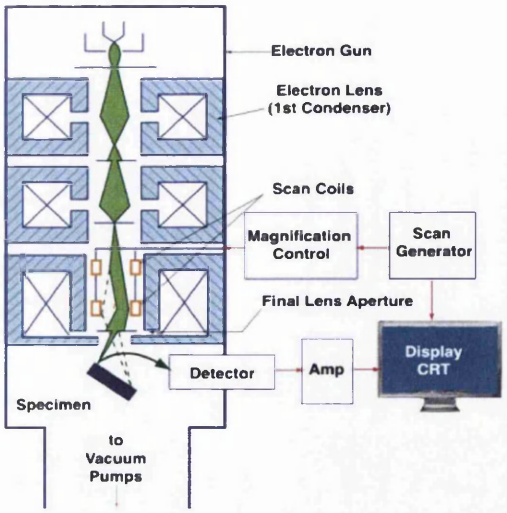

Figure 3.14 The main components of a typical SEM, (Zhou et al., 2007)

Membranes top surface, cross-section and bottom surface can be studied using Scanning Electron Microscopy (SEM). In addition, SEM is able to estimate the surface porosity, pore size and pore size distribution as shown in micrographs.

The Polyvinylidene fluoride (PVDF) membranes at different pore sizes used through this study have been characterised with scanning electron microscopy (SEM). A scanning electron microscope (HITACHI S-4800II) was used to take images of the prepared membranes. The surface and cross-section images of these membranes were taken in high vacuum mode (5 kV).

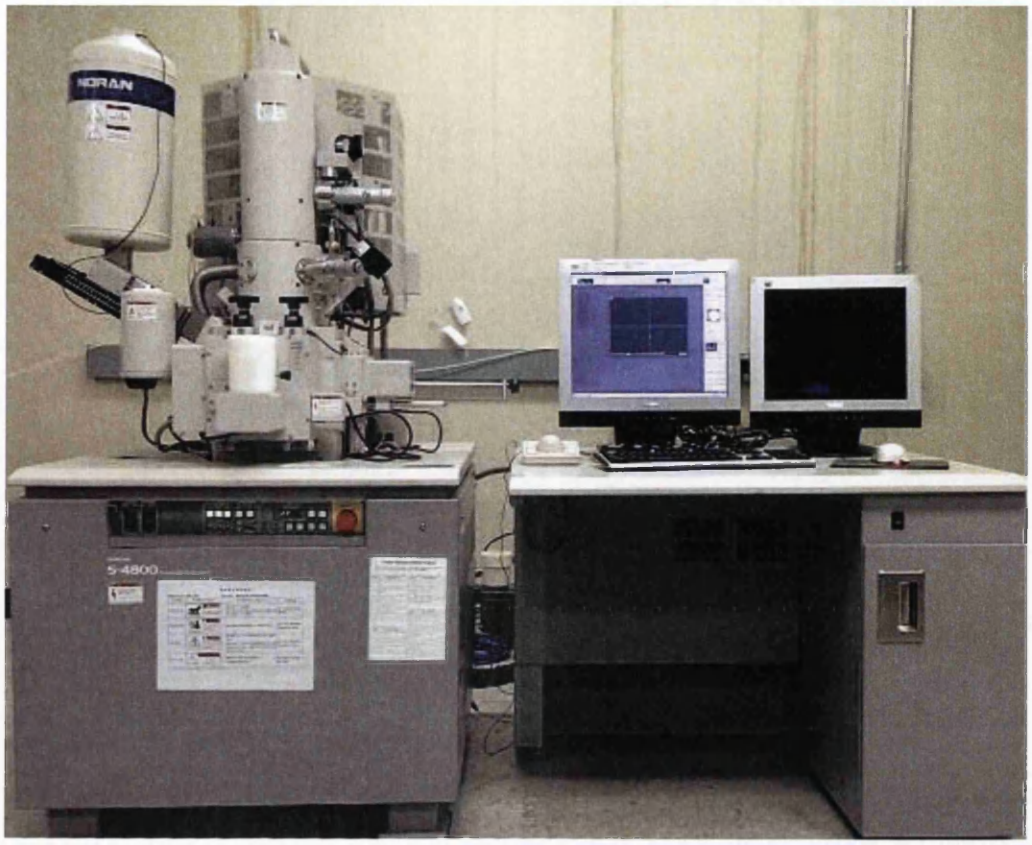

Figure 3.15 A photo of The scanning electron microscope (SEM)

CHAPTER 4

The effect of operational parameters on Boron removal with Amberlite IRA743 resin

4.1 Introduction

In this chapter, the removal of boron from water using Amberlite IRA743 resin will be investigated. The aim of this investigation is to conduct comprehensive studies on boron removal from aqueous solution using Amberlite IR743 resin in batch system to obtain the interactions between dependent variable (Boron removal efficiency) and independent variables (contact time, resin particle size, initial boron concentration, pH, temperature, resin dosage and NaCl , Na_2SO_4 and $MgCl_2$ salts).

The boron removal R, was calculated using the following equation:

$$R=\frac{C_0-C_e}{C_0} \times 100 \qquad 3.1$$

Where C_0 and C_e are the initial and equilibrium boron concentration (mg/L), respectively.

4.2 Effect of resin particle size on removal efficiency

The effect of the resin particle size on boron removal from water was investigated using Amberlite IRA743 resin fractions with different particle sizes of 1-45 μm, 150-180 μm and 500-700 μm. The other parameters were kept constant (boron concentration= 3.0 mg/L, pH= 6.0, T= 25° C, resin dosage= 0.4 g/ L).

Particle size distribution is shown in Figure 4.1 and Figure 4.2 for the resin particle in the range 1-45 μm and 150-180 μm respectively. The BET surface area is shown in Figure 4.3 and Figure 4.4 for the resin particle in the range 1-45 μm and 150-180 μm respectively.

It was found that the surface area for the particle fraction 1-45 μm and 150-180 μm is 26.6 m^2/g and 24.5 m^2/g respectively while the BET surface area was 20.8 m^2/g for the particle 500-700 μm (Dambies *et al.*, 2004). The BET surface area of the three fractions are shown in Table 4.1.

Table 4.1 BET Surface area of different particle size of Amberlite IRA743

Fraction μm	BET surface Area (m^2/g)
500-700	20.8
150-180	24.5
1-45	26.6

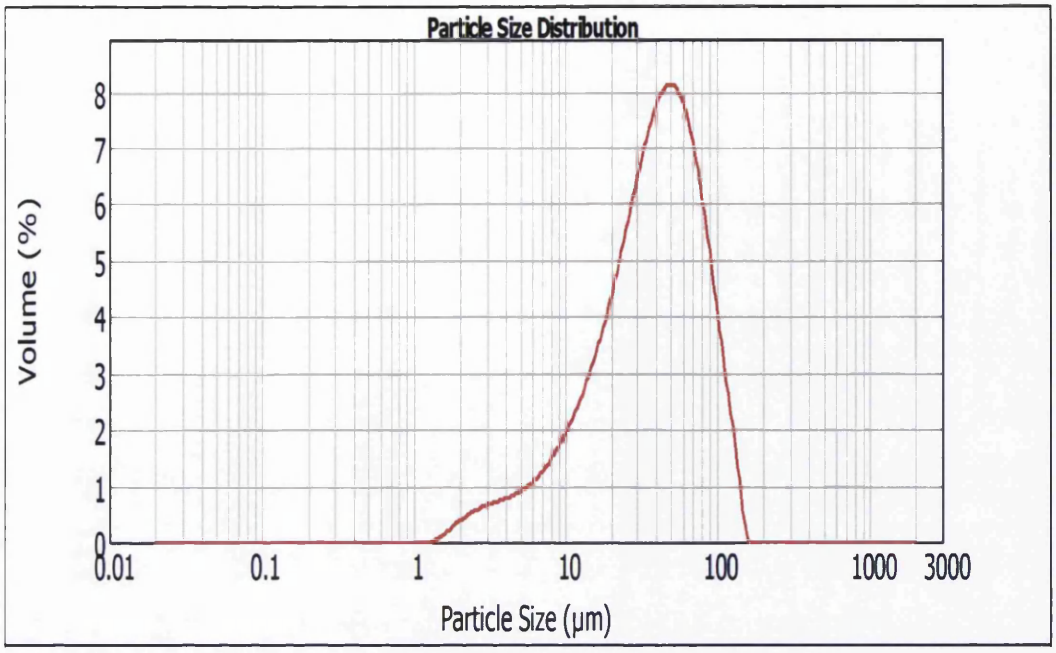

Figure 4.1 Particle size distribution for the fraction of Amberlite IRA743 resin over a particle size range of 1-45 µm

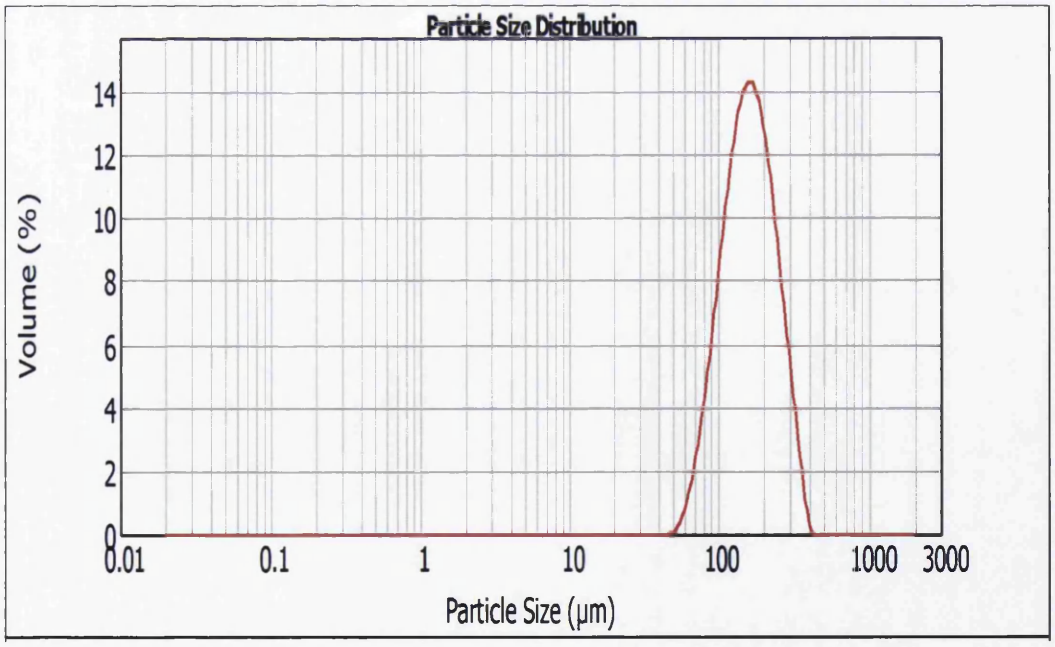

Figure 4.2 Particle size distribution for the fraction of Amberlite IRA743 resin over a particle size range of 150-180 µm

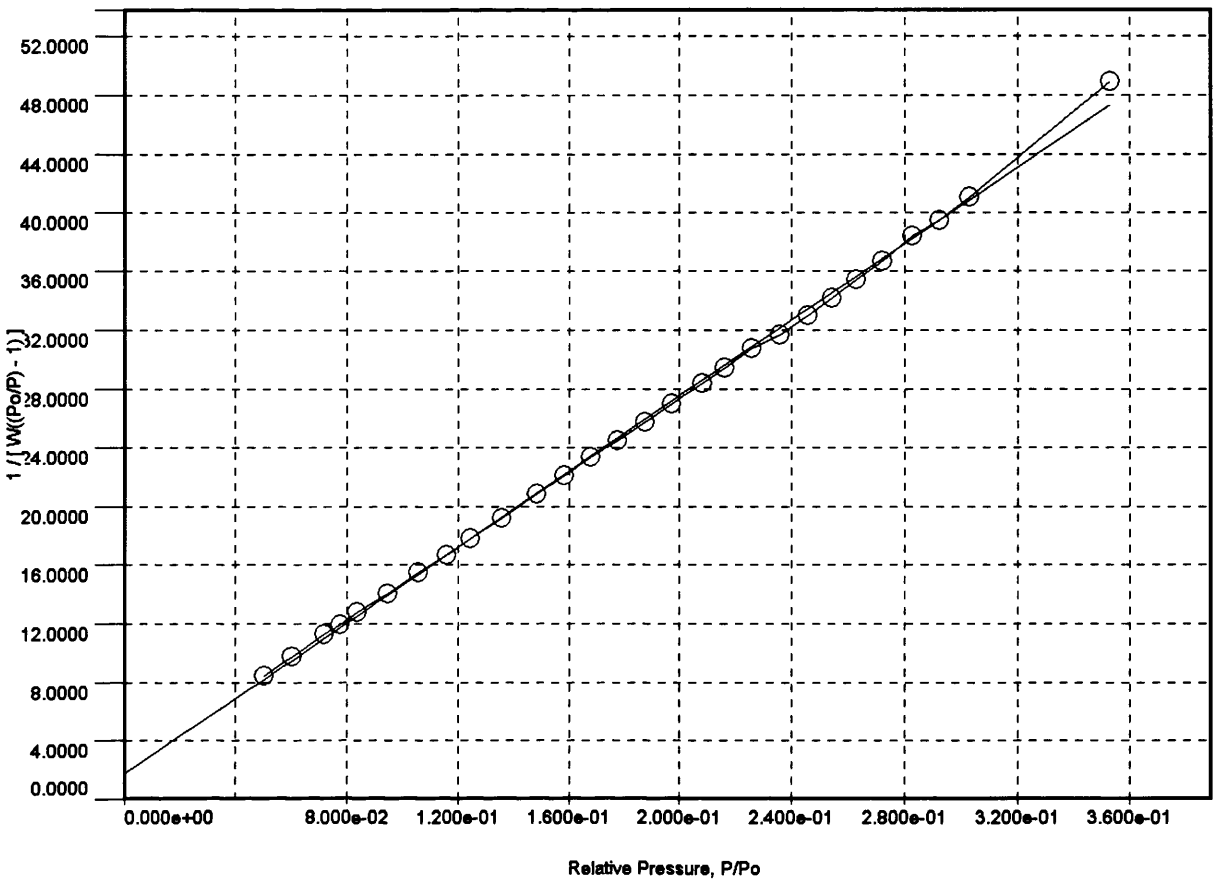

BET summary

Slope =	129.147
Intercept =	1.742e+00
Correlation coefficient, r =	0.999382
C constant=	75.137
Surface Area =	26.607 m^2/g

Figure 4.3 Surface area for the fraction of Amberlite IRA743 resin over a particle size range of 1-45 μm

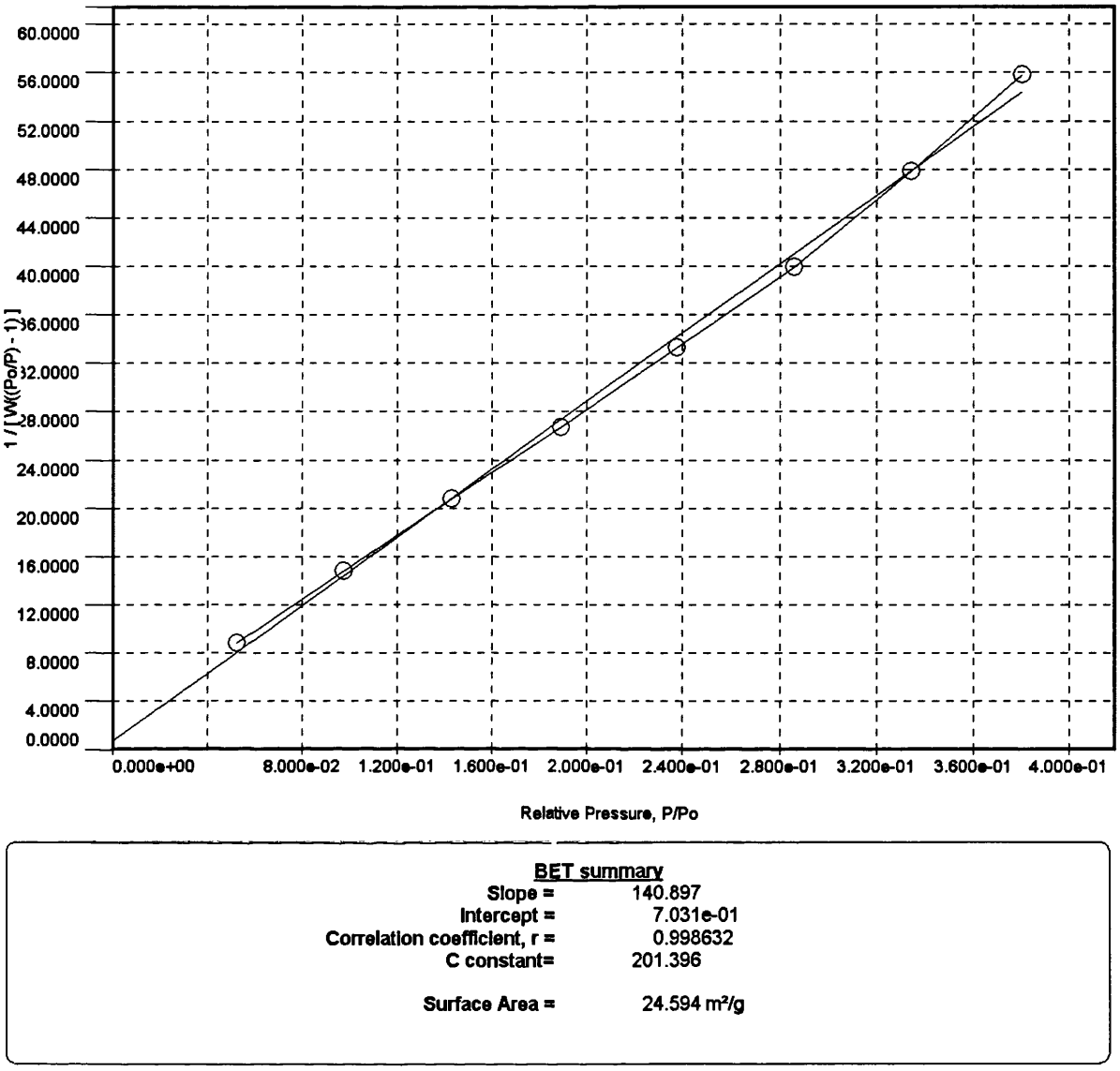

Figure 4.4 Surface area for the fraction of Amberlite IRA743 resin over a particle size range of 150-180 μm

As shown in Figure 4.5, the resin fraction with the smallest particle size removes boron better than resin fractions of larger particle size. Boron removal from water was 70.0, 54.8 and 6.5% for resin fractions with particle size of 1-45; 150-180 and 500-700 μm, respectively.

This finding may be explained by both increasing of total surface area and decreasing of diffusion resistance in resin particles with reducing of their size. These results support

the idea of applying ion exchange-membrane filtration for boron removal which uses fine ion exchange resin particles. Yilmaz-Ipek *et al.* (2011) found the same results by using Diaion CRB02 resin at different resin particle sizes such as 0.250–0.355, 0.355–0.500, 0.500–0.710, and 0.710–1.000 mm. Kabay *et al.* (2008) used CRB02 and XUS 43594.00 at two particle sizes (355-500 mm and 45-75 μm) and found the equilibrium half-time for boron removal was reached faster when using the smaller particles than the large particles.

The smallest resin particle size (1-45 μm) will be used to study the effect of other parameters since it gave the highest boron removal.

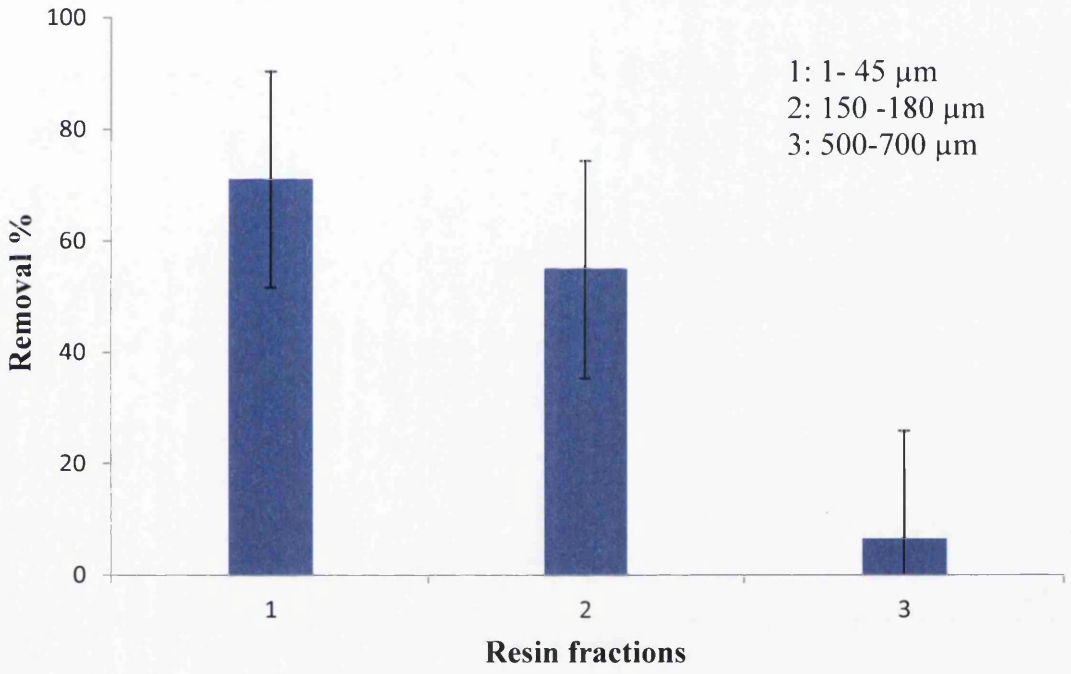

Figure 4.5 Effect of particle size of Amberlite IRA743 resin on boron removal efficiency, boron concentration= 3.1 mg/L, pH= 6.0, T= 25° C, resin dosage= 0.4 g/ L

4.3 Effect of contact time and resin dosage

The effect of contact time between boron solution and the resin on boron removal and boron concentration remains in solution was studied at two boron concentrations of 1.5 and 5.0 mgB/L at three different resin concentrations. The other parameters were kept constant (pH=8.0 and T= 25°C).

The boron concentration in the solution was measured at 1, 5, 10, 30, 60, and 120 min by taking samples from the solution at these times and measuring the boron concentration. Figure 4.6 and Figure 4.8 show the percentage of boron removed from the solution over time while Figure 4.7 and Figure 4.9 show the concentration of boron remaining in the solution over time.

The results for the solution containing boron concentration of 1.5 mg/L and resin dosage 0.4, 0.6 and 0.8 g resin/L are shown in Figure 4.6 and 4.7 while for the solution with initial boron concentration of 5 mg/L and the resin dosages used are 1, 2 and 3 g/L shown in Figure 4.8 and 4.9.

As can be seen from these figures, boron removal increases with the contact time and boron concentration remaining in the solution decreased. The boron removal increases with increasing in resin dosage.

From Figure 4.6, the removal of boron reached 13.33, 40, and 46.66% in the first minute when using 0.4, 0.6 and 0.8 g resin/L respectively and boron concentration goes down to zero in 10 minutes when using resin dosage of 0.8 g/L while it takes 30 minutes when using 0.6 g resin/L.

It is clear that the removal increase with the increase in resin dosage. The enhance in boron removal may be explained by increasing of surface area and a total number of binding sites on the resin surface with an increase of resin dosage. Same results were obtained by (Öztürk and Köse, 2008, Parsaei et al., 2011).

Clearly, since increasing the adsorbent doses provides a greater surface area and adsorption sites, the equilibrium concentration decreases with increasing adsorbent doses for a given initial concentration (Parsaei et al., 2011).

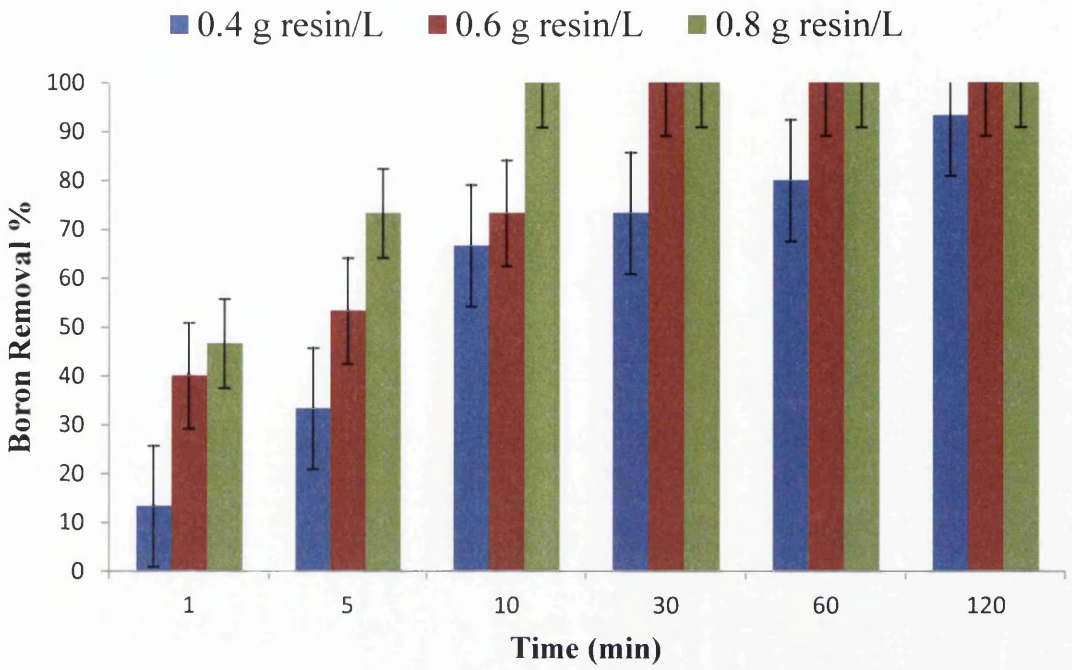

Figure 4.6 Effect of contract time on boron removal, Boron concentration = 1.5 mg/L, pH= 8.0, T =25°

As can be seen in Figure 4.8, the removal of boron in the first minute reached 12% with 1 g resin/L, 50% with 2 g resin/L, and 60% with 3 g resin/L. Boron was removed completely after 10 minutes when using 3 g resin/L and after 30 minutes with resin dosage of 2 g/L while it is removed completely after 120 minutes when 1 g resin/L was used as shown in Figure 4.9.

Figure 4.10 shows the effect of resin dosage on boron removal after 1 hour. By increasing the resin dosage from 0.2 to 1 g/L, the boron removal increased from 54 to 90 %. The removal reached 60, 74 and 84% when using 0.4, 0.6 and 0.8 g resin/L respectively.

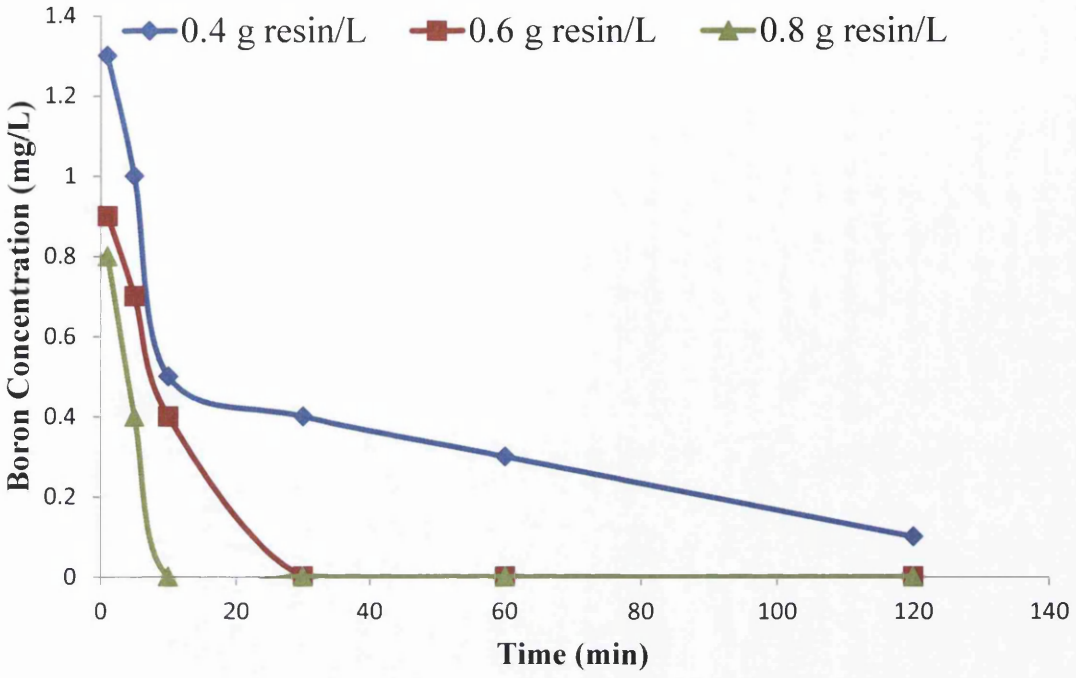

Figure 4.7 Effect of contact time on boron concentration. Initial boron concentration = 1.5 mg/L, pH= 8.0, T =25°C

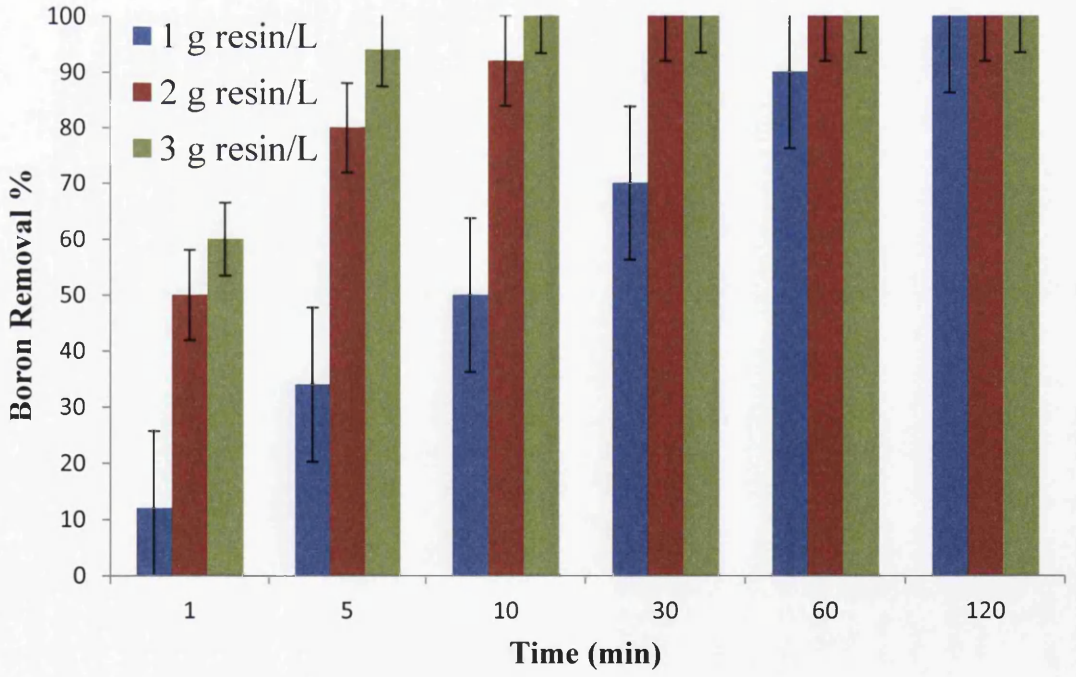

Figure 4.8 Effect of contact time on boron removal. Boron concentration = 5 mg/L, pH= 8.0, T =25°C

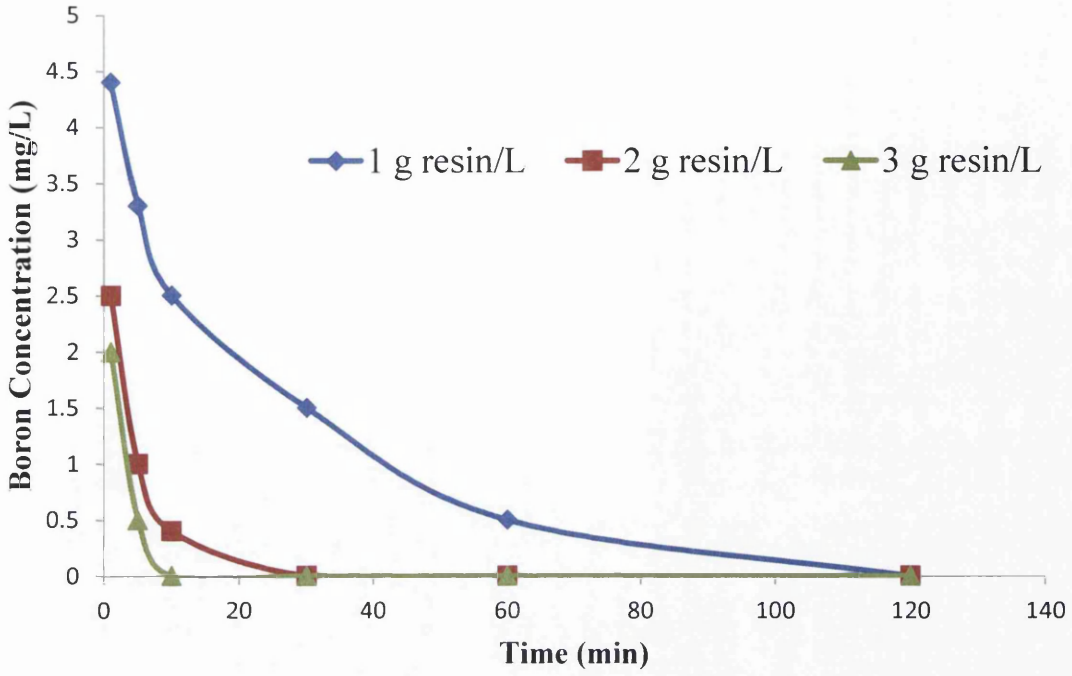

Figure 4.9 Effect of contact time on boron concentration. Initial boron concentration = 5 mg/L, pH= 8.0, T =25°C

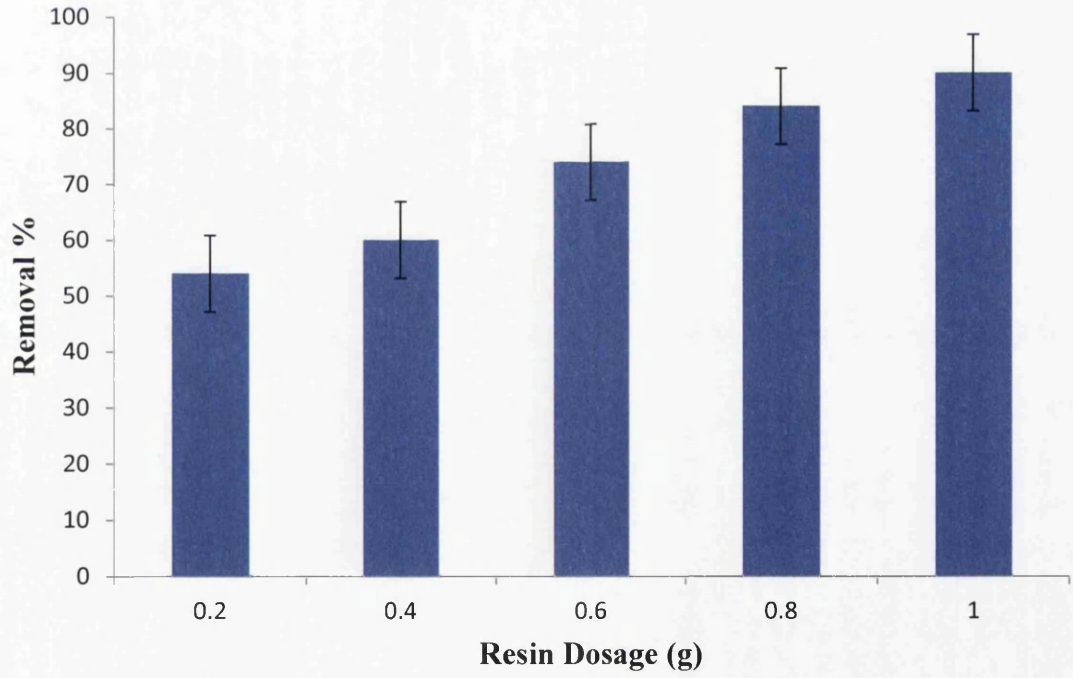

Figure 4.10 Effect of the resin dosage on boron removal. Boron concentration = 5.0 mg/L, pH=8.0, T=25 °C. Resin fraction (1-45 μm), time= 1 hr

4.4 Effect of Initial Boron Concentration

The effect of boron concentration in the solution on boron removal was studied at 3, 5, 10 and 15 mgB/L. The other parameters were kept constant at pH=8.0, T=25 °C and resin dosage of 0.2 g/L and each experiment ran for 1 hr. The boron removal decreased with increasing its concentration in the solution as shown in Figure 4.11. The removal was 18%, 27%, 54% and 90% from the initial boron concentration of 15, 10, 5 and 3 mg/L respectively. This might be because there were not enough active sites on the resin to adsorb so much boron with high initial concentrations. The equilibrium would be reached faster at lower initial concentration, probably because the more sorption sites are available to catch the available ions, which means faster adsorption in lower concentrations. As a result, reaching the equilibrium condition increased when the initial concentration of the solution increased (Ho et al., 1995, Parsaei et al., 2011).

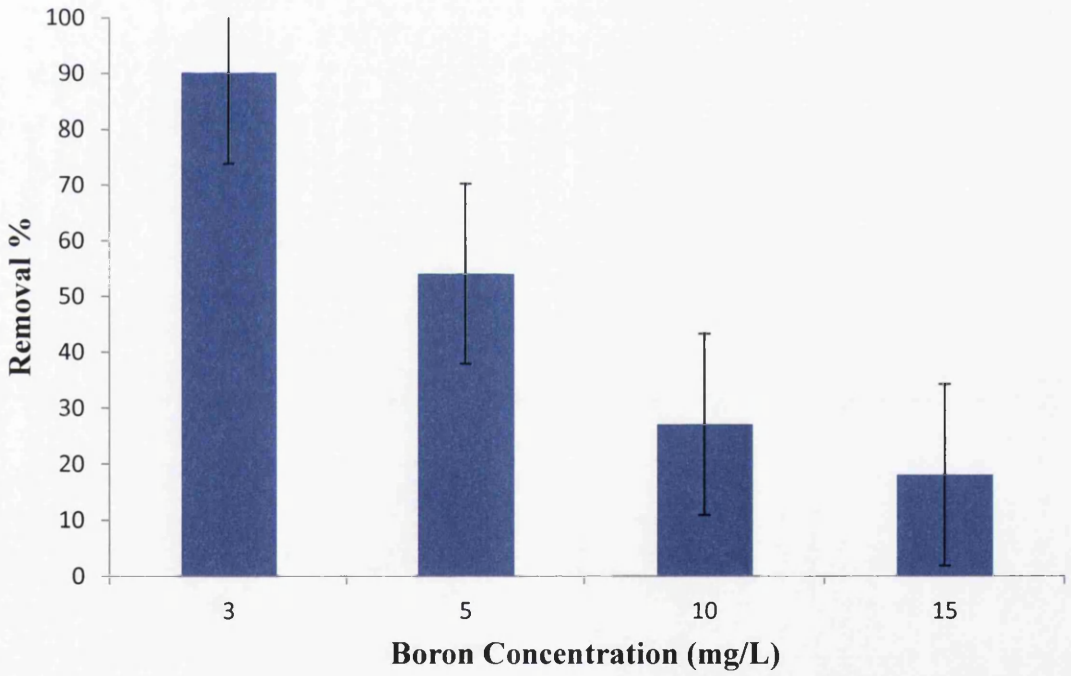

Figure 4.11 Effect of initial boron concentration on boron removal with Amberlite IRA743 resin (1-45 μm)

4.5 Effect of pH of Solution

In order to investigate pH effects on boron sorption, pH values of the $B(OH)_3$ solutions were adjusted to different values (4, 5, 6, 7, 8 and 10.5) by using NaOH or HCl solutions. The effect of solution pH on the efficiency of boron removal was evaluated in a batch system at constant temperature at 25°C, boron concentration of 5 mg/L at different resin dosages. As shown in Figure 4.12, the maximum sorption was achieved at pH=8 with removal efficiency of 90%. The lowest efficiency, on the other hand, was achieved at pH=4. To put it simply, the favorable pH range can be claimed as pH values between 7 and 8, as displayed in Figure 4.13. As was noted, at low pH(pH < 7), boric acid $B(OH)_3$ predominates in the solutions, while at higher pH, borate ion $B(OH)_4^-$ is the primary anion. Due to OH^- ions on the resin being exchanged with $B(OH)_4^-$ ions in solution, maximum boron removal was obtained at pH 8 (Öztürk and Kavak, 2008, Öztürk and Köse, 2008, Bektaş *et al.*, 2004, Bektaş and Öztürk, 2004). The pH dependence of boron removal may be interpreted by taking into account the formation of tetradentate complex of borate with N-methyl-D-glucamine and the dissociation process of $B(OH)_3$ (Yoshimura *et al.*, 1998, Li *et al.*, 2011).

Selective adsorption process of boron is driven by the formation of tetradentate complex, and increasing pH is favorable for the formation of tetradentate complex and thus for higher boron removal.

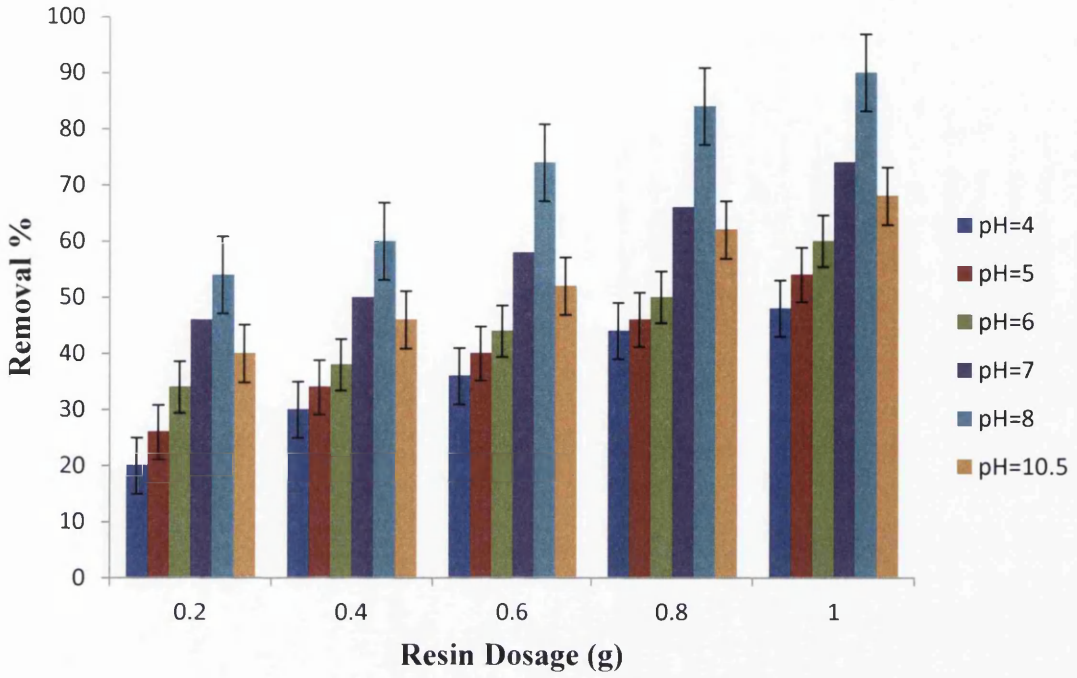

Figure 4.12 Effect of pH on efficiency of boron removal with Amberlite IRA743 resin (1-45 μm). Boron concentration = 5 mg/L, T=25 °C, time = 1 hr

However, a rise in pH also favor the dissociation process from $B(OH)_3$ into tetrahydroxyborate anion $B(OH)_4^-$, which exert an adverse effect on boron removal. At pH values around 9.0, $B(OH)_3$ reach the dissociation equilibrium (pKa = 9.2). Herein, increasing pH is more favorable to the formation of $B(OH)_4^-$ than of tetradentate complex, resulting in a decrease in boron removal efficiency; while in the pH range of 4.0–8.0, the amount of adsorbed boron and also the species of $B(OH)_4^-$ increase with the rise of pH.It was also found that the Amberlite IRA743 resin works as a chelating resin and shows high selectivity for the boron at basic pH (Pelin Demirçivi, 2008). The boron complexation at basic pH is carried out by the resin's hydroxyl groups which have different affinity for the species $B(OH)_3$ and $B(OH)_4^-$ (García-Soto and Munoz Camacho, 2005, Cengeloglu *et al.*, 2007).

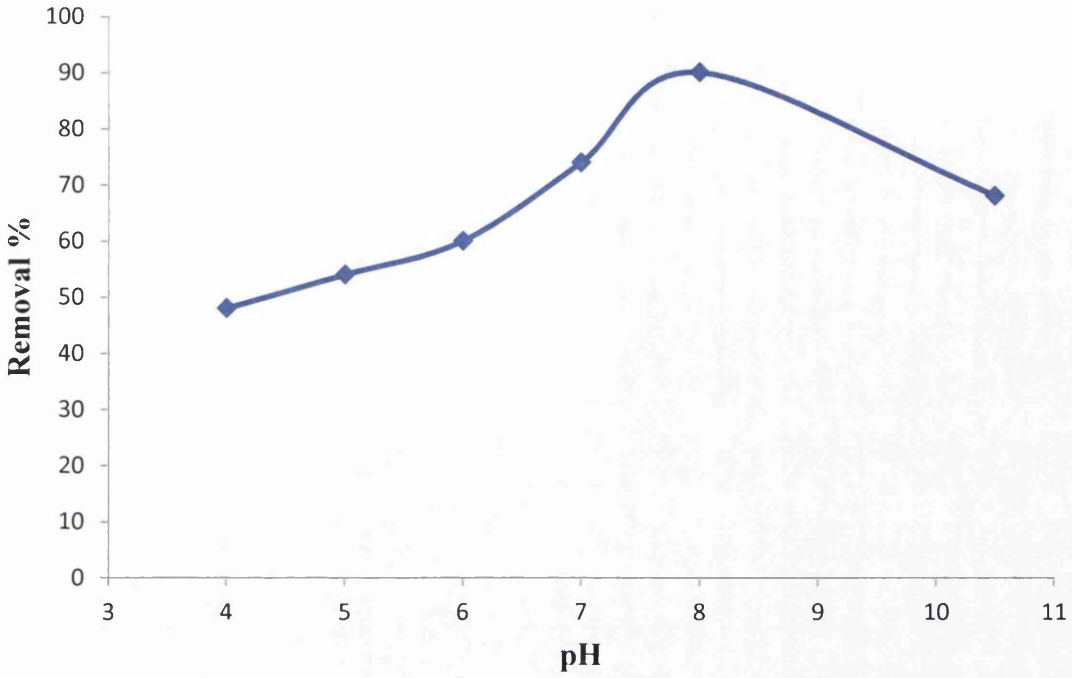

Figure 4.13 Variation of boron removal efficiency with Amberlite IRA743 resin (1-45 μm) with solution pH

4.6 Effect of Temperature

The effect of temperature on boron removal was studied at 15, 20, 25, 30 and 35°C at different resin dosage. Boron concentration of 5 mg/L and pH 8 were kept constant.

The results obtained are presented in Figure 4.14 which shows that boron removal increases when temperature of the solution increases from 15 to 35 °C. The removal increased from 42% at temperature 15°C to 70% at temperature 35°C when using resin concentration 0.2 g/L. The removal increases with increasing temperature at all the resin dosage used. This finding can be explained by accelerating of the random motion of boron molecules in solution when temperature increases. Such acceleration promotes the exchange process and as result binding of boron with the resin increases (Yan *et al.*, 2008, Xiao *et al.*, 2012). Also the fraction of borate ion increases with an increase of temperature of water (Hilal *et al.*, 2011).

Baek *et al.* (2007) studied the effect of temperature in the range of 10-70 °C using Amberlite IRA743 and found that the removal increased with increase in temperature from 10-40 °C and the profile for the removal of boron did not change at temperatures above 40 °C. same results were found by Yilmaz *et al.* (2005b), Boncukcuoğlu *et al.* (2004) and Xiao *et al.* (2012) while Bektaş and Öztürk (2004) found the removal decreased with increasing temperature.

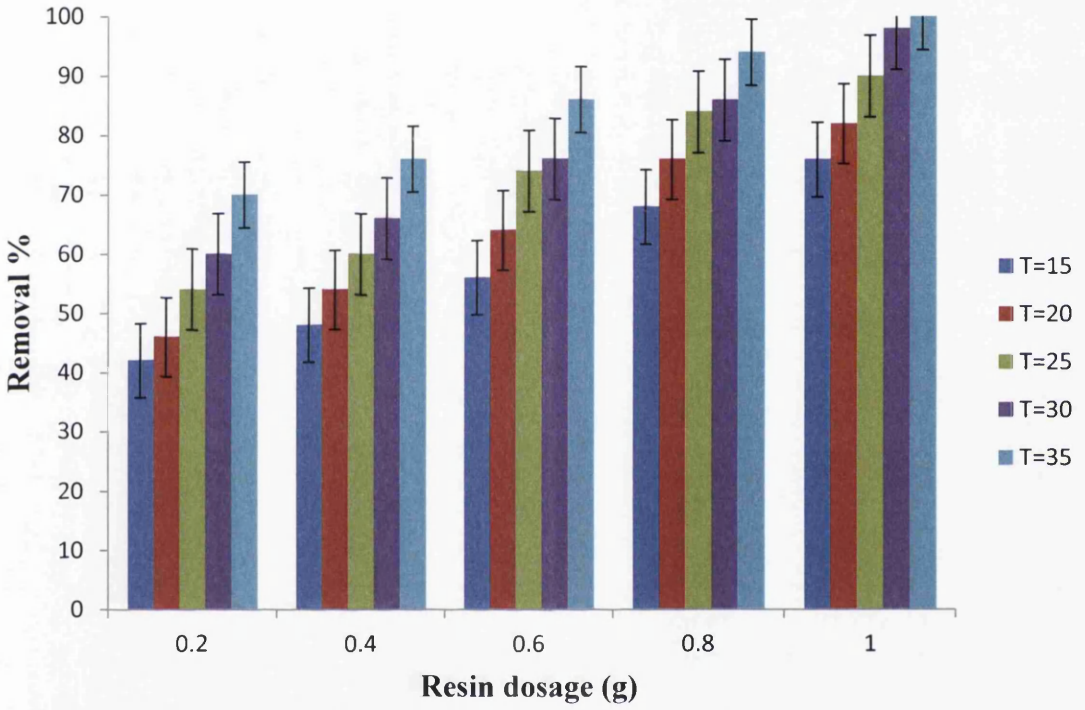

Figure 4.14 Effect of solution temperature on boron removal. Boron concentration = 5 mg/L, pH= 8, time = 1 hr

4.7 Effect of other ions

In the previous sections of this chapter, the effect of these parameters on boron removal with ion-exchange resin was studied in pure $B(OH)_3$ model solution . However in real aqueous systems, several other ions are usually presented which can affect boron removal by Amberlite IRA743 resin. To check the possibility of theses ions effect on

boron removal, boron removal with Amberlite IRA743 resin was examined in the presence of NaCl , Na_2SO_4 and $MgCl_2$ salts. Table 4.2 shows the investigated salts and their used concentrations and Table 4.3 shows the concentration of anions and cations of the salts mixture used.

Table 4.2 The investigated salts and their concentration ranges

Salt	**NaCl**	**Na_2SO_4**	**$MgCl_2$**
Lowest concentration (mg/L)	5000	3000	5000
Highest concentration (mg/L)	35000	10000	20000

Table 4.3 The ions concentration for the investigated salt mixture

Ion	Mixture (NaCl + $MgCl_2$ + Na_2SO_4)
Na^+	10880
Cl^-	18250
Mg^{+2}	1320
SO_4^{-2}	2720

The experiments run with change in the salts concentration while the other parameters were kept constant (T = 25°C, pH = 8, boron concentration = 5 mg/L, resin dosage = 2 g/L, time = 10 minutes).

The increase in NaCl concentration results are shown in Figure 4.15. From this Figure, it can be seen that there is a slightly decrease in boron removal with the presence of NaCl

salt. There is no relationship between the decrease in the boron removal and the increase in salt concentration.

Figure 4.16 shows the results of increasing $MgCl_2$ concentration on boron removal. As can be seen from this Figure, there is an improvement in the removal at $MgCl_2$ concentrations 5000 and 10000 mg/L while there is a slight decrease at 20000 mg/L.

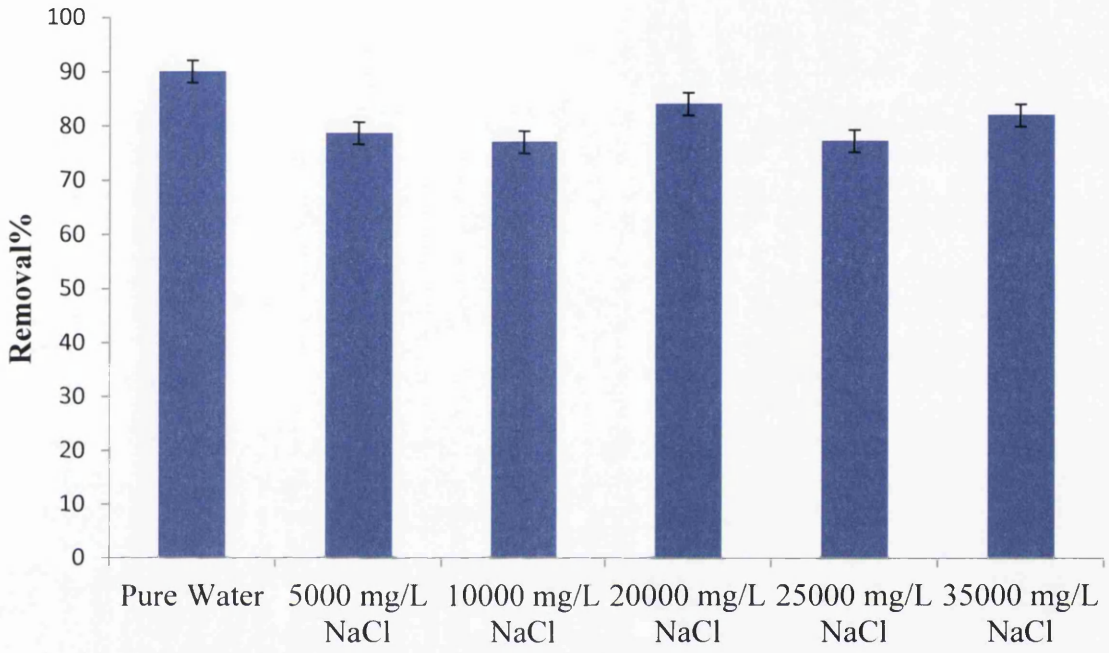

Figure 4.15 Effect of NaCl and concentration on boron removal by Amberlite IRA743

The effect of increasing Na_2SO_4 concentration on boron removal is shown in Figure 4.17. There is a small decrease in the removal at Na_2SO_4 concentration of 3000 mg/L while there is no effect of the salt at 5000 and 10000 mg/L Na_2SO_4.

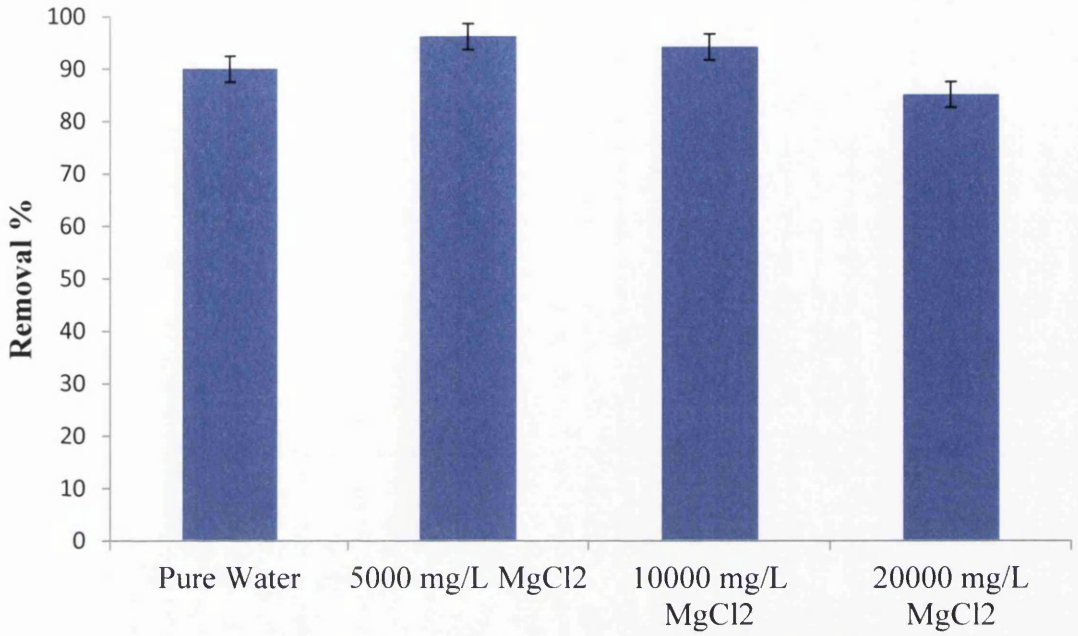

Figure 4.16 Effect of $MgCl_2$ concentration on boron removal by Amberlite IRA743

The presence of these salts at concentrations representing their concentrations in seawater (Table 4.4) on boron removal is shown in Figure 4.18. There is no noticeable change in the boron removal in the presence of these salts.

Öztürk and Köse (2008) found that the sorption of boron by Dowex 2×8 resin was significantly decreased by the addition of NaCl, $CaCl_2$ and Na_2SO_4. Badruk and Kabay (2003) found the same results as the presence of NaCl lead to decrease in boron sorption by CRB02 resin. The increase in boron removal in the presence of $MgCl_2$ may explained as the fact of precipitation of Mg ions in hydroxide form in the microenvironment of the resin phase. Apparently hydroxide ions are produced by tertiary amine function of the resin and hydroxide ions cause precipitation of $Mg(OH)_2$ on resin particles and magnesium hydroxides form corresponding borates which are insoluble in water which has some affectivities on boron sorbents (Biçak *et al.*, 2001).

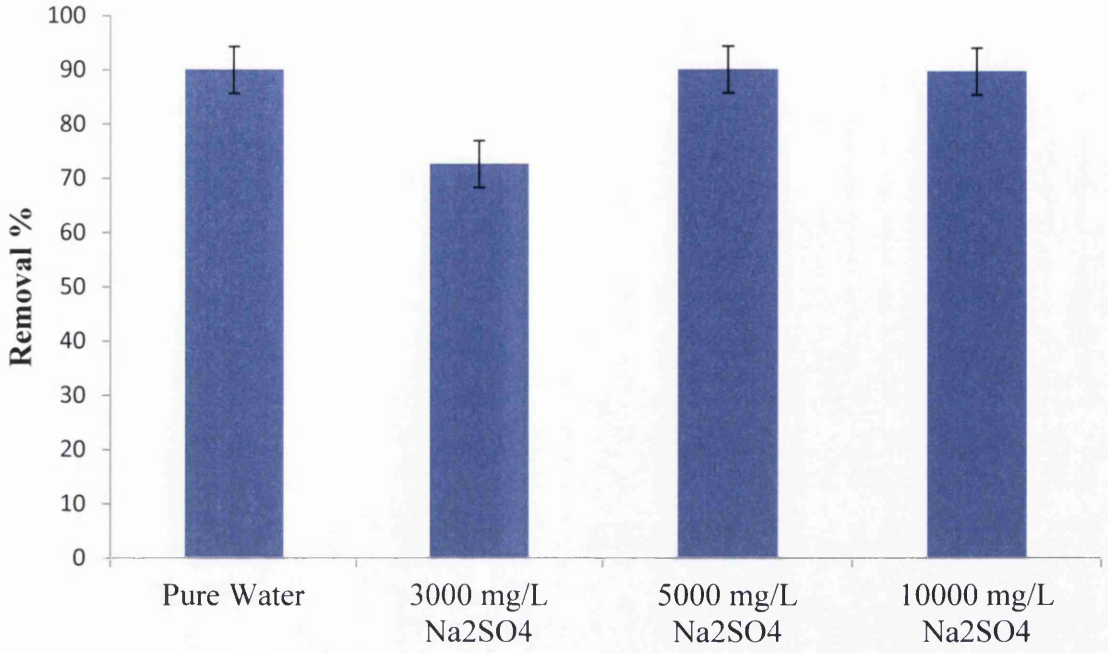

Figure 4.17 Effect of Na_2SO_4 concentration on boron removal by Amberlite IRA743

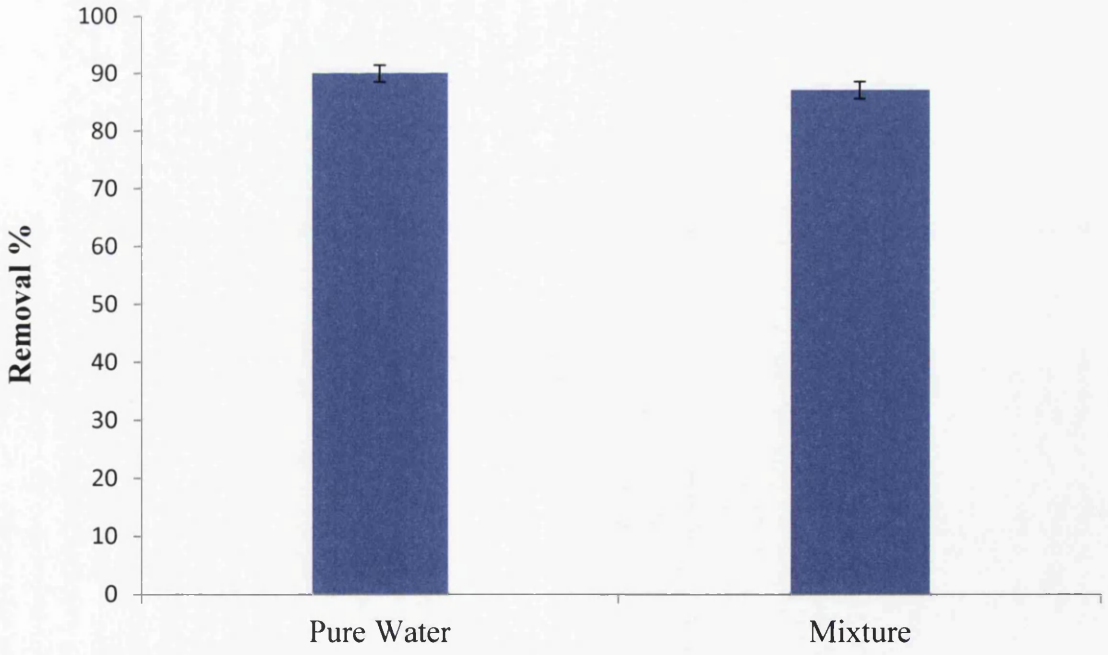

Figure 4.18 Effect of salt mixture on boron removal by Amberlite IRA743

4.8 Adsorption behaviour of boron

The modeling of the adsorption kinetics is fundamentally important in water treatment process design (Morisada *et al.*, 2011). In the present study, the pseudo-second order model was employed to evaluate the adsorption kinetic data for the resin used obtained at two boron concentrations , 1.5 and 5 mg/L, because this model expression provides the best correlation of the experimental data in many cases (Ho and McKay, 1999, Sağ and Aktay, 2002). The kinetic equation for the pseudo-second order model is described as:

$$\frac{dq}{dt} = k_2(q_e - q)^2 \qquad 3.2$$

where k_2 is the pseudo-second order rate constant. Integrating Eq. (2) with the boundary conditions, t = 0 to t = t and q = 0 to q = q, gives

$$\frac{1}{(q_e - q)} = \frac{1}{q_e} + k_2 t \qquad 3.3$$

Above equation can be rewritten as (Chowdhury and Saha, 2010):

$$q_t = \frac{k_2 q_e^2 t}{1 + k_2 q_e t} \qquad 3.4$$

Where q_t and q_e are the amount of boron adsorbed at time t and at equilibrium (mg/g) and k_2 (g/ mg.min) is the pseudo-second-order rate constant for the adsorption process. Equation 3.4 can be linearized to (Chowdhury and Saha, 2010):

$$\frac{t}{q_t} = \frac{1}{k_2 q_e^2} + \frac{1}{q_e} t \qquad 3.5$$

The constant k_2 and the amount of boron adsorbed at equilibrium q_e can be obtained by plotting t/q_t vs. t.

Figure 4.19 shows the time course variations for boron adsorption at boron concentration of 1.5 mg/L , pH = 8 , T= 25°C and resin dosage 0.4 g/L while Figure 4.20 shows the

time variation of boron concentration at 5 mg/L with the same conditions. Linear relationships between t and $^{t}/_{q_t}$ were obtained, indicating the adsorption behavior of boron by the resin agreed with pseudo-second order kinetics. The rate constant k_2 and q_e calculated from equation 3.5, are summarized in Table 4.4, together with equations of the regression lines and correlation coefficients (R^2).

Table 4.4 The pseudo-second order constant

Initial boron concentration, mg/L	Equation	R^2	$\mathbf{q_e}$, **mg/g**	$\mathbf{k_2}$, $\frac{\mathbf{g}}{\mathbf{mg.min}}$
1.5	y = 0.2728x + 2.2484	0.9949	3.67	0.033
5	y = 0.1846x + 2.1332	0.9963	5.41	0.016

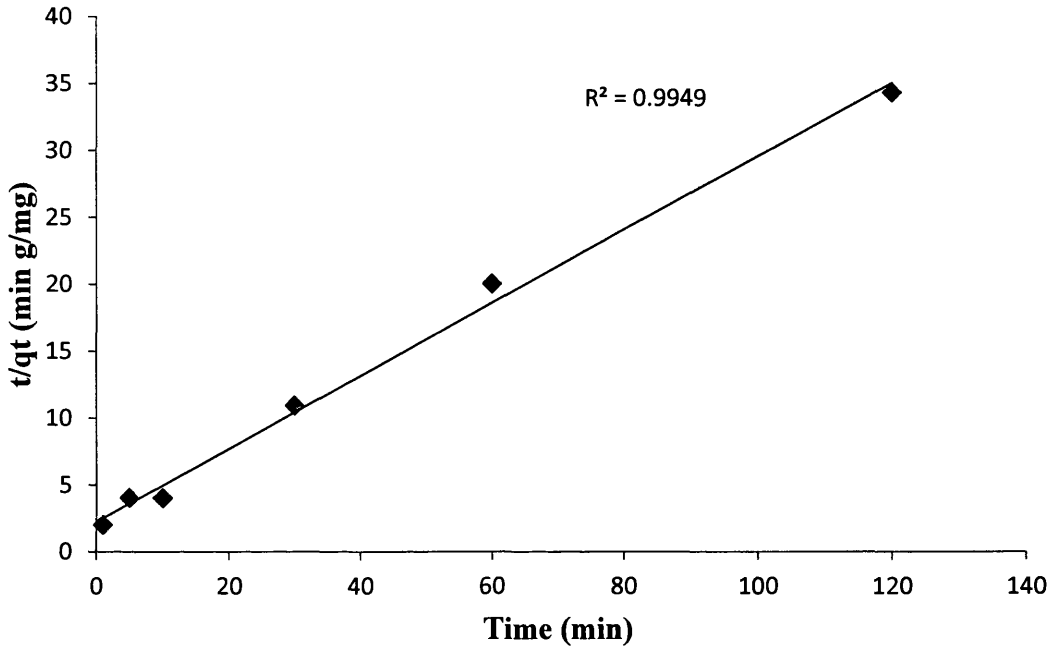

Figure 4.19 Pseudo-second-order kinetics for adsorption of boron on Amberlite IRA743, boron concentration=1.5 mg/L, resin dosage=0.4 g/L, pH=8, T=25°C

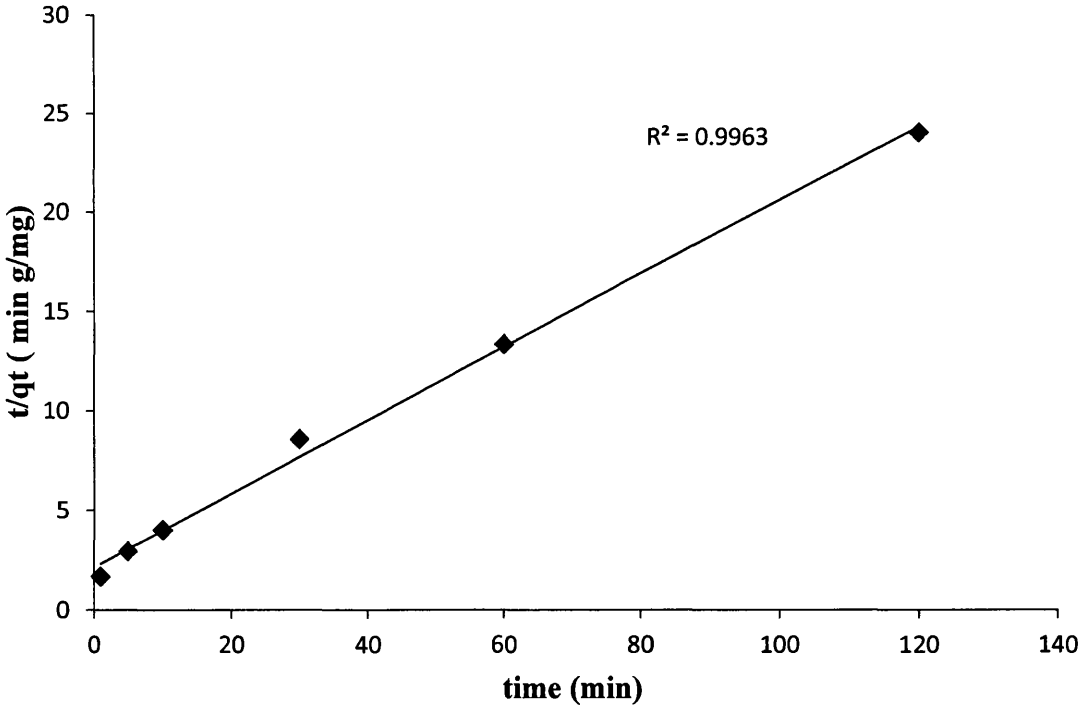

Figure 4.20 Pseudo-second-order kinetics for adsorption of boron on Amberlite IRA743, boron concentration=5 mg/L, resin dosage=0.4 g/L, pH=8, T=25°C

4.9 Conclusions

In this chapter, the impact of operational parameters on boron removal by Amberlite IRA743 resin was studied in a batch system. The effect of contact time, resin particle size, boron concentration, solution temperature, pH, resin dosage and NaCl, Na_2SO_4 $MgCl_2$ and salts mixture on boron removal from water were studied and the results showed that:

- The fraction of Amberlite IRA743 resin with the smaller particle size remove boron faster than the fraction of larger particle size due to higher surface area. The fraction in the range of (1-45 μm) was faster in removing boron than the particles with size of (150-180 μm) and (500-700 μm).
- The increase in contact time of boron solution with the resin will lead to decrease the boron concentration in the solution and enhance the removal.
- The boron removal increases with increasing pH up to 8 and decreased at pH 10.5. At low pH(pH < 7), boric acid $B(OH)_3$ predominates in the solutions, while at higher pH, borate ion $B(OH)_4^-$ is the primary anion.
- The boron removal increased with increasing the temperature of the solution which is due to the acceleration of the random motion of boron molecules in solution.
- The increase in resin dosage will increase the removal since the increase of the adsorbent doses provides a greater surface area and adsorption sites.
- The increase in feed boron concentration will decrease the boron removal because there were not enough active sites on the resin to adsorb so much boron with high initial concentrations.
- Increasing the concentration of NaCl will cause a slight decrease in the boron removal. There is an improvement in the boron removal when the solution contains 5000 and 10000 mg/L of $MgCl_2$ while the removal decreases with the presence of 20000 mg/L of $MgCl_2$. In case of increasing Na_2SO_4, there is a slight decrease in boron removal when using a solution with 3000 mg/L of Na_2SO_4, but the removal doesn't change in the presence of 5000 and 10000 mg/L of Na_2SO_4.

CHAPTER 5

The effect of operational parameters on permeate flux for hybrid adsorption-microfiltration process of boron removal

5.1 Introduction

The hybrid adsorption-microfiltration process combines two processes, adsorption and filtration of the suspension by microfiltration membrane. In the previous chapter, the adsorption process was investigated by studying the effect of different parameters on the adsorption of boron by the boron selective ion exchange Amberlite IRA resin.

Microfiltration is a separation technique for removing micron-sized particles uses membrane filters with pores in the approximate size range 0.1 to 10 μm, which are permeable to the fluid, but retain the particles, thus causing separation (Huisman, 2000).

The water flux (J) through a membrane is expressed as the amount of water V [L] flowing through a certain membrane area A [m^2] in time t [h]:

$$J=\frac{V}{A\,t} \qquad 5.1$$

The permeability K of the membrane is defined as

$$K=\frac{J}{TMP} \qquad 5.2$$

Where TMP is the trans-membrane pressure calculated as follows:

$$TMP=\frac{P_{inlet}+P_{outlet}}{2}-P_{permeate} \qquad 5.3$$

It is well known that in pressure-driven cross flow microfiltration (CFMF), suspended particles are transported to the membrane by the permeate flow resulting in clogging of the membrane pores or forming a deposit layer. It affects the membrane performance.

The presence of a deposit layer introduces additional resistance to permeate flow while the pore clogging changes the effective membrane pore size distribution (Tarleton and Wakeman, 1994, Kwon *et al.*, 2000a, Kwon *et al.*, 2000b).

In this chapter the separation of ion exchange Amberlite IRA743 resin loaded with boron from water by microfiltration was investigated by studying the effect of different operational parameters on the membrane permeate flux. The effect of membrane pore size, resin concentration, transmembrane pressure, pH and addition of NaCl , Na_2SO_4 and $MgCl_2$ salts in feed on permeate flux has been studied.

Three different pore size polyvinylidene fluoride (PVDF) membranes were used in these experiments. The trans-membrane pressure used was ranging from 0.2-1.5 bar while the range of Amberlite IRA743 resin concentration was 0.2-1 g resin/L. The solution pH varied between 4 and 10.5. The concentrations of NaCl, $MgCl_2$ and Na_2SO_4 were chosen in the range of their concentration in seawater.

The pure water fluxes for the membranes (0.1, 0.22 and 0.45 μm) are shown in Figures 5.1, 5.2 and 5.3. The permeability values of these membranes is, 3325 L/m².hr , 7581 L/m².hr and 26439 L/m².hr for 0.1 μm PVDF, 0.22 μm PVDF and 0.45 μm PVDF, respectively.

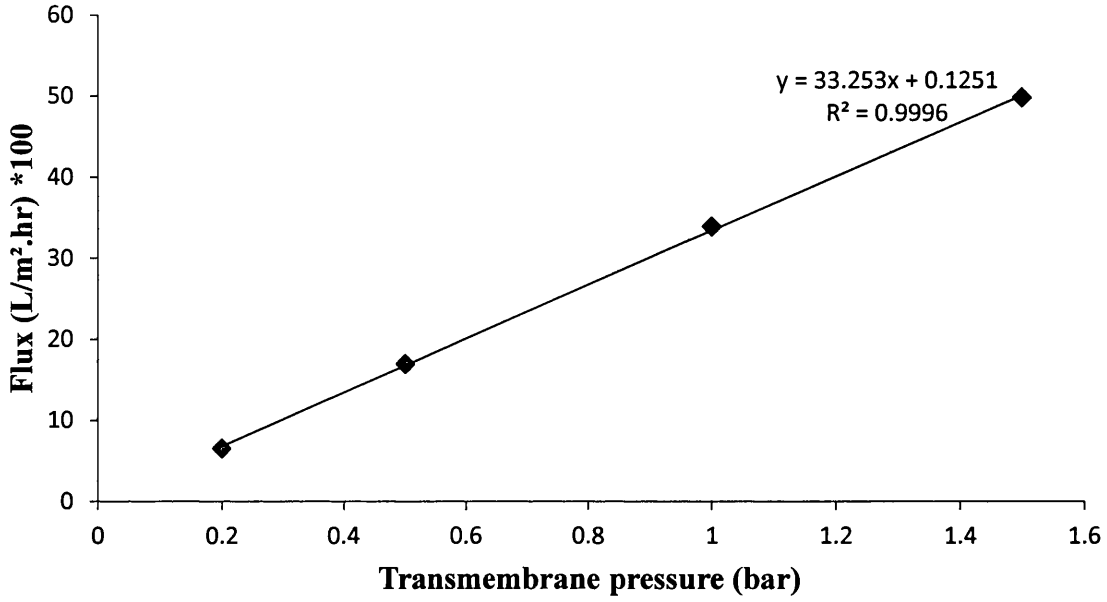

Figure 5.1 Pure water flux of 0.1μm PVDF membrane at various operating pressures

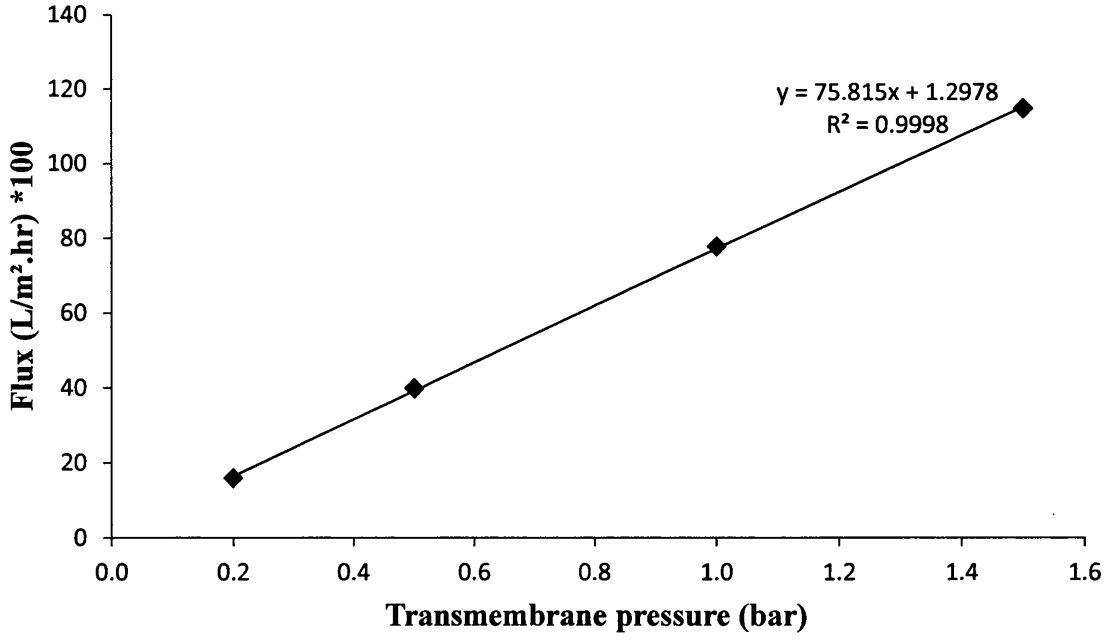

Figure 5.2 Pure water flux of 0.22μm PVDF membrane at various operating pressures

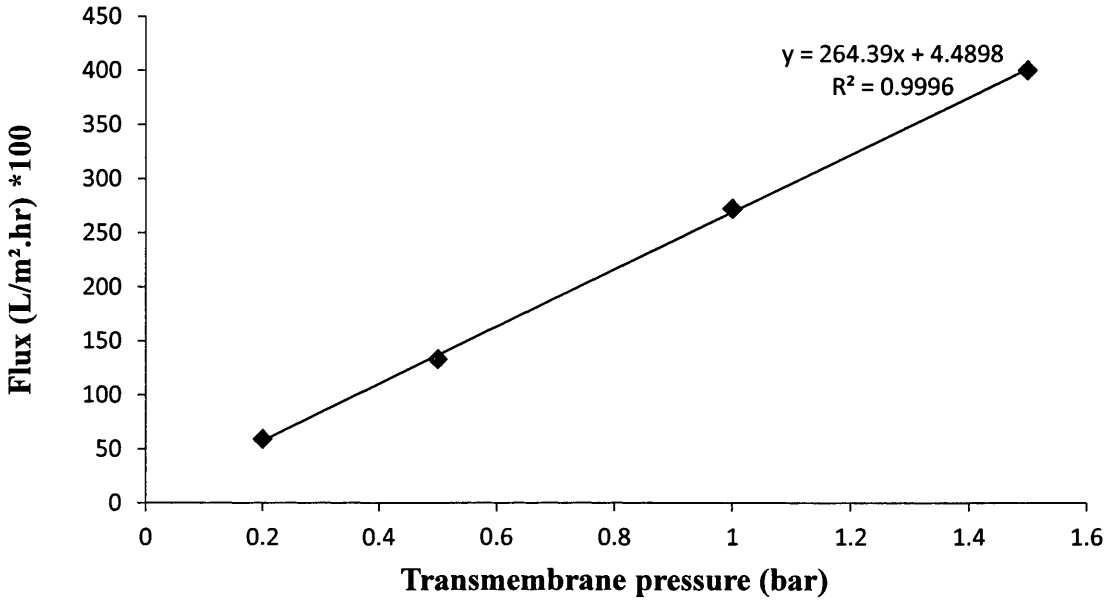

Figure 5.3 Pure water flux of 0.45μm PVDF membrane at various operating pressures

5.2 Effect of membrane pore size on permeate flux

In this section, the effect of membrane pore size on permeate flux and volume of permeate was investigated. Three microfiltration PVDF membranes with pore size of 0.1, 0.22 and 0.45 μm have been used. The particle size of Amberlite IRA743 resin used was in the range of 1-45 μm. The other parameters were kept constant as pH= 6 and T= 25°C. Two different operating pressures were applied (0.5 and 1.5 bar). The results shown in Figure 5.4 and Figure 5.5 present the permeate flux as a function of time while Figure 5.6 and Figure 5.7 shows the volume of permeate collected at the end of each experiment. The results from Figure 5.4 and 5.5 show that the flux increased when the membrane pore size increased form 0.1 μm to 0.22 μm whereas there is a decline in the flux as the membrane with pore size of 0.45 μm is used. Pseudo-steady fluxes were 275, 389, and 358 L/m².hr for the membranes 0.1, 0.22 and 0.45 μm respectively at pressure of 0.5 bar and 401, 655, and 600 L/m².hr at pressure of 1.5 bar. The permeate flux in the

beginning of the filtration is 2280, 1976 and 1066 L/m².hr for the membrane with pore size 0.22, 0.45 and 0.1 μm respectively.

The variation of filtration flux can be divided into two stages, a quickly decay and a pseudo-steady stage. At the early period of filtration, the flux attenuates very quickly due to the quicker membrane blocking and particle deposition which leads to the reduction in membrane porosity (Hwang *et al.*, 2008, Dizge *et al.*, 2011). In fact, the fluxes approach pseudo-steady values in some conditions, and the flux is quicker to reach the pseudo-steady value under a lower filtration pressure (Hwang *et al.*, 2008). In addition, the lowest filtration flux was found for the membrane with the largest pore size of 0.45 μm. This is due to severe pore blocking when more particles can accumulate in the wide-porous structure of the membrane. This phenomenon becomes less obvious under a lower filtration pressure (Hwang *et al.*, 2008). As can be seen in Figure 5.4, the fluxes of the membranes with different pore sizes are very close at operating pressure of 0.5 bar while the fluxes are essentially varied when the pressure applied increased to 1.5 bar as shown in Figure 5.5.

As can be seen in the Figure 5.8, the deposited particles were capable of clogging the pores more completely in the membrane with larger pore size (Kwon *et al.*, 2000a).

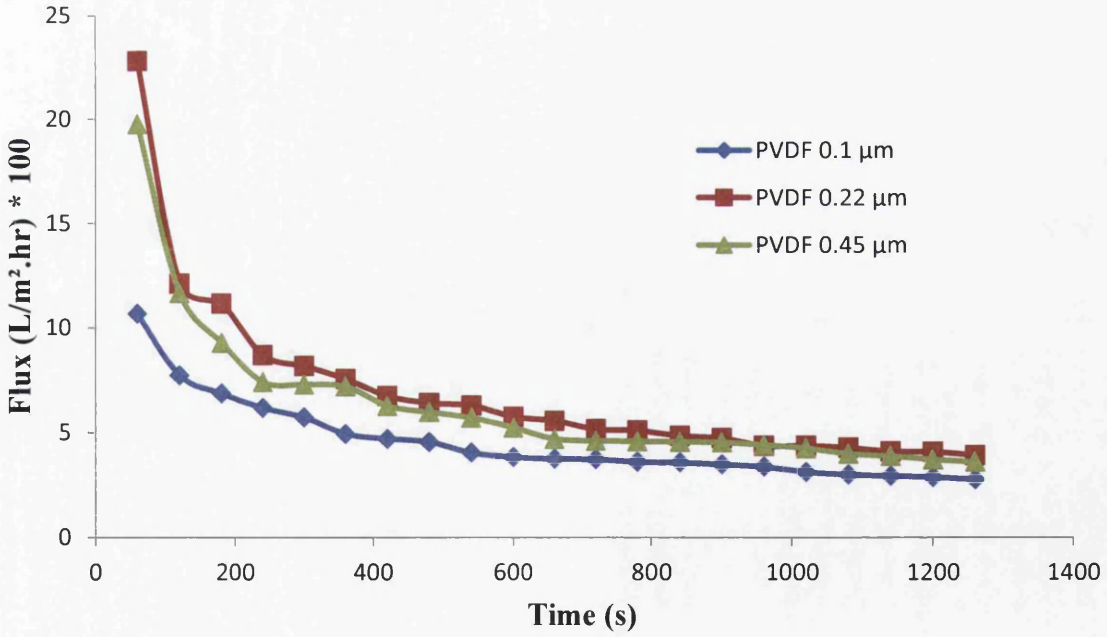

Figure 5.4 Effect of membrane pore size on permeate flux at microfiltration of Amberlite IRA743 resin suspension at operating pressure of 0.5 bar. Resin concentration=1g/L

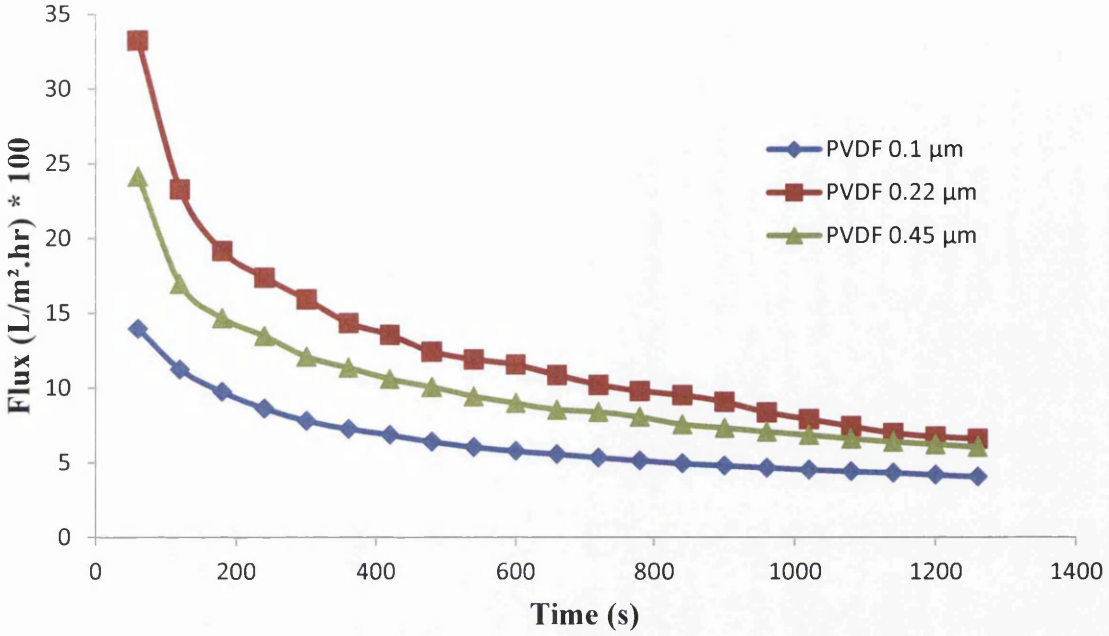

Figure 5.5 Effect of membrane pore size on permeate flux at microfiltration of Amberlite IRA743 resin suspension at operating pressure of 1.5 bar. Resin concentration=1g/L

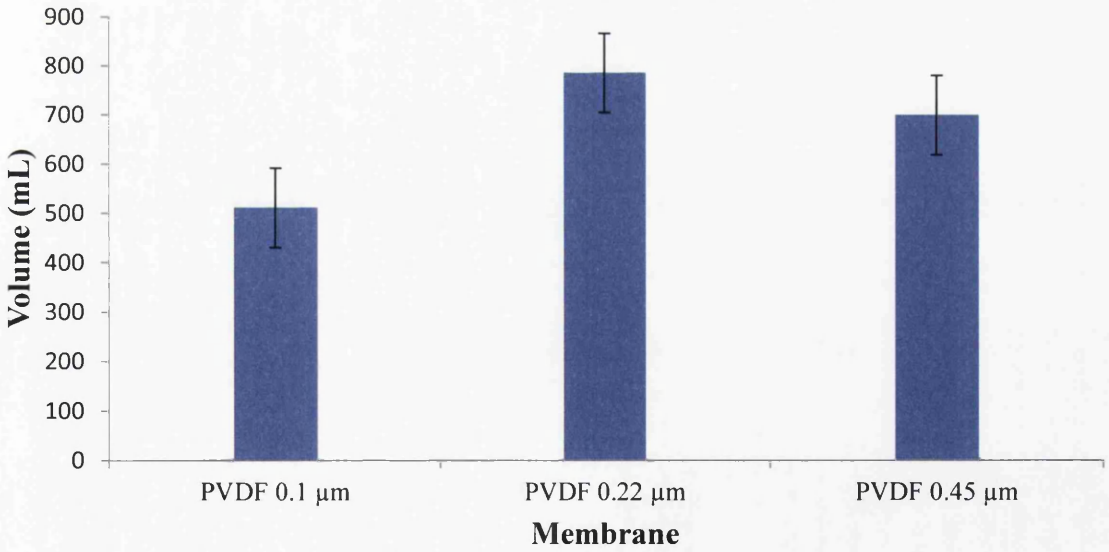

Figure 5.6 Effect of membrane pore size on permeate volume at microfiltration of Amberlite IRA743 resin suspension at operating pressure of 0.5 bar . Filtration time is 21 min. Resin concentration=1g/L

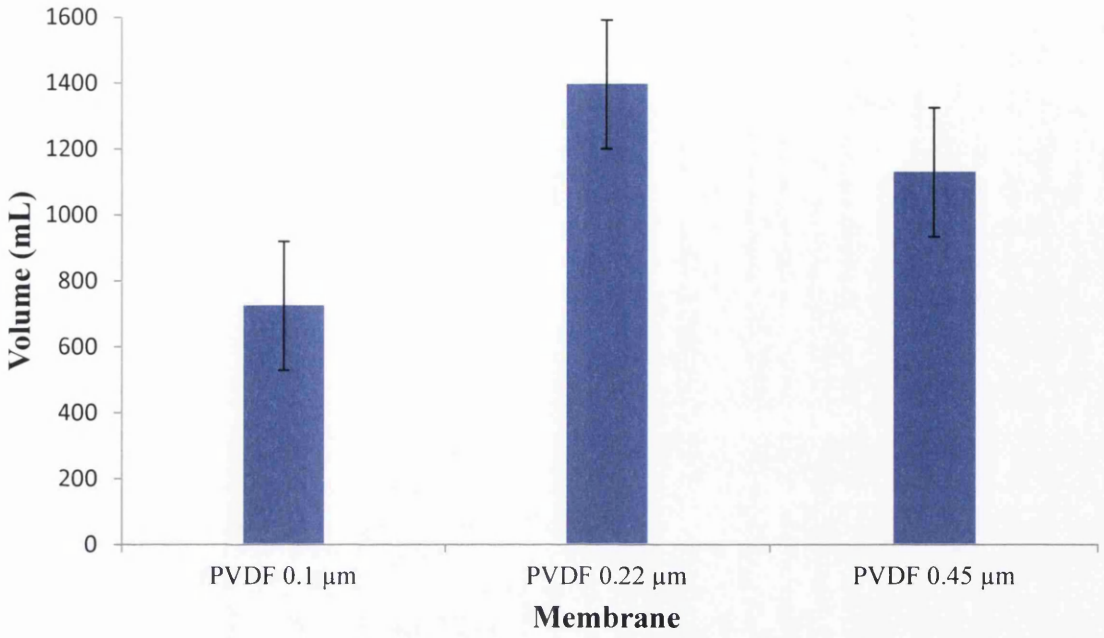

Figure 5.7 Effect of membrane pore size on permeate volume at microfiltration of Amberlite IRA743 resin suspension at operating pressure of 1.5 bars . Filtration time is 21 min. Resin concentration=1g/L

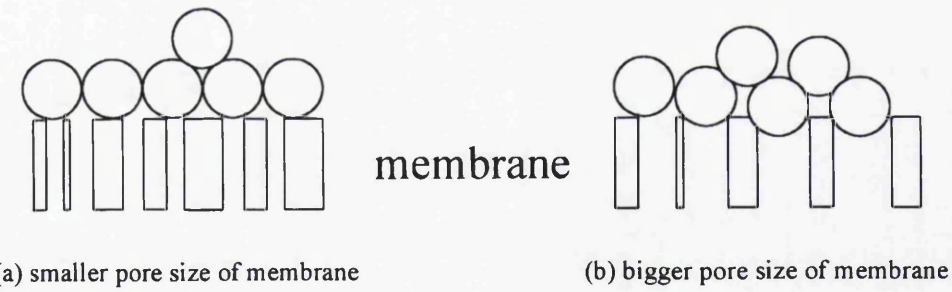

Figure 5.8 Schematic presentation of deposited particles onto membranes with smaller and larger pore sizes, (Kwon et al., 2000a)

The permeate was analyzed to check a content of total dissolved solids (resin particles) and found the concentration ranged between 0-2 mg/L as shown in Table 5.1 and no relationship between membrane pore size and the resin particles found in the permeate.

Table 5.1 Resin concentration in the permeate, resin concentration in the feed= 1 g/L

Membrane	**Resin** concentration in the permeate (**mg/L**)	
	At pressure 0.5 bar	At pressure 1.5
0.1 µm PVDF	0	2
0.22 µm PVDF	0	1
0.45 µm PVDF	0	0

5.3 Effect of transmembrane pressure on permeate flux

The effect of transmembrane pressure on permeate flux and permeate volume was studied at 0.2, 0.5, 1, and 1.5 bars for the three different pore size PVDF membranes (0.1, 0.22, and 0.45 μm) at two resin dosages of 0.2 and 1 g/L. The other parameters were kept constant as pH=6, and T=25°C. The change in flux with time at different pressures and the resin dosage of 0.2 g/L is shown in figures 5.9, 5.11 and 5.13 for the membranes with pore size 0.1μm PVDF, 0.22 μm PVDF and 0.45 μm PVDF respectively. Figures 5.10, 5.12 and 5.14 present the change of flux with time at different pressures and resin dosage of 1 g/L 13 for the membranes with pore size 0.1μm PVDF, 0.22 μm PVDF and 0.45 μm PVDF respectively.

As seen in these Figures, an increase in filtration pressure leads to a higher filtration flux due to the higher driving force.

From Figure 5.9, the permeate flux in the beginning of the filtration was 4028, 2769, 1730 and 761 L/m².hr at 1.5, 1 , 0.5 and 0.2 bar for the membrane with pore size of 0.1 μm. As can be seen in Figures 5.9-5.14, higher applied pressure leads to higher initial fluxes however little effect is seen after initial deposition of particles on the membrane. For example, in Figure 5.10, the initial permeate flux is 1393 and 258 L/m².hr at 1.5 and 0.2 bar respectively while the permeate flux at the end of experiments is 401 and 129 L/m².hr at 1.5 and 0.2 bar respectively. The results show that permeate flux declines more rapidly with increasing transmembrane pressure (Hong *et al.*, 1997). As can be seen from Figure 5.10, the permeate flux declines by 44.22% after 5 minutes when the pressure is 1.5 bar while it decreases by 16.27% after the same period when applying a pressure at 0.2 bar. This behavior shown can be explained by the increase in particle deposition rate at higher transmembrane pressures. Particle flux into the cake layer is enhanced at high transmembrane pressures because of the increased permeate flux, causing increased particle accumulation in the cake layer (Hong *et al.*, 1997).

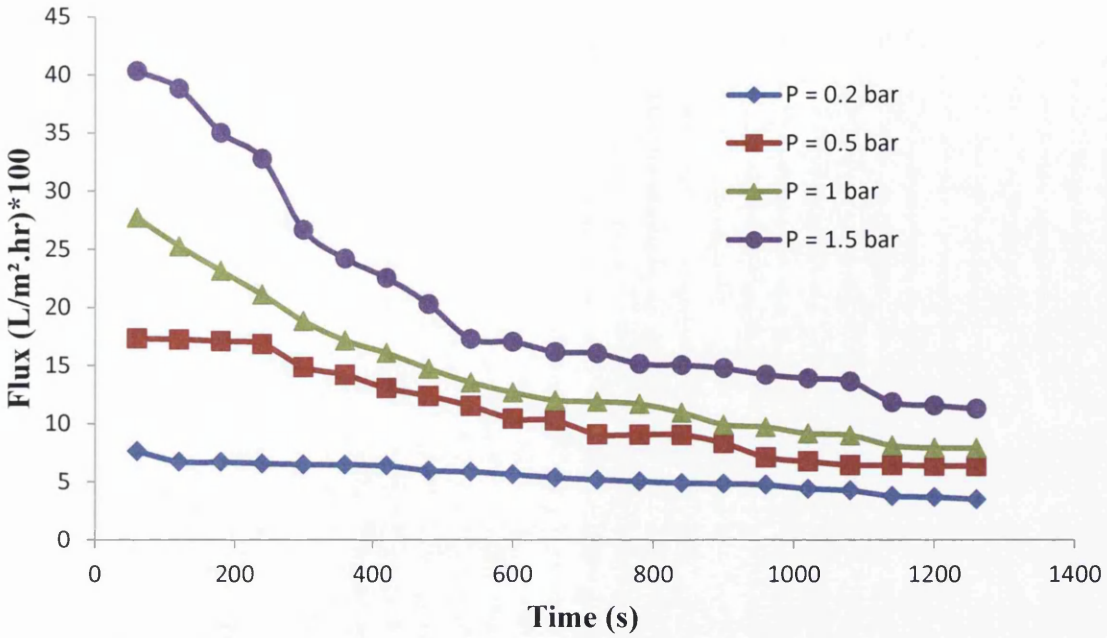

Figure 5.9 Effect of operating pressure on flux at microfiltration of Amberlite IRA743 resin suspension through the PVDF membrane with pore size of 0.1 μm. The resin concentration is 0.2 g/L

Faster flux decline at high transmembrane pressure may also be attributed to the formation of a more densely packed cake layer. It has been experimentally shown that cake layers can be more compressed at high transmembrane pressures due to the drag force induced by permeate flow (Chudacek and Fane, 1984).

As time progresses toward pseudo-steady state, the difference between the permeate fluxes for the used membranes with the applied pressures decreases. Figure 5.13 shows that the difference between the permeate fluxes in the beginning of the filtration at pressure 0.5 and 0.2 bar is 62.06% while this difference decreases to 19.24% at the end of the experiment.

At this stage of the filtration process, the flux behavior is controlled to a large extent by the resistance of the cake layer. Since thicker, and thus more resistant, cake layers are formed at higher applied pressures, the effect of the increased pressure on the permeate flux at the latter stages of the cross flow filtration is not as significant (Hong et al., 1997).

Blahušiak *et al.* (2009), Blahušiak and Schlosser (2009) and Onderková *et al.* (2009) used XUS-43594 resin and Blahušiak *et al.* (2009) and Onderková *et al.* (2009) used XUS-G3 resin and their results showed that with the increasing trans-membrane pressure difference, the permeate flux increases significantly.

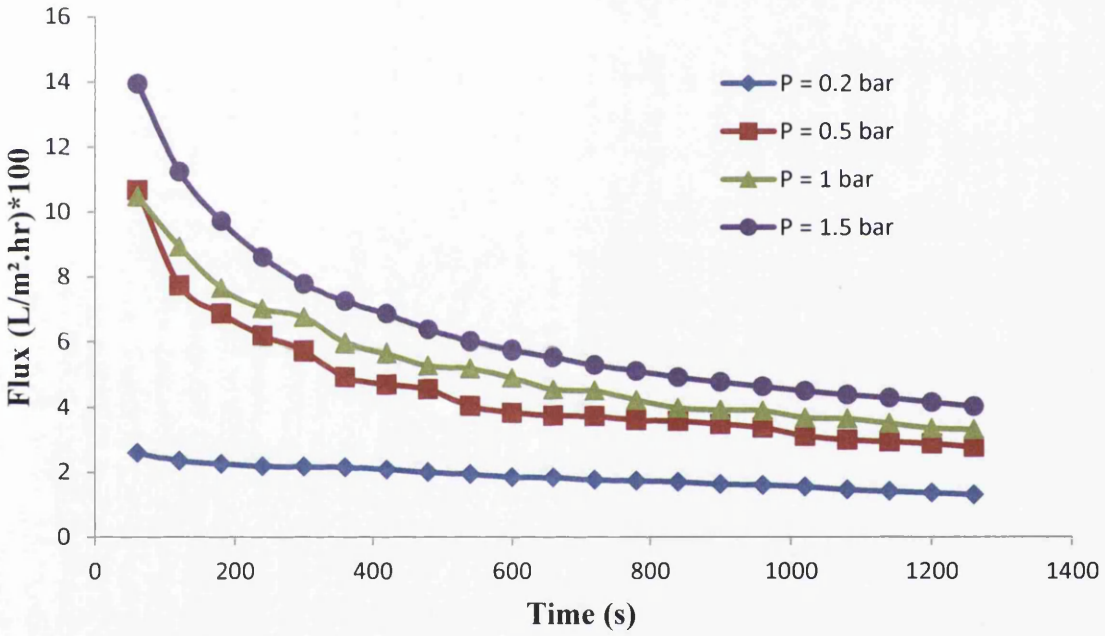

Figure 5.10 Effect of operating pressure on flux at microfiltration of Amberlite IRA743 resin suspension through the PVDF membrane with pore size of 0.1 μm. The resin concentration is 1.0 g/L

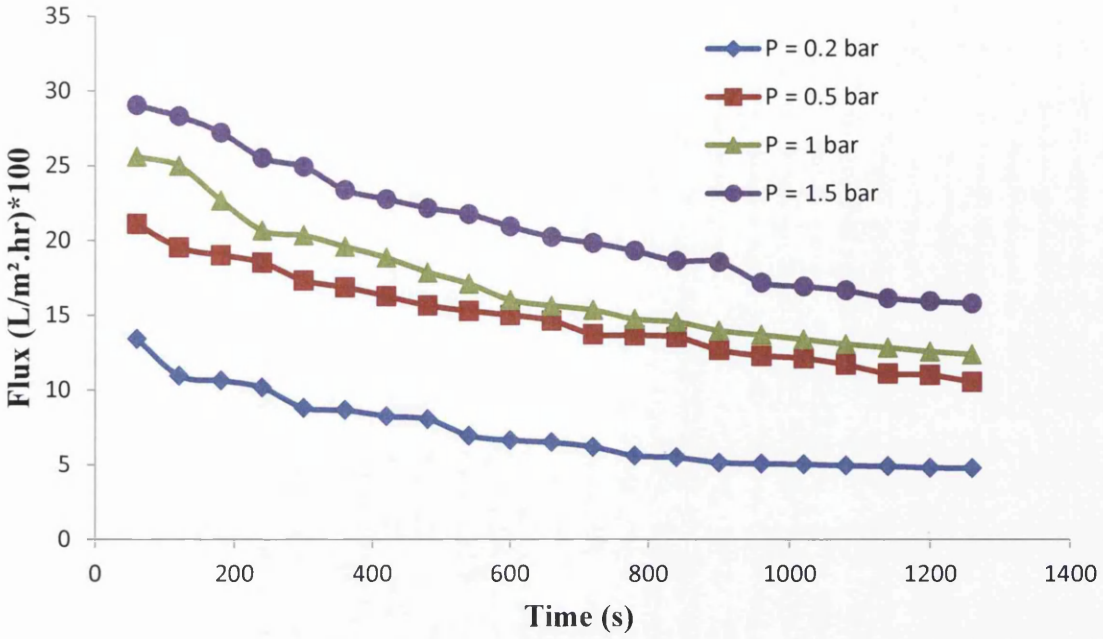

Figure 5.11 Effect of operating pressure on flux at microfiltration of Amberlite IRA743 resin suspension through the PVDF membrane with pore size of 0.22 µm. The resin concentration is 0.2 g/L

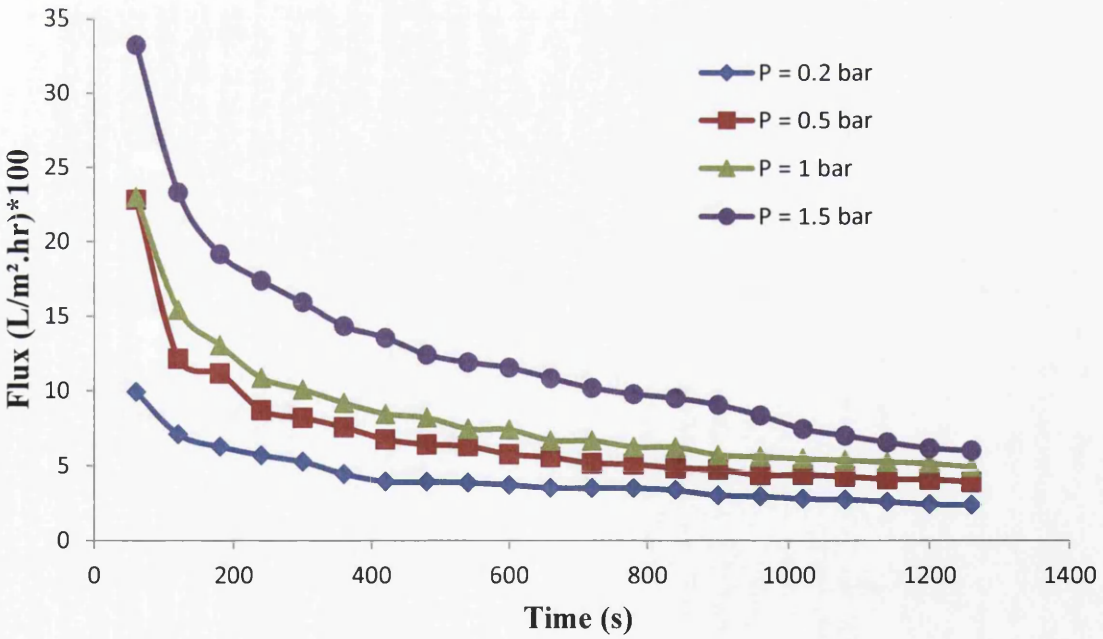

Figure 5.12 Effect of operating pressure on flux at microfiltration of Amberlite IRA743 resin suspension through the PVDF membrane with pore size of 0.22 µm. The resin concentration is 1.0 g/L

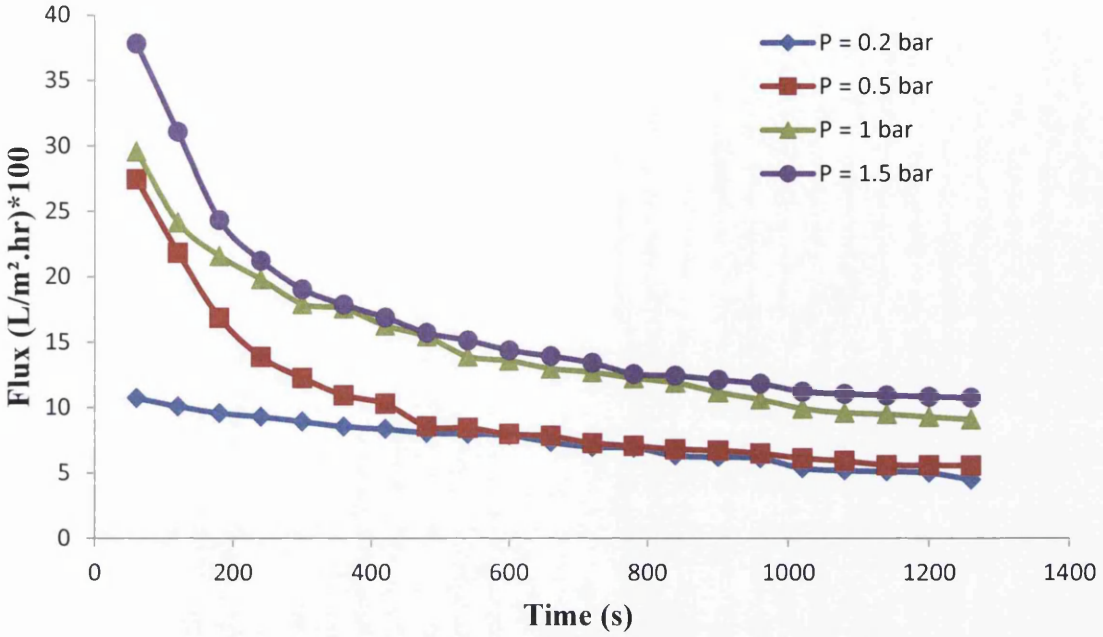

Figure 5.13 Effect of operating pressure on flux at microfiltration of Amberlite IRA743 resin suspension through the PVDF membrane with pore size of 0.45 µm. The resin concentration is 0.2 g/L

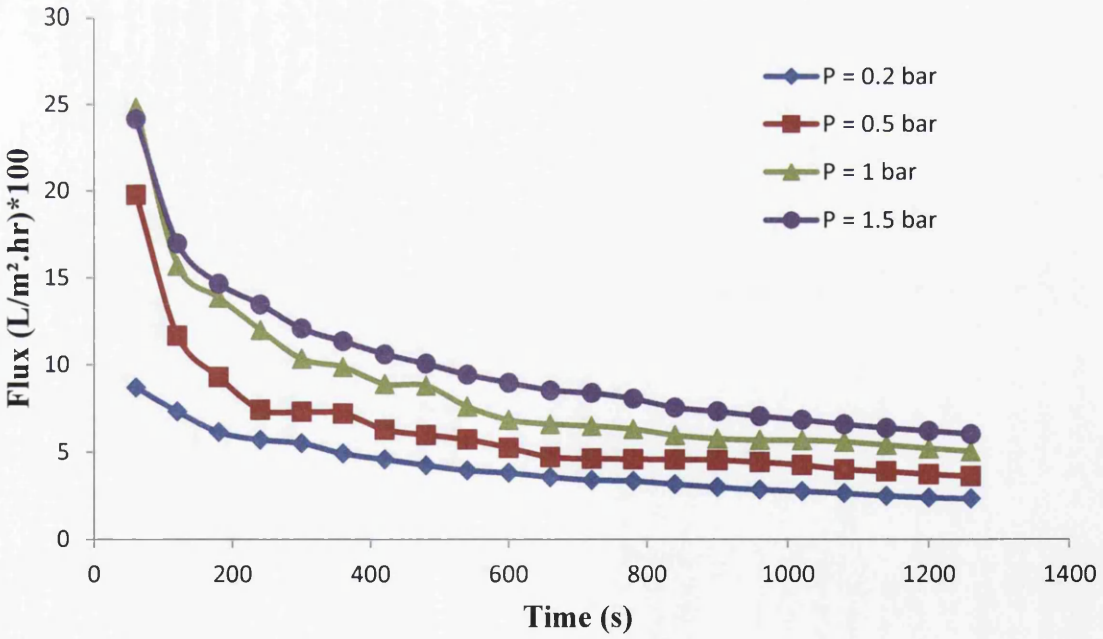

Figure 5.14 Effect of operating pressure on flux at microfiltration of Amberlite IRA743 resin suspension through the PVDF membrane with pore size of 0.45 µm. The resin concentration is 1 g/L

The concentration of the resin in the permeate is shown in Table 5.2, 5.3 and 5.4 for the membranes with pore size 0.1 μm PVDF, 0.22 μm PVDF and 0.45 μm PVDF respectively. As shown in these Tables, the applied pressure doesn't affect the concentration of the resin in the permeate.

Table 5.2 The concentration of Amberlite IRA743 resin in the permeate at microfiltration of the resin suspension through the PVDF membrane with pore size of 0.1 μm

Pressure, bar	**Resin** concentration in the permeate (**mg/L**)	
	At resin dosage 0.2 g/L	At resin dosage 1 g/L
0.2	1	2
0.5	0	0
1	3	0
1.5	0	2

Table 5.3 The concentration of Amberlite IRA743 resin in the permeate at microfiltration of the resin suspension through the PVDF membrane with pore size of 0.22 μm

Pressure, bar	**Resin** concentration in the permeate (**mg/L**)	
	At resin dosage 0.2 g/L	At resin dosage 1 g/L
0.2	2	0
0.5	0	0
1	0	0
1.5	0	1

Table 5.4 The concentration of Amberlite IRA743 resin in the permeate at microfiltration of the resin suspension through the PVDF membrane with pore size of 0.45 μm

Pressure, bar	**Resin** concentration in the permeate (**mg/L**)	
	At resin dosage 0.2 g/L	At resin dosage 1 g/L
0.2	1	1
0.5	3	0
1	0	0
1.5	4	0

The change of the permeate volume with time at different pressures is shown in figures 5.15, 5.16 and 5.17 for 0.45 μm PVDF, 0.22 μm PVDF and 0.1 μm respectively. The permeate volume increases with increasing the pressure for the three membranes used.

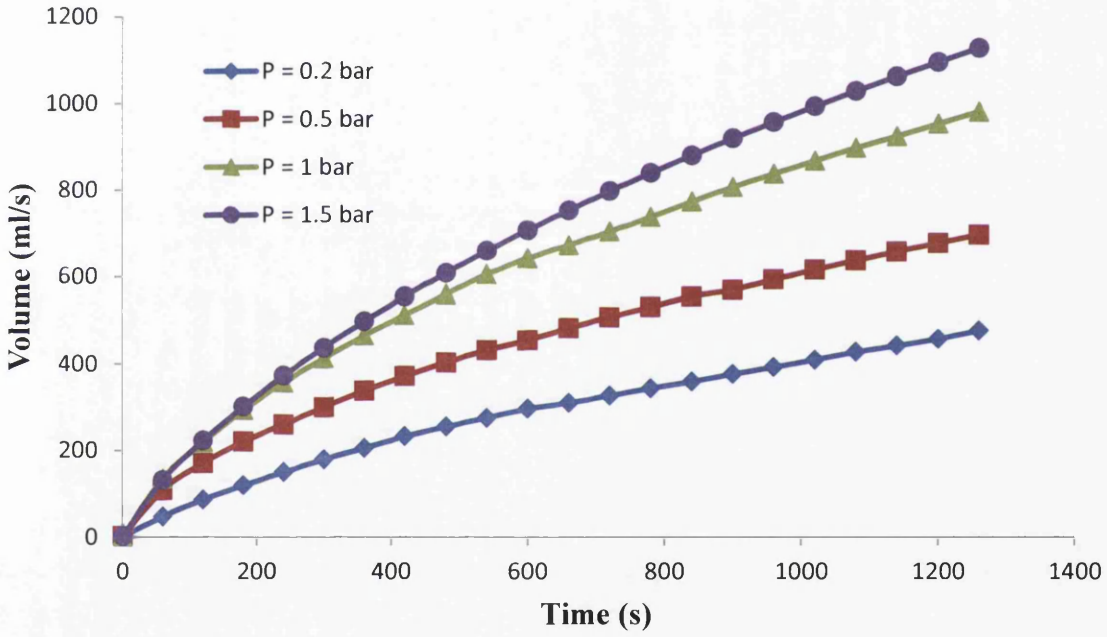

Figure 5.15 Effect of operating pressure on permeate volume with time at microfiltration of Amberlite IRA743 resin suspension through the PVDF membrane with pore size of 0.45 μm. The resin concentration is 1 g/L

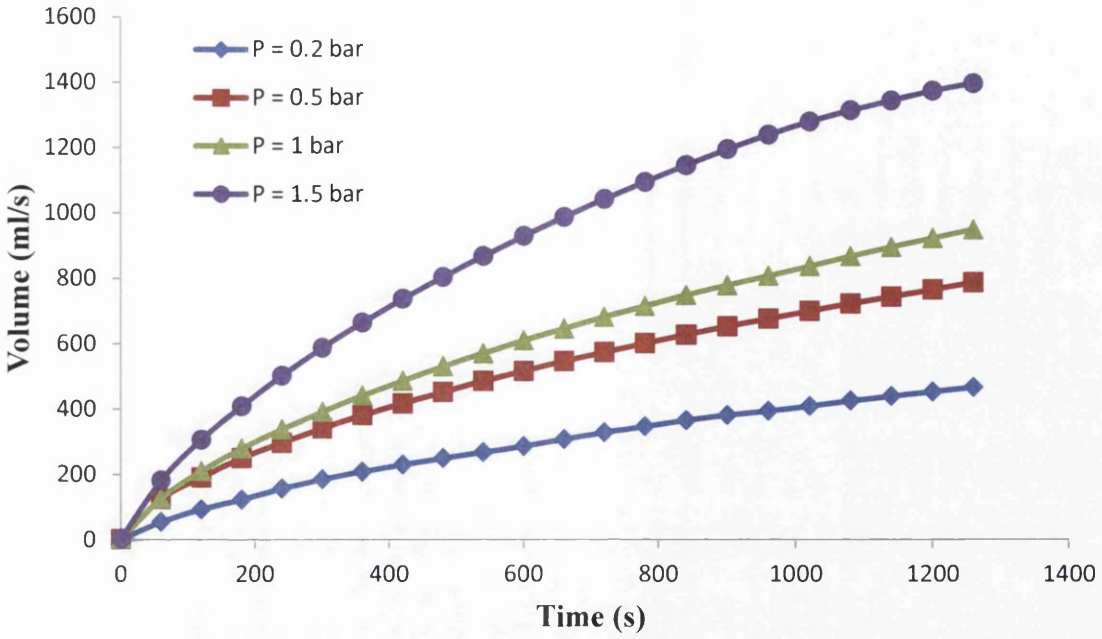

Figure 5.16 Effect of operating pressure on permeate volume with time at microfiltration of Amberlite IRA743 resin suspension through the PVDF membrane with pore size of 0.22 μm. The resin concentration is 1 g/L

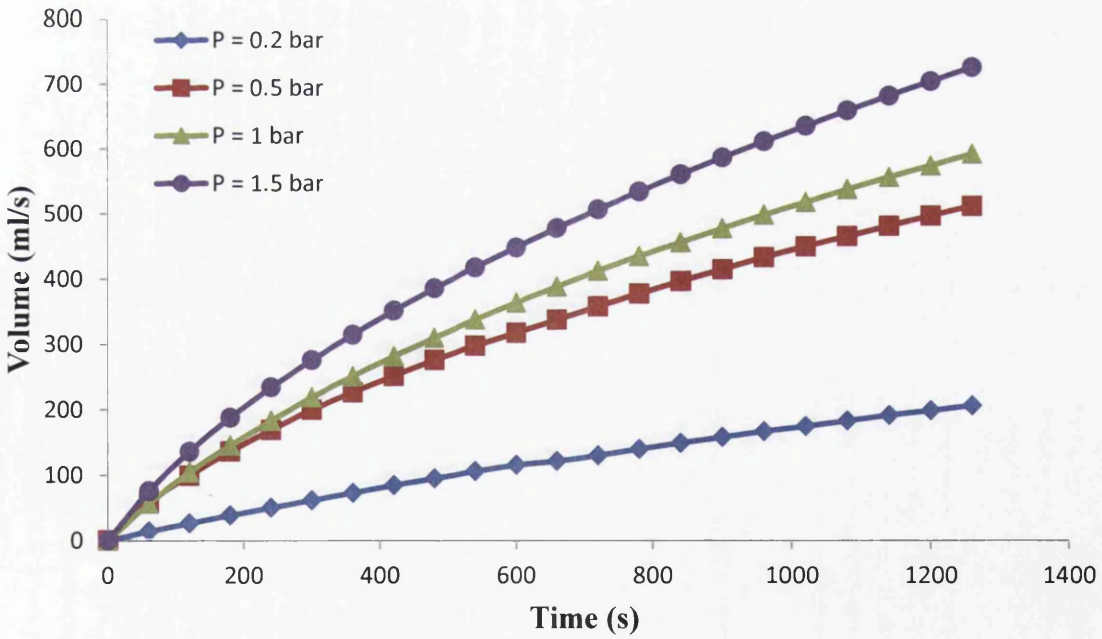

Figure 5.17 Effect of operating pressure on permeate volume with time at microfiltration of Amberlite IRA743 resin suspension through the PVDF membrane with pore size of 0.1 μm. The resin concentration is 1 g/L

5.4 Effect of the resin concentration

To study the effect of Amberlite IRA743 resin concentration in the feed solution on permeate flux, the filtration of the resin suspensions with concentrations of 0.2- 1.0 g/L through three PVDF membranes with pore sizes of 0.1-0.45 μm at different operating pressures was used. The other parameters were kept constant as pH=6 and T=25°C.

The results are shown in Figures 5.18- 5.23. The permeate flux decreased slightly with the increase in the resin concentration in the feed solution. It might be due to the fact that the particle deposition at higher feed concentration would be higher than that at lower feed concentration (Kwon *et al.*, 2000a, Lu and Ju, 1989).

From Figure 5.18, the initial permeate fluxes are 761, 672, 597, and 258 L/m².hr at resin concentration 0.2, 0.4, 0.6 and 1 g/L respectively with the membrane with a pore size of 0.1 μm and transmembrane pressure 0.2 bar. The initial value of the permeate flux was inversely proportional to the resin concentration; for instance, an increase in resin concentration from 0.2 to 1 g /L lead to an decrease of initial flux from 2769 to 1047 L/m².hr approximately as shown in Figure 5.19 with the membrane with pore size of 0.1 μm and transmembrane 1 bar.

The larger permeate flux decline at higher resin concentration in the feed solution is attributed to the increased particle transfer rate to the cake layer (Hong et al., 1997). Chudacek and Fane (1984) demonstrated that the specific resistance of a cake layer composed of resin particles increased with increasing particle concentration. Blahušiak *et al.* (2009), Blahušiak and Schlosser (2009) used Dowex XUS-43594 resin and Blahušiak *et al.* (2009) and Onderková *et al.* (2009) used XUS-G3 resin and they found the same results, the permeate flux of the membranes used decreases as the concentration of the suspension increases.

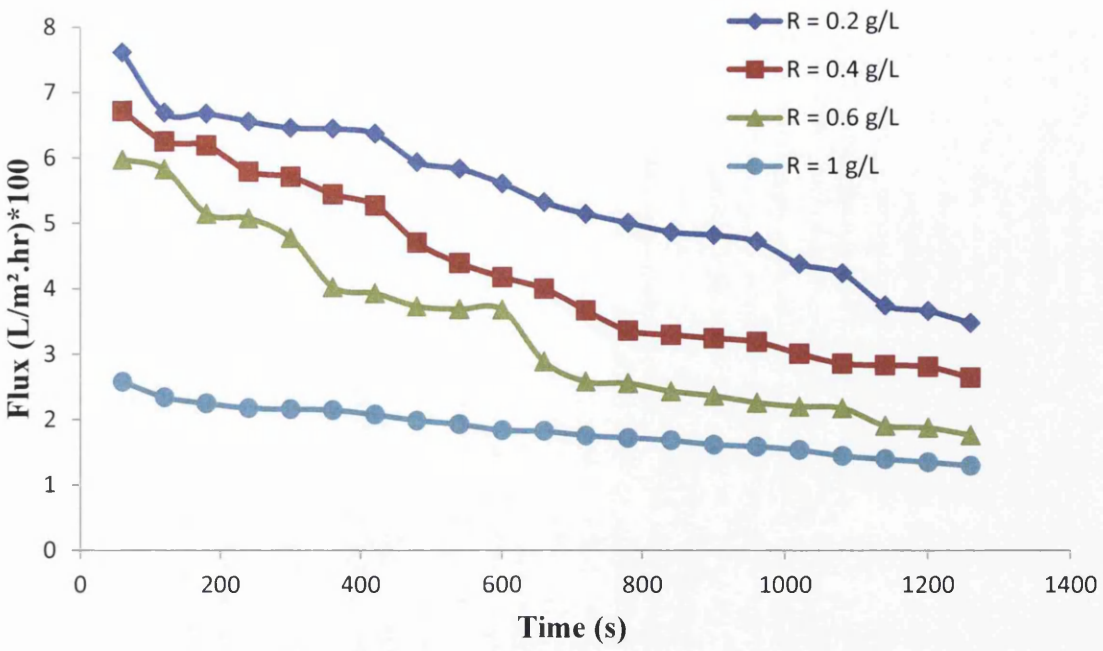

Figure 5.18 Effect of resin concentration on flux at microfiltration of Amberlite IRA743 resin suspension through the PVDF membrane with pore size of 0.1 μm. pH=6, T=25°C, pressure = 0.2 bar

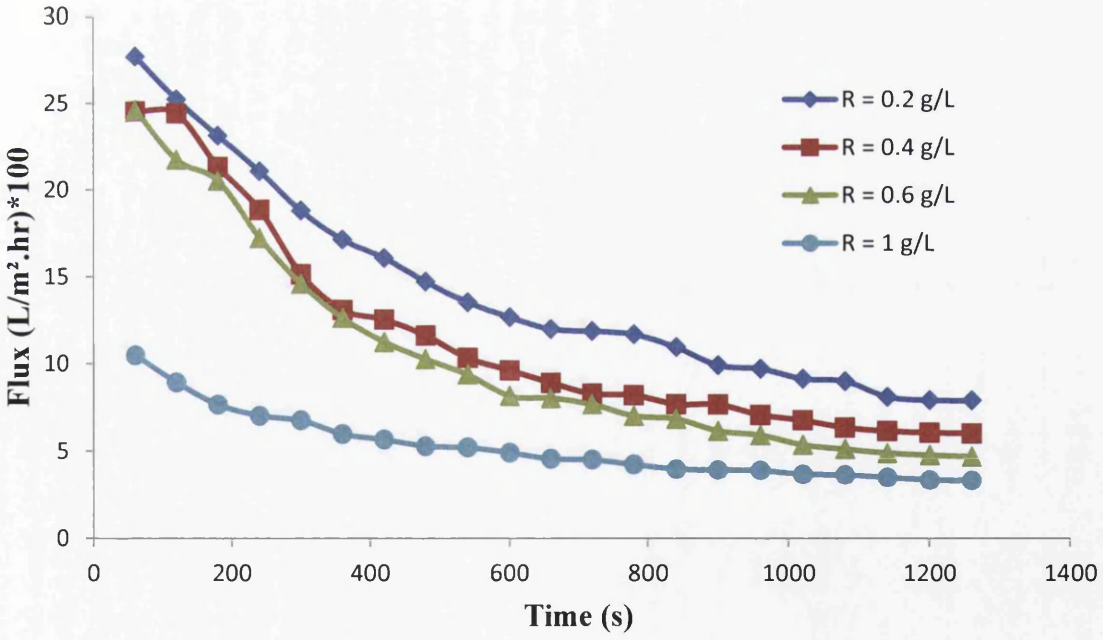

Figure 5.19 Effect of resin concentration on flux at microfiltration of Amberlite IRA743 resin suspension through the PVDF membrane with pore size of 0.1 μm. pH=6, T=25°C, pressure = 1 bar

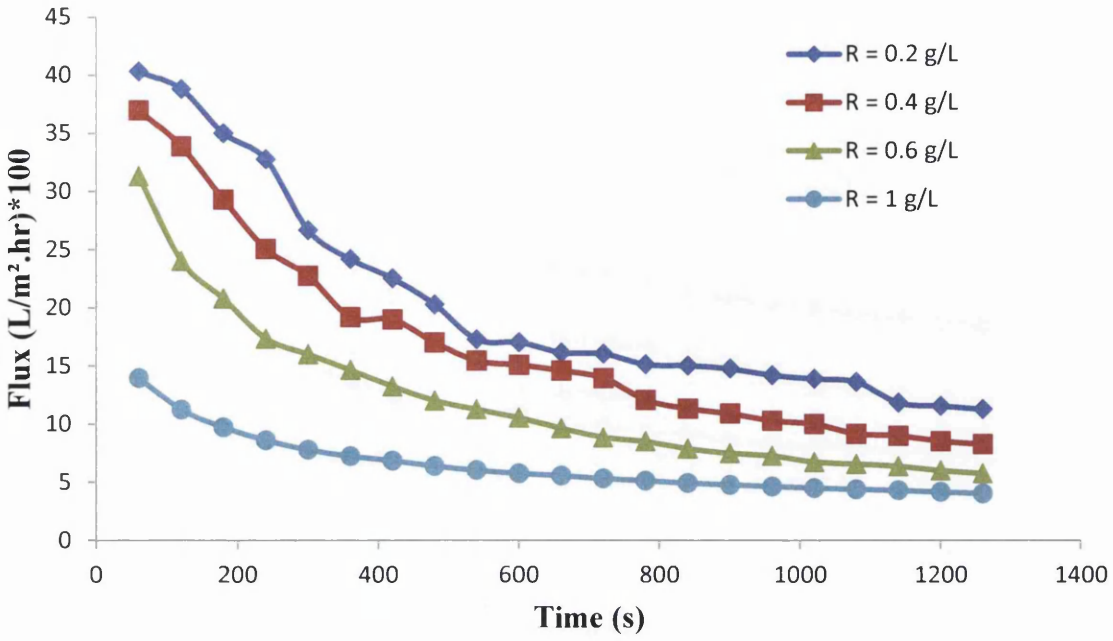

Figure 5.20 Effect of resin concentration on flux at microfiltration of Amberlite IRA743 resin suspension through the PVDF membrane with pore size of 0.1 µm, pH=6, T=25°C, pressure = 1.5 bar

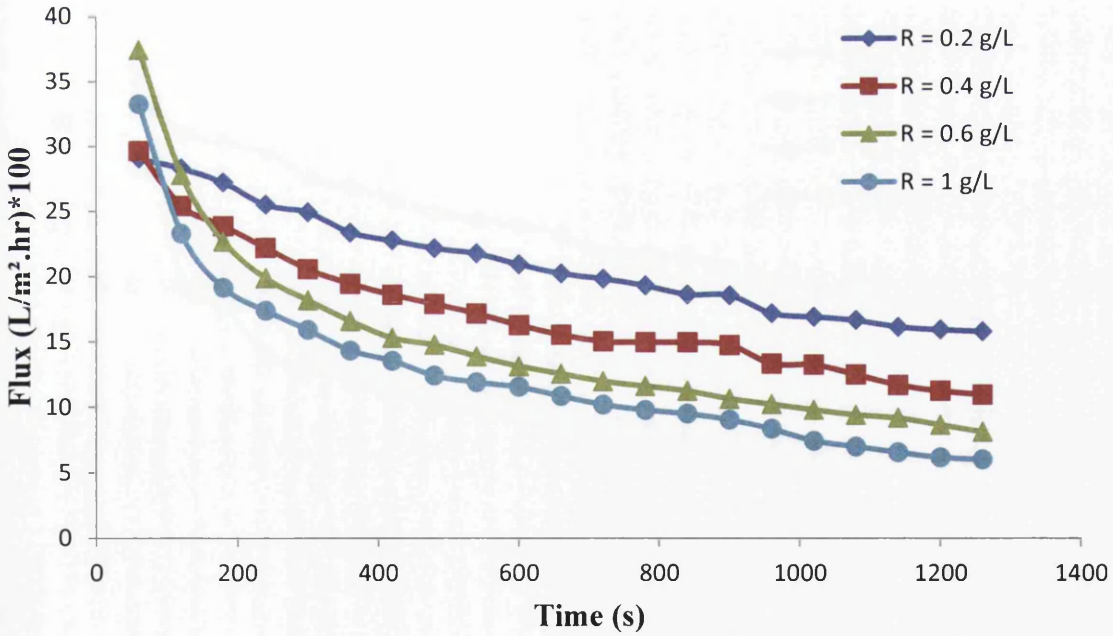

Figure 5.21 Effect of resin concentration on flux at microfiltration of Amberlite IRA743 resin suspension through the PVDF membrane with pore size of 0.22 µm, pH=6, T=25°C, pressure = 1.5 bar

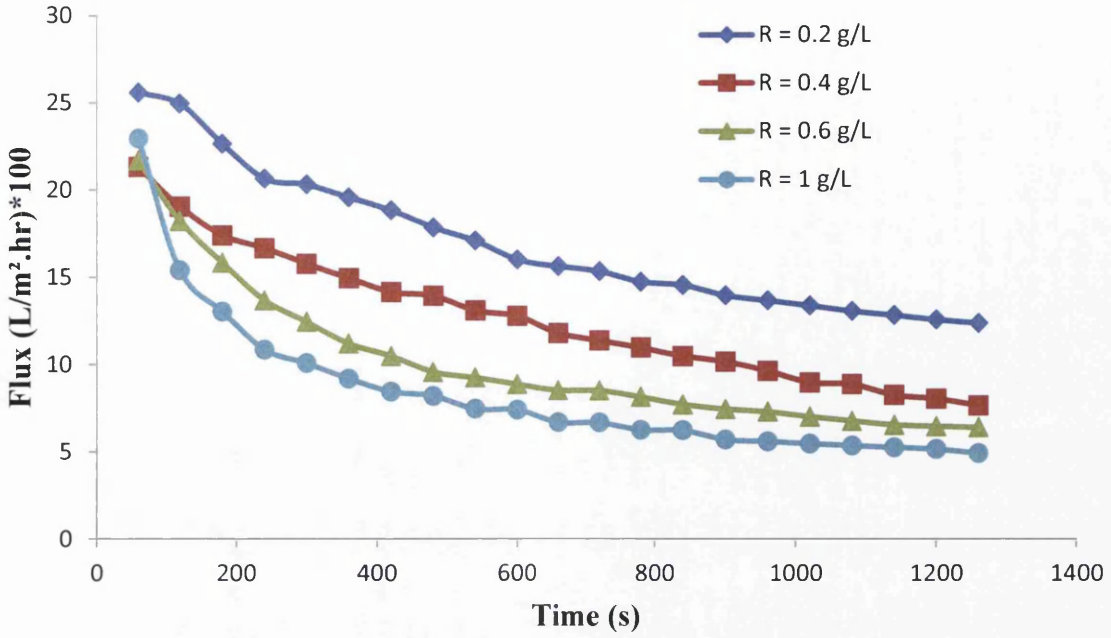

Figure 5.22 Effect of resin concentration on flux at microfiltration of Amberlite IRA743 resin suspension through the PVDF membrane with pore size of 0.22 µm, pH=6, T=25°C, pressure = 1 bar

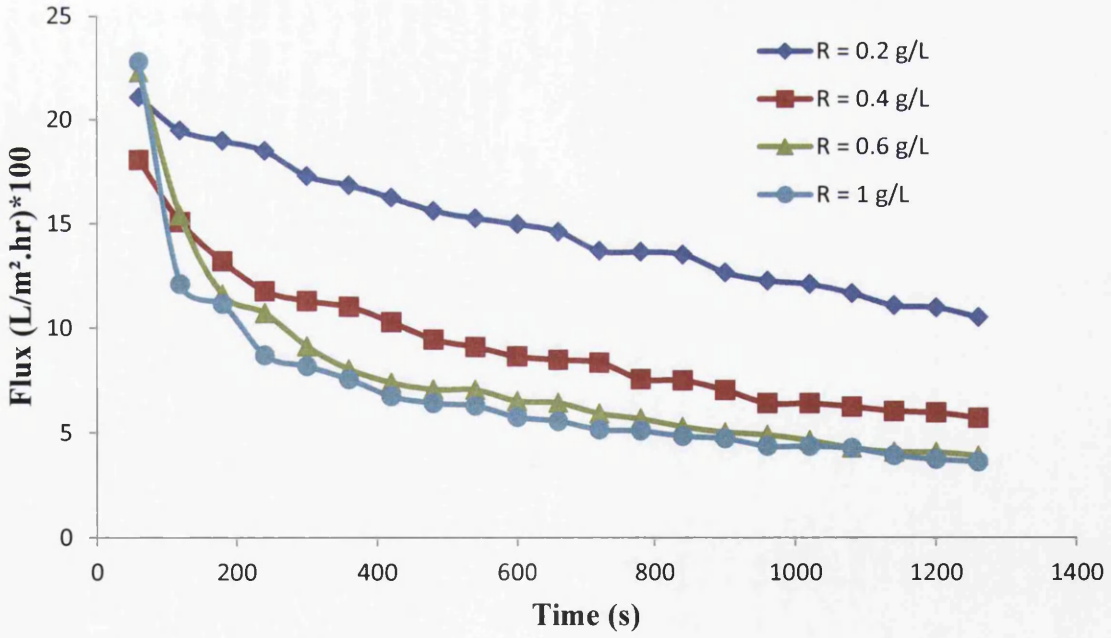

Figure 5.23 Effect of resin concentration on flux at microfiltration of Amberlite IRA743 resin suspension through the PVDF membrane with pore size of 0.22 µm, pH=6, T=25°C, pressure = 0.5 bar

5.5 Effect of pH

The effect of pH on permeate flux was studied by changing the pH of the feed suspension from 4 to 10.5. The other operating parameters were kept constant at T=25°C, operating pressure of 0.5 bar and resin concentration of 1 g/L. PVDF membrane with pore size of 0.22 µm was used.

As shown in Figure 5.24, the flux increased with increasing pH from 4 to 8. However, raising the pH to 10.5 decreases the flux to a value between that observed at pHs of 4 and 6. Increasing pH from 4 to 6 increased the permeate flux from 1681 to 2280 while the permeate flux increased to 2977 at pH 8. The flux decreased to 1563 when the pH of the solution increased to 10.5.

Permeate flux is higher at pH near the isoelectric point (IEP) and lower at pH far away from the IEP. Particles tend to agglomerate when the pH approaches the IEP, which mainly due to attractive Van der Waals forces and hence the fouling deposit formed has a lower overall resistance. The filtrate flux is high when the IEP is reached (Xu et al., 2002).

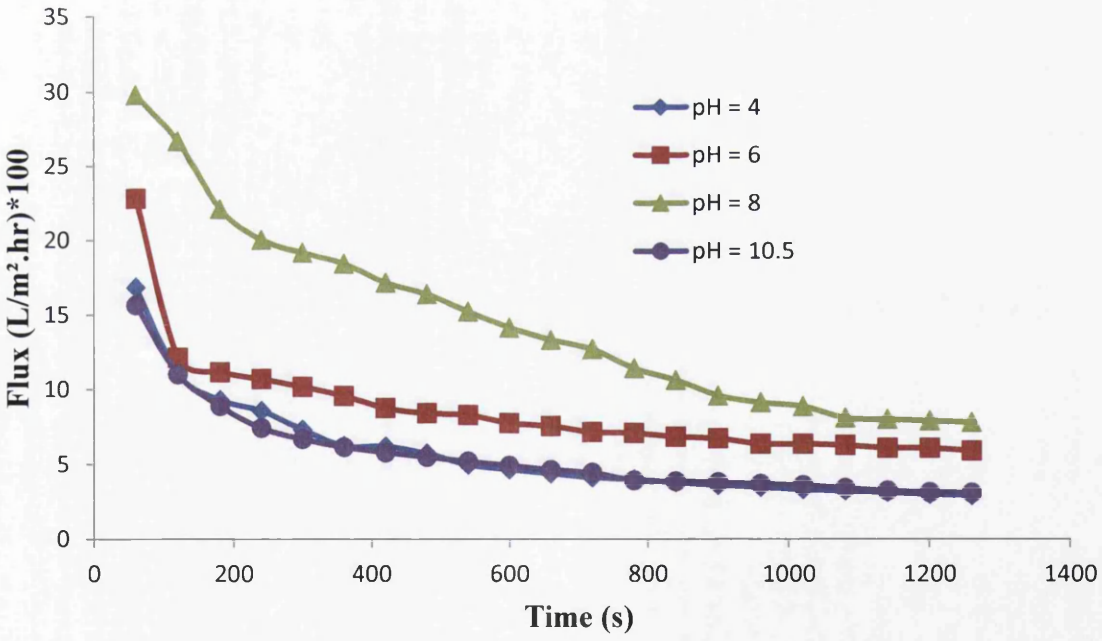

Figure 5.24 Effect of pH on flux with time at microfiltration of Amberlite IRA743 resin suspension through the PVDF membrane with pore size of 0.22 µm. P=0.5 bar, T=25°C, the resin concentration= 1 g/L

5.6 Effect of ionic strength on permeate flux

In this section, the effect of ionic strength on permeate flux was investigated. The effect of the presence of NaCl, Na_2SO_4 and $MgCl_2$ on permeate flux is shown in Figures 5.25, 5.26 and 5.27 respectively. As seen from Figure 5.25, the permeate flux increases with increasing the NaCl concentration in the feed solution 5000 to 35000 mg/L compared with the flux of pure solution with no NaCl exists. The flux increased from 682 L/m².hr when no NaCl in the feed solution to 1290 L/m².hr when 5000 mg/L of NaCl was added to the feed solution and to 1401 L/m².hr with solution of 35000 mg/L NaCl.

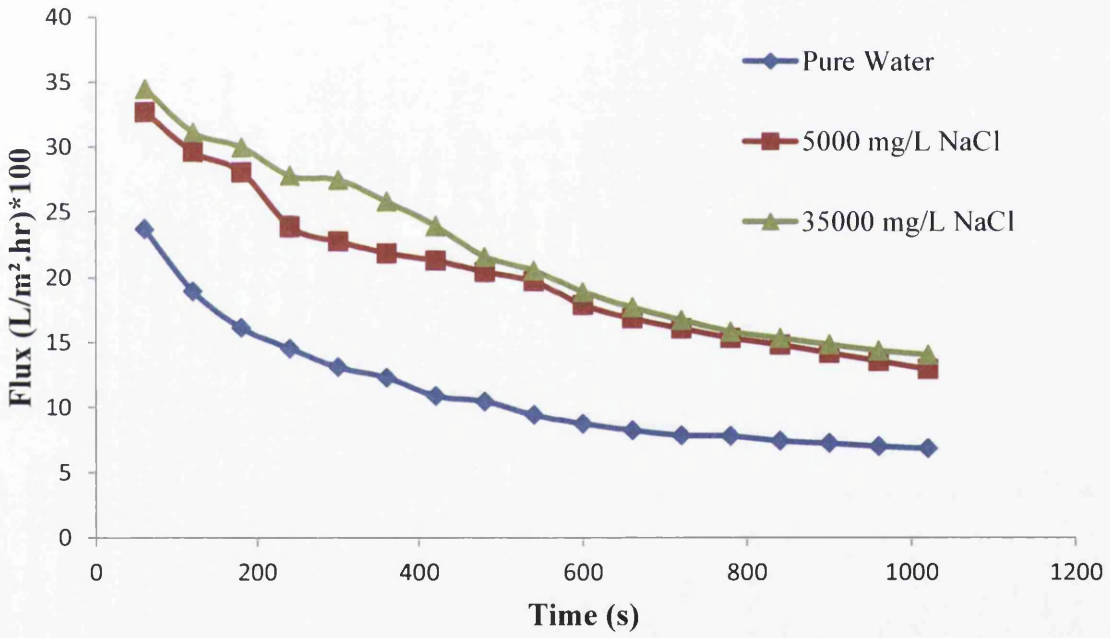

Figure 5.25 Effect of NaCl concentration on permeate flux

Figure 5.26 shows the effect of Na_2SO_4 on the flux of the suspension of boron with Amberlite IRA743. The permeate flux was 682 L/m².hr when no Na_2SO_4 salt exists in the solution. The permeate flux increased to 1588 L/m².hr and 1435 L/m².hr when adding 10000 mg/L and 3000 mg/L of Na_2SO_4 to the feed solution.

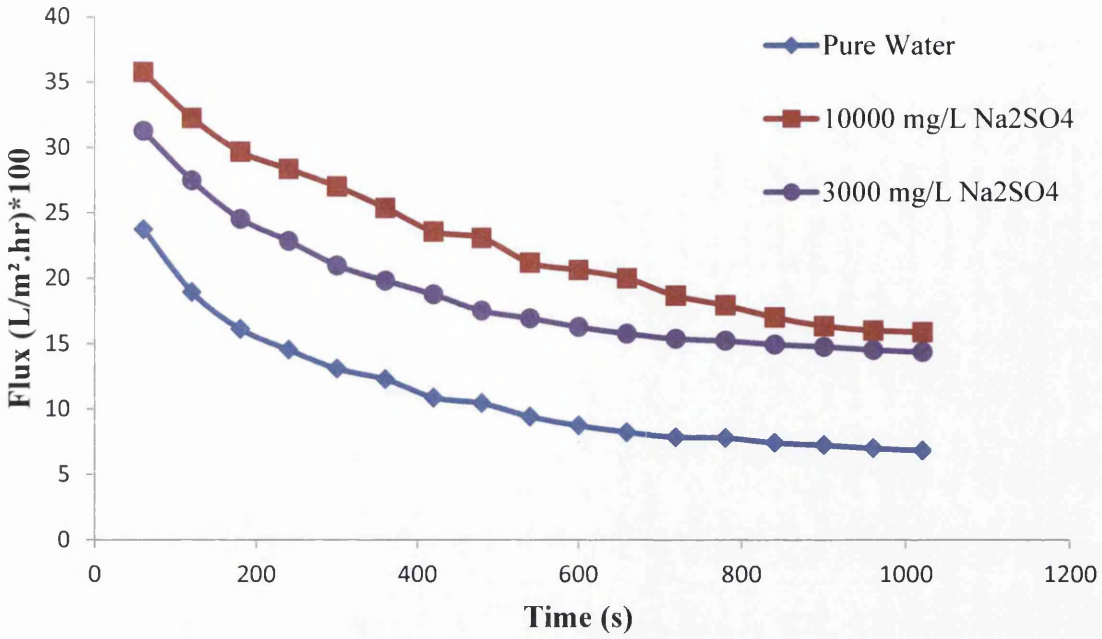

Figure 5.26 Effect of Na_2SO_4 Concentration on permeate flux

The results of the effect of $MgCl_2$ salt on the flux is shown in Figure 5.27. The existence of $MgCl_2$ in the feed solution will lead to increase in the flux. The flux increased from 682 L/m².hr 1040 L/m².hr when the concentration of $MgCl_2$ in the feed solution was 3000 mg/L and increased to 1400 mg/L with 2000 mg/L of $MgCl_2$.

Zhao *et al.* (2005) found the permeate flux of TiO_2 suspension increased with increasing the ionic strength. They explain this phenomena due to an increase in TiO_2 particle size with increasing ionic strength due to the decrease in zeta potentials caused by the compression of the diffuse layer at high ionic strength.

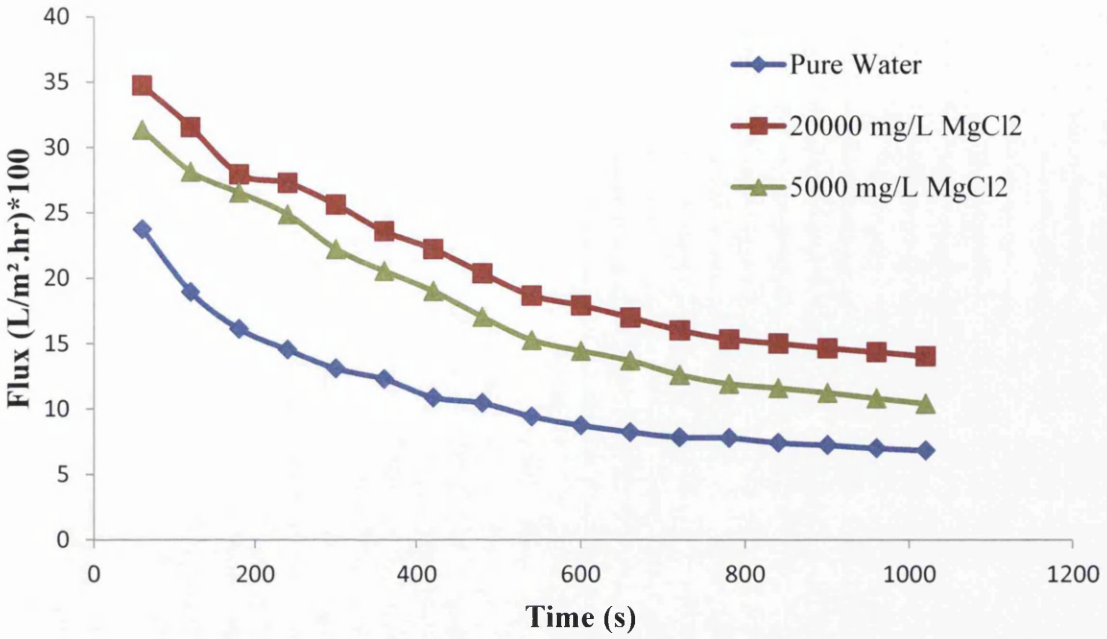

Figure 5.27 Effect of $MgCl_2$ concentration on permeate flux

5.7 Characterisation of the membranes

The membranes have been characterized with both scanning electron microscopy (SEM) and atomic force microscopy (AFM). A scanning electron microscope (HITACHI S-4800II) was used to take images of the membranes. The surface and cross-section images of new membranes were taken by both SEM and AFM. The fouled membranes images were taken by SEM.

Figure 5.28 (a) and (b) shows surface and cross section SEM image of the new 0.1 μm PVDF membrane respectively. As seen, the membrane pores are open and show no fouling. The SEM images of the used membrane for the filtration of the solution with resin dosages of 0.2 g/L and 1 g/L are shown in Figure 5.29 and 5.30. Figure 5.29 (a) and (b) shows the surface and cross section images of the used membrane with 0.2 g resin/L while Figure 5.30 (a) and (b) is for the membrane used for the filtration of the solution with 1 g resin/L.

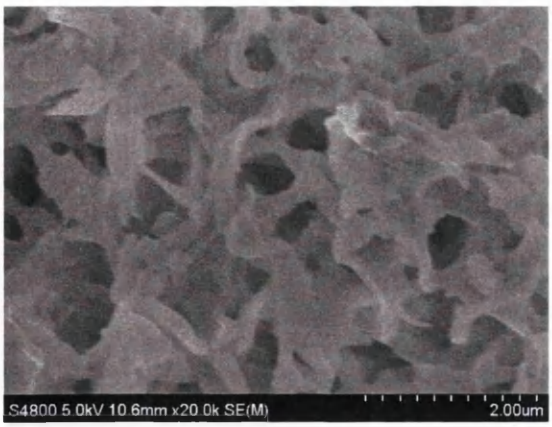

(b)

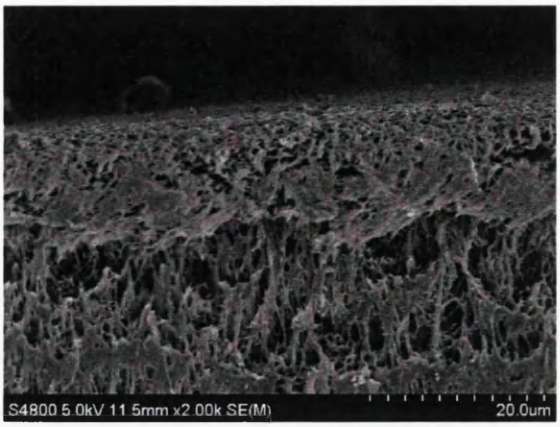

Figure 5.28 SEM micrographs of the new 0.1 μm PVDF membranes: (a)surface (b)cross section

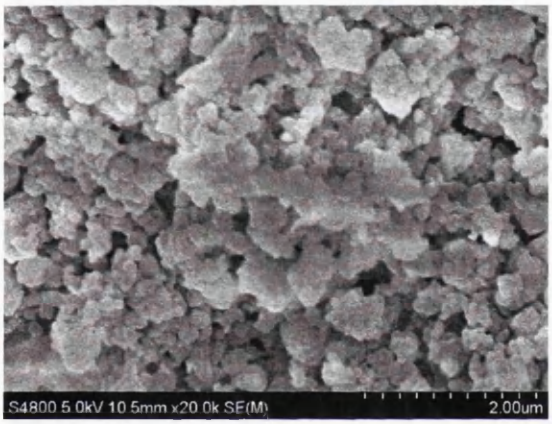

(b)

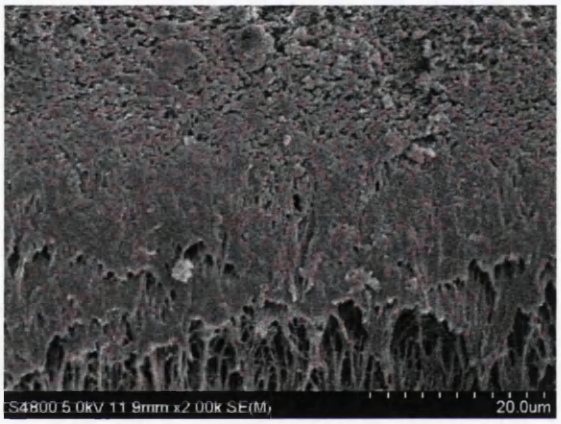

Figure 5.29 SEM micrographs of 0.1 μm PVDF membranes after filtering solution with 0.2g resin/L: (a)surface (b)cross section

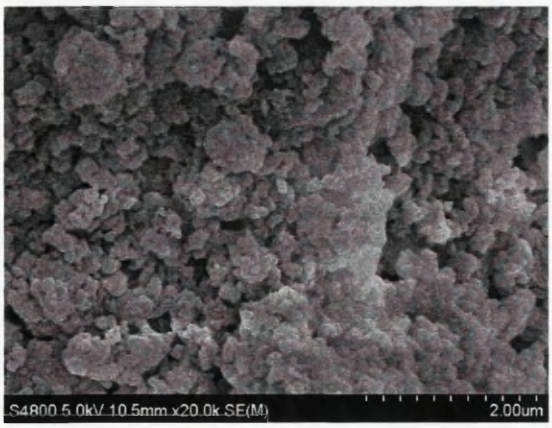

(b)

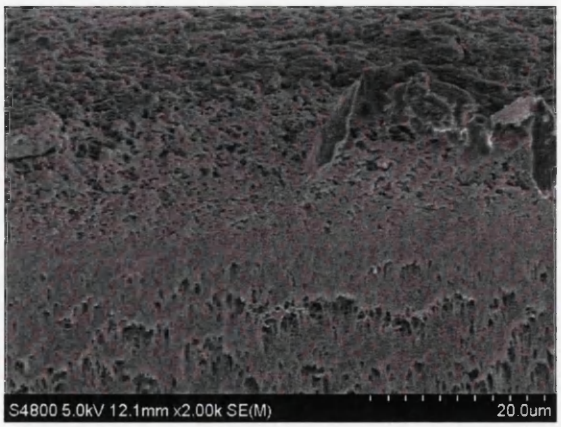

Figure 5.30 SEM micrographs of 0.1 μm PVDF membranes after filtering solution with 1g resin/L: (a)surface (b)cross section

The surface and cross section images of the new 0.22 μm PVDF membrane is shown in Figure 5.31(a) and (b) respectively. The surface and cross section SEM images of the used membranes are shown in Figure 5.32 (a) and (b) for the membrane used with a solution with 0.2 g resin/L and Figure 5.33 (a) and (b) for the membrane used for the filtration the solution with 1 g resin/L.

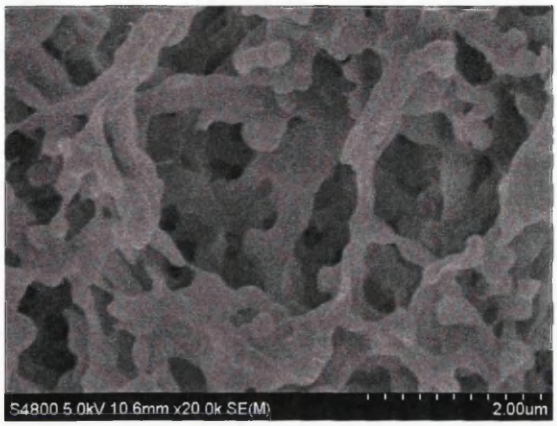

(b)

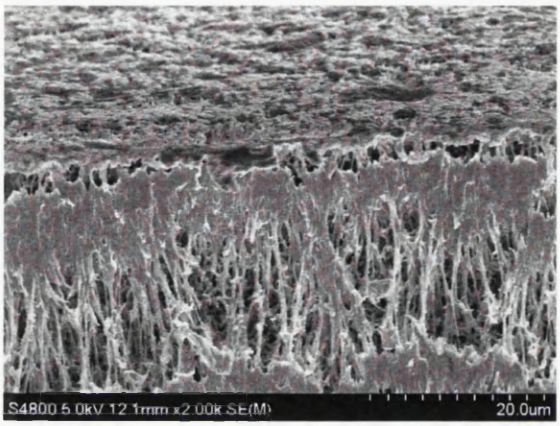

Figure 5.31 SEM micrographs of the new 0.22 μm PVDF membranes: (a)surface (b)cross section

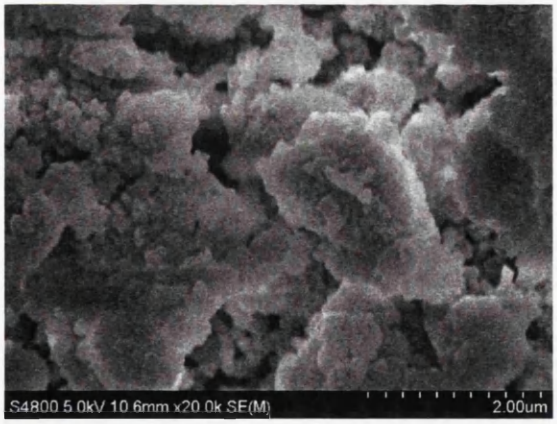

(b)

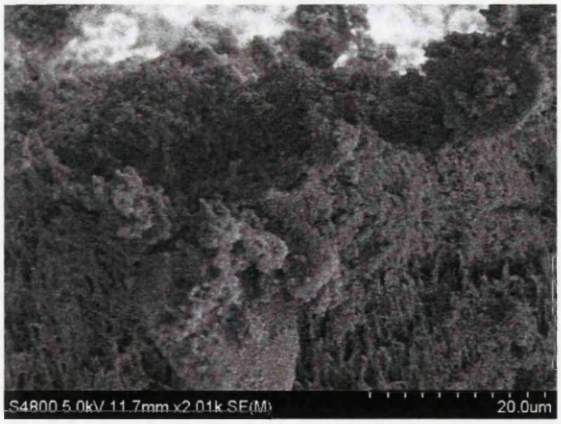

Figure 5.32 SEM micrographs of 0.22 μm PVDF membranes after filtering solution with 0.2g resin/L (a)surface (b)cross section

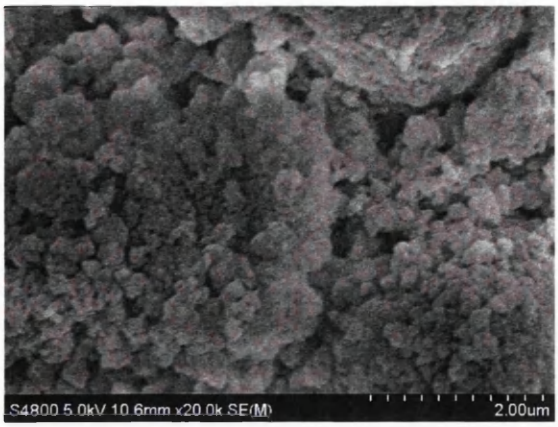

(b)

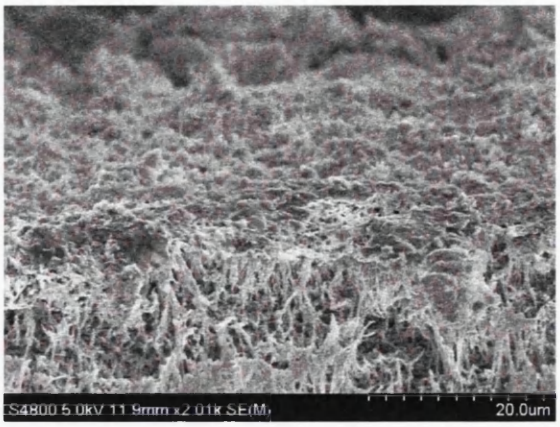

Figure 5.33 SEM micrographs of 0.22 μm PVDF membranes after filtering solution with 1g resin/L: (a)surface (b)cross section

The new 0.45 μm PVDF images are presented in Figure 5.34 (a) and (b) while Figure 5.35 (a) and (b) and Figure 5.36 (a) and (b) show the used 0.45 μm PVDF membranes for the filtration of the solutions containing 0.2 g resin/L and 1 g resin/L respectively. These images show that the resin particles deposited on the membrane surfaces for the membranes with pore size of 0.1 and 0.22 μm and no pore blockage was noticed. the images of the membrane with pore size of 0.45 μm supported the results of the permeate flux reduction (section 5.2) when using this membrane as the pores blocked by the resin particles.

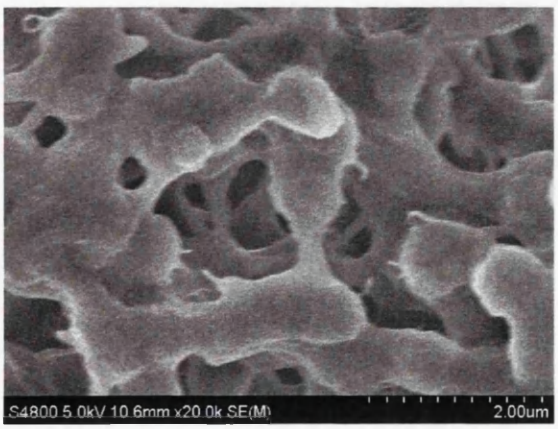

(b)

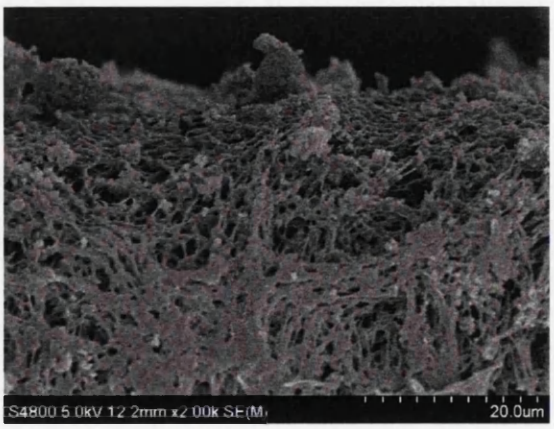

Figure 5.34 SEM micrographs of the new0.45 μm PVDF membranes: (a)surface (b)cross section

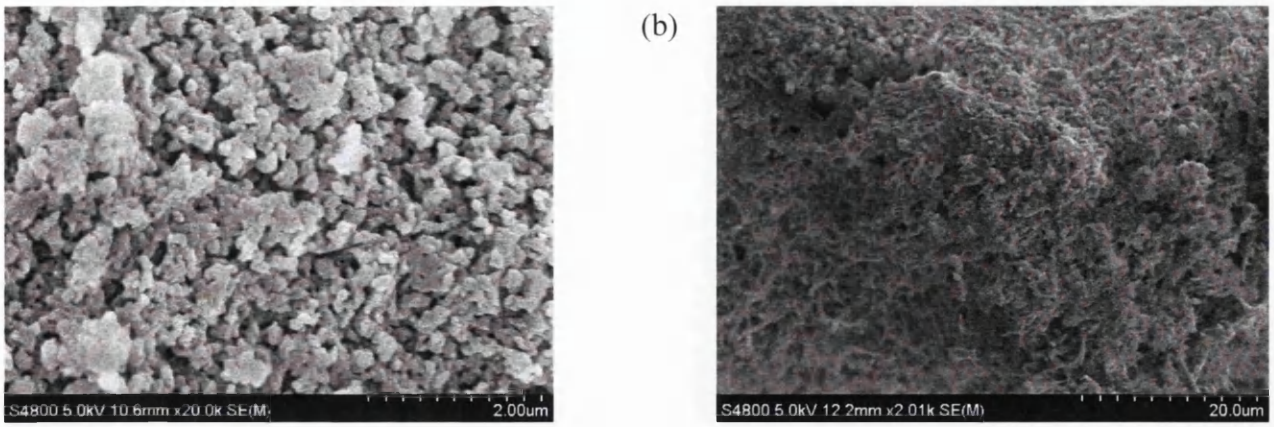

Figure 5.35 SEM micrographs of 0.45 μm PVDF membranes after filtering solution with 0.2 g resin/L: (a)surface (b)cross section

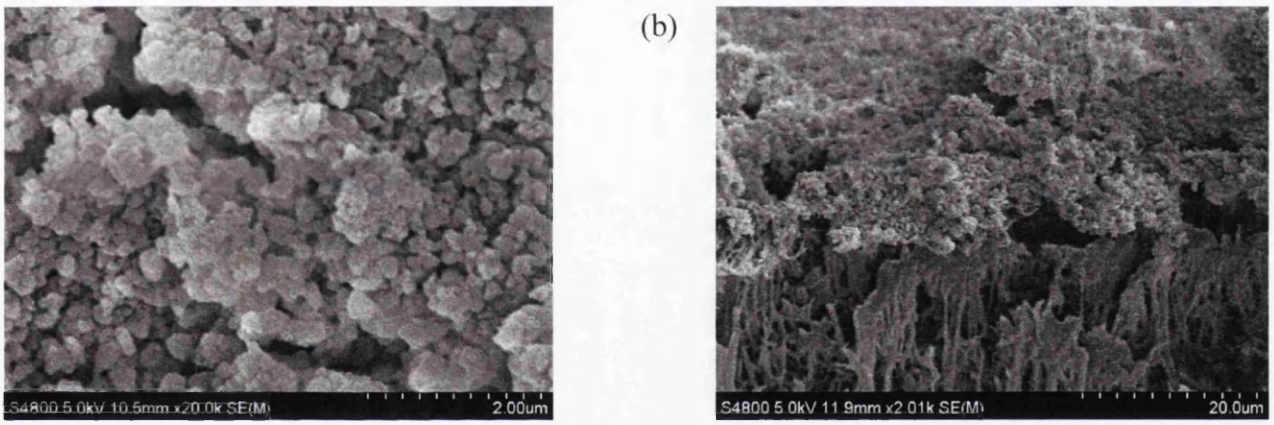

Figure 5.36 SEM micrographs of 0.45 μm PVDF membranes after filtering solution with 1g resin/L: (a) surface (b) cross section

The AMF images of the new membranes are shown in Figure 5.37a,b,c for the membrane with pore size 0.1 μm, 0.22 μm and 0.45 μm respectively.

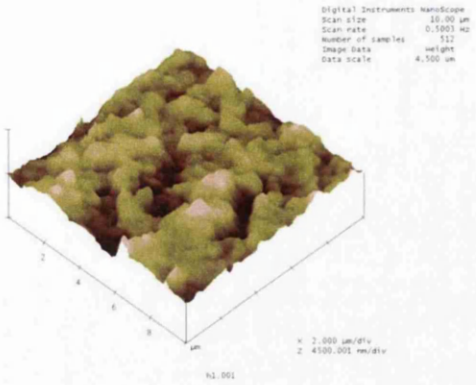

(a)

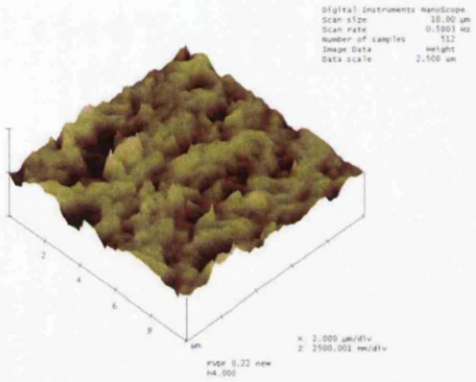

(b)

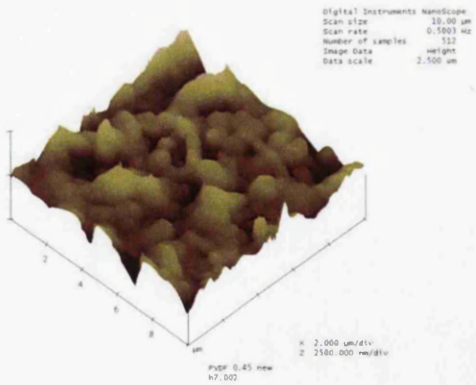

(c)

Figure 5.37 AFM images for the new membranes: a) 0.1 μm, b) 0.22 μm, c) 0.45 μm

Table 5.5 Surface characteristics of PVDF membranes as measured by AFM

Membranes	RMS (nm)	R_a	Surface Area Difference %
PVDF (0.1 μm)	423.81	329.62	133.73
PVDF (0.22 μm)	200.98	152.43	58.82
PVDF (0.45 μm)	341.12	258.12	93.95

Results in Figure 5.37 and Table 5.9 show that PVDF 0.1 μm has higher roughness than the other two membranes while PVDF 045 μm has higher roughness than 0.22 μm membrane. PVDF 0.1 μm has RMS of 423.81 nm and R_a of 329.62 nm compared to RMS of 200.98 nm and R_a of 152.43 for PVDF 0.22 μm and RMS of 341.12 nm and R_a of 258.12 for PVDF 0.45 μm membrane.

5.8 Conclusions

This chapter was focusing on the impacts of different operational parameters on the separation of the suspension of loaded resin with boron. The main parameters studied in this chapter were, the membrane pore size, transmembrane pressure, resin concentration in the feed solution and pH of the solution. The main findings may summarised as follows:

1- The permeate flux increased with increasing the membrane pore size from 0.1 to 0.22 μm and decreased after that when the pore size increased to 0.45 μm. this may due pore blocking when more particles can accumulate in the wide-porous structure of the membrane.

2- The trans-membrane pressure has a directly proportional effect on the permeate flux as the increase in pressure leads to an increase in permeate flux because of the higher driving force.
3- The resin concentration in the feed solution is inversely proportional to the permeate flux at different pressure and membrane pore size. It might be due to the fact that the particle deposition at higher feed concentration would be higher than that at lower feed concentration.
4- The increase in solution pH from 4-8 will result in permeate flux increasing, while there is a reduction in the permeate as pH increased to 10.5.
5- The permeate flux improved with the presence of NaCl, $MgCl_2$ and Na_sSO_4 salts. The flux increased with increasing in these salts concentrations in the feed solutions.
6- SEM images were taken for the membranes used in the experiments. The images supported the results found for the permeate flux reduction. The images showed the blockage of the membrane with pore size 0.45 μm while the particles deposited on the surface of the other membranes used in this thesis.

CHAPTER 6

Regeneration of Amberlite IRA743 Resin after Boron Removal

6.1 Introduction

Usually, the ion exchange is performed in cyclic operations. Each cycle is divided into three main stages: (1) sorption, (2) elution, and (3) regeneration, as shown in the ion operation cycle schematized in Figure 6.1 (Inamuddin and Luqman, 2012) .

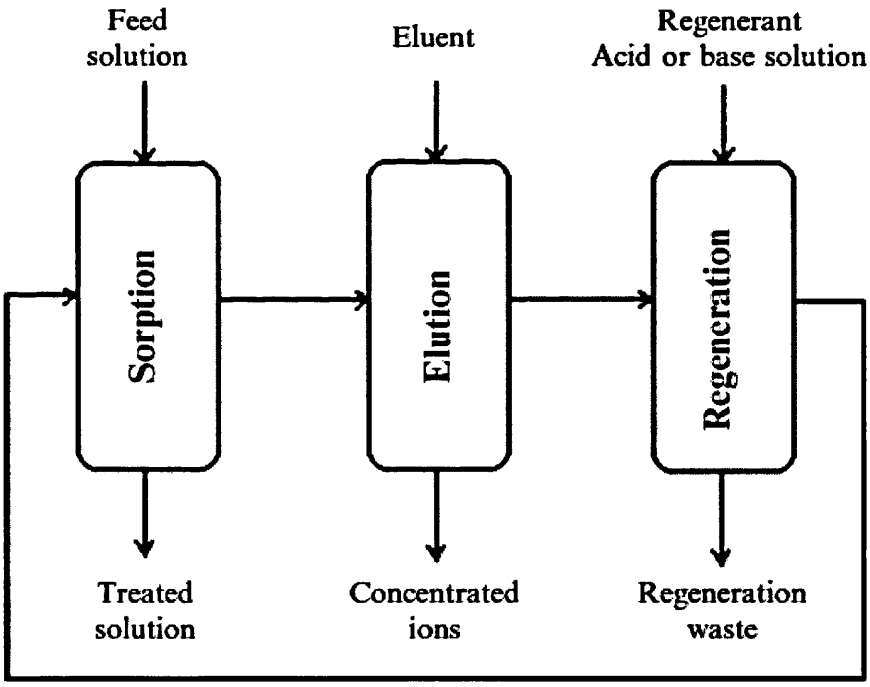

Figure 6.1 Schematic representation of ion exchange operation cycle, (Inamuddin and Luqman, 2012)

Let us take ion exchange removal of ion *B* from a solution. The ion exchange material is in the form of ion *A*, the treatment is described by the ion exchange reaction (Zagorodni, 2006)

$$Z_B\overline{RZ_AA} + Z_AB = Z_A\overline{RZ_BB} + Z_BA \qquad 6.1$$

Reaction (6.1) is the first stage of the operation called the *sorption* step. When the *sorption* is completed, the ion B must be split out of the exchanger phase through a procedure called *elution*. Then the material must be reconverted to the *A* form for the next ion exchange cycle. Such re-conversion is called *regeneration*.

It was reported that boron liberating hydrolysis is relatively easy at pH less than 1.0 and therefore, acid is required for the complete and rapid elution of the boric acid from boron selective resin (Kabay *et al.*, 2010). It was mentioned that additional amount of acid is required in the elution step since NMG functional group is linked to styrenic matrix through amine groups that entrap protons (Kabay *et al.*, 2010).

Generally, regeneration process consists of two main steps, deboronation using acid regenerants, such as HCl and H_2SO_4, and neutralisation using basic regenerant, typically, NaOH (Hilal *et al.*, 2011). Regeneration with sulfuric acid and polishing with soda caustic gives far better results relative to regeneration with sulfuric acid alone. Because the polishing with soda caustic improves the gross uniformity of the resins' chemical potential (Nadav, 1999). However, it is well-known that the saturated resin IRA 743 must be reconverted, or regenerated, to the free amine form by eluting with acid first and then alkalis before it is reused (Figure 6.2) (Xu and Jiang, 2007, Şahin, 2002).

Since the amine group of the resin was neutralized during the acid regeneration to form the acid sulphate, hydrolysis of the amine acid sulphate during the subsequent exhaustion cycle results in a very acidic effluent. To avoid this, the resin is then converted back to the free amine form with NaOH solution. The following scheme expressed the loading and elution of the boron-specific resin (Şahin, 2002):

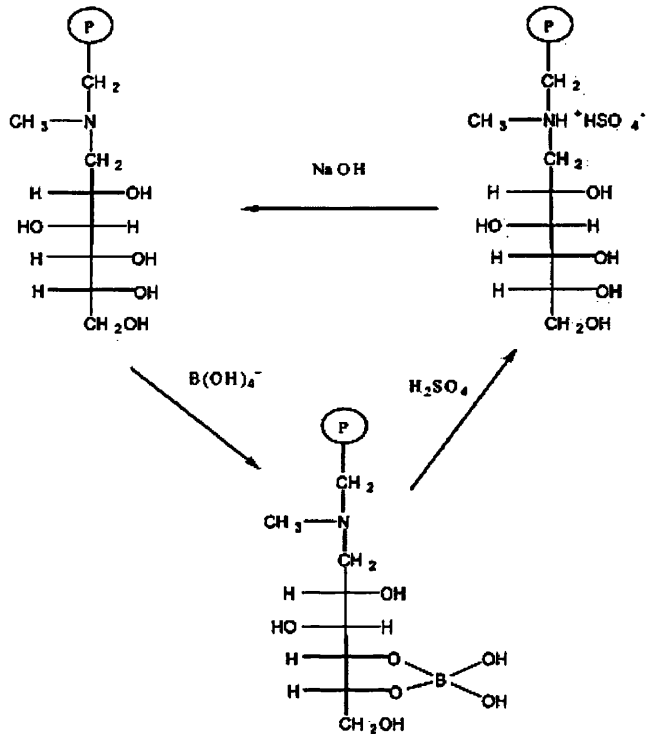

Figure 6.2 Loading and regeneration of the boron specific resin, (Şahin, 2002)

To evaluate the effect of acid concentration, elution of boron from the exhausted Amberlite IRA743 resin was studied using HCl and H_2SO_4 at different concentrations with batch method. Five sorption-elution-washing-regeneration-washing cycles were performed to evaluate a possibility of the resin regeneration and reuse.

6.2 Regeneration with HCl and NaOH

In this section, hydrochloric acid (HCl) was used at different concentrations (0.2, 0.5, 1 and 2M) to study the effect of changing the acid concentration on the resin performance. The adsorption experiment was performed using a solution containing 5 mg boron/L at pH of 8 and temperature at 25°C and resin dosage of 2 g/L. Each adsorption experiment lasts 10 min. After filtering the solution, the resin was rinse in 100 ml of hydrochloric acid (HCl).

To check the optimum time for the regeneration, the regeneration was tested at two time intervals (10 and 30 min).

As shown in Figure 6.3, boron removal improved and increased from 90% before regeneration to 100% after regeneration for 10 and 30 min. This implies that boron stripping by acid treatment is fast as in the case for loading. Gazi *et al.* (2008) used a novel functional polymer resin to remove boron from water and found boron was released from the loaded resin in 30-35 min as in the case for loading.

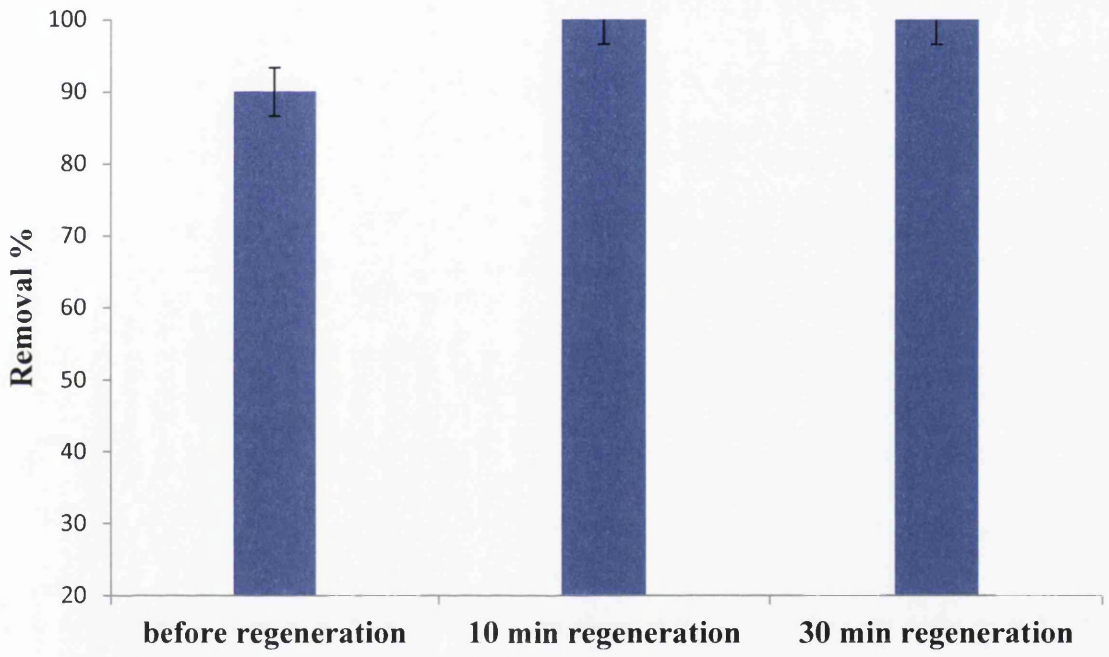

Figure 6.3 Effect of regeneration time with 0.2M HCl on boron removal. Boron concentration=5 mg/L, the resin dosage=2 g/L, pH=8, T=25°C

Figures 6.4-6.7 show the results of the resin regeneration with HCl at different acid concentrations. Five sorption-elution-washing-regeneration-washing cycles were applied to the resin.

Figure 6.4 shows the regeneration of the resin using 0.2M HCl. The boron removal was found to be 92.72% in the first exhausted step. The boron removal didn't change at the first cycle of regeneration. The boron removal increased up to 100% after second and third cycles of regeneration. The boron removal after fourth and fifth regeneration cycles was 92.72% which the same as before regeneration.

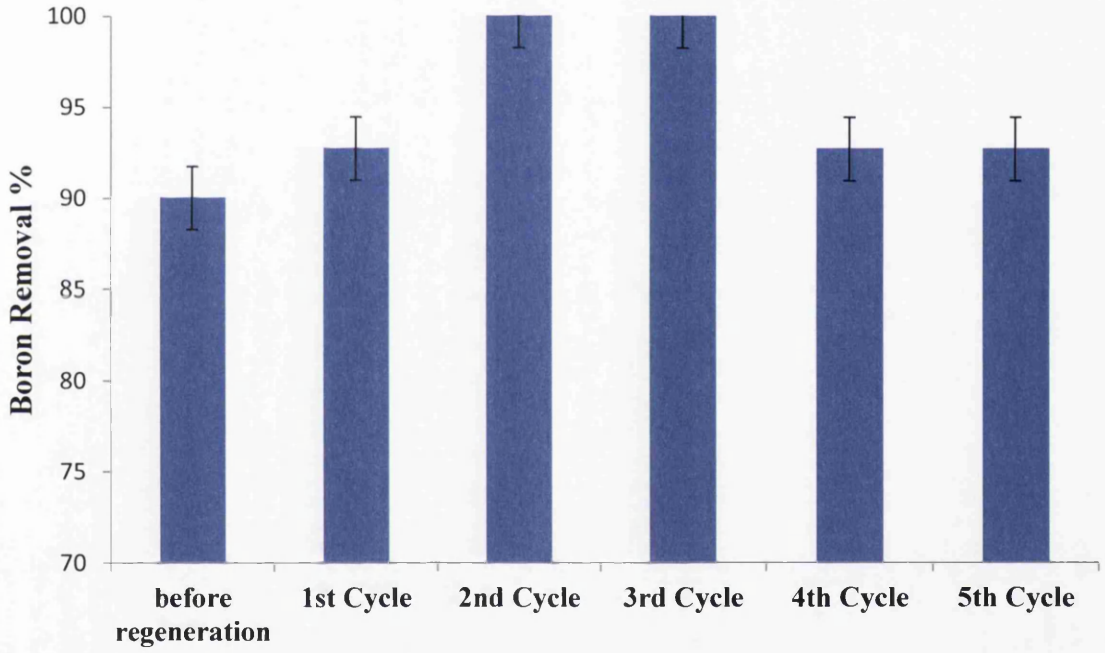

Figure 6.4 Regeneration of Amberlite IRA743 resin using 0.2M. HCl. Boron Concentration=5 mg/L, resin dosage=2 g/L, pH=8, T=25°C.

Figure 6.5 shows the results of the resin regeneration with 0.5M HCl. The initial removal (before regeneration) was 93.56% and the results show an increase in the boron removal after regeneration. The removal was 100% for the first, second and third cycles of the regeneration while the removal was 98.38% for the fourth and fifth cycles.

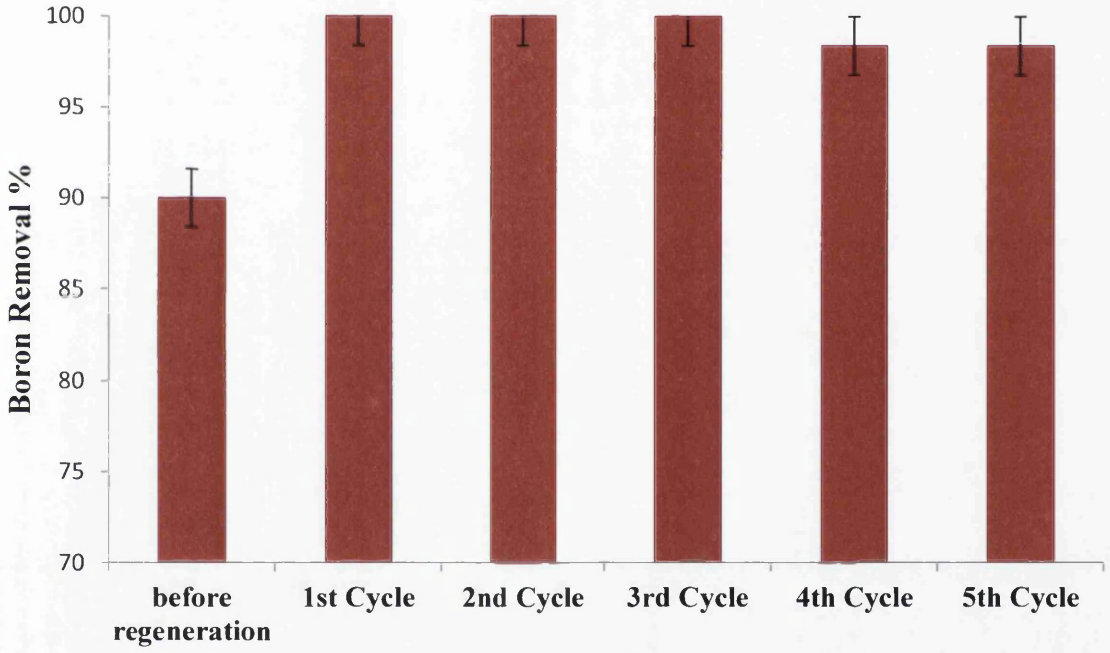

Figure 6.5 Regeneration of Amberlite IRA743 resin using 0.5 M HCl, Boron Concentration=5 mg/L, resin dosage=2 g/L, pH=8, T=25°C.

Figure 6.6 presents the regeneration cycles using 1M HCl. The initial removal of boron was 98.18%. The removal increased from the second cycle until the fifth cycle and the removal reached 100%.

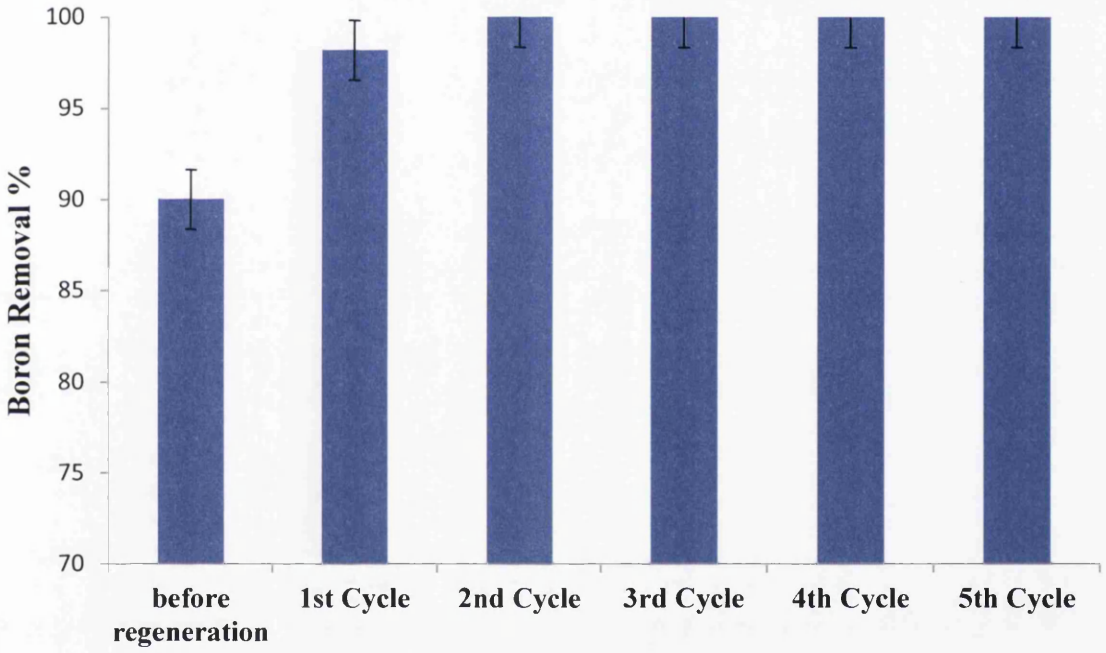

Figure 6.6 Regeneration of Amberlite IRA743 resin using 1M HCl, Boron Concentration=5 mg/L, resin dosage=2 g/L, pH=8, T=25°C.

The regeneration cycles using 2M HCl are shown in Figure 6.7. The boron removal increased to 100% after the regeneration. The improvement in the boron removal could be due to activation of functional sites on the resin by reconditioning with NaOH during the regeneration step (Badruk *et al.*, 1999, Koseoglu *et al.*, 2008a).

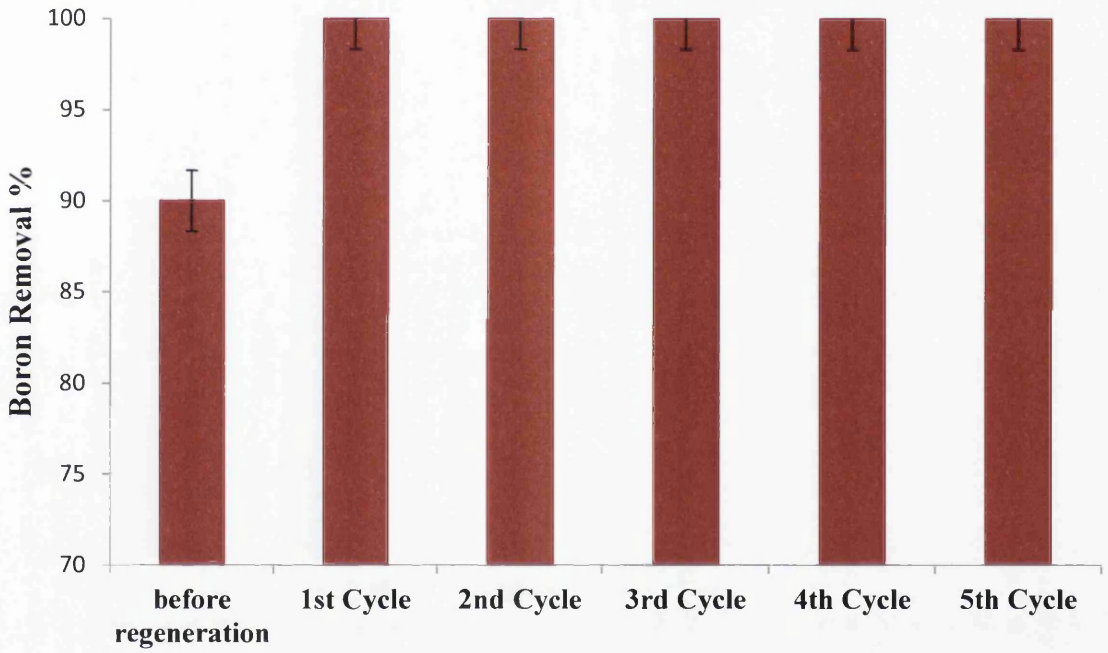

Figure 6.7 Regeneration of Amberlite IRA743 resin using 2M HCl, Boron concentration=5 mg/L, resin dosage=2 g/L, pH=8, T=25°C.

The additional set of regeneration experiments was performed using HCl acid at two different acid concentrations (0.2 and 2M HCl) for feed solution containing 1.5 mgB/L at pH 8, temperature 25°C and resin dosage of 0.4 g/L.

Figure 6.8 shows the results of the resin regeneration using 0.2M HCl. The regeneration increased the boron removal from 90% before regeneration to 98.18% in the first regeneration cycle. The removal increased to 100% in the second, third, fourth and fifth regeneration cycles.

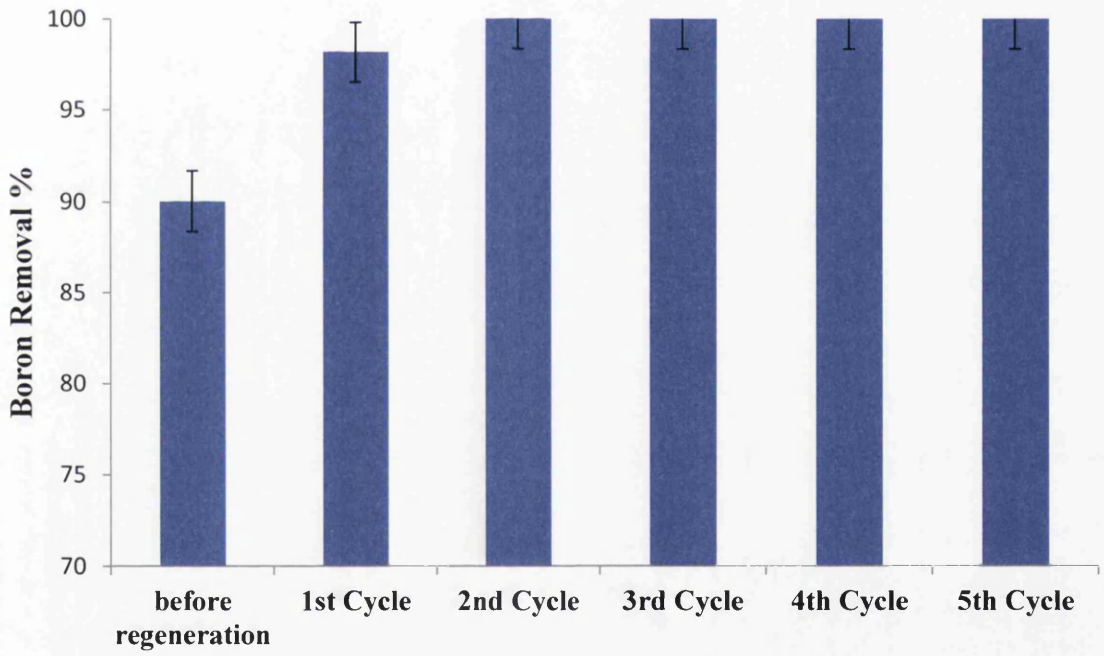

Figure 6.8 Regeneration of Amberlite IRA743 resin using 0.2M HCl , Boron Concentration=1.5 mg/L, resin dosage=0.4 g/L, pH=8, T=25°C

The results of boron removal by Amberlite IRA743 after regeneration using 2M HCl is shown in Figure 6.9. The boron removal was 66.66% before regeneration. Five cycles of regeneration were applied to the resin and the removal reached 100% after these cycles of regeneration.

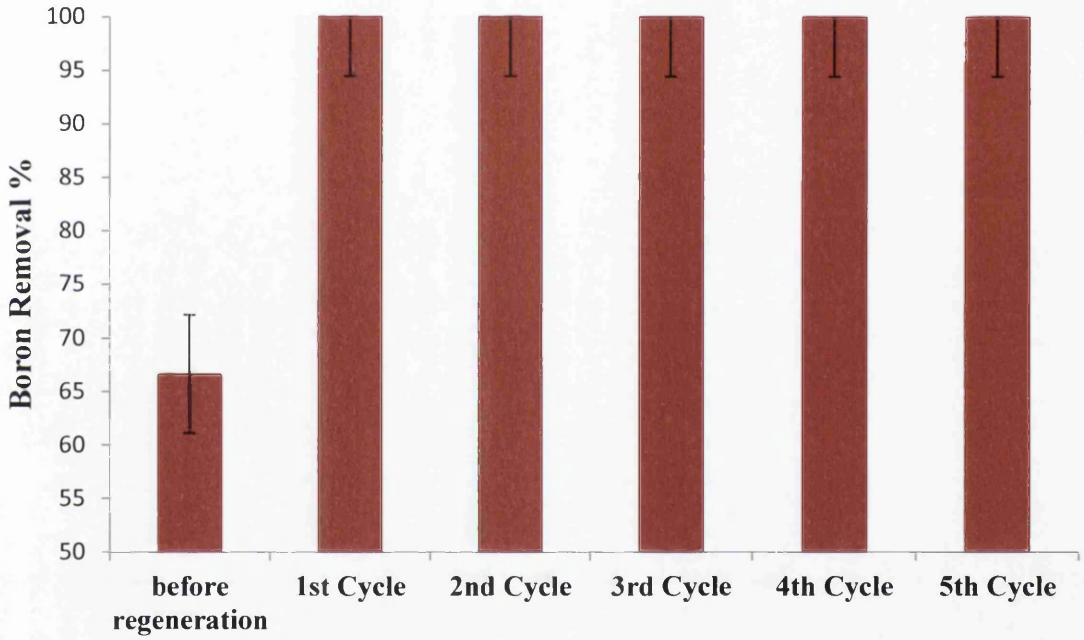

Figure 6.9 Regeneration of Amberlite IRA743 resin using 2M . HCl . Boron Concentration=1.5 mg/L, resin dosage=0.4 g/L, pH=8, T=25°C

6.3 Regeneration with H_2SO_4 and NaOH

Figures 6.10-6.13 show the regeneration results using H_2SO_4 acid at different concentrations. Figure 6.10 shows the results of the regeneration of the resin with 0.2M H_2SO_4. The initial boron removal with the resin was 90% and it increased to 100% after five cycles of regeneration.

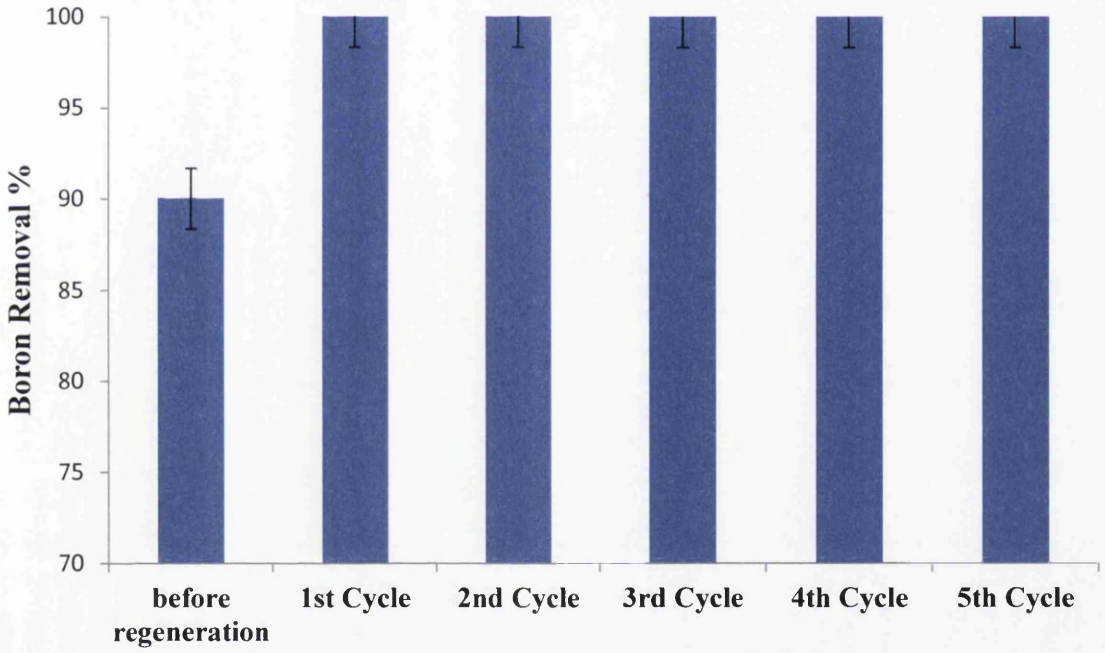

Figure 6.10 Regeneration of Amberlite IRA743 resin using 0.2M H_2SO_4 , Boron Concentration=5 mg/L, resin dosage=2 g/L, pH=8, T=25°C

The regeneration using 0.5M H_2SO_4 is shown in Figure 6.11. The boron removal increased from 90% before the resin regeneration to 100% after regeneration for the five cycles of regeneration. The results of the resin regeneration using 1 M H_2SO_4 is shown in Figure 6.12. The removal increased from 90% to 92.45% and 96.22% after the first and second cycle of regeneration respectively while it reached 100% at the third , fourth and fifth regeneration cycles.

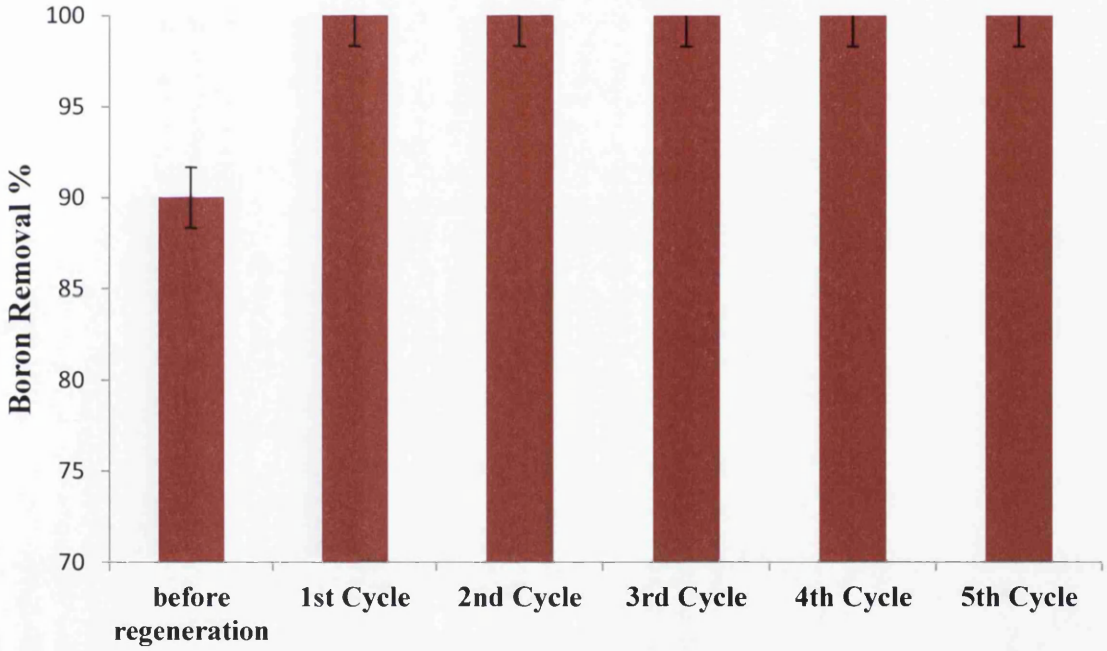

Figure 6.11 Regeneration of Amberlite IRA743 resin using 0.5M H_2SO_4 , Boron Concentration=5 mg/L, resin dosage=2 g/L, pH=8, T=25°C

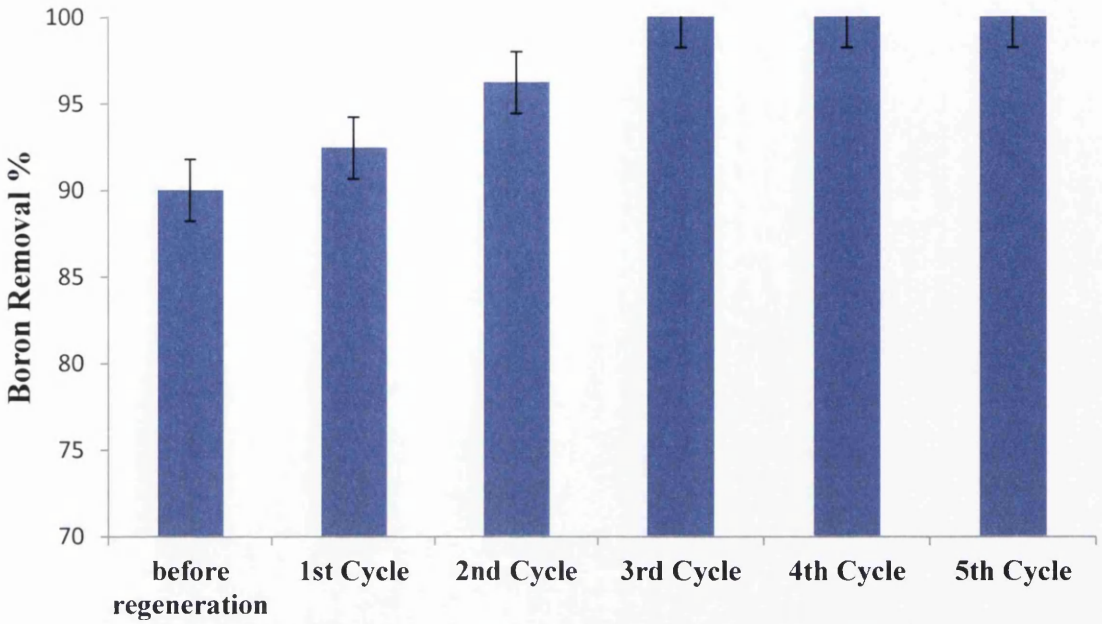

Figure 6.12 Regeneration of Amberlite IRA743 resin using 1M H_2SO_4 , Boron Concentration=5 mg/L, resin dosage=2 g/L, pH=8, T=25°C.

Figure 6.13 presents the result of the regeneration of the resin with 2M H_2SO_4. The initial boron removal reached 90% and it increased to 92.45% after the first regeneration cycle and 96.22% in the second cycle. The boron was removed completely from the water after the third, fourth and fifth cycles of regeneration.

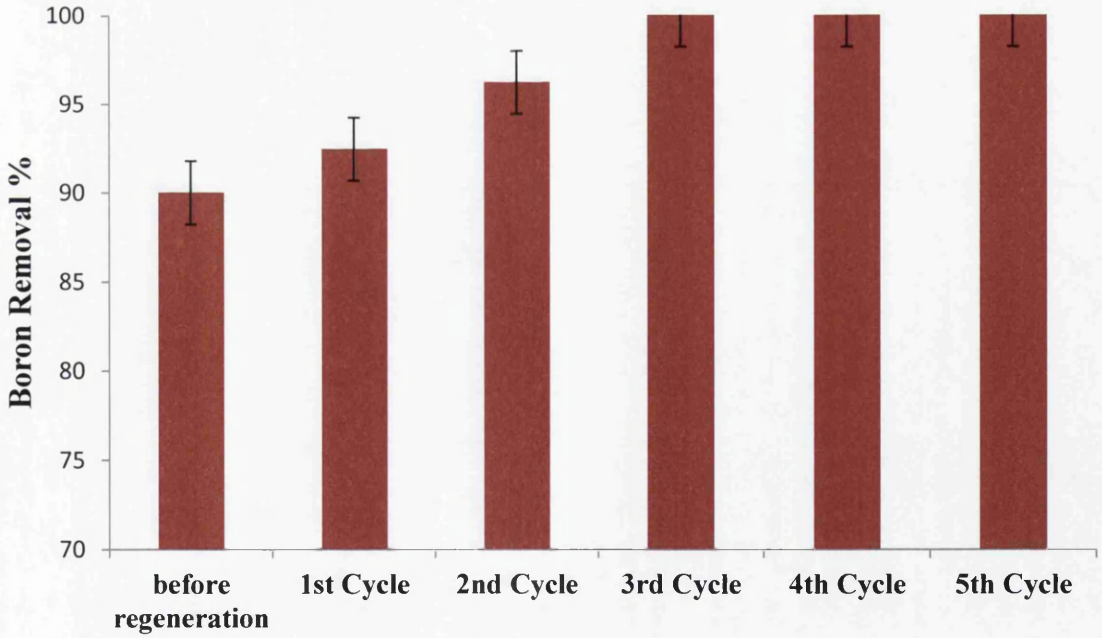

Figure 6.13 Regeneration of Amberlite IRA743 resin using 2M H_2SO_4. Boron Concentration=5 mg/L, resin dosage=2 g/L, pH=8, T=25°C.

The additional set of regeneration experiments was performed using H_2SO_4 acid at two different acid concentrations (0.2 and 2M) for feed solution containing 1.5 mgB/L at pH 8, temperature 25°C and resin dosage of 0.4 g/L.

The results of the regeneration using 0.2M H_2SO_4 is shown in Figure 6.14. The regeneration increased the boron removal from 66.66% before regeneration to 100% in the first to the fifth regeneration cycles.

Figure 6.15 shows the boron removal results after resin regeneration with 2M H_2SO_4 . The boron removal was 66.66% before regeneration. Five cycles of regeneration were applied to the resin and the removal reached 100% after these cycles of regeneration.

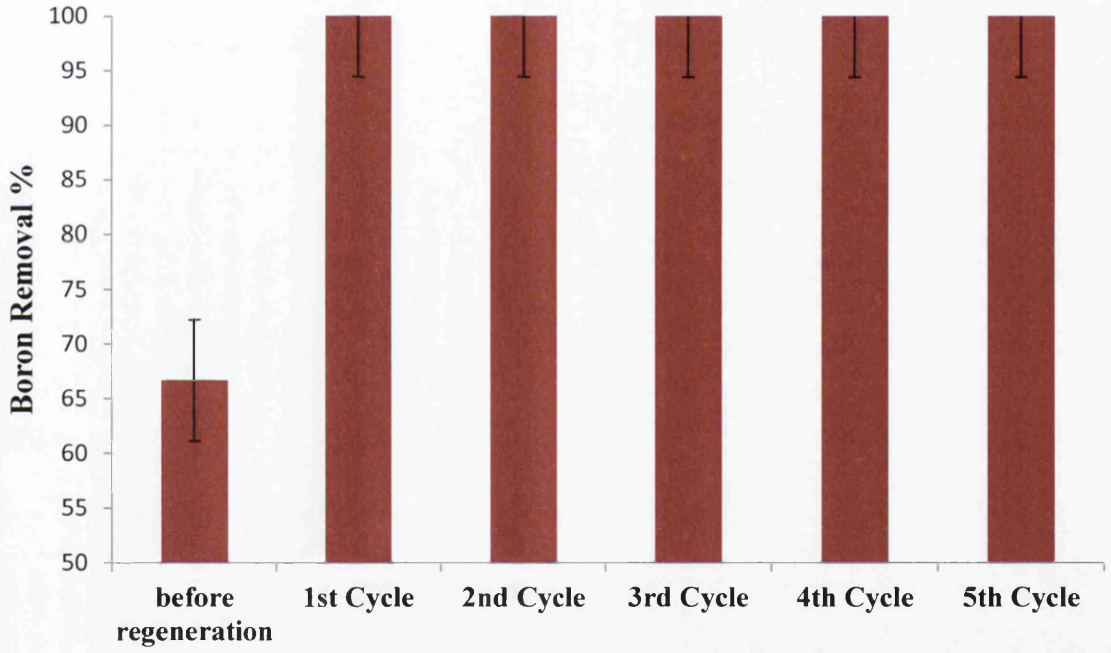

Figure 6.14 Regeneration of Amberlite IRA743 resin using 0.2M H_2SO_4 , Boron Concentration=1.5 mg/L, resin dosage=0.4 g/L, pH=8, T=25°C.

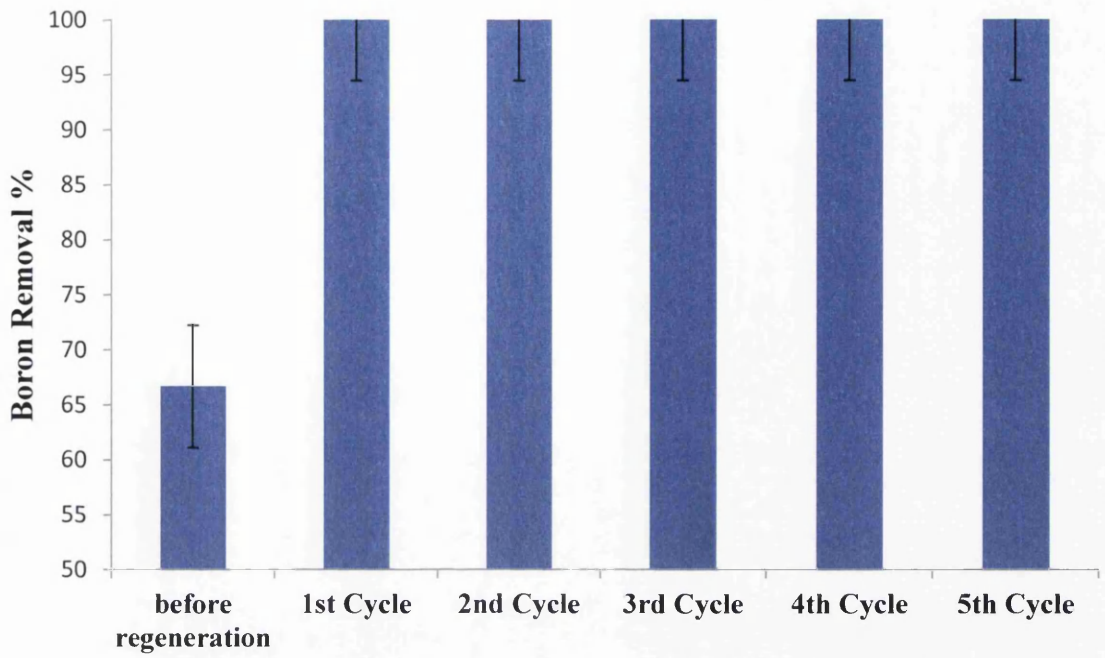

Figure 6.15 Regeneration using 2M H_2SO_4 , Boron Concentration=1.5 mg/L, resin dosage=0.4 g/L, pH=8, T=25°C.

It should be noted that Kabay *et al.* (2004a) found a complete stripping of boron from Diaion CRB 01 and Purolite S 108 (1) resins with H_2SO_4 as low as 0.05 M. They also used HCl at 0.1, 0.2, 0.5 and 1.0 M and H_2SO_4 at 0.05, 0.1, 0.25 and 0.5M for the resin regeneration.

6.4 Effect of regeneration treatment on particle size of the resin

In these experiments, the Amberlite IRA743 resin beads were ground using ball mill to get fine particles of the resin. When the resin particles are ground by a mechanical grinding, it is possible that swelling stress may cause the additional disruption of the polymer matrix and lower the particle diameter (Bryjak *et al.*, 2009). To evaluate this phenomenon, after simulations of five cycles of regeneration cycles, the particle size distribution of the resin particles was measured. The samples of Amberlite IRA743 resin were subjected to consecutive immersion in HCl, H_2SO_4 and NaOH solutions. Particle

size distribution was measured after each experiment. The results are shown in Table 6.1. The presented data show that the immersion in the acids and base does not result in additional breaking in the resin particles. Hence, it was concluded that the ground resin might be used for boron separation in the AMF system (Bryjak *et al.*, 2009). Figures 6.16-23 show the particle size distribution of the resin after five cycles of regeneration.

Table 6.1 Particle Size of the resin after 5 cycles of acid-base immersion

Sample	d_{10} (μm)	d_{50} (μm)	d_{90} (μm)	SPAN
Before cycling	9.69	38.82	88.76	2.036
After regeneration with 0.2M HCl	32.48	66.50	125.76	1.402
After regeneration with 0.5M HCl	19.21	48.19	98.68	1.649
After regeneration with 1M HCl	17.59	47.58	98.65	1.703
After regeneration with 2M HCl	14.88	43.76	95.45	1.841
After regeneration with 0.2M H_2SO_4	17.52	46.58	98.64	1.741
After regeneration with 0.5M H_2SO_4	12.63	41.05	92.14	1.936
After regeneration with 1M H_2SO_4	19.17	51.04	103.87	1.659
After regeneration with 2M H_2SO_4	22.62	52.27	114.91	1.765

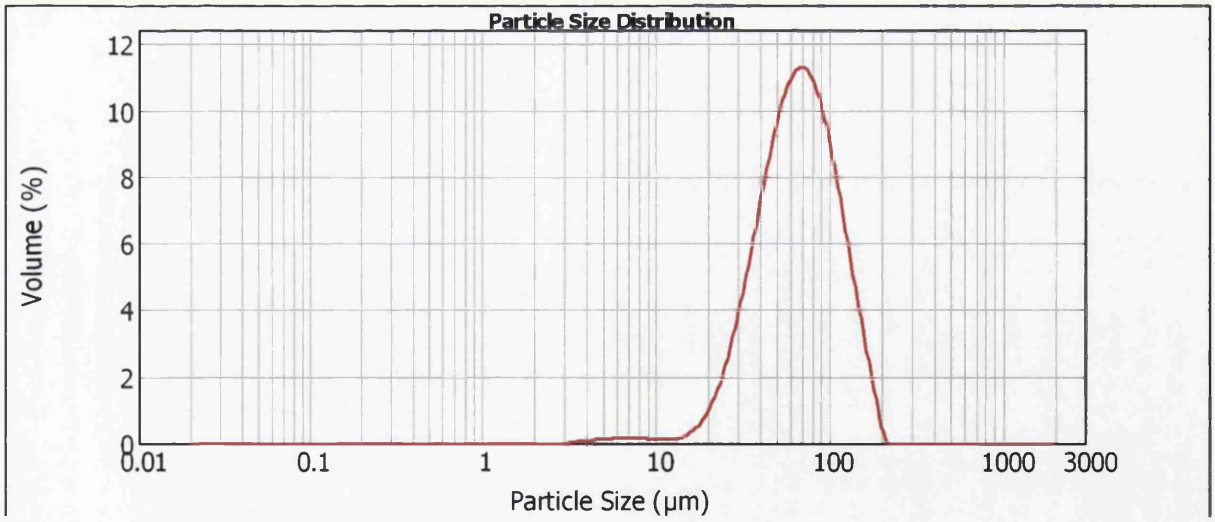

Figure 6.16 Particle size distribution for the fraction of Amberlite IRA743 resin after regeneration with 0.2M HCl

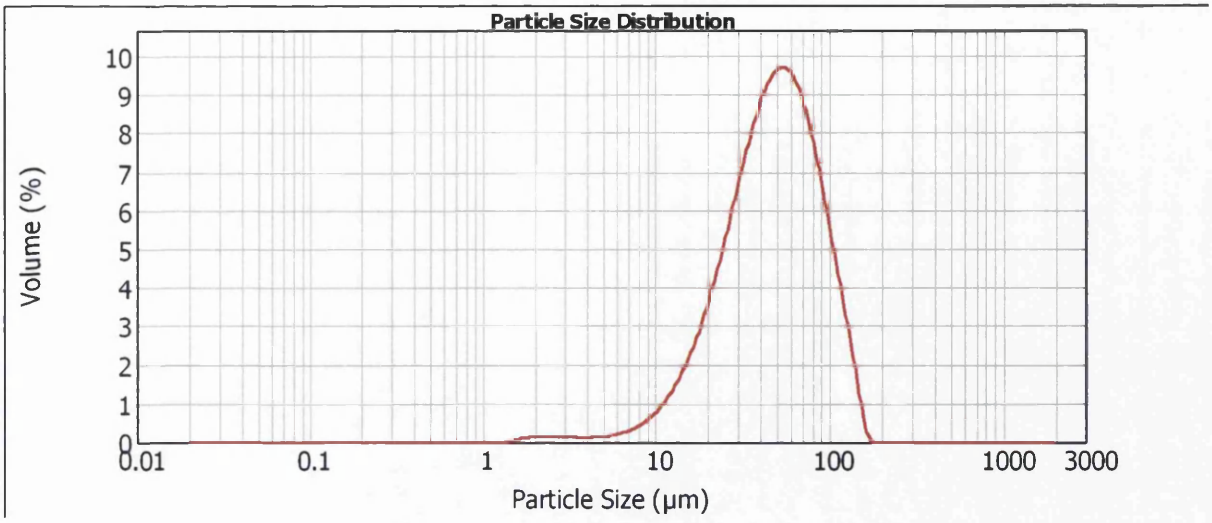

Figure 6.17 Particle size distribution for the fraction of Amberlite IRA743 resin after regeneration with 0.5M HCl

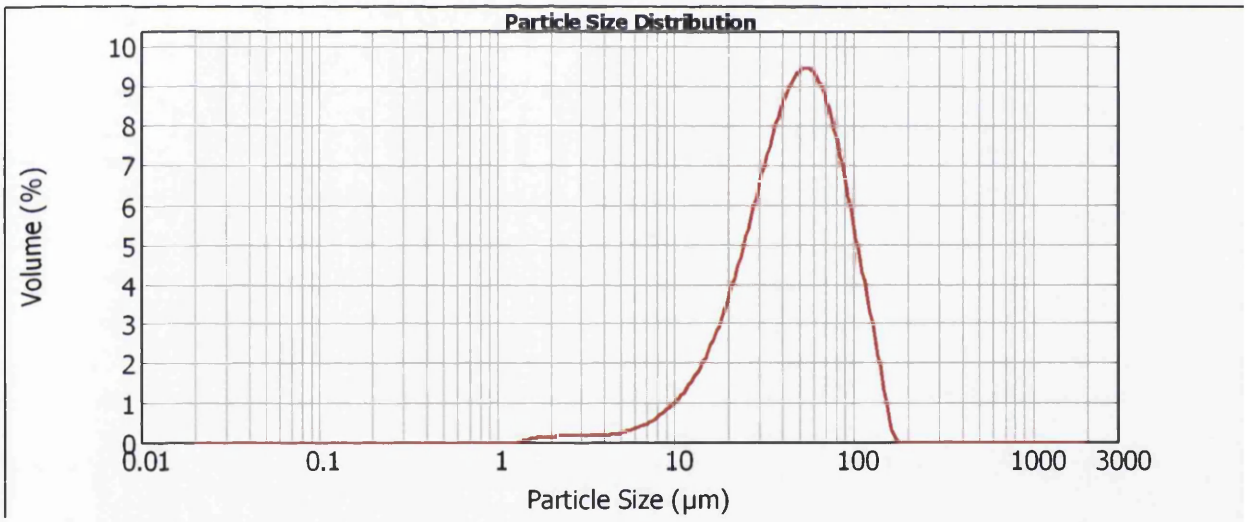

Figure 6.18 Particle size distribution for the fraction of Amberlite IRA743 resin after regeneration with 1M HCl

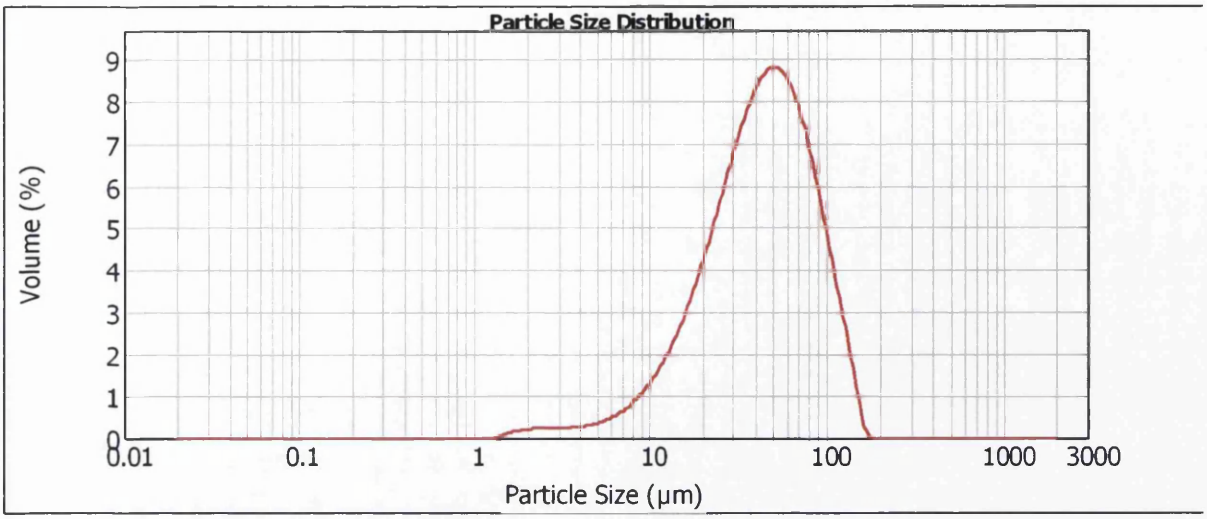

Figure 6.19 Particle size distribution for the fraction of Amberlite IRA743 resin after regeneration with 2M HCl

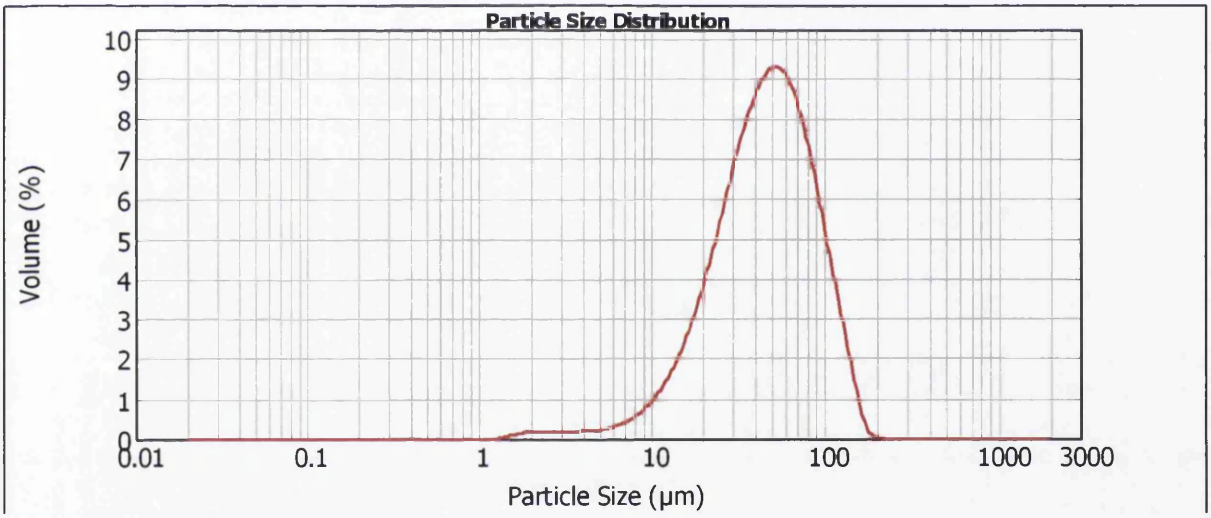

Figure 6.20 Particle size distribution for the fraction of Amberlite IRA743 resin after regeneration with 0.2M H_2SO_4

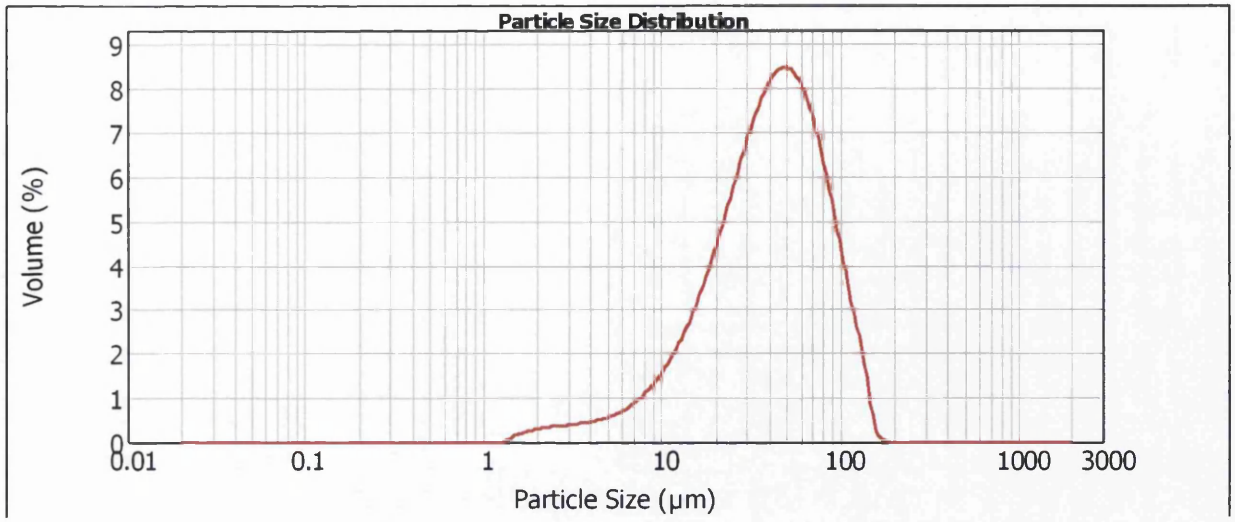

Figure 6.21 Particle size distribution for the fraction of Amberlite IRA743 resin after regeneration with 0.5M H_2SO_4

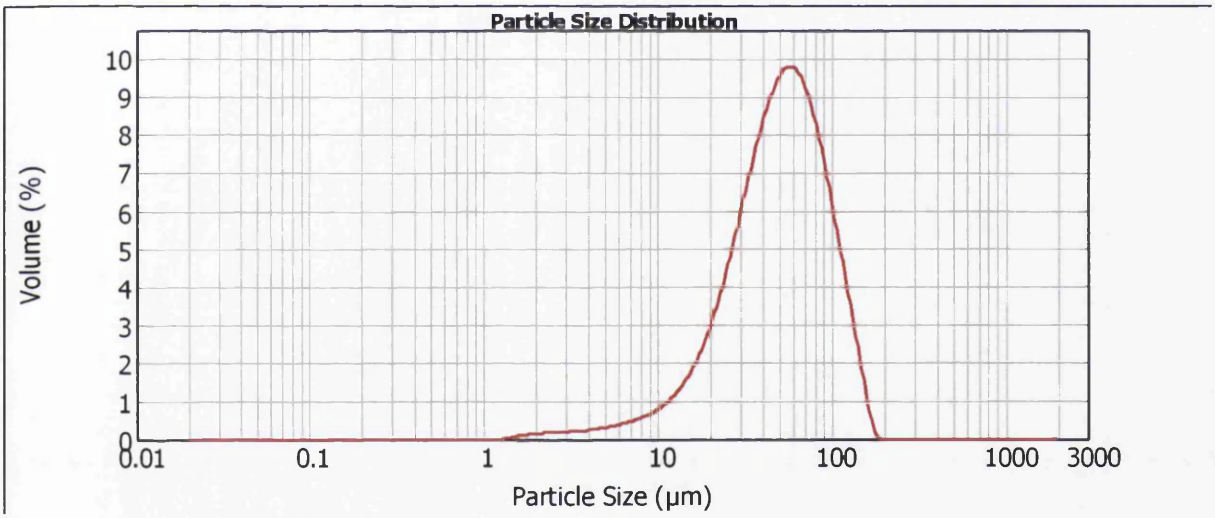

Figure 6.22 Particle size distribution for the fraction of Amberlite IRA743 resin after regeneration with 1 M H_2SO_4

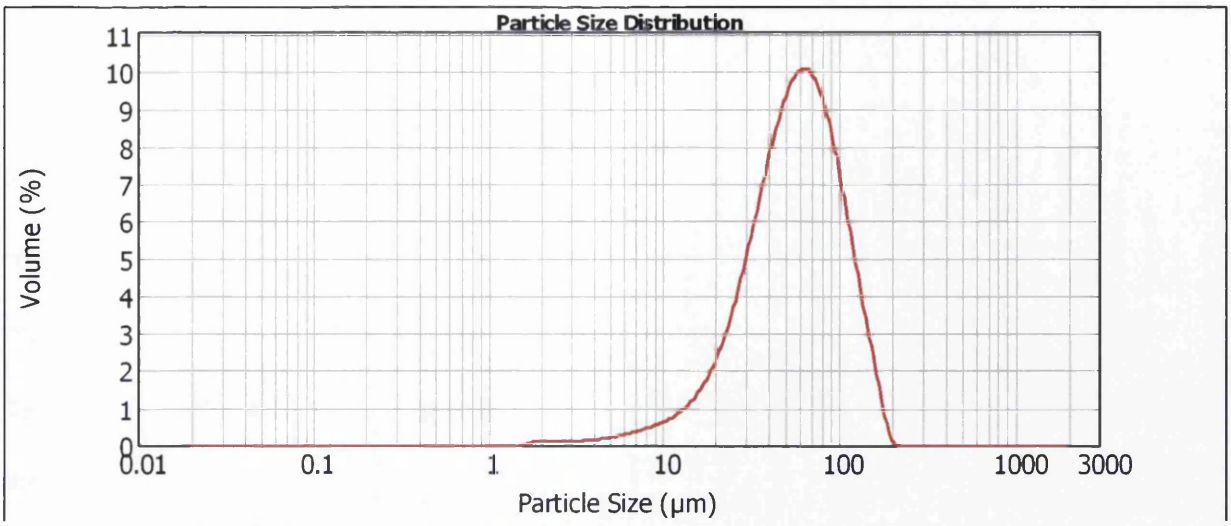

Figure 6.23 Particle size distribution for the fraction of Amberlite IRA743 resin after regeneration with 2M H_2SO_4

6.5 Conclusions

The regeneration of the saturated Amberlite IRA743 resin with boron was investigated in this chapter and its reusability for boron removal from water was tested. The regeneration process was performed by two steps, elution of boron from the loaded resin by acid (HCl or H_2SO_4) and then washing with NaOH. Different concentrations of the used acids were tested and the main findings are summarized as follows:

1- The exhausted Amberlite IRA743 resin saturated with boron can be efficiently regenerated and reused after treatment with HCl or H_2SO_4 solutions followed by NaOH treatment.
2- The boron removal from water improved after the resin regeneration using both HCl and H_2SO_4 at different concentrations obviously due to activation of functional sites on the resin by reconditioning with NaOH during the regeneration step.
3- The particle size distribution of the resin doesn't change after five sorption-elution-washing-regeneration-washing cycles using both HCl and H_2SO_4 at different concentrations.
4- The time to elute boron from the resin is about the same as the time of adsorption.
5- The ground resin might be used for boron separation in the AMF system since there is no additional breaking in the resin particles after cycles of regeneration.

CHAPTER 7

Integrated AMF Process of Boron Removal from Water

7.1 Introduction

In the previous chapters, the adsorption of boron using the selective-boron resin Amberlite IRA743 and the resin regeneration with acid and base were done in a batch system.

The impact of operational parameters such resin particle size, pH, temperature, boron concentration, resin dosage on boron removal using fine particles of the selective-boron Amberlite IRA743 resin have been studied. The regeneration of the loaded resin using acid followed by base washing has been tested in a previous chapter. Two acids, HCl and H_2SO_4, were tested for the regeneration of the saturated resin in a batch system.

In this chapter, the integrated system which combines the adsorption of boron using fine particles of the resin and the elution and regeneration of the loaded resin in one system has been investigated. For this purpose, a hybrid adsorption-microfiltration system was designed and investigated.

The integrated system includes two separation loops, as shown in Figure 7.1 (Borokhov Akerman *et al.*, 2012, Kabay *et al.*, 2010, Kabay *et al.*, 2009):

Loop 1: Binding of boron (B) on Amberlite IRA743 resin (S), which is subsequently followed by separation of this (BS) complex from the water by means of semi-permeable microfiltration membrane. Here, pure water (W) is the main product whereas the complex (BS) passes to the second stage of separation. This is sorption step.

Loop 2: Splitting of the complex BS onto the free resin (S) and boron (B) followed by membrane separation is carried out in the second stage of separation (regeneration). This step allows to reuse the resin and to recycle it in the system.

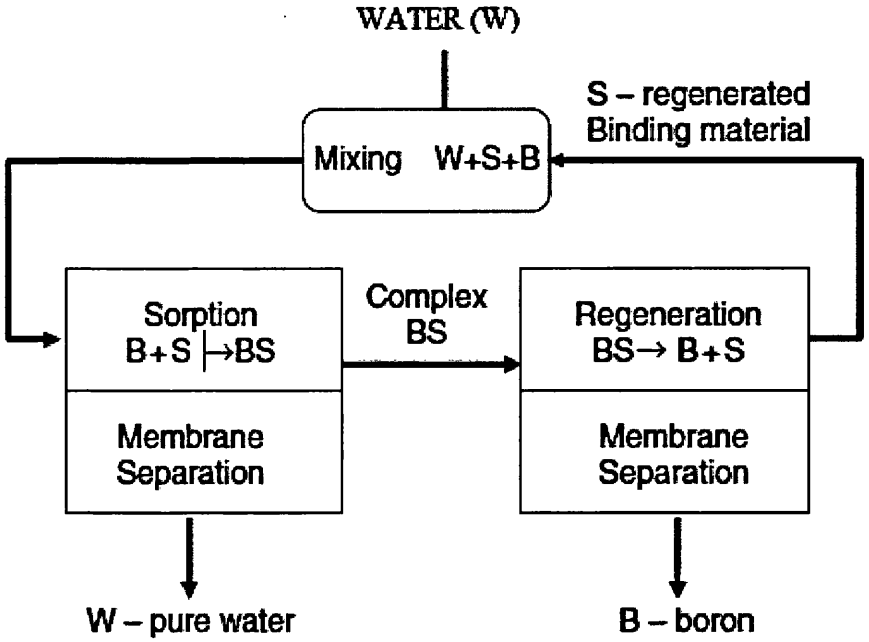

Figure 7.1 Integrated AMF System for boron removal from water, (Borokhov Akerman et al., 2012)

7.2 Design basis

The flow sheet of the hybrid adsorption-microfiltration (AMF) process used in this study is shown in Figure 7.2. Feed solution is mixed with the resin in tank 1 (T1). Loaded adsorbent suspension is pre-concentrated in microfiltration cell MF1. Permeate from MF1 is permeate 1. To suspension in tank 2 (T2) is added the stripping agent, usually acid, to decrease pH and desorb the solute (boron) from the saturated Amberlite IRA743 resin, which is achieved in relatively short time. A suspension of the regenerated adsorbent is further concentrated by microfiltration in the cross-flow module MF2. In Tank 3 (T3), the excess of solute and acid is removed from suspension by diafiltration (washing) with distilled water and after pH adjusting to the level needed for adsorption , the concentrated suspension in tank3 (T3) is concentrated by microfiltration in the cross-flow module MF3 and returned to the AMF process.

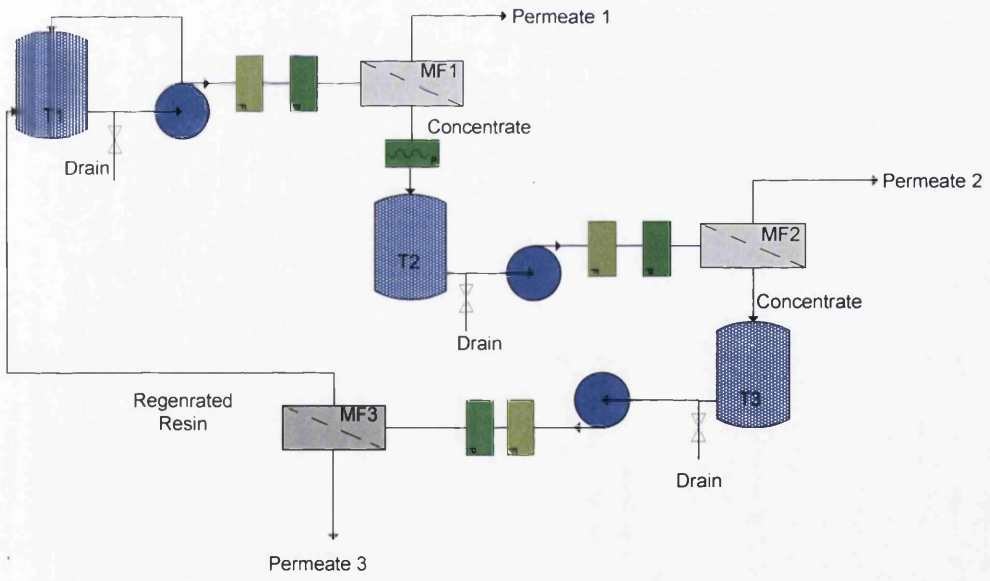

Figure 7.2 A Flow sheet of hybrid AMF process.

7.3 Plant equipment

The integrated system for boron removal is shown in Figure 7.3. The system is consisting from three tanks; tank1 is used for the adsorption step where the solution containing boron is kept in contact with the boron-selective Amberlite IRA743 resin so the removal is happening in this step. Tank2 is used for the elution step where the loaded resin is collecting and the acid is added to elute the boron from the saturated resin. The washing with distilled water and NaOH is performed in tank3 before returning the regenerated resin to the system to be used for the next step of adsorption; the three tanks have a diameter of 21 cm and a height of 20 cm, so the volume of each tank equals 7 litres. All the equipment plant parts are made from stainless steel to avoid any corrosion may happen especially when using acid for the elution step. The pipes used in this study were made of stainless steel with an inner diameter of 4 mm and outer diameter of 6 mm.

Figure 7.3 Adsorption Membrane Filtration (AMF) unit

The microfiltration cells which used in this study are shown in Figure 7.4. Two different polyvinylidene fluoride (PVDF) pore size membranes (0.1 μm and 0.22 μm) were used. The membrane effective area is 0.00332 m^2. Cell1 was connected to tank1 to concentrate the loaded resin and sent it to tank2 as a concentrate for the elution step with acid while the permeate is collected and analysed to measure the boron concentration and calculate the removal efficiency. Cell2 is connected to tank2 where the elution step happened as described earlier and the microfiltration cell2 is separating the eluted resin from the acid solution. The concentrate (eluted resin) from cell2 is collected in tank3 for the washing step with NaOH and water. Cell3 separating the regenerated resin which is collected in Tank1 for the next adsorption step.

Figure 7.4 Microfiltration Cells of the integrated system

To test this process, two polyvinylidene fluoride (PVDF) membranes with pore size 0.1 and 0.22 μm were used. Solutions with different boron concentrations (1.5 and 5 mg/L) were used as a feed solution. The two boron concentrations were chosen as these represent the concentration of boron in seawater (5 mg/L) and the concentration of boron in the permeate from the first stage of reverse osmosis (RO). The resin dosage used was

0.4g/L for the solution with boron concentration 1.5 mg/L and 2 g resin/L for the solution with 5 mg boron/L.

The permeate flux and boron removal efficiency were checked after each cycle.

The pure water fluxes for the membranes (0.1 and 0.22 μm) are shown in Figures 7.5 and 7.6. The permeability of these membranes is, 3325 L/m².hr and 7581 L/m².hr for PVDF 0.1 μm and PVDF 0.22 μm respectively.

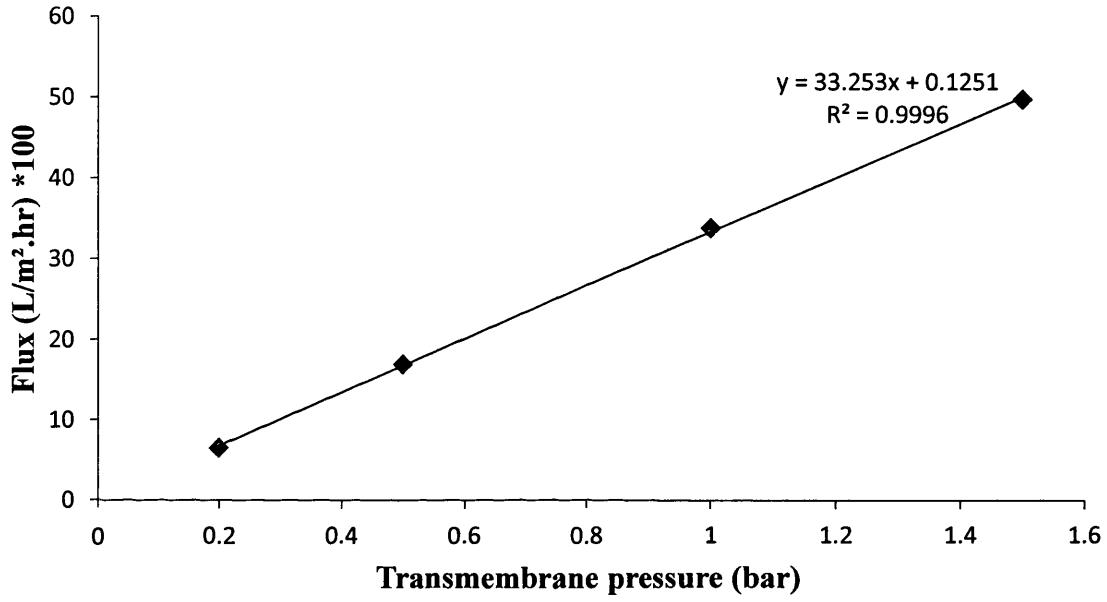

Figure 7.5 Pure water flux of 0.1μm PVDF membrane at various operating pressures

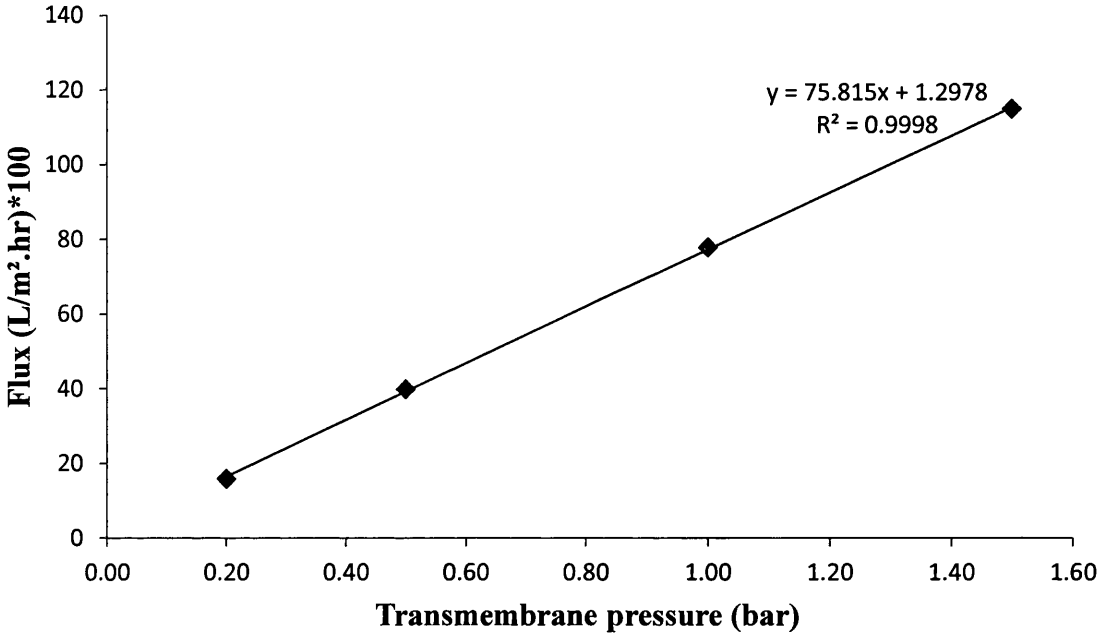

Figure 7.6 Pure water flux of 0.22μm PVDF membrane at various operating pressures

7.4 Hybrid (AMF) Process with 0.22 μm PVDF Membrane

In this section, the AMF system is studied using polyvinylidene difluoride (PVDF) microfiltration membrane with pore size 0.22 μm. Two different boron concentration solutions are used as feed solution. The permeate fluxes for the three microfiltration cells were measured. The results of these fluxes are shown in Figures 7.7-7.9 for the solution with boron concentration of 1.5 mg/L and resin concentration 0.4 g/L and in Figures 7.10-7.12 for the solution with boron concentration of 5 mg/L and resin concentration 2 g/L. The other parameters were kept constant at pH=8 and temperature = 25°C. The trans-membrane pressure applied in this section was 0.5 bar. The boron solution was kept circulated in contact with the boron-selective resin IRA743 for then minutes before the filtration by the microfiltration cell1. The permeate weight (mass) was measured by an electronic balance (Precisa, Model XB3200C) connected to a computer.

Figure 7.7 shows the change in permeate flux with time. The permeate flux decreases with time due to the cake layer formation on the membrane surface as shown in the SEM images illustrated in membrane characterisation section (7.4) in Figure 7.17 (a and b). Cycle0 represents the permeate flux with time for the suspension before resin regeneration. The permeate flux at the beginning of filtration in cycle1 is 3234 L/m².hr and it reaches 1388 L/m².hr at the end of the experiment. Cycle1, 2 and 3 represent the first, second and third cycles after regeneration respectively.

In cycle1, the permeate flux decreases from 2935 L/m².hr in the first minute to 1165 L/m².hr at the end of the experiment which is about 60%. In cycle2 the reduction in permeate flux is about 49% from 1610 to 827 L/m².hr, while in cycle3 the permeate flux decreases from11.85 to 5.43 L/m².hr.

The boron removal was calculated after each cycle by analysing the concentration of boron in the permeate and the results are shown in Table 7.1. The removal was 73.33% at cycle0 and it remains the same after the first cycle of regeneration. The removal improved and increased in cycle2 and cycle3 and it reached 86.66%. The improvement in the boron removal could be due to activation of functional sites on the resin by reconditioning with NaOH during the regeneration step (Badruk *et al.*, 1999, Koseoglu

et al., 2008a, Koseoglu *et al.*, 2008b). The deposition of the resin on the membrane surface may lead to the loss of some quantity of the resin and hence the resin dosage of next cycle is less than the previous one.

The membranes characterisation is shown in section 7.4 in Figure 7.17 (a and b) by taken the surface and cross section images by Scanning electron spectroscopy (SEM). The plot showed that the resin particles deposited on the surface of the membrane and no blockage happened in the membrane pores.

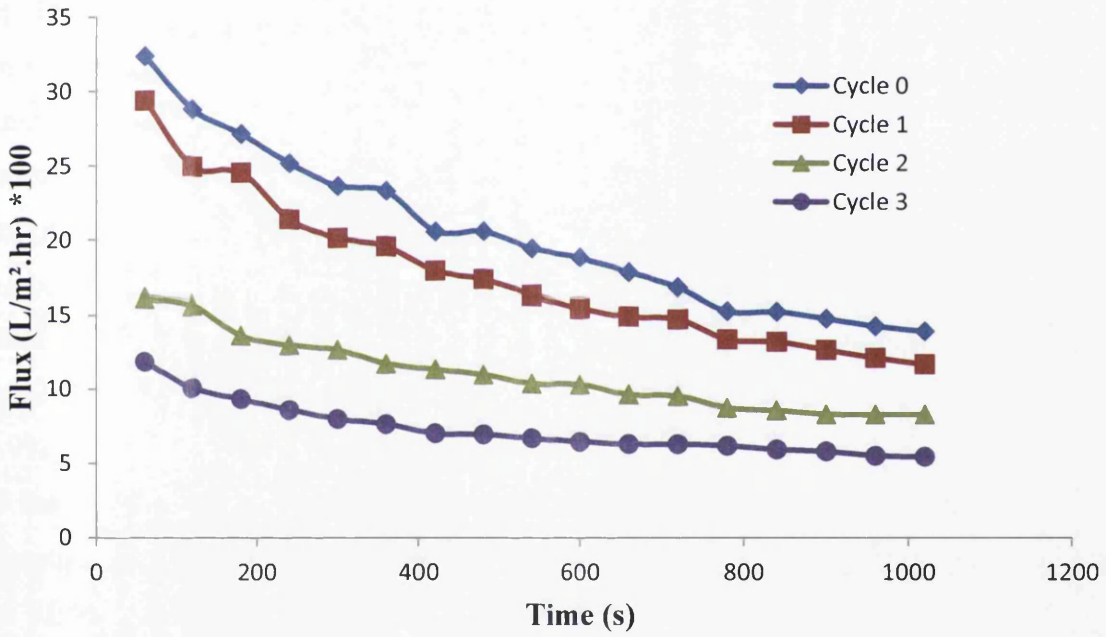

Figure 7.7 Change of permeate flux with time for the adsorption step using 0.22 μm PVDF, Boron concentration= 1.5 mg/L, T=25°C, pH=8, resin dosage= 0.4 mg/L

Table 7.1 The efficiency of boron removal after different regeneration cycles with 0.22 μm PVDF membrane

Cycle	Removal %
0	73.33
1	73.33
2	86.66
3	86.66

The saturated resin (concentrate) from cell1 is collected in tank2 (T2) for the elution step. In this tank, 120 ml of 0.2M HCl is added to the solution and the pH of the solution was reduced to 0.9 and circulated bypass for ten minutes as the adsorption time was 10 minutes and it was found earlier in chapter 6 that the time of elution equals the time of elution and the solution is pumped through cell2. The permeate is measured while the concentrate collected in tank3 (T3) for the next step.

The permeate (acid) flux with time is shown in Figure 7.8. The initial fluxes in cycle1, cycle2 and cycle3 are 2119, 1531 and 1145 L/m².hr respectively. The initial flux in cycle2 decreases by 27.7% compared to the initial flux in cycle1 while it decreased by 45.9% in cycle3 compared to the flux in cycle1. The flux in at the end of the experiment for the three cycles was 856, 682 and 450 L/m².hr for cycle1, cycle2 and cycle3 respectively.

The SEM images of this membrane was taken after these cycles and shown in Figure 7.18 (a and b) in section 7.4. Surface and cross section images were taken for this membrane.

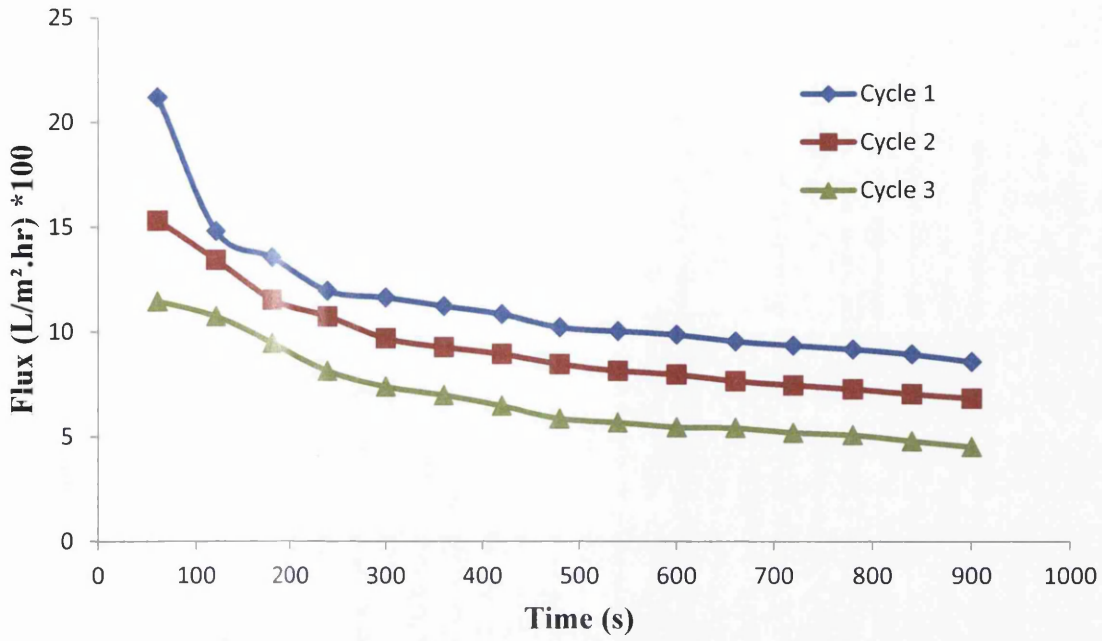

Figure 7.8 Change of permeate flux with time for the elution step in AMF process with 0.22 μm PVDF, 120 ml of 0.2M HCl

In Tank 3 (T3), the excess of solute and acid is removed from suspension by diafiltration (washing) with distilled water and after pH adjusted to neutral pH by adding 80 ml of NaOH , the concentrated suspension in tank3 (T3) is concentrated by microfiltration in in cell3. The concentrate from cell3 is returned to tank1 for the next adsorption cycle. Figure 7.9 shows the change of the flux with time for the three cycles. In cycle1, the flux dropped from 3743 to 961 L/m².hr at the end of the experiment. In cycle2, the flux decreases 46% from 11.13 to 5.99 L/m².hr while at cycle3 is 50% reduction in the flux from 837 to 415 L/m².hr.

The SEM images of this membrane was taken after these cycles and shown in Figure 7.19 (a and b) in section 7.4. Surface and cross section images were taken for this membrane.

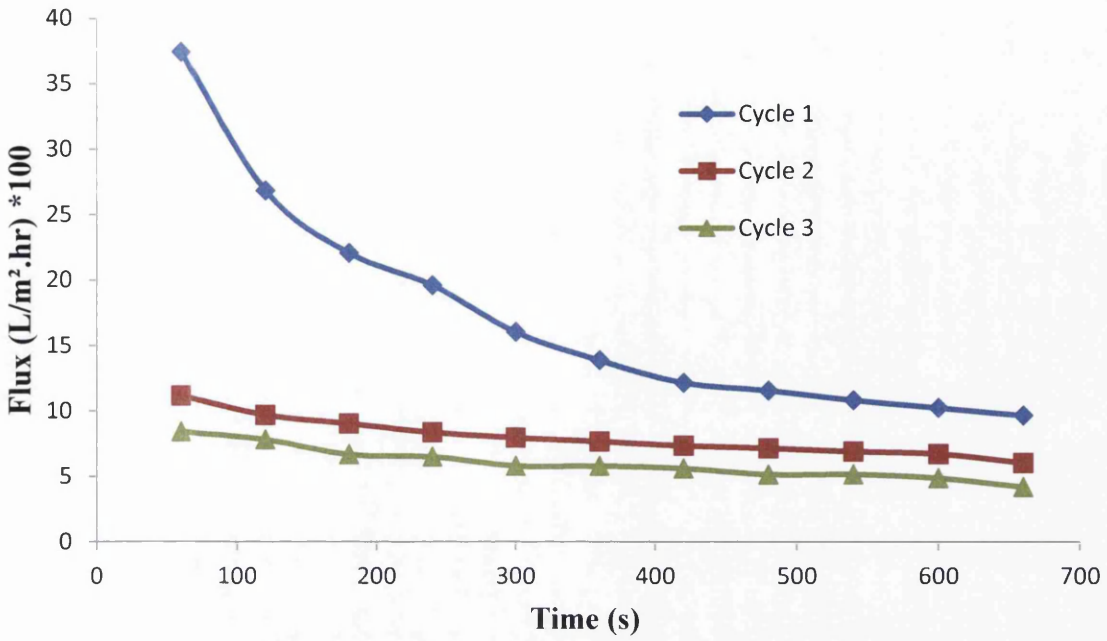

Figure 7.9 Change of permeate flux with time for the regeneration step of AMF process with 0.22 μm PVDF membrane, 80 ml of 0.2M NaOH

The AMF system will be tested using higher boron concentration and resin dosage than the previous section using the same membrane (0.22 μm). The system will be studied using a solution containing 5 mg boron/L and 2 g resin/L. the other parameters were, T=25°C , pH= 8 and contact time is 10 min.

The change of fluxes in the three cycles with time shown in Figure 7.10.

In cycle1, the flux decreased 58% from 1929 L/m².hr in the first minute to 799 L/m².hr at the end of the filtration. The reduction in flux in cycle2 is 56% from 1460 L/m².hr to 631 L/m².hr. In cycle3, the flux declined from 891 L/m².hr to 391 L/m².hr at the end of the experiment. The removal efficiency after each cycle is presented in Table 7.2. The initial boron removal is 90% and it stays the same in the second cycle. In the third cycle, the removal efficiency improves and reaches 100%.

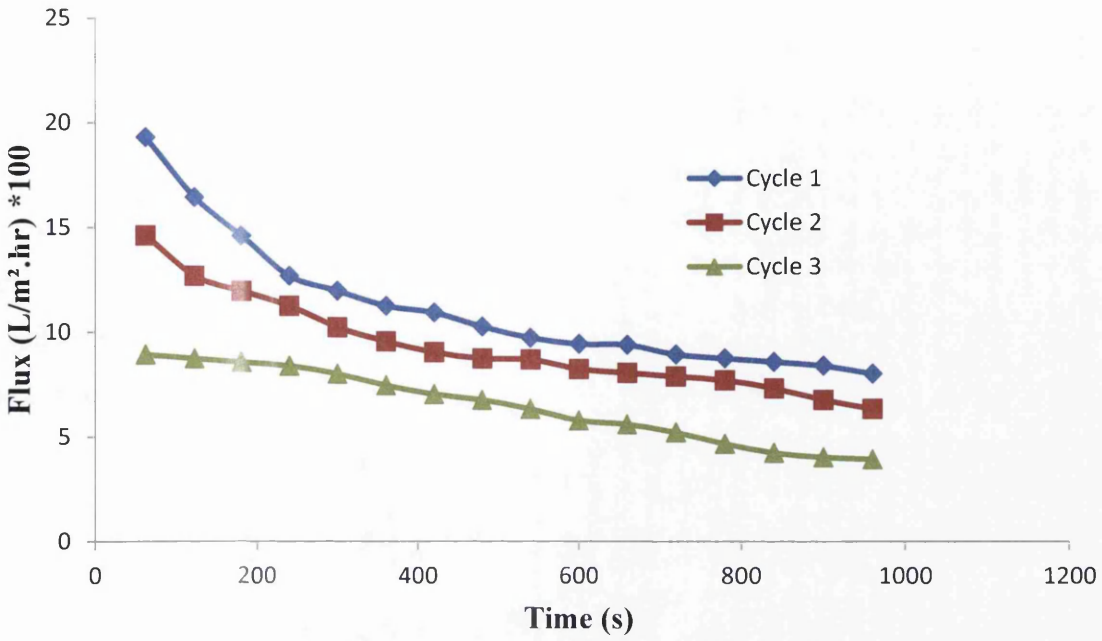

Figure 7.10 Change of permeate flux with time for the adsorption step of AMF process with 0.22 μm PVDF membrane, Boron concentration= 5 mg/L, T=25°C, pH=8, resin dosage= 2 mg/L

Table 7.2 The efficiency of boron removal after different regeneration cycles with 0.1 μm PVDF membrane

Cycle	Removal %
1	90
2	90
3	100

Figure 7.11 shows the change in flux of the acid with time. Here, 600 ml of HCl was added to the saturated resin and the pH is lowered to 0.9 for the elution step and kept circulated for ten minutes. Then, the solution is pumped and filtered and the flux is measured.

As seen from Figure 7.11, the flux decreases with time for the three cycles. The flux in cycle1 decreased from 813 L/m².hr to 418 L/m².hr while it decreases from 616 L/m².hr to 330 L/m².hr and from 550 L/m².hr to 264 L/m².hr in cycle2 and cycle3 respectively. The concentrate from this step is collected in tank3 for the regeneration step with NaOH.

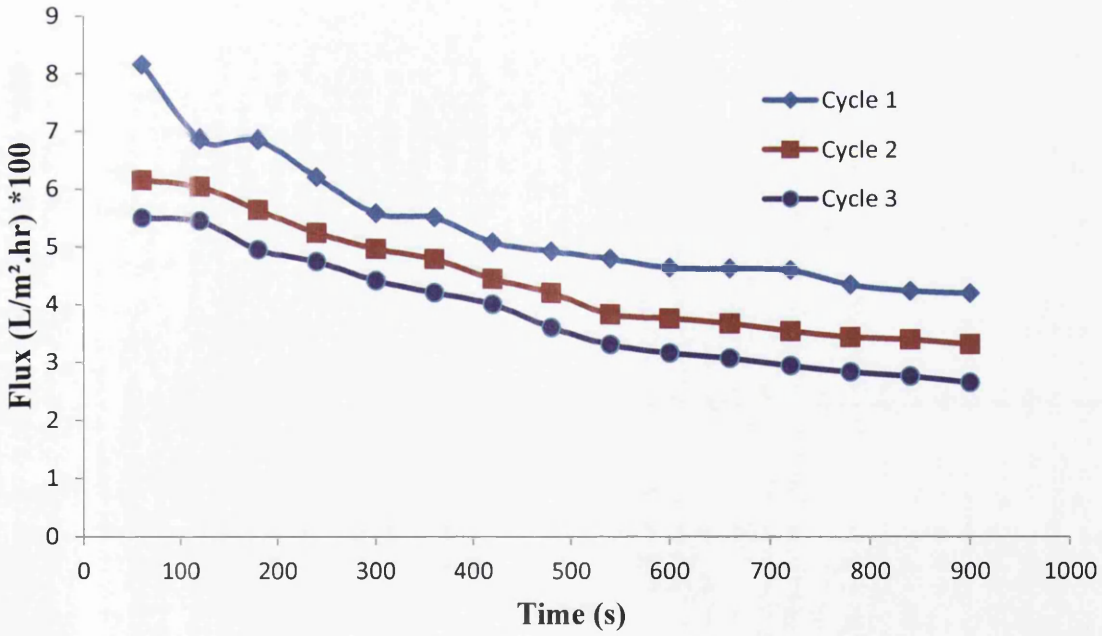

Figure 7.11 Change of permeate flux with time for the elution step of AMF process with 0.22 μm PVDF membrane, 600 ml of 0.2M HCl

After collecting the resin after elution step, 300 ml of NaOH was added to the solution and kept circulated for ten minutes before filtering it by microfiltration. Diafiltration of regenerated adsorbent by washing it with distilled water decreases the concentration of boron and acid in the regenerated suspension.

Figure 7.12 shows the flux with time for this step, the flux reduced in cycle1 by 68% from 1806 L/m².hr to 559 L/m².hr. the reduction in the flux in cycle2 and cycle3 was 49% from 876 L/m².hr to 444 L/m².hr for cycle1 and about 33% from 617 L/m².hr to 408 L/m².hr for cycle2. By measuring the reduction in the flux for the three cycles, it was found that the flux decreases from 1806 L/m².hr to 408 L/m².hr which equal to 77%.

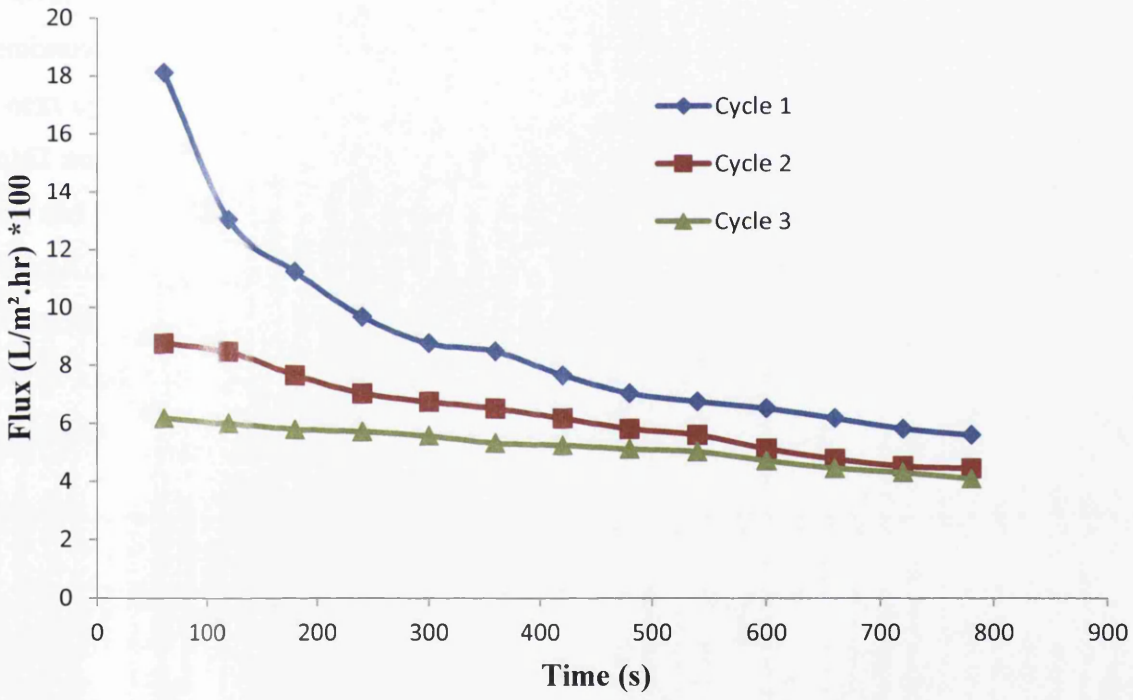

Figure 7.12 Change of permeate flux with time for the regeneration step using 0.22 μm PVDF, 300 ml of 0.2M NaOH

7.5 Hybrid (AMF) Process with 0.1 μm PVDF Membrane

Another PVDF membrane with a pore size of 0.1 μm was used to test the AMF process. A solution with boron concentration of 1.5 mg/L, temperature 25°C, pH 8 and resin concentration of 0.4 g/L was used for this purpose.

The results of the permeate flux of the adsorption step is shown in Figure 7.13. As can be seen from this Figure, there is a reduction in the flux with time for the four cycles due to the deposition of the resin on membrane. the permeate flux decreases from 1458 to 813 L/m².hr, 1069 to 722 L/m².hr, 956 to 638 L/m².hr, and from 714 to 549 L/m².hr for cycle1, cycle2, cycle3 and cycle4 respectively.

The removal efficiency of the regenerated resin is shown in Table 7.3. The removal was 68.75% in cycle1 and it remains the same after the first cycle of regeneration. The removal efficiency improved in cycel3 and cycle4. The deposition of the resin on the membrane surface may lead to the loss quantity of the resin and hence the resin dosage of next cycle is less than the previous one. The improvement in the boron removal in cycle2 and 3 as explained earlier could be due to activation of functional sites on the resin and this covers the loss of the resin quantity (Badruk *et al.*, 1999, Koseoglu *et al.*, 2008a, Koseoglu *et al.*, 2008b).

The SEM images of this membrane was taken after these cycles and shown in Figure 7.21 (a and b) in section 7.4. Surface and cross section images were taken for this membrane.

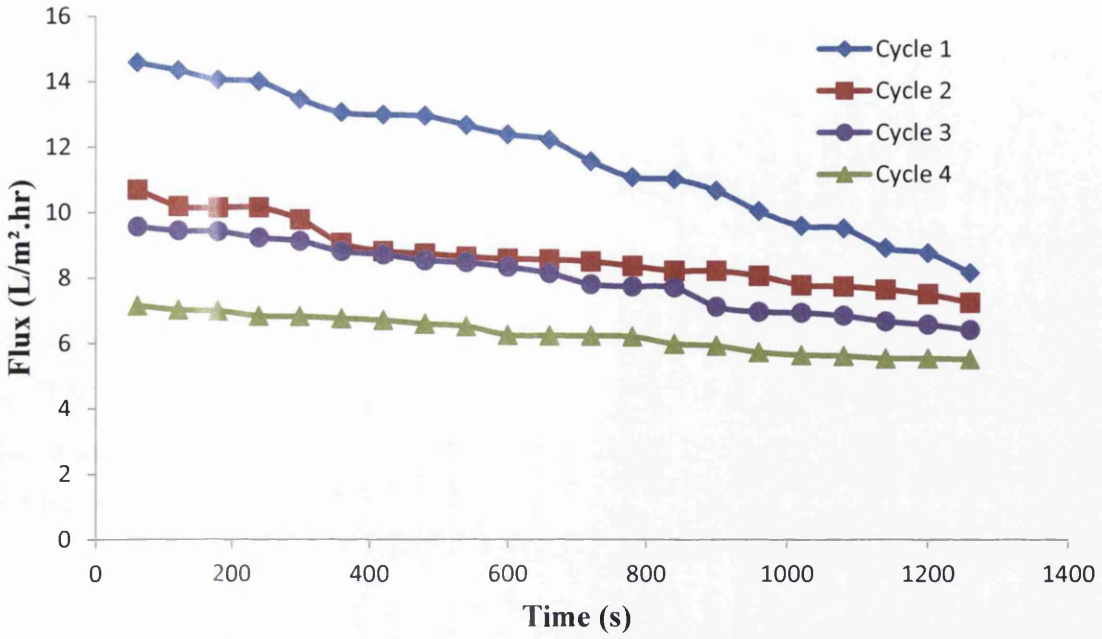

Figure 7.13 Change of permeate flux with time for the adsorption step of AMF process with 0.1 µm PVDF, Boron concentration= 1.5 mg/L, T=25°C, pH=8, resin dosage= 0.4 mg/L

Table 7. 3 The efficiency of boron removal after different regeneration cycles with 0.1 µm PVDF membrane

Cycle	Removal %
1	68.75
2	68.75
3	86.66
4	86.66

The saturated resin was eluted using 120 ml of 0.2M HCl and kept circulated for ten minutes and then filtered through 0.1 μm PVDF membranes. The change in the flux with time is shown in Figure 7.14. The flux decreased with time for all cycles of regeneration. In cycle1, the flux declined from 1320 L/m².hr at the beginning of the filtration to 576 L/m².hr at the end of the experiment. The flux also decreased from 994 L/m².hr to 461 L/m².hr and from 800 L/m².hr to 381 L/m².hr in cycle2 and cycle3 respectively.

The SEM images of this membrane was taken after these cycles and shown in Figure 7.22 (a and b) in section 7.4. Surface and cross section images were taken for this membrane.

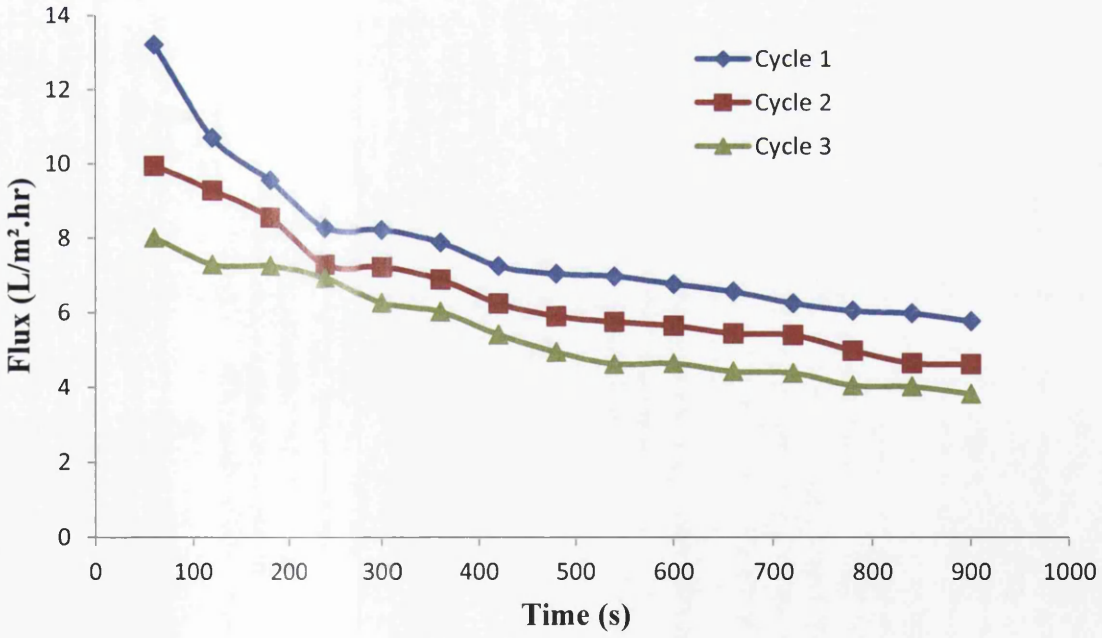

Figure 7.14 Change of permeate flux with time for the elution step of AMF process with 0.1 μm PVDF membrane, 120 ml of 0.2M HCl.

The change in the flux with time for the regeneration step with 0.2M NaOH is shown in Figure 7.15. In this step, the eluted resin was washed with distilled water and regenerated with 80 ml of 0.2M NaOH. The solution was circulated for ten minutes and then filtered using 0.1 μm PVDF membrane. The change in flux with time is shown in Figure 7.15. The flux decreased from 1608 L/m².hr to 461 L/m².hr in cycle1 of regeneration wile it decreased from 528 L/m².hr to 308 L/m².hr and from 377 L/m².hr to 303 L/m².hr in cycle2 and cycle3 respectively.

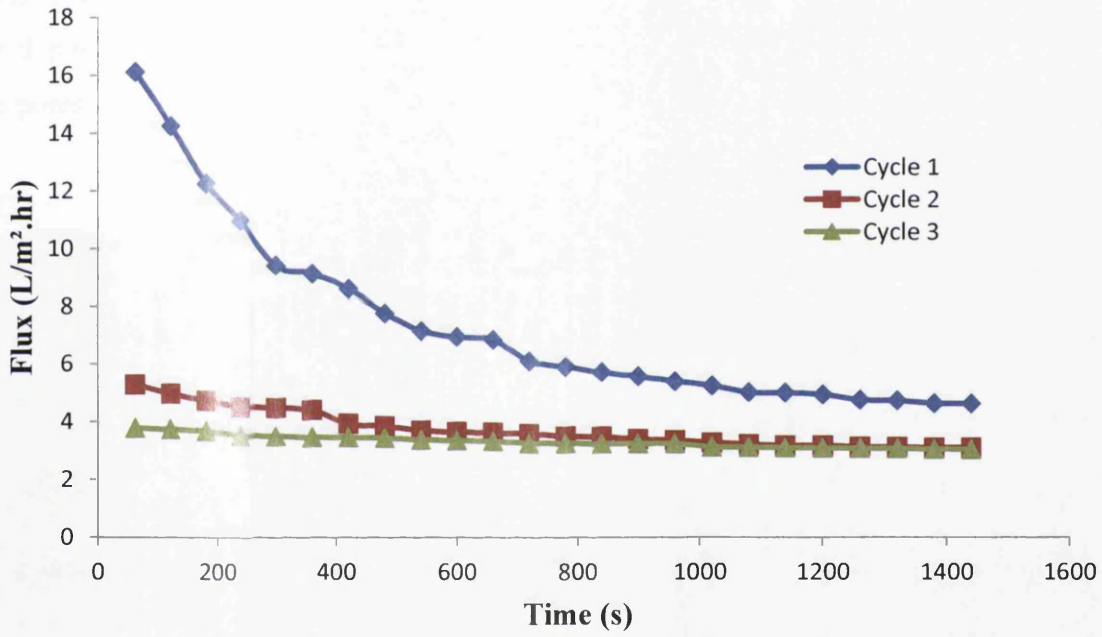

Figure 7.15 Change of permeate flux with time for the regeneration step using 0.1 μm PVDF, 80 ml of 0.2M NaOH

7.6 Characterisation of the membranes

The used PVDF membranes were scanned using Scanning Electron Microscope (SEM).SEM images are shown in Figures 7.16-7.23. Figure 7.12 (a) and (b) shows the surface and cross section images of the clean 0.22 μm PVDF membrane. Figure 7.17 (a) and (b) shows the surface and cross section images of the membrane after filtration of a solution containing 0.4 g resin/L, Figure 7.18 (a) and (b) shows the surface and cross section images of the membrane after elution step of the same solution while Figure 7.19 (a) and (b) shows the surface and cross section images of the membrane after regeneration with 0.2M NaOH. Figures 7.20-7.23 show the surface and cross section images of 0.1 μm PVDF membrane used in the AMF of a solution containing 1.5 mgB/L. From these Figures for both surface and cross section images, it ca be seen that the deposition of the resin happens in the surface of the membrane and nothing blocked the pores.

(a) (b)

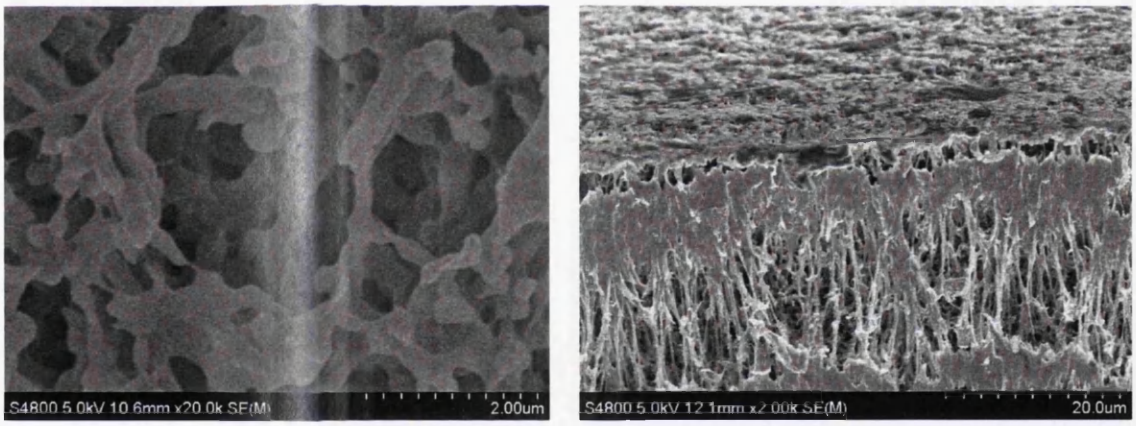

Figure 7.16 SEM micrographs of the new 0.22 μm PVDF membranes: (a)surface (b)cross section

(a) (b)

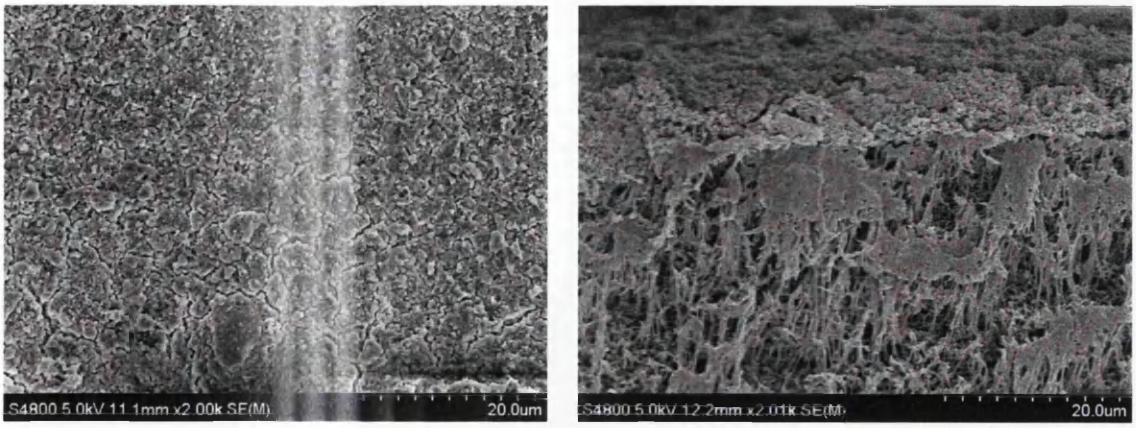

Figure 7.17 SEM micrographs of the 0.22µm used PVDF membranes for adsorption step: (a)surface (b)cross section

(a) (b)

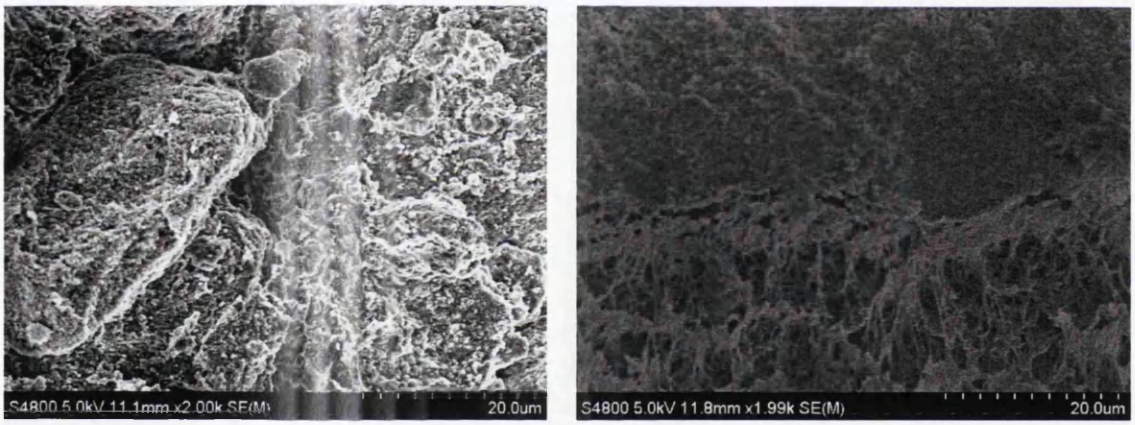

Figure 7.18 SEM micrographs of the 0.22µm used PVDF membranes for Elution step using 0.2M HCl: (a)surface (b)cross section

(a) (b)

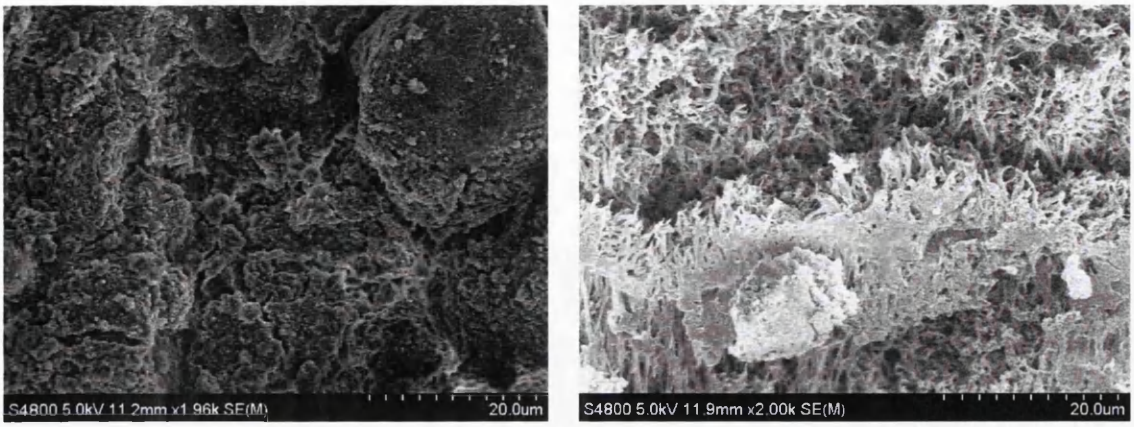

Figure 7.19 SEM micrographs of the 0.22μm used PVDF membranes for regeneration step using 0.2M NaOH: (a)surface (b)cross section

a) b)

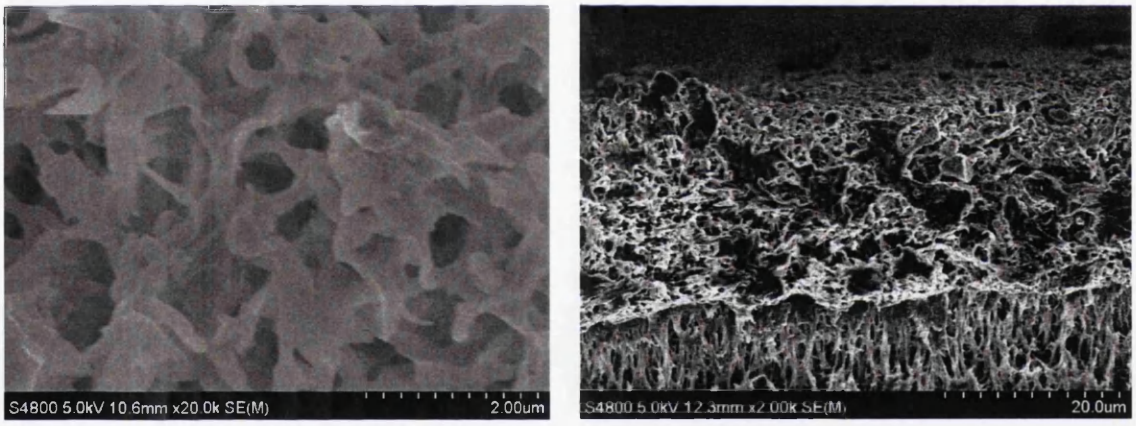

Figure 7.20 SEM micrographs of the 0.1μm New PVDF membranes: (a)surface (b) cross section

(a) (b)

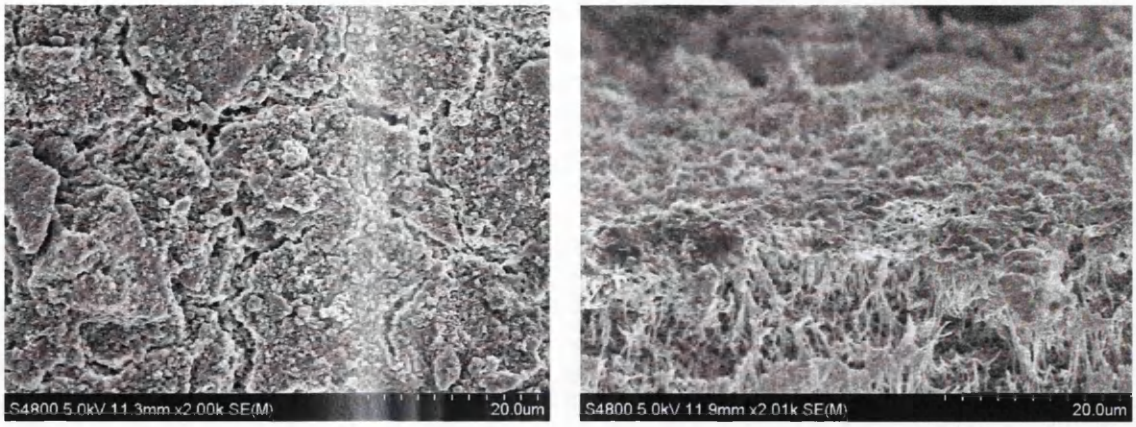

Figure 7.21 SEM micrographs of the 0.1μm used PVDF membranes for adsorption step: (a)surface (b)cross section

(a) (b)

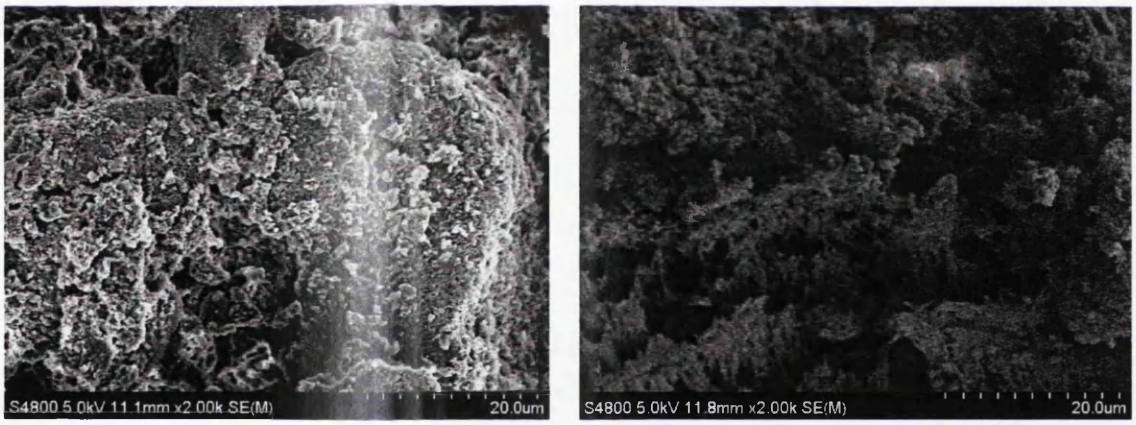

Figure 7.22 SEM micrographs of the 0.22μm used PVDF membranes for Elution step using 0.2M HCl : (a)surface (b)cross section

(a) (b)

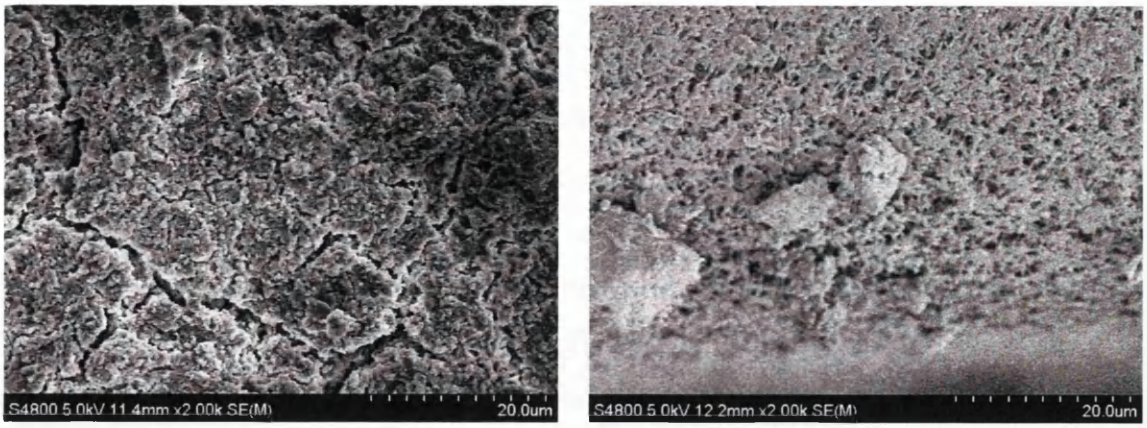

Figure 7.23 SEM micrographs of the 0.22µm used PVDF membranes for regeneration step using 0.2M NaOH: (a)surface (b)cross section

7.7 conclusions

The objective in this part of the thesis is to build a hybrid Adsorption-Microfiltration system at pilot scale and test its ability to desalinate saline water. The integrated process for boron adsorption by Amberlite IRA743 resin and resin regeneration was studied in this chapter. Two different PVDF pore size membranes were used and the change in flux was measured. Feed solutions with different boron concentrations and resin dosages were evaluated. The removal efficiency of the regenerated resin was measured. The major findings can be summarised as follows:

- The flux decreased with time for the two PVDF membranes used for adsorption, elution and regeneration due to the deposition of the resin on the membrane surface as shown in the SEM images.
- There is an improvement in the removal efficiency after repeated regeneration cycles.
- The boron-saturated resin after regeneration can be used repeatedly for efficient boron removal from water .
- According to the SEM images, the deposition of the resin happens on the surface and the pores weren't blocked by the resin particles.

CHAPTER 8

Conclusion, recommendation and future work

8.1 Conclusions

The hybrid process has gained the attention of process engineers lately as it can be used for the removal of very small quantities of harmful substances like boron from water. The hybrid process combines two phenomena: i) sorption on fine particles and ii) membrane separation of B-loaded bodies.

The comparison among the methods used for the removal of boron from water shows that ion exchange is the most effective for water deboronation. The application of the ion exchanger at very fine particles will increase the interface area and results in enhancement of the process rate and results in higher uptakes and better kinetics.

The main benefit of the adsorption membrane filtration (AMF) hybrid process is the higher efficiency and lower costs of the process as compared to the classical fixed bed column sorption and the opportunity of using very fine particles of the sorbent.

The goal of this thesis was to check the possibility to use adsorption-membrane filtration (AMF) hybrid process for cost reduction of boron removal from first stage RO permeate in some seawater desalination plants and from seawater. Two boron concentrations were studied in details, 1.5 mg/L which represents boron concentration in the permeate from the first stage of reverse osmosis (RO) and 5 mg/L which is the boron concentration in seawater.

The integrated adsorption membrane filtration (AMF) hybrid process for boron removal from saline water consists of three main stages, adsorption, filtration and regeneration. For this reason, the aim for this thesis was to apply experimentally the hybrid adsorption-membrane system for boron removal from saline water and study the impact of some parameters on the boron removal and on permeate flux during the microfiltration, the regeneration of the loaded resin was taken in consideration as it plays an important stage in the hybrid system.

For the adsorption stage, the impact of resin particle size, pH, temperature, resin concentration, boron concentration and the presence of foreign ions like NaCl, $MgCl_2$ and Na_2SO_4 boron removal efficiency was investigated. pH plays an important role in the boron removal from saline water as pH increases, the removal increases. No effect of the different salts on the removal which indicate that the resin can remove boron at different environments.

At the filtration step using microfiltration, the effect of membrane pore size, trans-membrane pressure, resin concentration, pH and the presence of foreign ions like NaCl, $MgCl_2$ and Na_2SO_4 on the permeate flux was studied. Three polyvinylidene fluoride (PVDF) microfiltration membranes with different pore sizes (0.1, 0.22 and 0.45 μm) were used and tested. The membrane with a pore size of 0.22 μm has the highest permeate flux compared with the other membranes. The increase in trans-membrane pressure and pH enhance the permeate flux while the resin dosage decreases it.

The regeneration stage was performed using different acids at different concentration. Both HCl and H_2SO_4 at different concentration (0.2, 0.5, 1 and 2 M) showed a good regeneration results and an improvement in the removal efficiency. The results showed that, the time to elute boron from the loaded resin is the same as the time of the sorption of boron from water. The particle size distribution of the resin was measured after each regeneration experiment to check if the immersion with acid breaks the particles and the results showed that no reduction happened in the particles size and this result gives a good indication of using the fine particle in the hybrid system.

The combination of these processes in one system was the main part of this thesis and the results showed that this technology is a promising technique for the removal of boron from saline water. Two different pore size polyvinylidene fluoride (PVDF) microfiltration membranes were used in this part of the study. These membranes are PVDF (0.1 μm and 0.22 μm). The flux and boron concentration in the permeate were measured. The fouling and deposition of the resin particle size were the main problem faced in this study. The boron removal results after three cycles of regeneration indicated that the technology is effective and a promising technology.

8.2 Recommendations

Despite the several achievements in the present work, some suggestions and recommendations should be taken in consideration for future work on the use of Adsorption-microfiltration process for boron removal from seawater. These recommendations are listed below:

- As cross section microfiltration configuration used in this study, the main problem found was fouling, so, another configuration should be tested like submerged microfiltration.
- The regeneration stage consumes large quantity of acid and base, so another regeneration method like donnan dialysis is recommended to be tested in future works.
- In the regeneration unit, the pH of the solution needs to be lowered less than 1 and for that the membrane used in this unit should be capable to work at this pH for long time.

REFERENCES

ADAIR, R. 2007. *Boron*, The Rosen Publishing Group.

AHMARUZZAMAN, M. 2010. A review on the utilization of fly ash. *Progress in Energy and Combustion Science,* 36, 327-363.

AL-ABRI, M. Z. 2007. *Combined macromolecular adsorption and coagulation for improving pre-treatment of membrane processes in desalination plants.* PhD, Nottingham.

ALBERT, B. & HILLEBRECHT, H. 2009. Boron: Elementary Challenge for Experimenters and Theoreticians. *Angewandte Chemie-International Edition,* 48, 8640-8668.

ALI, H. A., DEMBITSKY, V. M. & SREBNIK, M. 2005. *Contemporary Aspects of Boron: Chemistry and Biological Applications: Chemistry and Biological Applications*, Elsevier Science.

ALKHUDHIRI, A. I. 2013. *Treatment of saline solutions using air gap membrane distillation (AGMD).* PhD, Swansea University.

ANDERSON, J. L., EYRING, E. M. & WHITTAKER, M. P. 1964. Temperature jump rate studies of polyborate formation in aqueous boric acid. *J Phys Chem,* 68, 1128-1132.

ARGUST, P. 1998. Distribution of boron in the environment. *Biological Trace Element Research,* 66, 131-143.

AUBERT, H. & PINTA, M. 1997. *Trace elements in soils,* Amsterdam, Elsevier Scientific.

AY, A. N., ZÜMREOGLU-KARAN, B. & TEMEL, A. 2007. Boron removal by hydrotalcite-like, carbonate-free Mg–Al–NO3-LDH and a rationale on the mechanism. *Microporous and Mesoporous Materials,* 98, 1-5.

AYYILDIZ, H. F. & KARA, H. 2005. Boron removal by ion exchange membranes. *Desalination,* 180, 99-108.

BADRUK, M. & KABAY, N. Removal of boron from Kizildere-Denizli geothermal brines using ion-exchange method. Second United Nations Symposium on the Development and Use of Geothermal Resources, San Francisco, California, 2003. 8.

BADRUK, M., KABAY, N., DEMIRCIOGLU, M., MORDOGAN, H. & IPEKOGLU, U. 1999. Removal of Boron from Wastewater of Geothermal Power Plant by Selective Ion-Exchange Resins. II. Column Sorption–Elution Studies. *Separation Science and Technology,* 34, 2981-2995.

BAEK, K. W., SONG, S. H., KANG, S. H., RHEE, Y. W., LEE, C. S., LEE, B. J., HUDSON, S. & HWANG, T. S. 2007. Adsorption kinetics of boron by anion exchange resin in packed column bed. *Journal of Industrial and Engineering Chemistry,* 13, 452-456.

BANASIAK, L. J. & SCHAFER, A. I. 2009. Removal of boron, fluoride and nitrate by electrodialysis in the presence of organic matter. *Journal of Membrane Science,* 334, 101-109.

BEATTY, R. 2005. *Boron*, Benchmark Books.

BEKTAŞ, N., ÖNCEL, S., AKBULUT, H. Y. & DIMOGLO, A. 2004. Removal of boron by electrocoagulation. *Environmental Chemistry Letters,* 2, 51-54.

BEKTAŞ, T. E. & ÖZTÜRK, N. 2004. Boron Removal from Aqueous Solution by Ion-Exchange Resin. *2nd International Boron Symposium.* Eskişehir.

BELCHER, R., TULLY, G. W. & SVEHLA, G. 1970. A Comparative Study of Various Complexing Agents (Polyols) Used in Titration of Boric Acid. *Analytica Chimica Acta,* 50, 261-&.

BIÇAK, N., BULUTÇU, N., ŞENKAL, B. F. & GAZI, M. 2001. Modification of crosslinked glycidyl methacrylate-based polymers for boron-specific column extraction. *Reactive and Functional Polymers,* 47, 175-184.

BICAK, N., GAZI, M. & SENKAL, B. F. 2005. Polymer supported amino bis-(cis-propan 2,3 diol) functions for removal of trace boron from water. *Reactive and Functional Polymers,* 65, 143-148.

BıÇAK, N., ÖZBELGE, H. Ö., YILMAZ, L. & SENKAL, B. F. 2000. Crosslinked polymer gels for boron extraction derived fromN-glucidol-N-methyl-2-hydroxypropyl methacrylate. *Macromolecular Chemistry and Physics,* 201, 577-584.

BICAK, N. & SENKAL, B. F. 1998. Sorbitol-modified poly (N-glycidyl styrene sulfonamide) for removal of boron. *Journal of applied polymer science,* 68, 2113-2119.

BLAHUŠIAK, M., ONDERKOVÁ, B., SCHLOSSER, Š. & ANNUS, J. 2009. Microfiltration of microparticulate boron adsorbent suspensions in submerged hollow fibre and capillary modules. *Desalination,* 241, 138-147.

BLAHUŠIAK, M. & SCHLOSSER, Š. 2009. Simulation of the adsorption—microfiltration process for boron removal from RO permeate. *Desalination,* 241, 156-166.

BONCUKCUOĞLU, R., ERDEM Y11MAZ, A., MUHTAR KOCAKERIM, M. & ÇOPUR, M. 2004. An empirical model for kinetics of boron removal from boron-containing wastewaters by ion exchange in a batch reactor. *Desalination,* 160, 159-166.

BOROKHOV AKERMAN, E., V. SIMHON, M. & GITIS, V. 2012. Advanced treatment options to remove boron from seawater. *Desalination and Water Treatment,* 46, 285-294.

BOUGUERRA, W., MNIF, A., HAMROUNI, B. & DHAHBI, M. 2008. Boron removal by adsorption onto activated alumina and by reverse osmosis. *Desalination,* 223, 31-37.

BOWEN, W. R. & HILAL, N. 2009. *Atomic Force Microscopy in Process Engineering: An Introduction to AFM for Improved Processes and Products*, Elsevier Science.

BOWEN, W. R. & TEODORA, A. D. 2007. Atomic Force Microscopy of Membranes. *Encyclopedia of Surface and Colloid Science, Second Edition.* Taylor & Francis.

BRADY, N. & WEIL, R. 2008. *The nature and properties of soils,* Prentice Hall, Upper Saddle River.

BRUNAUER, S., EMMETT, P. H. & TELLER, E. 1938. Adsorption of gases in multimolecular layers. *Journal of the American Chemical Society,* 60, 309-319.

BRYJAK, M., GANCARZ, I., POŹNIAK, G. & TYLUS, W. 2002. Modification of polysulfone membranes 4. Ammonia plasma treatment. *European Polymer Journal,* 38, 717-726.

BRYJAK, M., KABAY, N., GULER, E., PIEKACZ, J., YILMAZ-IPEK, I. & YUKSEL, M. 2008a. boron removal from seawater reverse osmosis permeate by sorption-membrane filtration hybrid method. *xxiii ars separatoria.* Toruń, Poland.

BRYJAK, M., WOLSKA, J. & KABAY, N. 2008b. Removal of boron from seawater by adsorption–membrane hybrid process: implementation and challenges. *Desalination,* 223, 57-62.

BRYJAK, M., WOLSKA, J., SOROKO, I. & KABAY, N. 2009. Adsorption-membrane filtration process in boron removal from first stage seawater RO permeate. *Desalination,* 241, 127-132.

BURSALı, E. A., SEKI, Y., SEYHAN, S., DELENER, M. & YURDAKOÇ, M. 2011. Synthesis of chitosan beads as boron sorbents. *Journal of Applied Polymer Science,* 122, 657-665.

BUTTERWICK, L., OUDE, N. & RAYMOND, K. 1989. Safety Assessment of Boron in Aquatic and Terrestrial Environments. *Ecotoxicology and Environmental Safety,* 17, 339-371.

CDW 2008. Guidelines for Canadian drinking water quality. Ottawa.

CELIK, Z. C., CAN, B. Z. & KOCAKERIM, M. M. 2008. Boron removal from aqueous solutions by activated carbon impregnated with salicylic acid. *J Hazard Mater,* 152, 415-22.

CENGELOGLU, Y., ARSLAN, G., TOR, A., KOCAK, I. & DURSUN, N. 2008. Removal of boron from water by using reverse osmosis. *Separation and Purification Technology,* 64, 141-146.

CENGELOGLU, Y., TOR, A., ARSLAN, G., ERSOZ, M. & GEZGIN, S. 2007. Removal of boron from aqueous solution by using neutralized red mud. *J Hazard Mater,* 142, 412-7.

CHAHBOUN, A., CORATGER, R., AJUSTRON, F., BEAUVILLAIN, J., AIMAR, P. & SANCHEZ, V. 1992. Comparative study of micro-and ultrafiltration membranes using STM, AFM and SEM techniques. *Ultramicroscopy,* 41, 235-244.

CHAPELLE, S. & VERCHERE, J. F. 1988. A B-11 and C-13 Nmr Determination of the Structures of Borate Complexes of Pentoses and Related Sugars. *Tetrahedron,* 44, 4469-4482.

CHOI, W. W. & CHEN, K. Y. 1979. Evaluation of Boron Removal by Adsorption on Solids. *Environmental Science & Technology,* 13, 189-196.

CHOWDHURY, S. & SAHA, P. 2010. Pseudo-second-order kinetic model for sorption of malachite green onto sea shell: Comparison of linear and non-linear methods. *IIOAB J,* 1, 3-7.

CHUDACEK, M. W. & FANE, A. G. 1984. The dynamics of polarisation in unstirred and stirred ultrafiltration. *Journal of Membrane Science,* 21, 145-160.

COTTON, F. A. & WILKINSON, G. 1980. *Advanced Inorganic Chemistry,* New York, Wiley.

DAMBIES, L., SALINARO, R. & ALEXANDRATOS, S. D. 2004. Immobilized N-methyl-D-glucamine as an arsenate-selective resin. *Environmental science & technology,* 38, 6139-6146.

DEAN, J. A. 1999. *Lange's Handbook of Chemistry,* New York, McGraw-Hill.

DEL MAR DE LA FUENTE GARCÍA-SOTO, M. & CAMACHO, E. M. 2006. Boron removal by means of adsorption with magnesium oxide. *Separation and Purification Technology,* 48, 36-44.
DEMBITSKY, V. M., SMOUM, R., AL-QUNTAR, A. A., ABU ALI, H., PERGAMENT, I. & SREBNIK, M. 2002. Natural occurrence of boron-containing compounds in plants, algae and microorganisms. *Plant Science,* 163, 931-942.
DEMETRIOU, A. & PASHALIDIS, I. 2012. Adsorption of boron on iron-oxide in aqueous solutions. *Desalination and Water Treatment,* 37, 315-320.
DEMIRÇIVI, P. & NASÜN-SAYGILI, G. 2010. Removal of boron from waste waters using HDTMA-modified zeolites. *Desalination and Water Treatment,* 23, 110-117.
DICKSON, A. G. 1990. Thermodynamics of the Dissociation of Boric-Acid in Synthetic Seawater from 273.15-K to 318.15-K. *Deep-Sea Research Part a-Oceanographic Research Papers,* 37, 755-766.
DIZGE, N., SOYDEMIR, G., KARAGUNDUZ, A. & KESKINLER, B. 2011. Influence of type and pore size of membranes on cross flow microfiltration of biological suspension. *Journal of Membrane Science,* 366, 278-285.
DOĞANAY, C. O., ÖZBELGE, H. Ö., BıÇAK, N., AYDOĞAN, N. & YıLMAZ, L. 2011. Use of Specifically Tailored Chelating Polymers for Boron Removal from Aqueous Solutions by Polymer Enhanced Ultrafiltration. *Separation Science and Technology,* 46, 581-591.
DOMINGUEZ-TAGLE, C., ROMERO-TERNERO, V. J. & DELGADO-TORRES, A. M. 2011. Boron removal efficiency in small seawater Reverse Osmosis systems. *Desalination,* 265, 43-48.
DUBOIS, I. E. 2011. *Specific surface area of some minerals commonly found in granite.* KTH.
DYDO, P. 2013. Transport model for boric acid, monoborate and borate complexes across thin-film composite reverse osmosis membrane. *Desalination,* 311, 69-79.
DYDO, P., TUREK, M., CIBA, J., TROJANOWSKA, J. & KLUCZKA, J. 2005. Boron removal from landfill leachate by means of nanofiltration and reverse osmosis. *Desalination,* 185, 131-137.
EDZWALD, J. K. & HAARHOFF, J. 2011. Seawater pretreatment for reverse osmosis: Chemistry, contaminants, and coagulation. *Water Research,* 45, 5428-5440.
EEA 1998. The quality of water intended for human consumption. Council Directive 98/83/EC.
EIGEN, M. & HAMMES, G. 1963. Elementary steps in enzyme reactions. *In:* NORD, F. F. (ed.) *Advances in Enzymology.* New York: Wiley.
EMSLEY, J. 1991. *The Elements,* Oxford, Oxford University Press.
ERSAN, H. Y. & PINARBASI, S. 2011. Boron removal by glucamine-functionalized hydrogel beads in batch fashion. *Journal of Applied Polymer Science,* 121, 1610-1615.
FARHAT, A., AHMAD, F. & ARAFAT, H. 2013. Analytical techniques for boron quantification supporting desalination processes: A review. *Desalination,* 310, 9-17.

FERREIRA, O. P., DE MORAES, S. G., DURAN, N., CORNEJO, L. & ALVES, O. L. 2006. Evaluation of boron removal from water by hydrotalcite-like compounds. *Chemosphere,* 62, 80-8.

FOX, K. K., DANIEL, M., MORRIS, G. & HOLT, M. S. 2000. The use of measured boron concentration data from the GREAT-ER UK validation study (1996-1998) to generate predicted regional boron concentrations. *Science of the Total Environment,* 251, 305-316.

FREGER, V., GILRON, J. & BELFER, S. 2002. TFC polyamide membranes modified by grafting of hydrophilic polymers: an FT-IR/AFM/TEM study. *Journal of Membrane Science,* 209, 283-292.

FUJITA, Y., HATA, T., NAKAMARU, M., IYO, T., YOSHINO, T. & SHIMAMURA, T. 2005. A study of boron adsorption onto activated sludge. *Bioresour Technol,* 96, 1350-6.

GARCÍA-SOTO, M. D. M. D. L. F. & MUNOZ CAMACHO, E. 2005. Boron removal by processes of chemosorption. *Solvent extraction and ion exchange,* 23, 741-757.

GAZI, M. & BICAK, N. 2007. Selective boron extraction by polymer supported 2-hydroxylethylamino propylene glycol functions. *Reactive and Functional Polymers,* 67, 936-942.

GAZI, M., GALLI, G. & BICAKA, N. 2008. The rapid boron uptake by multi-hydroxyl functional hairy polymers. *Separation and Purification Technology,* 62, 484-488.

GAZI, M., SENKAL, B. F. & BICAK, N. 2004. Modification of Crosslinked Poly(styrene) Based Polymers for Boron-Specific Extraction. *Macromolecular Symposia,* 217, 215-222.

GEFFEN, N., SEMIAT, R., EISEN, M. S., BALAZS, Y., KATZ, I. & DOSORETZ, C. G. 2006. Boron removal from water by complexation to polyol compounds. *Journal of Membrane Science,* 286, 45-51.

GEORGHIOU, G. & PASHALIDIS, I. 2007. Boron in groundwaters of Nicosia (Cyprus) and its treatment by reverse osmosis. *Desalination,* 215, 104-110.

GORIN, P. A. J. & MAZUREK, M. 1973. C-13 Resonance Spectroscopic Studies on Formation of Borate and Diphenylborinate Complexes of Polyhydroxy Compounds. *Canadian Journal of Chemistry-Revue Canadienne De Chimie,* 51, 3277-3286.

GREENWOOD, N. N. 1973. Boron. *Comprehensive Inorganic Chemistry.* Oxford: Pergamon Press.

GROVER, P. K. & RYALL, R. L. 2004. Critical Appraisal of Salting-Out and Its Implications for Chemical and Biological Sciences. *Chemical Reviews,* 105, 1-10.

GÜLER, E., KABAY, N., YÜKSEL, M., YAVUZ, E. & YÜKSEL, Ü. 2011a. A comparative study for boron removal from seawater by two types of polyamide thin film composite SWRO membranes. *Desalination,* 273, 81-84.

GÜLER, E., KABAY, N., YÜKSEL, M., YIĞIT, N. Ö., KITIŞ, M. & BRYJAK, M. 2011b. Integrated solution for boron removal from seawater using RO process and sorption-membrane filtration hybrid method. *Journal of Membrane Science,* 375, 249-257.

HANAY, A., BONCUKCUOGLU, R., KOCAKERIM, M. & YILMAZ, A. 2003. Boron removal from geothermal waters by ion exchange in a batch reactor. *Fresenius Environmental Bulletin,* 12, 1190-1194.
HARADA, A., TAKAGI, T., KATAOKA, S., YAMAMOTO, T. & ENDO, A. 2011. Boron adsorption mechanism on polyvinyl alcohol. *Adsorption,* 17, 171-178.
HEBBLETHWAITE, R. L. & EMBERSON, P. 1993. Rising from the ashes. *Landscape Des,* 10, 31-34.
HILAL, N., AL-KHATIB, L., AL-ZOUBI, H. & NIGMATULLIN, R. 2005. Atomic force microscopy study of membranes modified by surface grafting of cationic polyelectrolyte. *Desalination,* 184, 45-55.
HILAL, N., BOWEN, W., ALKHATIB, L. & OGUNBIYI, O. 2006. A review of atomic force microscopy applied to cell interactions with membranes. *Chemical Engineering Research and Design,* 84, 282-292.
HILAL, N., KIM, G. J. & SOMERFIELD, C. 2011. Boron removal from saline water: A comprehensive review. *Desalination,* 273, 23-35.
HILAL, N. & KOCHKODAN, V. 2003. Surface modified microfiltration membranes with molecularly recognising properties. *Journal of Membrane Science,* 213, 97-113.
HO, Y.-S. & MCKAY, G. 1999. Pseudo-second order model for sorption processes. *Process Biochemistry,* 34, 451-465.
HO, Y., JOHN WASE, D. & FORSTER, C. 1995. Batch nickel removal from aqueous solution by sphagnum moss peat. *Water Research,* 29, 1327-1332.
HO, Y. & MCKAY, G. 1998. Sorption of dye from aqueous solution by peat. *Chemical Engineering Journal,* 70, 115-124.
HOLLIS, J. F., KEREN, R. & GAL, M. 1988. Boron Release and Sorption by Fly Ash as Affected by pH and Particle Size. *Journal of Environment Quality,* 17, 181.
HONG, S., FAIBISH, R. S. & ELIMELECH, M. 1997. Kinetics of permeate flux decline in crossflow membrane filtration of colloidal suspensions. *Journal of colloid and interface science,* 196, 267-277.
HOSHINA, H., SEKO, N., UEKI, Y. & TAMADA, M. 2007. Synthesis of Graft Adsorbent with N-Methyl-D-glucamine for Boron Adsorption. *Journal of Ion Exchange,* 18, 236-239.
HOU, D., WANG, J., SUN, X., LUAN, Z., ZHAO, C. & REN, X. 2010. Boron removal from aqueous solution by direct contact membrane distillation. *J Hazard Mater,* 177, 613-9.
HU, H. N., PENN, S. G., LEBRILLA, C. B. & BROWN, P. H. 1997. Isolation and characterization of soluble boron complexes in higher plants - The mechanism of phloem mobility of boron. *Plant Physiology,* 113, 649-655.
HUERTAS, E., HERZBERG, M., ORON, G. & ELIMELECH, M. 2008. Influence of biofouling on boron removal by nanofiltration and reverse osmosis membranes. *Journal of Membrane Science,* 318, 264-270.
HUISMAN, I. H. 2000. Membrane separations | Microfiltration. *In:* WILSON, I. D. (ed.) *Encyclopedia of Separation Science.* Oxford: Academic Press.
HUNG, P. V. X., CHO, S.-H. & MOON, S.-H. 2009. Prediction of boron transport through seawater reverse osmosis membranes using solution–diffusion model. *Desalination,* 247, 33-44.

HWANG, K.-J., LIAO, C.-Y. & TUNG, K.-L. 2008. Effect of membrane pore size on the particle fouling in membrane filtration. *Desalination,* 234, 16-23.
HYUNG, H. & KIM, J.-H. 2006. A mechanistic study on boron rejection by sea water reverse osmosis membranes. *Journal of Membrane Science,* 286, 269-278.
INAMUDDIN, M. & LUQMAN, M. 2012. *Ion Exchange Technology I* New York, Springer.
INUKAI, Y., KAIDA, Y. & YASUDA, S. 1997. Selective adsorbents for germanium (IV) derived from chitosan. *Analytica chimica acta,* 343, 275-279.
INUKAI, Y., TANAKA, Y., MATSUDA, T., MIHARA, N., YAMADA, K., NAMBU, N., ITOH, O., DOI, T., KAIDA, Y. & YASUDA, S. 2004. Removal of boron(III) by N-methylglucamine-type cellulose derivatives with higher adsorption rate. *Anal Chim Acta,* 511, 261-265.
IRAWAN, C., LIU, J. C. & WU, C.-C. 2011. Removal of boron using aluminum-based water treatment residuals (Al-WTRs). *Desalination,* 276, 322-327.
JACOB, C. 2007. Seawater desalination: Boron removal by ion exchange technology. *Desalination,* 205, 47-52.
JAHIRUDDIN, M., SMART, R., WADE, A. J., NEAL, C. & CRESSER, M. S. 1998. Factors regulating the distribution of boron in water in the River Dee catchment in north east Scotland. *Science of the Total Environment,* 210, 53-62.
JOLLY, W. L. 1984. *Modem inorganic chemistry,* New York, McGraw-Hill.
KABAY, N., BRYJAK, M., SCHLOSSER, S., KITIS, M., AVLONITIS, S., MATEJKA, Z., AL-MUTAZ, I. & YUKSEL, M. 2008. Adsorption-membrane filtration (AMF) hybrid process for boron removal from seawater: an overview. *Desalination,* 223, 38-48.
KABAY, N., GÜLER, E. & BRYJAK, M. 2010. Boron in seawater and methods for its separation — A review. *Desalination,* 261, 212-217.
KABAY, N., KÖSEOĞLU, P., YAPıCı, D., YÜKSEL, Ü. & YÜKSEL, M. 2013a. Coupling ion exchange with ultrafiltration for boron removal from geothermal water-investigation of process parameters and recycle tests. *Desalination,* 316, 17-22.
KABAY, N., KÖSEOĞLU, P., YAVUZ, E., YÜKSEL, Ü. & YÜKSEL, M. 2013b. An innovative integrated system for boron removal from geothermal water using RO process and ion exchange-ultrafiltration hybrid method. *Desalination,* 316, 1-7.
KABAY, N., SARP, S., YUKSEL, M., ARAR, Ö. & BRYJAK, M. 2007. Removal of boron from seawater by selective ion exchange resins. *Reactive and Functional Polymers,* 67, 1643-1650.
KABAY, N., YILMAZ-IPEK, I., SOROKO, I., MAKOWSKI, M., KIRMIZISAKAL, O., YAG, S., BRYJAK, M. & YUKSEL, M. 2009. Removal of boron from Balcova geothermal water by ion exchange–microfiltration hybrid process. *Desalination,* 241, 167-173.
KABAY, N., YILMAZ, İ., BRYJAK, M. & YÜKSEL, M. 2006. Removal of boron from aqueous solutions by a hybrid ion exchange–membrane process. *Desalination,* 198, 158-165.
KABAY, N., YıLMAZ, I., YAMAC, S., SAMATYA, S., YUKSEL, M., YUKSEL, U., ARDA, M., SAĞLAM, M., IWANAGA, T. & HIROWATARI, K. 2004a. Removal and recovery of boron from geothermal wastewater by selective ion

exchange resins. I. Laboratory tests. *Reactive and Functional Polymers,* 60, 163-170.
KABAY, N., YILMAZ, I., YAMAC, S., YUKSEL, M., YUKSEL, U., YILDIRIM, N., AYDOGDU, O., IWANAGA, T. & HIROWATARI, K. 2004b. Removal and recovery of boron from geothermal wastewater by selective ion-exchange resins — II. Field tests. *Desalination,* 167, 427-438.
KABAYA, N., SARPA, S., YUKSELA, M., KITISB, M., LUB, H. K., ARARC, Ö., BRYJAKD, M. & SEMIATE, R. 2008. Removal of boron from SWRO permeate by boron selective ion exchange resins containing N-methyl glucamine groups. *Desalination,* 223, 49-56.
KAFTAN, Ö., AÇıKEL, M., EROĞLU, A. E., SHAHWAN, T., ARTOK, L. & NI, C. 2005. Synthesis, characterization and application of a novel sorbent, glucamine-modified MCM-41, for the removal/preconcentration of boron from waters. *Anal Chim Acta,* 547, 31-41.
KAMBOH, M. A. & YILMAZ, M. 2013. Synthesis of N-methylglucamine functionalized calix[4]arene based magnetic sporopollenin for the removal of boron from aqueous environment. *Desalination,* 310, 67-74.
KARAHAN, S., YURDAKOC, M., SEKI, Y. & YURDAKOC, K. 2006. Removal of boron from aqueous solution by clays and modified clays. *J Colloid Interface Sci,* 293, 36-42.
KAVAK, D. 2009. Removal of boron from aqueous solutions by batch adsorption on calcined alunite using experimental design. *J Hazard Mater,* 163, 308-14.
KEHAL, M., REINERT, L. & DUCLAUX, L. 2010. Characterization and boron adsorption capacity of vermiculite modified by thermal shock or H2O2 reaction and/or sonication. *Applied Clay Science,* 48, 561-568.
KELLY, R. N. & KAZANJIAN, J. 2006. Commerical reference shape standards use in the study of particle shape effect on laser diffraction particle size analysis. *AAPS PharmSciTech,* 7, E126-E137.
KEMP, P. H. 1956. *The chemistry of borates,* Ipswich, W.S. Cowell LTD.
KHAYET, M., KHULBE, K. C. & MATSUURA, T. 2004. Characterization of membranes for membrane distillation by atomic force microscopy and estimation of their water vapor transfer coefficients in vacuum membrane distillation process. *Journal of Membrane Science,* 238, 199-211.
KHAYET, M., MENGUAL, J. & ZAKRZEWSKA-TRZNADEL, G. 2005. Direct contact membrane distillation for nuclear desalination. Part I: Review of membranes used in membrane distillation and methods for their characterisation. *International journal of nuclear desalination,* 1, 435-449.
KHULBE, K., FENG, C., MATSUURA, T. & KHAYET, M. 2006. AFM images of the cross-section of polyetherimide hollow fibers. *Desalination,* 201, 130-137.
KIM, B.-C., HUNG, P. V. X. & MOON, S.-H. 2010. Boron removal from seawater by combined system of seawater reverse osmosis membranes and ion exchange process: a pilot-scale study. *Desalination and Water Treatment,* 15, 178-182.
KIR, E. & ALKAN, E. 2006. Fluoride removal by Donnan dialysis with plasma-modified and unmodified anion-exchange membranes. *Desalination,* 197, 217-224.

KIR, E., GURLER, B. & GULEC, A. 2011. Boron removal from aqueous solution by using plasma-modified and unmodified anion-exchange membranes. *Desalination,* 267, 114-117.
KLIEGEL, W. 1980. *Bor in Biologie,* New York, Springer-Verlag.
KLUCZKA, J., CIBA, J., TROJANOWSKA, J., ZOLOTAJKIN, M., TUREK, M. & DYDO, P. 2007. Removal of boron dissolved in water. *Environmental Progress,* 26, 71-77.
KLUCZKA, J., KOROLEWICZ, T., ZOŁOTAJKIN, M., SIMKA, W. & RACZEK, M. 2013. A new adsorbent for boron removal from aqueous solutions. *Environ Technol,* 1-8.
KÖSE, T. E., DEMIRAL, H. & ÖZTÜRK, N. 2011. Adsorption of boron from aqueous solutions using activated carbon prepared from olive bagasse. *Desalination and Water Treatment,* 29, 110-118.
KOSEOGLU, H., HARMAN, B. I., YIGIT, N. O., GULER, E., KABAY, N. & KITIS, M. 2010. The effects of operating conditions on boron removal from geothermal waters by membrane processes. *Desalination,* 258, 72-78.
KOSEOGLU, H., KABAY, N., YÜKSEL, M. & KITIS, M. 2008a. The removal of boron from model solutions and seawater using reverse osmosis membranes. *Desalination,* 223, 126-133.
KOSEOGLU, H., KABAY, N., YÜKSEL, M., SARP, S., ARAR, Ö. & KITIS, M. 2008b. Boron removal from seawater using high rejection SWRO membranes — impact of pH, feed concentration, pressure, and cross-flow velocity. *Desalination,* 227, 253-263.
KRAUSKOPF, K. B. 1972. Geochemistry of micronutrients. *In:* MORTVEDT, J. J., GIORDANO, P. M. & LINDSAY, W. L. (eds.). Madison: Soil Science Society of America.
KRAWCZYK, D. & GONGLEWSKI, N. 1959. Determining suspended solids using a spectrophotometer. *Sewage and Industrial Wastes,* 31, 1159-1164.
KREBS, R. E. 2006. *The history and use of our earth's chemical elements: a reference guide*, Greenwood Publishing Group.
KUROKAWA, H., SHIBAYAMA, M., ISHIMARU, T., NOMURA, S. & WU, W. I. 1992. Phase-Behavior and Sol-Gel Transition of Poly(Vinyl Alcohol) Borate Complex in Aqueous-Solution. *Polymer,* 33, 2182-2188.
KWON, D., VIGNESWARAN, S., FANE, A. & AIM, R. B. 2000a. Experimental determination of critical flux in cross-flow microfiltration. *Separation and Purification Technology,* 19, 169-181.
KWON, D. Y., VIGNESWARAN, S., FANE, A. G. & AIM, R. B. 2000b. Experimental determination of critical flux in cross-flow microfiltration. *Separation and Purification Technology,* 19, 169-181.
LEE, I. P., SHERINS, R. J. & DIXON, R. L. 1978. Evidence for Induction of Germinal Aplasia in Male Rats by Environmental Exposure to Boron. *Toxicology and Applied Pharmacology,* 45, 577-590.
LENZ, R. W. & HEESCHEN, J. P. 1961. The application of NMR to structural studies of carbohydrates in aqueous solution. *J. Polymer Soc.,* 51, 247–255.
LI-NA, W., TAO, Q. & YI, Z. 2006. Synthesis of Novel Chelating Adsorbents for Boron Uptake from Aqueous Solutions. *The Chinese Journal of Process Engineering,* 6, 375-379.

LI, X., LIU, R., WU, S., LIU, J., CAI, S. & CHEN, D. 2011. Efficient removal of boron acid by N-methyl-d-glucamine functionalized silica–polyallylamine composites and its adsorption mechanism. *Journal of Colloid and Interface Science,* 361, 232-237.

LIU, H., QING, B., YE, X., GUO, M., LI, Q., WU, Z., LEE, K., LEE, D. & LEE, K. 2009a. Boron adsorption mechanism of a hybrid gel derived from tetraethoxysilane and bis(trimethoxysilylpropyl)amine. *Current Applied Physics,* 9, e280-e283.

LIU, H., QING, B., YE, X., LI, Q., LEE, K. & WU, Z. 2009b. Boron adsorption by composite magnetic particles. *Chemical Engineering Journal,* 151, 235-240.

LIU, H., YE, X., LI, Q., KIM, T., QING, B., GUO, M., GE, F., WU, Z. & LEE, K. 2009c. Boron adsorption using a new boron-selective hybrid gel and the commercial resin D564. *Colloids and Surfaces A: Physicochemical and Engineering Aspects,* 341, 118-126.

LIU, R., MA, W., JIA, C.-Y., WANG, L. & LI, H.-Y. 2007. Effect of pH on biosorption of boron onto cotton cellulose. *Desalination,* 207, 257-267.

LU, W.-M. & JU, S.-C. 1989. Selective particle deposition in crossflow filtration. *Separation Science and Technology,* 24, 517-540.

LUTZ, O., HUMPFER, E. & SPRAUL, M. 1991. Ascertainment of Boric-Acid Esters in Wine by B-11 Nmr. *Naturwissenschaften,* 78, 67-69.

M. SUZUKI, T., A. PACHECO TANAKA, D., YOKOYAMA, T., MIYAZAKI, Y. & YOSHIMURA, K. 1999. Complexation and removal of trace boron from aqueous solution by an anion exchange resin loaded with chromotropic acid (disodium 2,7-dihydroxynaphthalene-4,5-disulfonate). *Journal of the Chemical Society, Dalton Transactions,* 0, 1639-1644.

MAGARA, Y., TABATA, A., KOHKI, M., KAWASAKI, M. & HIROSE, M. 1998. Development of boron reduction system for sea water desalination. *Desalination,* 118, 25-33.

MAKKEE, M., KIEBOOM, A. P. G. & VANBEKKUM, H. 1985. Studies on Borate Esters .3. Borate Esters of D-Mannitol, D-Glucitol, D-Fructose and D-Glucose in Water. *Recueil Des Travaux Chimiques Des Pays-Bas-Journal of the Royal Netherlands Chemical Society,* 104, 230-235.

MATSUNAGA, T. & NAGATA, T. 1995. In-Vivo B-11 Nmr Observation of Plant-Tissue. *Analytical Sciences,* 11, 889-892.

MELLEN, R. H., BROWNING, D. G. & SIMMONS, V. P. 1983. Investigation of Chemical Sound-Absorption in Seawater. *Journal of the Acoustical Society of America,* 74, 987-993.

MIYAZAKI, Y., MATSUO, H., FUJIMORI, T., TAKEMURA, H., MATSUOKA, S., OKOBIRA, T., UEZU, K. & YOSHIMURA, K. 2008. Interaction of boric acid with salicyl derivatives as an anchor group of boron-selective adsorbents. *Polyhedron,* 27, 2785-2790.

MNIF, A., HAMROUNI, B. & DHAHBI, M. 2009. Boron removal by membrane processes. *Desalination and Water Treatment,* 5, 119-123.

MOE 2009. Management of Drinking Water Quality. Republic of Korea: Ministry of Environment.

MOH 2005. Drinking-water Standards for New Zealand. Wellington: Ministry of Health.

MORGAN, V. 1980. *Boron chemistry,* New York, Longman.
MORISADA, S., RIN, T., OGATA, T., KIM, Y. H. & NAKANO, Y. 2011. Adsorption removal of boron in aqueous solutions by amine-modified tannin gel. *Water Res,* 45, 4028-34.
MULDER, M. 1996. *Basic Principles of Membrane Technology Second Edition,* Kluwer Academic Pub.
NA, J. W. & LEE, K. J. 1993. Characteristics of boron adsorption on strong-base anion-exchange resin. *Annals of Nuclear Energy,* 20, 455-462.
NADAV, N. 1999. Boron removal from seawater reverse osmosis permeate utilizing selective ion exchange resin. *Desalination,* 124, 131-135.
NEAL, C., FOX, K. K., HARROW, M. & NEAL, M. 1998. Boron in the major UK rivers entering the North Sea. *Science of the Total Environment,* 210, 41-51.
NHMRC 2004. Australian drinking water guidelines. Canberra: National Health and Medical Research Council.
NIKITIN, Y. I. & PETASYUK, G. 2008. Specific surface area determination methods, devices, and results for diamond powders. *Journal of Superhard Materials,* 30, 58-70.
NIPH 2006. Seawater Desalination Facility on Okinawa. Japan.
NISHIHAMA, S., SUMIYOSHI, Y., OOKUBO, T. & YOSHIZUKA, K. 2013. Adsorption of boron using glucamine-based chelate adsorbents. *Desalination,* 310, 81-86.
NUNES, S. P. & PEINEMANN, K.-V. 2006. *Membrane technology: in the chemical industry,* John Wiley & Sons.
OHE, K., OKAMOTO, K., NAKAMURA, S. & BABA, Y. 2003. Synthesis of Glycidyl Methacrylate-Divinylbenzene Microspheres with Aminoalcohol Groups and Their Adsorption Properties for Boron. *Journal of Ion Exchange,* 14, 325-328.
ONDERKOVÁ, B., ŠCHLOSSER, Š., BLAHUŠIAK, M. & BÚGEL, M. 2009. Microfiltration of suspensions of microparticulate boron adsorbent through a ceramic membrane. *Desalination,* 241, 148-155.
OO, M. H. & SONG, L. 2009. Effect of pH and ionic strength on boron removal by RO membranes. *Desalination,* 246, 605-612.
OWEN, B. B. 1934. The dissociation constant of boric acid from 10 to 50 C. *J. Am. Chem. Soc.,* 56, 1695-97.
OZTURK, N. & KAVAK, D. 2005. Adsorption of boron from aqueous solutions using fly ash: batch and column studies. *J Hazard Mater,* 127, 81-8.
ÖZTÜRK, N. & KAVAK, D. 2008. Boron removal from aqueous solutions by batch adsorption onto cerium oxide using full factorial design. *Desalination,* 223, 106-112.
ÖZTÜRK, N. & KÖSE, T. E. 2008. Boron removal from aqueous solutions by ion-exchange resin: Batch studies. *Desalination,* 227, 233-240.
PARSAEI, M., GOODARZI, M. S. & NASEF, M. M. 2011. Adsorption Study for Removal of Boron Using Ion Exchange Resin in Bach System. *2nd International Conference on Environmental Science and Technology* Singapore.
PARSCHOVÁ, H., MIŠTOVÁ, E., MATĚJKA, Z., JELÍNEK, L., KABAY, N. & KAUPPINEN, P. 2007. Comparison of several polymeric sorbents for selective boron removal from reverse osmosis permeate. *Reactive and Functional Polymers,* 67, 1622-1627.

PEAK, D., LUTHER, G. W. & SPARKS, D. L. 2003. ATR-FTIR spectroscopic studies of boric acid adsorption on hydrous ferric oxide. *Geochimica et Cosmochimica Acta,* 67, 2551-2560.

PELIN DEMIRÇIVI, A. G. N.-S. 2008. Removal of Boron from Waste Waters by Ion-Exchange in a Batch System. *International Journal of Chemical and Biological Engineering,* 1, 135-138.

PICARD, T., CATHALIFAUD-FEUILLADE, G., MAZET, M. & VANDENSTEENDAM, C. 2000. Cathodic dissolution in the electrocoagulation process using aluminium electrodes. *Journal of Environmental Monitoring,* 2, 77-80.

PIEROTTI, R. & ROUQUEROL, J. 1985. Reporting physisorption data for gas/solid systems with special reference to the determination of surface area and porosity. *Pure Appl Chem,* 57, 603-619.

PIZER, R. D., RICATTO, P. J. & TIHAL, C. A. 1993. Thermodynamics of Several Boron Acid Complexation Reactions Studied by Variable-Temperature H-1 and B-11 Nmr-Spectroscopy. *Polyhedron,* 12, 2137-2142.

POLAT, H., VENGOSH, A., PANKRATOV, I. & POLAT, M. 2004. A new methodology for removal of boron from water by coal and fly ash. *Desalination,* 164, 173-188.

POLOWCZYK, I., ULATOWSKA, J., KOŹLECKI, T., BASTRZYK, A. & SAWIŃSKI, W. 2013. Studies on removal of boron from aqueous solution by fly ash agglomerates. *Desalination,* 310, 93-101.

POWER, P. P. & WOODS, W. G. 1997. The chemistry of boron and its speciation in plants. *Plant and Soil,* 193, 1-13.

PRATS, D., CHILLON-ARIAS, M. F. & RODRIGUEZ-PASTOR, M. 2000. Analysis of the influence of pH and pressure on the elimination of boron in reverse osmosis. *Desalination,* 128, 269-273.

RAJAKOVIĆ, L. V. & RISTIĆ, M. D. 1996. Sorption of boric acid and borax by activated carbon impregnated with various compounds. *Carbon,* 34, 769-774.

REMY, P., MUHR, H., PLASARI, E. & OUERDIANE, I. 2005. Removal of boron from wastewater by precipitation of a sparingly soluble salt. *Environmental Progress,* 24, 105-110.

ROY, R. N., ROY, L. N., LAWSON, M., VOGEL, K. M., MOORE, C. P., DAVIS, W. & MILLERO, F. J. 1993. Thermodynamics of the Dissociation of Boric-Acid in Seawater at S=35 from 0-Degrees-C to 55-Degrees-C. *Marine Chemistry,* 44, 243-248.

ROZANSKA, A., WISNIEWSKI, J. & WINNICKI, T. 2006. Donnan dialysis with anion-exchange membranes in a water desalination system. *Desalination,* 198, 236-246.

SABARUDIN, A., OSHITA, K., OSHIMA, M. & MOTOMIZU, S. 2005. Synthesis of cross-linked chitosan possessing N-methyl-d-glucamine moiety (CCTS-NMDG) for adsorption/concentration of boron in water samples and its accurate measurement by ICP-MS and ICP-AES. *Talanta,* 66, 136-44.

SAĞ, Y. & AKTAY, Y. 2002. Kinetic studies on sorption of Cr (VI) and Cu (II) ions by chitin, chitosan and< i> Rhizopus arrhizus</i>. *Biochemical Engineering Journal,* 12, 143-153.

SAH, R. N. & BROWN, P. H. 1997. Boron determination - A review of analytical methods. *Microchemical Journal,* 56, 285-304.
ŞAHIN, S. 2002. A mathematical relationship for the explanation of ion exchange for boron adsorption. *Desalination,* 143, 35-43.
SALENTINE, C. G. 1983. High-Field B-11 Nmr of Alkali Borates - Aqueous Polyborate Equilibria. *Inorganic Chemistry,* 22, 3920-3924.
SANDERSON, B. R. (ed.) 1980. *Coordinated compounds of boric acid,* New York: Longman.
SANTANDER, P., RIVAS, B. L., URBANO, B. F., YıLMAZ İPEK, İ., ÖZKULA, G., ARDA, M., YÜKSEL, M., BRYJAK, M., KOZLECKI, T. & KABAY, N. 2013. Removal of boron from geothermal water by a novel boron selective resin. *Desalination,* 310, 102-108.
SASO 2000. Bottled drinking water. Saudi Arabian Standards Organization.
SCHLOSSER, S., BLAHUIAK, M. & KABAY, N. 2008. A new hybrid adsorption-mf process for water treatment with microparticluate adsorbent. *12th Aachener Membran Kolloquium.* Aachen (DE).
SCHMITT-KOPPLIN, P., HERTKORN, N., GARRISON, A. W., FREITAG, D. & KETTRUP, A. 1998. Influence of borate buffers on the electrophoretic behavior of humic substances in capillary zone electrophoresis. *Analytical Chemistry,* 70, 3798-3808.
SENKAL, B. F. & BICAK, N. 2003. Polymer supported iminodipropylene glycol functions for removal of boron. *Reactive and Functional Polymers,* 55, 27-33.
SEYHAN, S., SEKI, Y., YURDAKOC, M. & MERDIVAN, M. 2007. Application of iron-rich natural clays in Camlica, Turkey for boron sorption from water and its determination by fluorimetric-azomethine-H method. *J Hazard Mater,* 146, 180-5.
SIMONNOT, M. O., CASTEL, C., NICOLAI, M., ROSIN, C., SARDIN, M. & JAUFFRET, H. 2000. Boron removal from drinking water with a boron selective resin: Is the treatment really selective? *Water Research,* 34, 109-116.
SINGH, S., KHULBE, K., MATSUURA, T. & RAMAMURTHY, P. 1998. Membrane characterization by solute transport and atomic force microscopy. *Journal of Membrane Science,* 142, 111-127.
SINTON, S. W. 1987. Complexation Chemistry of Sodium-Borate with Polyvinyl-Alcohol) and Small Diols - a B-11 Nmr-Study. *Macromolecules,* 20, 2430-2441.
SMITH, B. F., ROBISON, T. W., CARLSON, B. J., LABOURIAU, A., KHALSA, G. R. K., SCHROEDER, N. C., JARVINEN, G. D., LUBECK, C. R., FOLKERT, S. L. & AGUINO, D. I. 2005. Boric acid recovery using polymer filtration: studies with alkyl monool, diol, and triol containing polyethylenimines. *Journal of Applied Polymer Science,* 97, 1590-1604.
SUTZKOVER, I., HASSON, D. & SEMIAT, R. 2000. Simple technique for measuring the concentration polarization level in a reverse osmosis system. *Desalination,* 131, 117-127.
TARLETON, E. & WAKEMAN, R. J. 1994. Understanding flux decline in crossflow microfiltration. Part 3-Effects of membrane morphology.
TING, T.-M., HOSHINA, H., SEKO, N. & TAMADA, M. 2013. Removal of boron by boron-selective adsorbent prepared using radiation induced grafting technique. *Desalination and Water Treatment,* 51, 2602-2608.

TSUDA, M., SHIROTANI, I., MINOMURA, S. & TERAYAMA, Y. 1976. Effect of Pressure on Dissociation of Weak Acids in Aqueous Buffers. *Bulletin of the Chemical Society of Japan,* 49, 2952-2955.
TU, K. L., CHIVAS, A. R. & NGHIEM, L. D. 2013. Enhanced boron rejection by NF/RO membranes by complexation with polyols: Measurement and mechanisms. *Desalination,* 310, 115-121.
TUREK, M., BANDURA-ZALSKA, B. & DYDO, P. 2009. Boron removal by Donnan dialysis. *Desalination and Water Treatment,* 10, 53-59.
TUREK, M., DYDO, P., TROJANOWSKA, J. & CAMPEN, A. 2007. Adsorption/co-precipitation—reverse osmosis system for boron removal. *Desalination,* 205, 192-199.
USEPA 2006. Edition of the drinking water standards and health advisories. Washington, DC.
USEPA 2008. Drinking water health advisory for boron. Washington, DC.
VANDUIN, M., PETERS, J. A., KIEBOOM, A. P. G. & VANBEKKUM, H. 1984. The Ph-Dependence of the Stability of Esters of Boric-Acid and Borate in Aqueous-Medium as Studied by B-11 Nmr. *Tetrahedron,* 40, 2901-2911.
VANDUIN, M., PETERS, J. A., KIEBOOM, A. P. G. & VANBEKKUM, H. 1985. Studies on Borate Esters .2. Structure and Stability of Borate Esters of Polyhydroxycarboxylates and Related Polyols in Aqueous Alkaline Media as Studied by B-11 Nmr. *Tetrahedron,* 41, 3411-3421.
VIEIRA, R. H. & VOLESKY, B. 2010. Biosorption: a solution to pollution? *International microbiology,* 3, 17-24.
WAHAB MOHAMMAD, A., HILAL, N. & NIZAM ABU SEMAN, M. 2003. A study on producing composite nanofiltration membranes with optimized properties. *Desalination,* 158, 73-78.
WANG, L., QI, T., GAO, Z., ZHANG, Y. & CHU, J. 2007. Synthesis of N-methylglucamine modified macroporous poly(GMA-co-TRIM) and its performance as a boron sorbent. *Reactive and Functional Polymers,* 67, 202-209.
WATON, G., MALLO, P. & CANDAU, S. J. 1984. Temperature-Jump Rate Study of the Chemical Relaxation of Aqueous Boric-Acid Solutions. *J. Phys.Chem.,* 88, 3301-3305.
WEAST, R. C., ASTLE, M. J. & W.H., B. 1985. CRC handbook of chemistry and physics. 69th ed. Boca Raton, FL: CRC Press.
WEDD, M. W. 2003. Determination of particle size distributions using laser diffraction. *Educational Resources for Particle Technology,* 4, 1-4.
WEIR, R. J. & FISHER, R. S. 1972. Toxicologic Studies on Borax and Boric-Acid. *Toxicology and Applied Pharmacology,* 23, 351-359.
WHO 1993. Guidelines for Drinking-Water Quality, 2nd edition. Geneva.
WHO 2003 Boron in Drinking Water. Geneva.
WHO 2009. Boron in drinking water - background document for development of WHO guidelines for drinking water quality.
WHO 2011. Guidelines for Drinking Water Quality, Fourth Edition. Zheneva.
WOLSKA, J. & BRYJAK, M. 2011. Preparation of polymeric microspheres for removal of boron by means of sorption-membrane filtration hybrid. *Desalination,* 283, 193-197.

WOLSKA, J. & BRYJAK, M. 2013. Methods for boron removal from aqueous solutions — A review. *Desalination,* 310, 18-24.
WOLSKA, J., BRYJAK, M. & KABAY, N. 2010. Polymeric microspheres with N-methyl-D-glucamine ligands for boron removal from water solution by adsorption-membrane filtration process. *Environ Geochem Health,* 32, 349-52.
WYNESS, A. J., PARKMAN, R. H. & NEAL, C. 2003. A summary of boron surface water quality data throughout the European Union. *Science of the Total Environment,* 314, 255-269.
XIAO, X., CHEN, B.-Z., SHI, X.-C. & CHEN, Y. 2012. Boron removal from brine by XSC-700. *Journal of Central South University,* 19, 2768-2773.
XIE, R., CHU, L.-Y., CHEN, W.-M., XIAO, W., WANG, H.-D. & QU, J.-B. 2005. Characterization of microstructure of poly(N-isopropylacrylamide)-grafted polycarbonate track-etched membranes prepared by plasma-graft pore-filling polymerization. *Journal of Membrane Science,* 258, 157-166.
XU, N., ZHAO, Y., ZHONG, J. & SHI, J. 2002. Crossflow microfiltration of micro-sized mineral suspensions using ceramic membranes. *Chemical Engineering Research and Design,* 80, 215-221.
XU, Y. & JIANG, J.-Q. 2007. Technologies for Boron Removal. *Industrial & Engineering Chemistry Research,* 47, 16-24.
YAN, C., YI, W., MA, P., DENG, X. & LI, F. 2008. Removal of boron from refined brine by using selective ion exchange resins. *J Hazard Mater,* 154, 564-71.
YAN, L., LI, Y. S., XIANG, C. B. & XIANDA, S. 2006. Effect of nano-sized Al2O3-particle addition on PVDF ultrafiltration membrane performance. *Journal of Membrane Science,* 276, 162-167.
YASUHIKO, K., YOSHINARI, I., SEIJI, Y., AKEHIRO, Y., KATSUYA, M., MASASHI, S. & TOSHIAKI, T. 2002. Adsorption Properties of Boron on Branched-Saccharide-Polyallylamine Resins. *Journal of Japan Society on Water Environment,* 25, 547-552.
YAVUZ, E., GÜLER, E., SERT, G., ARAR, Ö., YÜKSEL, M., YÜKSEL, Ü., KITIŞ, M. & KABAY, N. 2013a. Removal of boron from geothermal water by RO system-I—Effect of membrane configuration and applied pressure. *Desalination,* 310, 130-134.
YAVUZ, E., GURSEL, Y. & SENKAL, B. F. 2013b. Modification of poly(glycidyl methacrylate) grafted onto crosslinked PVC with iminopropylene glycol group and use for removing boron from water. *Desalination,* 310, 145-150.
YILMAZ-IPEK, I., KABAY, N. & ÖZDURAL, A. R. 2011. Non-equilibrium sorption modeling for boron removal from geothermal water using sorption–microfiltration hybrid method. *Chemical Engineering and Processing: Process Intensification,* 50, 599-607.
YILMAZ, A. E., BONCUKCUOĞLU, R., BAYAR, S., FIL, B. A. & KOCAKERIM, M. M. 2012. Boron removal by means of chemical precipitation with calcium hydroxide and calcium borate formation. *Korean Journal of Chemical Engineering,* 29, 1382-1387.
YILMAZ, A. E., BONCUKCUOGLU, R., KOCAKERIM, M. M. & KESKINLER, B. 2005a. The investigation of parameters affecting boron removal by electrocoagulation method. *J Hazard Mater,* 125, 160-5.

YILMAZ, A. E., BONCUKCUOGLU, R., KOCAKERIM, M. M., YILMAZ, M. T. & PALULUOGLU, C. 2008. Boron removal from geothermal waters by electrocoagulation. *J Hazard Mater,* 153, 146-51.

YILMAZ, A. E., BONCUKCUOGLU, R., YILMAZ, M. T. & KOCAKERIM, M. M. 2005b. Adsorption of boron from boron-containing wastewaters by ion exchange in a continuous reactor. *J Hazard Mater,* 117, 221-6.

YILMAZ, İ., KABAY, N., BRJYAK, M., YÜKSEL, M., WOLSKA, J. & KOLTUNIEWICZ, A. 2006. A submerged membrane–ion-exchange hybrid process for boron removal. *Desalination,* 198, 310-315.

YILMAZ IPEK, I., HOLDICH, R., KABAY, N., BRYJAK, M. & YUKSEL, M. 2007. Kinetic behaviour of boron selective resins for boron removal using seeded microfiltration system. *Reactive and Functional Polymers,* 67, 1628-1634.

YıLMAZ İPEK, İ., KABAY, N. & YÜKSEL, M. 2013. Modeling of fixed bed column studies for removal of boron from geothermal water by selective chelating ion exchange resins. *Desalination,* 310, 151-157.

YOSHIMURA, K., MIYAZAKI, Y., OTA, F., MATSUOKA, S. & SAKASHITA, H. 1998. Complexation of boric acid with the N-methyl-D-glucamine group in solution and in crosslinked polymer. *Journal of the Chemical Society, Faraday Transactions,* 94, 683-689.

YOU, L., WU, Z., KIM, T. & LEE, K. 2006. Kinetics and thermodynamics of bromophenol blue adsorption by a mesoporous hybrid gel derived from tetraethoxysilane and bis(trimethoxysilyl)hexane. *Journal of Colloid and Interface Science,* 300, 526-535.

ZABORSKA, W. 1995. Competitive inhibitors of free and chitosanimmobilized urease. *Acta Biochem. Polon.,* 42, 115-118.

ZAGORODNI, A. A. 2006. *Ion Exchange Materials: Properties and Applications: Properties and Applications*, Access Online via Elsevier.

ZEEBE, R. E., SANYAL, A., ORTIZ, J. D. & WOLF-GLADROW, D. A. 2001. A theoretical study of the kinetics of the boric acid-borate equilibrium in seawater. *Marine Chemistry,* 73, 113-124.

ZERZE, H., KARAGOZ, B., OZBELGE, H. O., BICAK, N., AYDOGAN, N. & YILMAZ, L. 2013a. Imino-bis-propane diol functional polymer for efficient boron removal from aqueous solutions via continuous PEUF process. *Desalination,* 310, 158-168.

ZERZE, H., OZBELGE, H. O., BICAK, N., AYDOGAN, N. & YILMAZ, L. 2013b. Novel boron specific copolymers with quaternary amine segments for efficient boron removal via PEUF. *Desalination,* 310, 169-179.

ZHAO, Y., ZHANG, Y., XING, W. & XU, N. 2005. Influences of pH and ionic strength on ceramic microfiltration of TiO2 suspensions. *Desalination,* 177, 59-68.

ZHOU, W., APKARIAN, R., WANG, Z. L. & JOY, D. 2007. Fundamentals of Scanning Electron Microscopy (SEM). *Scanning Microscopy for Nanotechnology.* Springer.